LBL--30200

DE91 014229

Synthesis and Reactivity of Compounds Containing Ruthenium-Carbon, -Nitrogen, and -Oxygen Bonds

John F. Hartwig

December, 1990

Ph. D. Thesis

Chemical Sciences Division
Lawrence Berkeley Laboratory
University of California
Berkeley, CA 94720

This work was supported by the Director, Office of Energy Research, Office of Basic Energy Sciences, Chemical Sciences Division, of the U.S. Department of Energy under Contract No. DE-AC03-76SF00098

Synthesis and Reactivity of Compounds Containing Ruthenium-Carbon, -Nitrogen, and -Oxygen Bonds

John F. Hartwig

Abstract

Chapters 1-3. The products and mechanisms of the thermal reactions of several complexes of the general structure $(PMe_3)_4Ru(X)(Y)$ and $(DMPM)_2Ru(X)(Y)$ where X and Y are hydride, aryl, and benzyl groups, have been investigated. The mechanism of decomposition depends critically on the structure of the complex and the medium in which the thermolysis is carried out. The alkyl hydride complexes are do not react with alkane solvent, but undergo C-H activation processes with aromatic solvents by several different mechanisms. Thermolysis of $(PMe_3)_4Ru(Ph)(Me)$ or $(PMe_3)_4Ru(Ph)_2$ leads to the ruthenium benzyne complex $(PMe_3)_4Ru(\eta^2\text{-}C_6H_4)$ (1) by a mechanism which involves initial reversible dissociation of phosphine. In many ways its chemistry is analogous to that of early rather than late organo transition metal complexes.

Chapters 4-7. The synthesis, structure, variable temperature NMR spectroscopy and reactivity of ruthenium complexes containing aryloxide or arylamide ligands are reported. These complexes undergo cleavage of a P-C bond in coordinated trimethylphosphine, insertion of CO and CO_2 and hydrogenolysis. Mechanistic studies on these reactions are described.

Chapters 8 and 9. The generation of a series of reactive ruthenium complexes of the general formula $(PMe_3)_4Ru(R)$(enolate) is reported. Most of these enolates have been shown to bind to the ruthenium center through the oxygen atom. Two of the enolate complexes 8 and 9 exist in equilibrium between the O- and C-bound forms. The reactions of these compounds are reported, including reactions to form oxygen-containing metallacycles. The structure and reactivity of these ruthenium metallacycles is reported, including their thermal chemistry and reactivity toward protic acids, electrophiles, carbon monoxide, hydrogen and trimethylsilane.

Acknowledgements

I have thoroughly enjoyed my four years in Berkeley, and I have many people to thank for this. By some unknown process I ended up working for the odd couple of Bob Bergman and Dick Andersen, and I couldn't have designed a more rewarding working environment. The two of them complemented each other perfectly, and their interest, time, expertise, ideas, and financial support will be appreciated for many years. We gratefully acknowledge support for this work from the National Institutes of Health (Grant no. GM-25459) and from the Director, Office of Energy Research, Office of Basic Energy Sciences, Chemical Sciences Division, of the U.S. Department of Energy under Contract No. DE-AC03-76SF00098.

This department is blessed with what must be one of the best academic NMR facilities, and I am grateful to Rudi Nunlist and Rich Mazzarisi for their dedication to this facility, as well as Rich's interest in insuring that I never missed a quality S.F. Opera performance. I am also thankful for Dr. F.J. Hollander's role in helping to identify several of my compounds. All but one crystal structure analyses were performed by him at the UC Berkeley X-ray crystallographic facility (CHEXRAY).

This department is also blessed with a brilliant group of students and post-docs with whom to work. Although the experiments contained in this thesis was performed with my hands, I must credit the other members of Bob's research group with many of the ideas. For those who dared, Karen Goldberg was always willing to help teach air sensitive techniques, and I will always provide her with a (silent) thank you for her role in getting me started. Page Stoutland, John Freudenberger, and Susan Kegley taught me the rest of what I learned in my infancy in Berkeley, including how to survive in the Sierras on foot during the summer and on cross-country skis during the winter. During my second and third years, Tom Foo always provided the insight I lacked; I have missed his advice and willingness to attend Jazz and Blues shows anywhere, anytime.

My classmate Dave Glueck was often a better source for literature than the library, and I thank him for an infinite number of discussions and references on late-metal heteroatom compounds. I often worked very closely with my other classmate Pat Walsh and I appreciate his motivating influence, numerous ideas, and late night company during these times. Other students on the second floor of Lewis have made it difficult for me to leave Berkeley. Kamal Bharucha answered my organic questions, listened to my travel tales, and kept me aware of my Eastern (U.S.) background. Many hours at Roma and evenings in the city were spent with Rick Michelman, Natalie Walsh; their ability to be uplifting at all times was essential to my sanity. Anne Baranger was a loyal friend to me for all two years we have been in Berkeley together; I have appreciated her support and willingness to eat everything I cooked except the sweetbreads. Mathew Butts taught me everything I know about the Simpson's and after moving into our air-free junkyard, showed me the pleasure of helping enthusiastic students get started in graduate school. Kevan Shokat has been a constant source of energy, which is always appreciated but was most necessary during our first year when he also worked on the second floor of Lewis.

I spent perhaps more than my fair share of time on vacation, but my time in Asia with Leslie Bienen, Europe with Christine Leimgruber, and across the USA with Marc Weiner and Martha Collins are some of my best memories.

I have been located as far away from my family as is possible in this country, but not by choice. They are always supportive, and I must thank them for their advice on all aspects of my non-scientific life, as well as always thinking I'm wonderful even when I'm (usually, always?) not. Whenever I speak of my family, I must also include Scott Callon, Jinel Anderberg, and Dave Hitz, my friends from college living in the South Bay, and Leslie Bienen, my loyal sidekick throughout Asia. They have provided everything one could wish for from a group of friends and I will miss them deeply next year.

Finally I would like to show my appreciation to Mr. Scott Murray and Mr. Kenneth Ashe my two sixth grade teachers who showed me the pleasures of learning and to my Grandfather Paul who showed my the joy and satisfaction of learning to make things.

Table of Contents

Chapter 1

Inter- and Intramolecular C-H Bond Forming and Cleavage Reactivity of Two Different Types of Poly(trimethylphosphine)ruthenium Intermediates

Introduction

Reductive elimination from alkyl(hydrido) metal complexes to form C-H bonds has been shown to be an important step in several catalytic processes.[1] Careful studies of this reaction have revealed different mechanisms for the process.[2,3] For example, studies with metals in the platinum triad have shown that reductive elimination can be induced by ligand dissociation as well as by ligand association. A saturated Ir^{III} system with labile ligands was shown to undergo a reductive elimination reaction induced both thermally[2j,k] and photochemically[2g] by ligand dissociation.

The microscopic reverse of this reaction, oxidative addition of C-H bonds, has also been looked at extensively in recent years in the hope of designing a system which will catalytically functionalize saturated hydrocarbons.[4] One approach to this problem involves oxidative addition of an alkane by the transition metal center followed by coordination of an unsaturated organic molecule, migratory insertion, and reductive elimination of the functionalized alkane. In fact, homogeneous catalytic systems that functionalize arenes (albeit with low turnover numbers) have been achieved both thermally and photochemically by this route.[5]

Several electron rich d^8 transition metal systems are now known which undergo $d^8 \rightarrow d^6$ oxidative addition of hydrocarbon C-H bonds, leading to alkyl hydride complexes.[2b-f,4,6] Many of these metal systems contain ancillary ligands that do not dissociate easily, and this has limited the ability of these complexes to open a coordination site and undergo insertion reactions into the alkyl or hydride ligand. Most recently, dihydride and alkyl hydride complexes that activate hydrocarbons and contain potentially labile phosphines as the other ligands have been identified.[6b-e,i] In these complexes, phosphine dissociation potentially provides a site of unsaturation for potential modification of the alkyl substituent. Examples include $(DMPE)Fe(H)_2$ (DMPE= dimethylphospinoethane), which oxidatively adds alkanes upon photochemical loss of H_2,[6d] and (DMPE)Ru(aryl)(H) which has been shown to undergo exchange of the aryl group with arene solvent.[6j] However, a common problem with polyphosphine systems has been the observation of intra- rather than intermolecular C-H oxidative addition reactions.[2b-f,6e,7]

Moreover, systems with chelating phosphines do not provide an open site as readily as a monodentate phosphines, and they make mechanistic studies difficult because the dissociation of one end of the phosphorus ligand is difficult to detect kinetically. The $(PMe_3)_4Os(R)(H)$ system (which possesses monodentate phosphine ligands) has been shown to cleanly insert into the C-H bond of benzene, but intramolecular insertion into the C-H bond of the phosphine is competitive with insertion into the C-H bond of methane.[2b]

We have studied the analogous ruthenium system $(PMe_3)_4Ru(R)(H)$ in order to improve the understanding of factors that control inter- and intramolecular oxidative addition reactions in systems containing labile phosphine ligands. Kinetic and labelling studies provide evidence for the generation of two types of intermediates, one of which shows entirely intramolecular oxidative addition and the other exclusively intermolecular reactivity. Moreover, these studies indicate that reductive elimination of alkane from the alkyl hydride complexes proceeds by a simple one step mechanism, unusual for most d^6 and d^8 metal systems possessing labile ligands.

Results

Synthesis of tetrakis(trimethylphosphine)ruthenium alkyl hydride and deuteride complexes. The benzyl hydride complex $(PMe_3)_4Ru(CH_2Ph)(H)$ (**1**) was synthesized as shown in equation **1**. The known methyl chloride complex **2**[8] was exposed to 3

$$\underset{\textbf{2}}{cis\text{-}(PMe_3)_4Ru(Me)(Cl)} \xrightarrow[Et_2O]{H_2\ (3\ atm)} \underset{\textbf{3}}{cis\text{-}(PMe_3)_4Ru(H)(Cl)} + CH_4 \qquad (1)$$

$$\xrightarrow[Et_2O]{PhCH_2MgCl} \underset{\textbf{1}}{cis\text{-}(PMe_3)_4Ru(H)(CH_2Ph)}$$

atm hydrogen in ether to yield hydrido chloride **3**[9] as the only compound observed by $^{31}P\{^1H\}$ NMR spectrometry. Attempts to isolate the hydrido chloride gave low yields; an insoluble light yellow precipitate was obtained upon removal of the ether solvent under vacuum. Therefore, **3** was used *in situ*. Treatment with 1.1 equivalents of benzyl magnesium chloride, followed by crystallization from pentane gave **1** in 67 % yield. The ^1H NMR spectrum of the benzyl hydride complex displayed a doublet of doublet of triplets in the hydride region of the ^1H NMR spectrum

and an A_2BC pattern in the $^{31}P\{^1H\}$ spectrum indicating a cis octahedral geometry. The benzyl deuteride was prepared in comparable yield by an analogous route, using 3 atm of deuterium in the first step. Neither the EI nor FAB mass spectroscopy provided a molecular ion for the benzyl hydride complex, so the isotopic purity of the phenyl deuteride could not be determined by this method. However, a minimum isotopic purity could be determined by ^1H and ^2H NMR spectroscopy. The ^2H NMR spectrum of a 0.043 mmol benzene solution of **1-d_1** showed only a signal corresponding to the deuteride resonance, and the ^1H NMR spectrum of a 0.029 mmol solution of **1-d_1** showed no signal for the hydride resonance. A 0.0014 mmol solution of **1-d_0** did show a detectable hydride resonance by ^1H NMR spectroscopy, providing a lower limit of 95% for the isotopic purity for **1-d_1**.

The phenyl hydride complex $(PMe_3)_4Ru(Ph)(H)$ (**5**) was most conveniently prepared by room temperature addition of one equivalent of isopropanol to a pentane solution of the recently reported[10] benzyne complex, $(PMe_3)_4Ru(\eta^2\text{-}C_6H_4)$ (**4**) (equation 2). Concentration of the

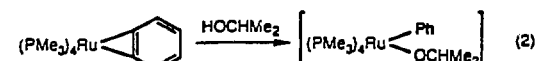

(2)

$\longrightarrow$ *cis*-$(PMe_3)_4Ru(H)(Ph)$ + Me_2CO

5

solution and cooling to -40 °C gave **5** in 48 % yield. The phenyl deuteride complex was synthesized by the addition of methanol-d_3 to a benzene solution of the benzyne complex, and was crystallized from pentane to give **5-d_1** in 43 % yield. Only a signal corresponding to the deuteride resonance was observed in the ^2H NMR spectrum, and no signal for the hydride resonance was observed in the ^1H NMR spectrum, again indicating >95% isotopic purity. The resonances in the phenyl region of the ^1H and $^{13}C\{^1H\}$ NMR spectra of **5** at room temperature were broad, but sharpened upon cooling to -40 °C, at which point rotation of the phenyl ring was slow on the ^1H and $^{13}C\{^1H\}$ NMR time scales. The hydride resonance in the ^1H NMR spectrum again appears as a doublet of doublet of triplets pattern, and the room temperature $^{31}P\{^1H\}$ NMR

spectrum displayed an A_2BC pattern indicating a *cis* geometry as was observed for the benzyl hydride complex **1**.

Thermolysis and Isotope Exchange Reactions. Thermolysis of the benzyl hydride complex in C_6D_6 solvent at 85 °C for 5 h yielded toluene and the cyclometallated complex $Ru(CH_2PMe_2)(PMe_3)_3(H)$ (**6**) in 97 % yield (^1H NMR spectroscopy) resulting from oxidative addition of the ligand C-H bond to the metal center (equation 3). This compound was reported by

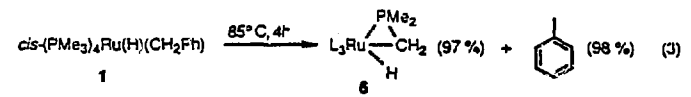

Werner as the product of the reduction of $Ru(PMe_3)_4(Cl)_2$ with Na/Hg.[7b] The $^{31}P\{^1H\}$ and ^1H NMR spectra of the product obtained from the thermolysis of **1** were identical to those of an independently prepared sample of **6** prepared in 22% yield by the method of Werner. The $^{31}P\{^1H\}$ NMR spectrum of the product showed an ABCD pattern and a characteristic high field resonance at -29 ppm for the phosphine in the metallated ring. No evidence for addition of solvent C-H bonds was observed in the thermolysis of **1**.

Thermolysis of the benzyl deuteride complex **1**-d_1 in cyclohexane yielded **6** in 97% yield, and exclusively toluene-d_1, as determined by comparison to an authentic sample prepared by the addition of D_2O to a solution of $PhCH_2MgBr$. The ^2H NMR spectrum of the reaction mixture showed no hydride signal, and GC/MS analysis of the volatile materials showed that the toluene consisted of only toluene-d_1. The reaction was run in cyclohexane so that the the aromatic and methyl regions of the toluene could be integrated in the ^2H NMR spectrum of the final reaction solution. The ratio of the signal for the methyl group on the product toluene-d_1 to the signal for the ortho position was 11:1. This small degree of deuteration in the aryl ring presumably occurred by reversible oxidative addition of the aryl C-H bond to the metal center, consistent with other *ortho*-metallation reactions in this system[10,11] and others.[12]

Thermolysis of the phenyl hydride complex **5** in cyclohexane-d_{12} at 135 °C for 8 h again yielded the cyclometallated complex **6** in 94 % yield by ^1H NMR spectroscopy (equation 4).

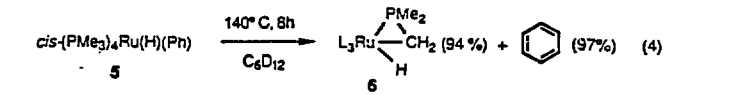

However, thermolysis of **5** in C_6D_6 at 140 °C for 8 h yielded the cyclometallated deuteride complex $Ru(CH_2PMe_2)(PMe_3)_3(D)$ **6**-d_1 in 90 % yield by ^1H NMR spectroscopy with deuterium incorporated into the hydride position (equation 5). When this reaction was run in C_6D_6 and

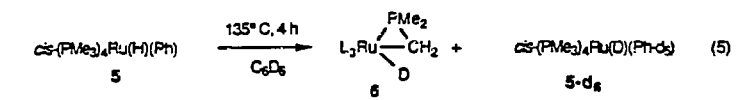

monitored after 4 h at 135 °C, the ^1H NMR spectrum showed an absence of both the aromatic signals and the hydride signal of the residual starting material and an increase in the solvent benzene peak (equation 5). The $^{31}P\{^1H\}$ NMR spectrum of the residual starting material exhibited the A_2BC part of an A_2BCX pattern, where X=D. The ^2H NMR spectrum contained resonances corresponding to the aromatic and hydride hydrogens of **5** in a ratio of 5:1, consistent with complete exchange of deuterated benzene into **5**. These data indicate that the rate of exchange between **5** and solvent benzene-d_6 is greater than the rate of reductive elimination to form **6**. Deuterium incorporation was also observed in the phosphine ligands by ^2H NMR spectroscopy; the ratio of deuterium in the phosphine region to deuterium in the hydride position was roughly 1:1.

Thermolysis of phenyl deuteride complex **5** was conducted in toluene at 140° C, monitoring the reaction by ^2H NMR spectrometry over the course of 4 h, followed by determination of the isotopic distribution in the benzene product by GC/MS of the volatile materials, and determination of the conversion of phenyl hydride to tolyl hydride by addition of acid to the organometallic products. Monitoring the reaction by ^2H NMR spectra showed a decrease in the hydride (deuteride) signal, an increase in the benzene resonance, and the appearance of signals

for the phosphine region. However, the ratio of deuterium in the phosphine region to deuterium in the benzene product was small, between 1:4 and 1:5 throughout the thermolysis. The amount of benzene-d_0 was found to be significantly greater than these values. The thermolysis was conducted twice, and the ratio of benzene-d_0 to benzene-d_1 was found to be 1:0.86 and 1:0.67 by GC/MS.

The extent of conversion from phenyl deuteride to tolyl hydride could not be simply determined by ^1H or $^{31}P\{^1H\}$ NMR spectroscopy because of the similar NMR spectra of the starting complex 5 and the ring exchange products. Instead, the conversion was determined by treating a portion of the non-volatile products with methanesulfonic acid in ether and determining the ratio of benzene to toluene by GC analysis. The ratio of phenyl to tolyl groups was found to be1:2.85 and 1:2.05 by this method for the two experiments. To confirm that all of the solvent toluene had been removed, a portion of the non-volatile materials which were not treated with acid was analyzed by ^1H NMR spectroscopy in C_6D_6. The spectrum contained no toluene resonances, but did contain a resonance at δ2.40 and δ2.37 corresponding to the methyl groups of the metal-bound tolyl groups, presumably *meta*- and *para*- substituted.

Thermolysis of the known $Ru(PMe_3)_4(H)_2$ in benzene-d_6 at 135 °C for 9.5 h yielded $Ru(PMe_3)_4(D)_2$ quantitatively by ^1H and ^2H NMR spectroscopy (equation 6). The hydride

$$cis\text{-}(PMe_3)_4Ru(H)_2 \xrightarrow[C_6D_6]{135°\,C,\ 4h} cis\text{-}(PMe_3)_4Ru(D)_2 \quad (6)$$

resonance was absent in the ^1H NMR spectrum of the reaction mixture after the thermolysis indicating at least 95% deuterium incorporation, and the deuteride signal was the only resonance observed in the ^2H NMR spectrum after the solvent was replaced with C_6H_6. The EI mass spectrum of the reaction product showed only a parent ion for $Ru(PMe_3)_4(D)_2$. No peak for $Ru(PMe_3)_4(H)_2$ or $Ru(PMe_3)_4(D)(H)$ was observed, indicating *complete* deuteration of the hydride position. Neither H_2 nor cyclometallated hydride, known to be stable at this temperature, was observed by ^1H NMR spectrometry. In fact, the dihydride complex remained unchanged in

alkane solvent up to 180 °C. Thermolysis of the dihydride in *n*-pentane-d_{12} did not yield a decrease in the hydride signal or an increase in the residual pentane resonances of the ^{1}H NMR spectrum. In addition, no deuteride resonances were observed in the ^{2}NMR spectrum of the thermolysis reaction when the deuterated solvent was removed under vacuum and replaced with undeuterated *n*-pentane.

Kinetic studies. The thermolysis of **1** in benzene-d_6 was conducted at 80 °C in NMR tubes sealed under vacuum. The course of the reaction was monitored by removing the tubes, cooling them quickly and then obtaining ^{1}H NMR spectra at ambient temperature. The growth of the methyl group resonance of the toluene product and the disappearance of the methylene resonance of the starting ruthenium complex were integrated against a ferrocene internal standard and provided identical rates. For one set of experiments, the reaction was run in 0.0410 M - 0.246 M solutions of trimethylphosphine in benzene-d_6 with a constant concentration of 0.0410 M ruthenium complex. Linear first order plots were obtained for greater than three half lives at all concentrations. No intermediates were detected. To confirm the first order behavior of the reductive elimination, the reaction was also run with an initial metal concentration of 0.0121 M. Within experimental error, the rate constants for all concentrations of phosphine and starting ruthenium complex were identical (Table 1).

To check for rapid dissociation of phosphine ligand, compound **1** was heated to 60 °C in the presence of 4.0 equivalents of PMe_3-d_9 in benzene-d_6 for 12 h. The initial solution showed only PMe_3-d_9 in the free phosphine region of the $^{31}P\{^1H\}$ NMR spectrum (the isotope shift of 0.26 ppm for each deuterium is large enough that all possible isotopes of PMe_3-d_0 to PMe_3-d_9 can be observed by $^{31}P\{^1H\}$ NMR spectrometry). Less than 10 % conversion of **1** to **6** and toluene was observed after the 12 h of thermolysis. However, the $^{31}P\{^1H\}$ NMR spectrum showed a 0.86:1.0 mixture of free PMe_3-d_9 and PMe_3-d_0. Although quantitative rate studies were not carried out on this substitution reaction, these observations make it clear that the rate of phosphine dissociation is much faster than the rate of reductive elimination.

Table 1. Rate constants for the thermolysis of **1** in the presence of added phosphine.

$k_{obs} \times 10^{-4}$ (sec^{-1})	[L] (M)
1.26 ± 0.19	0.0410
1.35 ± 0.20	0.123
1.22 ± 0.18	0.246
1.59 ± 0.24	0.492
1.14 ± 0.17	no added phosphine [1]=0.0412 M
1.38 ± 0.21	no added phosphine, [1] = 0.0121 M

Table 2. Rate constants for the thermolysis of **5** in the presence of added phosphine.

$k_{obs} \times 10^{-5}$ (sec^{-1})	[L] (mM)
2.93 ± 0.44	4.10
2.26 ± 0.34	8.36
3.06 ± 0.46	13.1
2.73 ± 0.41	27.9
2.87 ± 0.43	86.8

A quantitative study of the rate of reductive elimination of benzene from phenyl hydride **5** at 135 °C demonstrated that the rate was independent of phosphine concentration, as was the case for the reductive elimination of toluene from **1** at 80 °C. The thermolysis of **5** was conducted in cyclohexane-d_{12}, a solvent which does not react with **5**. The rate of the reaction was measuredat 135° C by removing the samples and monitoring the disappearance of a phosphine resonance of starting material **5** by ambient temperature ^{1}H NMR spectroscopy. The samples contained 0.00820 M **5** and between 0.00410 M and 0.0869 M added phosphine. All reactions were monitored for at least three half-lives and provided first order plots with correlation coefficients greater than 0.988. The rate constants were identical within experimental error at all phosphine concentrations, as shown in Table 2.

Obtaining quantitative rate data in benzene solvent was complicated by the two competing processes, ring exchange forming **5**-d_6 and reductive elimination forming **6**. We did, however, obtain the following qualitative information which is consistent with a phosphine independent rate for the reductive elimination process to form **6**, and a phosphine dependent rate for the ring exchange process to form **5**-d_6.

Thermolysis of the phenyl hydride complex **5** in benzene-d_6 was conducted at 135 °C for 12 h in two NMR tubes, side by side, one containing no additional phosphine and one containing 2 equivalents of PMe_3 (0.234 M solution). The amount of conversion of **5** to **6** after 12 h of thermolysis at 135 °C was nearly identical for the two samples: the one containing no added phosphine showed 55 % conversion, while the one containing 0.234 M PMe_3 showed 56 % conversion by $^{31}P\{^1H\}$ NMR spectroscopy. In contrast to the formation of **6** in either cyclohexane or benzene, the rate of ring exchange was strongly dependent on phosphine concentration. No signal in the hydride or phenyl region was observed in the ^{1}H NMR spectrum of the sample containing no added phosphine, indicating that complete exchange had occurred with solvent benzene. However, resonances in both regions were observed for the sample containing 0.234 M phosphine.

In an attempt to assure ourselves that phosphine inhibition was due to shifting the preequilibrium involving phosphine dissociation, rather than scavenging of some unknown trace catalyst by the added ligand, we attempted to run the thermolysis of phenyl hydride **5** in benzene-d_6 in the presence of a phosphine which would could trap such a species, but which would not be incorporated into **5**. Unfortunately, even addition of the larger tri-*n*-butylphosphine (4 equiv) led to substantial substitution for trimethylphosphine. Similarly, addition of the poorer electron donor triphenylphosphine led to free trimethylphosphine and a different (as yet unidentified) material, perhaps formed by orthometallation of the ligand aryl substituents. These results clearly confirm that PMe_3 dissociation occurs rapidly, and though we have not demonstrated absolutely that this step is required for the ring exchange process, our results remain strongly suggestive.

Like the rate of H/D exchange of phenyl hydride complex **5** with benzene, the rate of H/D exchange of the dihydride complex with benzene-d_6 appeared to depend of the concentration of phosphine. The exchange with benzene-d_6 was run at 135 °C for 9.5 h in two NMR tubes, side by side, one with no added phosphine and one with 10 equivalents PMe_3 (0.386 M). (As noted above, the dihydride is stable at these temperatures.) Again, a marked decrease in the rate of exchange was observed for the tube containing added phosphine. The ^1H NMR spectrum of the sample with no added phosphine contained no hydride resonances, while the sample with added phosphine did contain a hydride resonance.

Discussion

Mechanism of $(PMe_3)_4Ru(CH_2Ph)(H)$ thermolysis. *Three possible* mechanisms for reactions induced by thermolysis of the benzyl hydride complex (illustrated for the corresponding deuteride **1-d_1**) are shown in Scheme I. Pathway a involves reductive elimination directly from the coordinatively saturated 18-electron starting material. Both pathway b and pathway c are initiated by a rapid phosphine-dissociation preequilibrium. In the pathway b branch, oxidative addition of a ligand C-H bond to the ruthenium metal center is followed by reductive elimination to form toluene. Pathway c involves the same 5-coordinate ruthenium(II)

Scheme 1

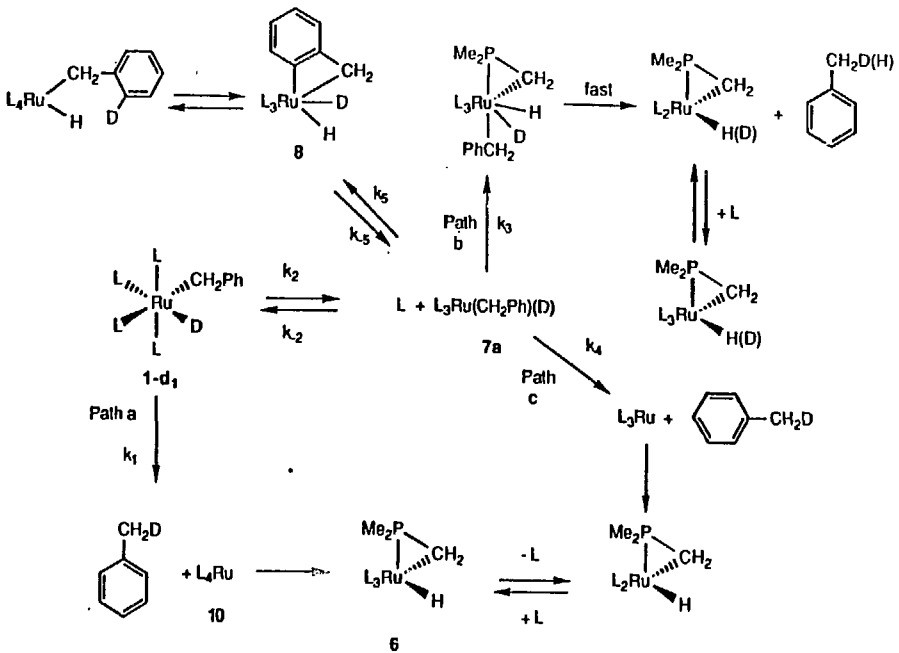
L4Ru
CH2
H
D
L3Ru
D
H
8
Me2P
CH2
L3Ru
H
D
PhCH2
fast
Me2P
CH2
L2Ru
H(D)
+
CH2D(H)
k5
k-5
Path b
k3
+ L
Me2P
CH2
L3Ru
H(D)
L
L
CH2Ph
Ru
L
D
L
1-d1
k2
k-2
L + L3Ru(CH2Ph)(D)
7a
k4
Path c
L3Ru +
CH2D
Path a
k1
CH2D
+ L4Ru
10
Me2P
CH2
L3Ru
H
6
- L
+ L
Me2P
CH2
L2Ru
H

unsaturated intermediate, but reductive elimination to form toluene precedes oxidative addition of the ligand C-H bond.

The distribution of deuterium observed during the thermolysis of **1**-d_1 provides information that supports pathway a as the dominant route to **6**. As shown in Scheme 1, pathway a would yield deuterium only in the methyl group of the toluene product with none in the final ruthenium complex. If reversible *ortho*-metallation were occurring competitively (for example, by competitive loss of L, generating **7a** and then **8**) it would scramble deuterium into the phenyl ring of the benzyl group. Even if this *ortho*-metallation occurs, elimination by pathway a would yield exclusively toluene-d_1. In pathway c, reductive elimination occurs from the unsaturated species **7a** before any ligand oxidative addition occurs, and so this mechanism also predicts that deuterium would be observed only in the toluene. Pathway b gives rise to intermediate **9** which contains a hydride and a deuteride on the same 7- coordinate metal center as the benzyl group. From this intermediate, reductive elimination of either toluene-d_1 or toluene-d_0 can occur, yielding products which contain deuterium both in the hydride position on the ruthenium and in the methyl group of the toluene. The formation of only toluene-d_1 and **6**-d_0 in the thermolysis of **1**-d_0 eliminates pathway b.

Our kinetic studies proved a means of distinguishing the two remaining mechanisms a and b, and are consistent only with pathway a. Pathway a predicts a simple first-order rate expression, assuming that the ratio of k_2/k_{-2} is small. Consistent with this assumption, no free phosphine was observed when monitoring this reaction by either ^1H or $^{31}P\{^1H\}$ NMR spectrometry. Reaction by either pathway b or pathway c would be inhibited by added phosphine if k_{-2} is fast compared to k_3 or k_4, and would show a linear inverse dependence on phosphine concentration (Equation 7). At 60° C free labeled phosphine exchanges with coordinated

$$\frac{d[6]}{dt} = \frac{k_2k_3[1]}{k_3 + k_{-2}[L]} \qquad k_{obs} = \frac{k_2k_3}{k_3 + k_{-2}[L]} \qquad (7)$$

phosphine at a much faster rate than reductive elimination occurs, demonstrating that k_{-2} is indeed larger than k_3 or k_4. Consequently, the identical rates at all concentrations of phosphine

rules out both pathways b and c. Thus, rapid dissociation of phosphine does not occur on the pathway to formation of **6**. We conclude that reductive elimination occurs directly from the coordinatively saturated complex **1** to form the 16-electron intermediate $(PMe_3)_4Ru$ (**10**), which oxidatively adds the ligand C-H bond.

Mechanism of $(PMe_3)_4Ru(Ph)(H)$ thermolysis. Mechanisms analogous to those shown in Scheme I for the benzyl deuteride complex are shown for the phenyl deuteride complex **5** in Scheme 2. Again, the three pathways are distinguishable using kinetic and labelling studies. In contrast to the behavior of **1**, the thermolysis of **5** follows two of the three pathways: reductive elimination of benzene proceeds *via* pathway a, and leads to intramolecular oxidative addition of the ligand C-H bond. In contrast, H/D exchange with aromatic solvent proceeds by pathway b as shown in Scheme 3.

The mechanisms of the intramolecular C-H activation processes are shown in Scheme 2. Formation of **6** from **5** in cyclohexane occurred without any intermolecular ring exchange with solvent. In all solvents, exchange of phosphine occurred at temperatures much lower than either ring exchange or formation of **6**. Quantitative rate data in cyclohexane demonstrated that the rate of formation of **6** was independent of phosphine concentration, consistent with pathway a.

The intermolecular C-H activation processes are shown in Scheme 3. In contrast to the behavior observed for the reductive elimination reactions, the rate of H/D exchange of **5** with aromatic solvents *was* inhibited by added phosphine. Thus, this reaction most likely involves rapid initial dissociation of PMe_3, leading to **7b**. In fact, the intermolecular C-H activation of solvent benzene *must* occur by way of a different intermediate from the $(PMe_3)Ru$ intermediate **10** because our results with benzyl hydride complex **1** demonstrated that intermediate **10** reacts exclusively intramolecularly in arene solvents.

Although pathways b and c are kinetically indistinguishable by our results, they do predict different results for the labelling experiments. If pathway b operates, the thermolysis of **5**-d_1 in toluene would result in the formation of both benzene-d_0 and benzene-d_1, whereas pathway c would lead to formation of only benzene-d_1. The observation of both benzene-d_1 and benzene-

Scheme 2

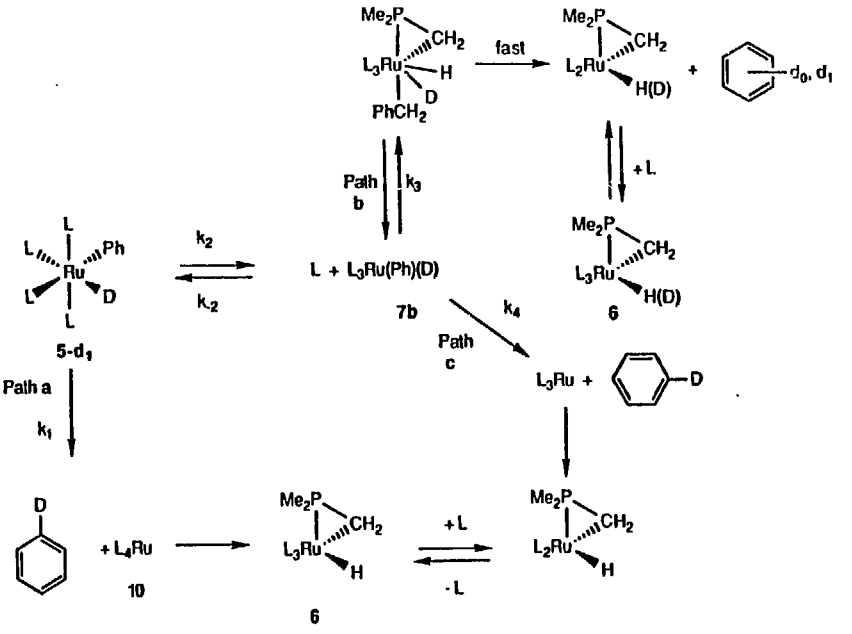
Me2P
CH2
L3Ru
H
D
PhCH2
fast
L2Ru
H(D)
d0, d1
+L
Path b
k3
k2
k-2
L
Ph
Ru
D
5-d1
L + L3Ru(Ph)(D)
7b
6
k4
Path c
L3Ru +
Path a
k1
+ L4Ru
10
+L
-L

Scheme 3

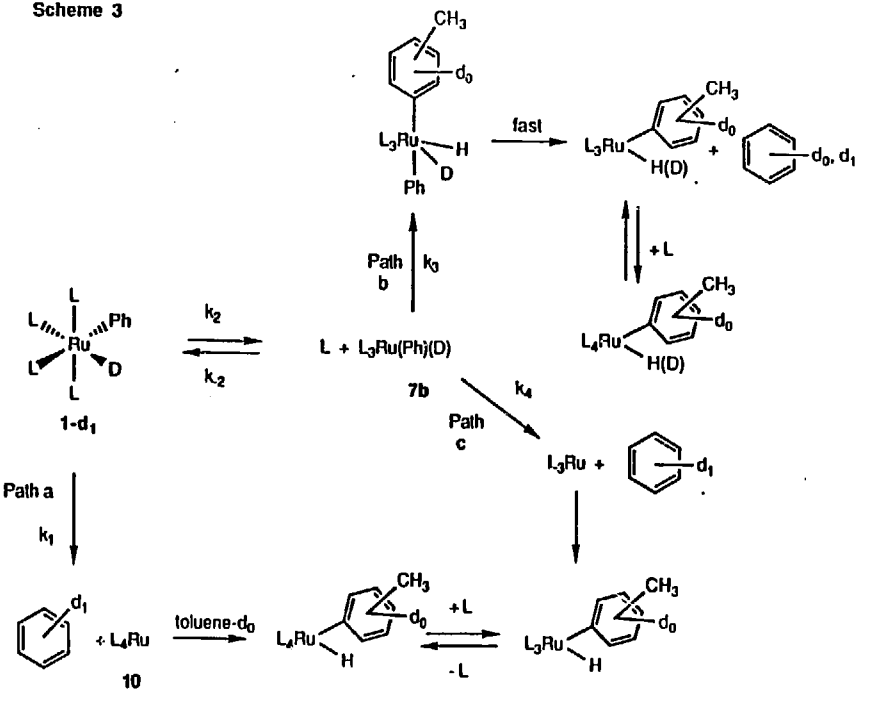
CH3
d0
L3Ru
H
D
Ph
fast
L3Ru
H(D)
+
d0, d1
+L
Path
b
k3
L4Ru
H(D)
L
Ph
Ru
D
k2
k2
L + L3Ru(Ph)(D)
7b
k4
Path
c
L3Ru +
d1
1-d1
Path a
k1
d1
+ L4Ru
10
toluene-d0
L4Ru
H
+L
-L
L3Ru
H

Scheme 4

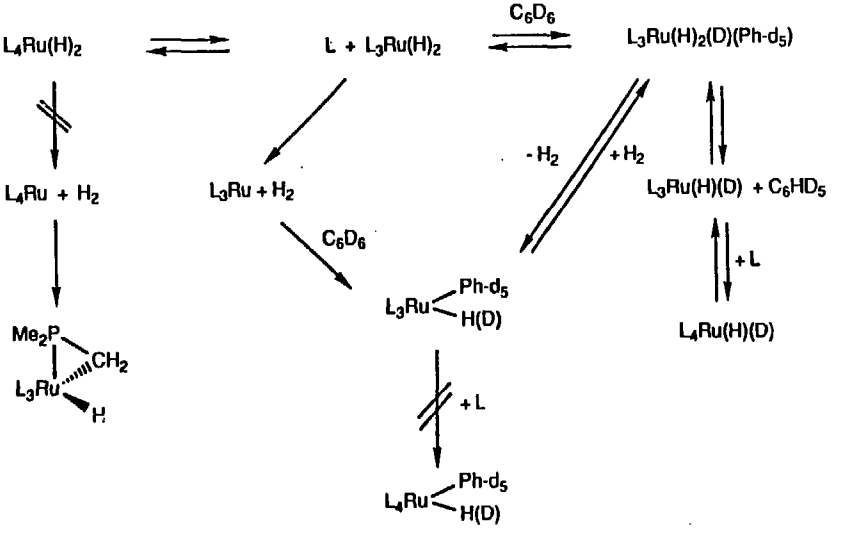
L4Ru(H)2
L + L3Ru(H)2
C6D6
L3Ru(H)2(D)(Ph-d5)
L4Ru + H2
L3Ru + H2
- H2
+ H2
L3Ru(H)(D) + C6HD5
C6D6
+ L
L3Ru
Ph-d5
H(D)
Me2P
CH2
L3Ru
H
+ L
L4Ru(H)(D)
L4Ru
Ph-d5
H(D)

d_0 in roughly equal amounts after 67-74% conversion to tolyl hydride complexes in the exchange of **5**-d_1 with toluene rules out c as the exclusive pathway.

Finally, the phosphine inhibition of H/D exchange of the dihydride complex $(PMe_3)Ru(H)_2$ with benzene solvent indicates that this process occurs by pathway b or c. As pictured in Scheme 4, pathway a would yield H_2 and cyclometallated product **6**. Pathway c involves reductive elimination of dihydrogen from the five-coordinate intermediate followed by successive oxidative addition of benzene and dihydrogen. Although our results do not rule out pathway c, a simpler mechanism is pathway b, and it is analogous to the mechanism of H/D exchange with phenyl hydride **5**. This mechanism involves reversible oxidative addition of benzene to the five coordinate dihydride intermediate to form a trihydride intermediate which allows for exchange, and this seems to be the most likely mechanism.

Selectivities. The propensity of the benzyl hydride, phenyl hydride, and dihydride complexes to undergo intramolecular or intermolecular oxidative addition can be traced to their abilities to undergo reductive elimination. The activation energy required to eliminate toluene from the saturated complex **1** is lower than the total activation energy required to dissociate PMe_3 and then add solvent or ligand to the resulting 5-coordinate intermediate **7a**, so C-H oxidative addition in **1** occurs *via* L_4Ru intermediate **10**. In contrast, the barrier to reductive elimination from the phenyl hydride complex is higher than it is from the benzyl hydride complex. As a result, phosphine dissociation followed by oxidative addition to the corresponding 5-coordinate species **7b** is competitive with direct reductive elimination. Because the barrier to reductive elimination of dihydrogen is too high to observe, even up to 180 °C, only the 5-coordinate intermediate $L_3Ru(H)_2$ is accessible in this case.

The inter- vs. intramolecular selectivity in benzene solvent is markedly different for the 5-coordinate Ru^{II} and 4-coordinate Ru^0 species which are generated by the thermolyses of these three compounds: the 4-coordinate L_4Ru (**10**) chooses only intramolecular reactivity, whereas the 5-coordinate $L_3Ru(R)(H)$ selects only intermolecular reactivity. Typically, systems are thought to be driven toward intramolecular reactivity when the metal center is sterically encumbered. We

propose that the intermediates with the higher coordination numbers in this study actually possess metal centers which are sterically *less* encumbered because they contain three rather than four bulky trimethylphosphine ligands.

Comparison of Reductive Elimination Mechanism to Other Systems. The reductive elimination reactions of d^6 metal systems that possess labile ligands are often accelerated by ligand dissociation. For example, elimination of maleic anhydride from the Ir(III) complexes, Ir(H)[σ-$CHCH_2C(O)OC(O)$](σ-carborane)(CO)(PhCN)(PPh_3)[2k] and of carborane from Ir(H)(Cl)(σ-carborane)(CO)$(PPh_3)_2$[2i] has been shown to involve predissociation of ligand. Reductive elimination of ketone from a rhodium enolate hydride complex involves predissociation of phosphine ligand,[2n] and photolytic elimination of dihydrogen from a series of Ir(III) and Rh(III) complexes involves initial photodissociation of ligand, followed by thermal elimination of H_2.[2g] In addition, some C-C reductive elimination reactions are accelerated by ligand dissociation.[2a, 3] In contrast, the rates of several C-H reductive elimination reactions are independent of free ligand concentration, because dissociation occurs more slowly than reductive elimination.[2h, i] For the ruthenium system discussed here, dissociation of phosphine was shown to occur more rapidly than reductive elimination, but the elimination process occurred directly from the saturated $L_4Ru(CH_2Ph)(H)$ and $L_4Ru(Ph)(H)$ species. Thus, this study presents an unusual case of a transition metal complex which undergoes rapid ligand dissociation, but which displays a preference for reductive elimination from the saturated 18 e⁻ species over reductive elimination from unsaturated 16 e⁻ species.

Comparison to $(PMe_3)_4Os(CH_2CMe_3)(H)$. Our results indicate that differences in the mechanisms for the ruthenium and osmium systems stem from the greater bond strengths[13] and more accessible M^{IV} oxidation state[14] of the third row over the second row transition metals. The differences in bond strength are manifested in the faster rate of reductive elimination directly from the saturated alkyl hydride complex for the ruthenium system, and the different oxidation potentials result in a slower rate of oxidative addition by the ruthenium(II) intermediate $(PMe_3)_3Ru(R)(H)$ to form the ruthenium(IV) intermediate $(PMe_3)_3Ru(R)(R')(H)_2$. Thus, thermolysis

of the ruthenium alkyl hydride complex results exclusively in formation of $(PMe_3)_4Ru$ (**10** in Scheme 1), while the osmium system reacts predominantly by oxidative addition of benzene solvent to the $(PMe_3)_3Os^{II}(R)(H)$ intermediate, forming the $(PMe_3)_3Os^{IV}(R)(Ph)(H)_2$. Aryl ring exchange by the ruthenium(phenyl)hydride complex **7** and H/D exchange by dihydride **8** occurs at 135-140 °C by way of Ru^{IV} intermediates as compared to 80 °C for the osmium system.

The selectivities of the $(PMe_3)_4M$ and $(PMe_3)_3M(R)(H)$ intermediates are similar for the two systems. Although the reaction to form $(PMe_3)_4Os$ from thermolysis of alkyl hydride complexes is much slower than reaction by $(PMe_3)_3Os$ or $(PMe_3)_3Os(R)(H)$, the four coordinated osmium(0) intermediate has been generated by phosphine dissociation from $(PMe_3)_5Os$, and like the ruthenium intermediate, this complex reacts intramolecularly to form $(PMe_3)_3Os(CH_2PMe_2)(H)$. It has been difficult to obtain kinetic evidence that the osmium(II) intermediate $(PMe_3)_3Os(R)(H)$ undergoes only intermolecular oxidative additions, since reaction by this intermediate must be distinguished from reaction by $(PMe_3)_3Os$ which also results from phosphine dissociation. However, the evidence that the intermediate $(PMe_3)Ru(Ph)(H)$ provides products resulting from only *intermolecular* C-H activation is clearcut: the rate of formation of $(PMe_3)_3Ru(CH_2PMe_2)(H)$ is independent of phosphine concentration.

A final difference between these two group 16 metal systems is their propensity to react *via* the $(PMe_3)_3M$ intermediate. Our labelling studies with $(PMe_3)_4Ru(Ph)(D)$ indicate that the major intermolecular pathway involves $(PMe_3)_3Ru(D)(Ph)$ and not $(PMe_3)_3Ru$. Flood and his coworkers have concluded from kinetic isotope experiments that the osmium system undergoes activation of methane, mesitylene, and tetramethylsilane by way of the $(PMe_3)_3Os$ intermediate, although ring exchange with benzene occurs *via* the $(PMe_3)_3Os(CH_2CMe_3)(H)$ intermediate. Although it is possible that the 14 electron, three-coordinate intermediate is important in the osmium system, we believe our labelling results rule out this intermediate as part of any major reaction pathway for the ruthenium system.

Experimental

General. Unless otherwise noted, all manipulations were carried out under an inert atmosphere in a Vacuum Atmospheres 553-2 drybox with attached M6-40-1H Dritrain, or by using standard Schlenk or vacuum line techniques.

^{1}H NMR spectra were obtained on either the 300, 400 or 500 MHz Fourier Transform spectrometers at the University of California, Berkeley (UCB) NMR facility. The 300 MHz instrument was constructed by Mr. Rudi Nunlist and interfaced with a Nicolet 1280 computer. The 400 and 500 MHz instruments were commercial Bruker AM series spectrometers. ^{1}H NMR spectra were recorded relative to residual protiated solvent. ^{13}C{^{1}H} NMR spectra were obtained at either 75.4, 100.6 MHz or 125.7 MHz on the 300, 400 or 500 MHz instruments, respectively and chemical shifts were recorded relative to the solvent resonance. Chemical shifts are reported in units of parts per million downfield from tetramethylsilane. ^{31}P{^{1}H} NMR spectra were obtained at either 121.6 or 162.1 MHz on the 300 or 400 MHz instruments, respectively and chemical shifts were recorded in units of parts per million downfield from 85% H_3PO_4. ^{2}H NMR spectra were recorded at 153.4 MHz on the 500 MHz instrument and chemical shifts are reported in units of parts per million downfield from tetramethylsilane.

IR spectra were obtained on a Perkin-Elmer Model 283 infrared spectrometer or on a Perkin-Elmer Model 1550 or 1750 FT-IR spectrometer using potassium bromide solution cells (0.1 or 0.025 mm path length) or potassium bromide ground pellets. Mass spectroscopic (MS) analyses were obtained at the UCB mass spectrometry facility on AEI MS-12 and Kratos MS-50 spectrometers. GC/MS results were obtained with either with a gas chromatograph in series with the Kratos MS-50 or using a Hewlett-Packard 5890A gas chromatograph in series with a Hewlett-Packard 5970 Mass Selective Detector using a 30 m column (0.25 mm i.d., 0.25 m film thickness), DB1701 from J&W Scientific. Elemental analyses were obtained from the UCB Microanalytical Laboratory.

Sealed NMR tubes were prepared by fusing Wilmad 505-PP and 504-PP tubes to ground glass joints which were then attached to a vacuum line with Kontes stopcocks or alternatively, the

tubes were attached via Cajon adapters directly to Kontes vacuum stopcocks.[15] High pressure valve NMR tubes refer to Wilmad Cat. #522-PV. Known volume bulb vacuum transfers were accomplished with an MKS Baratron attached to a high vacuum line.

Unless otherwise specified, all reagents (including Grignard reagents) were purchased from commercial suppliers and used without further purification. PMe_3 (Strem) was dried over NaK or a Na mirror and vacuum transferred prior to use. Ferrocene (Aldrich) was sublimed prior to use. Methanesulfonic acid was dried by azeotroping with benzene using a Dean-Stark trap followed by vacuum distillation under argon. Pentane, hexane, and cyclohexane (UV grade, alkene free) were distilled from $LiAlH_4$ under nitrogen. Benzene, toluene, diethyl ether and tetrahydrofuran were distilled from sodium benzophenone ketyl under nitrogen. Isopropanol and methanol-d_3 were dried over sodium and vacuum distilled. Deuterated solvents for use in NMR experiments were dried as their protiated analogues but were vacuum transferred from the drying agent. $(PMe_3)_3Ru(\eta^2\text{-}CH_2PMe_2)(H)$ was prepared by the method of Werner, but was isolated by sublimation at 85° C, followed by crystallization from pentane at -40° C.

$(PMe_3)_4Ru(Me)(Cl)$. We found the procedure provided here to be more convenient than the published procedure.[16] In a 250 mL round bottom flask, 1.50g of $(PMe_3)_4Ru(OAc)(Cl)$[17] was dissolved in 100 mL of toluene. To this stirred solution was added, at room temperature over 3 min, 0.50 mL (0.33 equiv.) of $AlMe_3$ as a 2.0 M solution in toluene. The solution was stirred for 1 h at room temperature over which time a fine white powder formed. The volume of the solution was reduced to 5-10 mL under vacuum and filtered while still cold from solvent removal in order to remove all aluminum salts. The resulting yellow solution was then layered with pentane to yield 0.629 g (46% yield) of yellow blocks. The supernatant was then cooled to -40 °C to obtain an additional 0.246 g (18%) of product. ^1H NMR (C_6D_6) δ1.27 (t, 18H, N=5.8) 1.20 (d, 9H, N=5.4), 0.91 (d, 9H, N=7.6), 0.27 (m, 3H); $^{31}P\{^1H\}$ NMR A_2BC, δA=-5.65, δB=15.16, δC=-16.09, J_{AB}=34.5, J_{AC}=24.4, J_{BC}=18.3. Lit: ^1H NMR (C_6D_6) δ1.27 (t, 18H, N=6) 1.19 (d, 9H, N=5), 0.90 (d, 9H, N=8), 0.29 (m, 3H); $^{31}P\{^1H\}$ NMR A_2BC δA=-5.8, δB=14.9, δC=-16.3 J_{AB}=34, J_{AC}=24, J_{BC}=18.

$Ru(PMe_3)_4(H)_2$ (7). Into a 250 mL round bottom flask was weighed 1.00 g (2.00 mmol) of $(PMe_3)_4Ru(OAc)(Cl)$.[17] Ether (100 mL) was added. To the stirred solution was added 0.250 mL (1.00 mmol) of a 2.0 M solution of lithium aluminum hydride in ether. The initial yellow solution became clear and contained a white precipitate after 15 min. After allowing the reaction to stir for an additional 1 h, the solvent was removed under reduced pressure, and the residue extracted with pentane (3 x 50 mL). The pentane was removed to yield 0.540 mg (66 % yield) of a white powder which ^1H and $^{31}P\{^1H\}$ NMR spectroscopy showed to be pure 7, as determined by comparison to literature data.[16] ^1H NMR (C_6D_6) δ1.37 (t, 18H, N=5.2) 1.24 (d, 18H, N=5.0), -9.71 (m, 2H); $^{31}P\{^1H\}$ NMR A_2B_2 δA=0.12, δB=-7.41, J_{AB}=26.1. Lit: ^1H NMR (C_6D_6) δ1.37 (t, 18H, N=5) 1.27 (d, 18H, N=5), -10.1 (m, 2H); $^{31}P\{^1H\}$ NMR A_2B_2 δA=2.7, δB=-4.8, J_{AB}=26.4.

$Ru(PMe_3)_4(CH_2Ph)(H)$ (1). A Fisher-Porter bottle was charged with 1.11 g (2.44 mmol) of $Ru(PMe_3)_4(Me)(Cl)$[8] in 10 ml tetrahydrofuran in the drybox, and then was filled with 100 psi H_2. The solution was stirred for 12 h at room temperature. The vessel was brought into the drybox, and 1.24 mL of 2.0 M $PhCH_2MgBr$ in THF was added to the reaction solution. This mixture was stirred for 5 h, after which time the solution had turned clear and a white solid had precipitated. The solvent was removed under vacuum and the residue extracted with 50 mL, 25 mL, and 25 mL portions of pentane. The pentane extracts were combined and filtered, concentrated to ~7 mL under vacuum and cooled to -40 °C to yield 0.681 g (55.0 %) analytically pure, white crystals. A second crop, also pure by ^1H NMR spectroscopy yielded 0.152 mg white crystals (12.3 %). ^1H NMR (C_6D_6) δ 7.90 (d, 7.6, 2H), 7.29 (t, 7.4, 2H), 7.04 (t, 7.8, 1H), 2.25 (m, 2H), 1.21 (t, N=4.7, 18H), 1.15 (d, N=5.5, 9H), 1.05 (d, N=4.9, 9H), -9.49 (ddt, J=89.8, 29.7, 22.1, 1H); $^{31}P\{^1H\}$ A_2BC, δ_A= -1.40, δ_B= -7.56, δ_C= -13.11, J_{AB}= 26.4, J_{AC} = 26.4, J_{BC}= 19.9; $^{13}C\{^1H\}$ δ 158.45 (d, 6.7), 132.41 (s), 127.11 (s), 121.53 (s), 28.26 (d, 18.6), 24.74 (tt, 12.4, 3.3), 22.79 (dq, 14.6, 2.7), 15.99 (dtd, 46.9, 13.4, 6.4); IR: 1856 (M-H, s); MS (EI) m/e 406 (M-CH_2Ph); Anal. Calcd. for $C_{19}H_{44}P_4Ru$: C, 45.87; H, 8.91. Found: C, 45.70; H, 8.81.

$Ru(PMe_3)_4(CH_2Ph)(D)$ (1-d_1). A procedure identical to that for the preparation of $Ru(PMe_3)_4(CH_2Ph)(H)$ was followed except D_2 was substituted for H_2, and the reaction was run

with 255 mg $Ru(PMe_3)_4(Me)(Cl)$ to yield 116 mg (41.6 %) of product in one crop. ^{1}NMR (C_6D_6) δ 7.90 (d, 7.6, 2H), 7.29 (t, 7.4, 2H), 7.04 (t, 7.8, 1H), 2.25 (m, 2H), 1.21 (t, N=4.7, 18H), 1.15 (d, N=5.5, 9H), 1.05 (d, N=4.9, 9H); ^{2}H {^{1}H} NMR δ -9.49 (dq, J=15, 4); ^{31}P {^{1}H} NMR A_2BCX, δ_A= -1.40, δ_B= -7.56, δ_C= -13.11, J_{AB}= 26.4, J_{AC} = 26.4, J_{AX}= 3.9, J_{BC}= 19.9; J_{BX} =0, J_{CX}= 13.8. IR: 1333 (M-D, s).

$Ru(PMe_3)_4(Ph)(H)$ (5). To a solution of 300 mg (0.627 mmol) of $Ru(PMe_3)_4(\eta^2$-$C_6H_4)$ in 5 mL pentane was added 47.7 μL (0.627 mmol) isopropanol in 0.5 mL pentane at room temperature. After allowing the mixture to react for 1 h, the volume was reduced under vacuum to 1 mL and cooled to -40 °C to yield 145 mg (48.2 %) white crystals. ^{1}H NMR (THF-d_8, -55 °C) δ 7.75 (m, 1H), 7.45 (m, 1H), 6.60 (m, 3H), 1.38 (d, N=5.4, 9H), 1.35 (d, N=5.8, 9H), 1.10 (t, N=5.2, 18H), -9.50 (dtd, J=92.6, 18.3, 18.3); ^{31}P {^{1}H} NMR A_2BC δ_A= -1.356, δ_B= -10.59, δ_C= -17.18, J_{AB}= 24.5, J_{AC}= 26.7, J_{BC}= 18.9; ^{13}C {^{1}H} NMR (THF-d_8, -55 °C) 174.20 (m), 153.10 (s), 146.55 (d, 8.8), 125.32 (s), 124.84 (s), 119.69 (s), 27.96 (d, 18.0), 24.67 (m), 23.59 (t, 12.2); IR 3060 (m), 2981 (m), 2966 (m), 1859 (M-H, s), 1561 (m), 1424 (m), 1419 (m), 1295 (s), 1278 (m); 940 (s); MS (EI) m/e 406 (M-C_6H_6), 330 (M-C_6H_6-PMe_3): Anal. Calcd. for $C_{18}H_{42}P_4Ru$: C, 44.71; H, 8.62. Found: C, 44.82; H, 8.83.

$Ru(PMe_3)_4(Ph)(D)$ (5-d_1). To a solution of 100 mg (0.209 mmol) of $Ru(PMe_3)_4(\eta^2$-$C_6H_4)$ in 3 mL benzene was added 18 μL MeOH-d_3 in 0.5 mL pentane. After allowing the mixture to react for 1 h, the benzene was removed under vacuum, and the residue was crystallized from pentane at -40 °C to yield 43.6 mg (43.4 %) white crystals. ^{1}H NMR (THF-d_8, -55 °C) δ 7.75 (m, 1H), 7.45 (m, 1H), 6.60 (m, 3H), 1.38 (d, N=5.4, 9H), 1.35 (d, N=5.8, 9H), 1.10 (t, N=5.2, 18H); ^{2}H {^{1}H} NMR (THF, 20 °C) δ -9.58 (dq, J=14.3, 4.0); ^{31}P {^{1}H} NMR δ 0 -1.356 (br t, J=25, 2P), -10.59 (m), -17.18 (m); IR; 3036 (m), 2981 (m), 2966 (m), 1561 (s), 1424 (m), 1420 (m), 1337 (M-H, m), 1295 (s), 1279 (s) 939 (s).

Thermolysis of $Ru(PMe_3)_4(CH_2Ph)(D)$ in cyclohexane. The ruthenium complex (15.0 mg, 0.0302 mmol) was dissolved in cyclohexane (0.7 mL), and the solution was transferred to an NMR tube. The sample was degassed and sealed under vacuum. The NMR

tubes were heated by submerging them completely in an oil bath heated to 85° C. $^{31}P\{^1H\}$ NMR spectroscopy showed quantitative conversion to 6, determined by comparison with a sample of 6 independently prepared as described in the general section. ^2H NMR spectroscopy showed an 11:1 integrated ratio of the methyl peak to aryl peaks of the toluene product. The tube was then cracked open under vacuum and the volatile materials collected in a glass tube cooled in a liquid nitrogen bath. GC/MS analysis of the volatile materials showed the absence of toluene-d_0. Only toluene-d_1 was detected, as determined by comparison of the mass spectrum of the toluene peak to that obtained for a sample of toluene-d_1 obtained by treating benzyl magnesium chloride with D_2O (99.8% isotopic purity).

Kinetic evaluation of the thermolysis of $Ru(PMe_3)_4(CH_2Ph)(H)$ in C_6D_6. Into a 5.00 mL volumetric flask was weighed 102 mg (0.205 mmol) $Ru(PMe_3)_4(CH_2Ph)(H)$ and 28 mg of ferrocene as an internal standard. C_6D_6 was added to the flask, making a 0.0412 M solution. In a typical experiment, 0.700 mL of this solution was added by syringe to a thin walled, 9" NMR tube. In an experiment to confirm the first order nature of the reaction, 4.2 mg (0.0084 mmol) of ruthenium complex was weighed into an NMR tube. To this tube was added 0.7 mL of C_6D_6 by syringe. Each tube was degassed, the appropriate amount of PMe_3 was condensed into it, and the tube was flame sealed to give a length of 8.5". The tubes were heated at 80° C +/- 0.1° C in a factory-calibrated Neslab Exocal Model 251 constant temperature bath filled with Dow Corning 200 silicone Fluid, and frozen rapidly in ice water after removal from the bath. All reactions were monitored to greater than 3 half-lives by ambient-temperature ^1H NMR spectrometry by integrating the methylene protons of the benzyl group vs. the ferrocene internal standard. The spectra were taken with a single acquisition and double checked with a second acquisition after a delay of at least 10 T_1. Formation of 6 was confirmed by comparing the ^1H NMR spectrum with that of an independently prepared sample of 6 as described in the general section. Rate constants are given in Table 1; all kinetic plots displayed excellent linearity with correlation coefficients of 0.95 or better.

Exchange of PMe_3-d_9 with $Ru(PMe_3)_4(CH_2Ph)(H)$. A sample of 11.0 mg (0.0221 mmol) $Ru(PMe_3)_4(CH_2Ph)(H)$ was dissolved in C_6D_6 and transferred to an NMR tube. The tube was degassed and 0.0885 mmol PMe_3-d_9 was added by vacuum transfer. The tube was sealed under vacuum and heated to 60 °C for 12 h. $^{31}P\{^1H\}$ NMR spectrometry showed a ratio of 1:0.8 for the peak at 61.44 (PMe_3) and 64.05 (PMe_3-d_9).

Thermolysis of $Ru(PMe_3)_4(Ph)(H)$ in C_6D_6. The ruthenium complex (10.8, 0.0224 mmol) was dissolved in 0.7 mL C_6D_6 and 2 mg of ferrocene was added as an internal standard. The solution was transferred to an NMR tube which was degassed and sealed under vacuum. The tube was submerged completely in a 140° bath for 18 h, and ^1H NMR spectroscopic analysis of the resulting solution showed formation of 6 in 90% yield.

Thermolysis of $Ru(PMe_3)_4(Ph)(H)$ in C_6D_6 with and without added PMe_3. The ruthenium complex (22.6 mg, 0.0464 mmol) was dissolved in 1.5 mL C_6D_6 and the solution was divided into two NMR tubes. One tube was degassed and sealed under vacuum, and the other was degassed and sealed under vacuum after the addition of 2 equivalents (0.0464 mmol) of PMe_3. The tubes were heated at 135° C for 9.5 h. Conversions for the two samples were determined by $^{31}P\{^1H\}$ NMR spectroscopy since the resonances are well separated. Approximate conversions of 55% for the sample with no added phosphine and 56% for the sample with 2 equivalents of phosphine were determined by comparing the total of all integrals for the two compounds. ^1H NMR spectroscopy showed no hydride or aromatic resonances for the sample containing no additional PMe_3. Only the phosphine resonances corresponding to 5 and 6 were observed. A hydride resonance and aryl resonances were observed for the sample containing 2 equivalents of PMe_3.

Thermolysis of $Ru(PMe_3)_4(Ph)(H)$ in cyclohexane-d_{12}. The ruthenium complex (11.0 mg, 0.0228 mmol) was dissolved in 0.7 mL cyclohexane and 2 mg of ferrocene was added as an internal standard. The solution was transferred to an NMR tube which was degassed and sealed under vacuum. The tube was submerged completely in a 135° bath for 18 h, and ^1H

NMR spectroscopic analysis of the resulting solution showed formation of 4 in 94% yield and benzene in 97% yield.

Kinetic evaluation of the thermolysis of $Ru(PMe_3)_4(Ph)(H)$ in cyclohexane-d_{12}. Into a 5.00 mL volumetric flask was weighed 19.8 mg (0.0410 mmol) $Ru(PMe_3)_4(CH_2Ph)(H)$ and 20 mg of mesitylene as an internal standard. Cyclohexane-d_{12} was added to the flask, making a 8.20 mM solution. In a typical experiment, 0.700 mL of this solution was added by syringe to a thin walled, 9" NMR tube. The tube was degassed, the appropriate amount of PMe_3 was condensed and the tube was flame sealed to give a length of 8.5". The tubes were heated at 80° C +/- 0.1° C in a factory-calibrated Neslab Exocal Model 251 constant temperature bath filled with Dow Corning 200 silicone Fluid, and frozen rapidly in ice water after removal from the bath. All reactions were monitored to greater than 3 half-lives by ambient-temperature ^1H NMR spectrometry by integrating the resonance due to the mutually trans phosphines of 5 vs. the mesitylene internal standard. The spectra were taken with a single acquisition and double checked with a second acquisition after a delay of at least 10 T_1. Rate constants are given in Table 2; all kinetic plots displayed excellent linearity with correlation coefficients of 0.98 or better.

Thermolysis of $Ru(PMe_3)_4(Ph)(D)$ in cyclohexane. The ruthenium complex (25.2 mg, 0.0517 mmol) was dissolved in 0.7 mL cyclohexane. The solution was transferred to an NMR tube which was degassed and sealed under vacuum. The tube was submerged completely in a 140° bath for 8 h, and ^2H NMR spectroscopic analysis of the sample was conducted every 2h during the thermolysis. The spectra showed a decrease in the hydride resonance for 5 and an increase in the resonances for benzene at 7.11 ppm and for the PMe_3 groups of 5 between 1.1 and 1.4 ppm. The integrated ratio of the benzene and phosphine signals in the final reaction mixture was roughly 2:1; an accurate value for this ratio could not be obtained due to overlap of the PMe_3 resonances with the cyclohexane solvent resonance. No signals were observed in the hydride region.

Thermolysis of $Ru(PMe_3)_4(Ph)(D)$ in toluene. The ruthenium complex (14.2-15.6 mg, 0.0323 mmol) was dissolved in toluene (0.7 mL) and transferred to an NMR tube which was then freeze pump thawed through three cycles. The sample was heated for 4 h at 140° C, after which time the NMR tube was cracked open under vacuum. The volatile materials were collected in a glass tube cooled with liquid nitrogen and analyzed by GC/MS at 90 ev. Two spectra were taken for each experiment, and the ratios agreed within 1-2 %. Using the m/e=78 and 79 peaks the ratio of benzene-d_1 to benzene-d_0 was calculated to be 0.86:1 for one experiment and 0.67:1 for the other. The remaining material was exposed to high vacuum for 4 h, dissolved in 1 mL of hexamethyldisiloxane and exposed to high vacuum for 8 h to remove any residual solvent. The solid was dissolved in ether and >3 equivalents of methanesulfonic acid in ether was added. A white solid rapidly formed, and the resulting solution was filtered through a plug of celite and analyzed by gas chromatography to determine the ratio of toluene to benzene as 2.85:1 in one experiment and 2.05:1 in the other.

Thermolysis of $Ru(PMe_3)_4(H)_2$ in C_6D_6 with and without added phosphine. The ruthenium complex (22.0 mg, 0.0543 mmol) was dissolved in 1.5 mL C_6D_6, 2 mg of ferrocene was added, and the solution was divided into two NMR tubes. One tube was degassed and sealed under vacuum, and the other tube was degassed and sealed under vacuum after the addition of 10 equivalents (0.272 mmol) of PMe_3 to give a PMe_3 concentration of 0.36 M. The tubes were heated at 135° for 9.5 h. ^1H NMR spectroscopy showed a hydride signal for the sample containing 10 equivalents of PMe_3, but no hydride signal for the sample containing no additional PMe_3.

Notes and References

1. Masters, C. *Homogeneous Transition-Metal Catalysis*, Chapman and Hall, New York, 1981. Yamamoto, A . *Organotransition Metal Chemistry*, John Wiley and Sons, Inc., New York, 1986.
2. a) Stille, J.K.; Lau, K.S.Y.; *Acc. Chem. Res.*, 1978, *10*, 343, and references therein. b) Desrosiers, P.J.; Shinomoto, R.S.; Flood, T.C. *J. Am. Chem. Soc.* 1986, *108*, 1346. c) Desrosiers, P.J.; Shinomoto, R.S.; Flood, T.C. *J. Am. Chem. Soc.* 1986, *108*, 7964. d) Harper, T.G.P.; Shinomoto, R.S.; Deming, M.A.; Flood, T.C. *J. Am. Chem. Soc.* 1988, *110*, 7915. e) Ermer, S.P.; Shinomoto, R.S.; Deming, M.A.; Flood, T.C. *Organometallics* 1989, *8*, 1377. f) Shinomoto, R.S.; Desrosiers, P.J.; Harper, G.P.; Flood, T.C. *J. Am. Chem. Soc.* 1990, *112*, 704. g) Wink, D.A.; Ford, P.C. *J. Am. Chem. Soc.* 1986, *108*, 4838. h) Periana, R.A.; Bergman, R.G.; *J. Am. Chem. Soc. 1986, 108*, 7332. i) Buchanan, J.M.; Stryker, J.M.; Bergman, R.G. *J. Am. Chem. Soc.*, 1986, *108*, 1537. j) Basato, M.; Morandini, F.; Longato, B.; Bresadola, S. *Inorg. Chem* 1984, *23*, 649. k) Basato, M.; Longato, B.; Morandini, F.; Bresadola, S. *Inorg. Chem* 1984, *23*, 3972. l) Michelin, R.A.; Faglia, S.; Uguagliati, P. *Inorg. Chem.* 1983, *22*, 1831. m) Abis, L.; San, A.; Halpern, J. *J. Am. Chem. Soc.* 1978, *100*, 2915. n) Milstein, D. *Acc. Chem. Res.* 1984, *17*, 221.
3. a) Tatsumi, K.; Nakamura, A.; Komiya, S.; Yamamoto, A.; Yamamoto, T. *J. Am. Chem. Soc.* 1984, *106*, 8181. b) Komiya, S.; Abe, Y.; Yamamoto, A.; Yamamoto, T. *Organometallics* 1983, *2*, 1466. C) DiCosimo, R.; Whitesides, G.M. *J. Am. Chem. Soc.* 1982, *104*, 3601. d) Tatsumi, K.; Hoffmann, R.; Yamamoto, A.; Stille, J.K. *Bull. Chem. Soc. Jpn.* 1981, *54*, 1857. e) Stille, J.K.; Gillie. A. *J. Am. Chem. Soc.* 1980, *102*, 4933. f) Akermark, B.; Johansen, H.; Roos, B.; Wahlgren, U. *J. Am. Chem. Soc.* 1979, *101*, 5876. g) Akermark, B.; Ljungqvist, A. *J. Organomet. Chem.* 1979, 182, 59. h) Akermark, B.; Ljungqvist, A. *J. Organomet. Chem.*, 1978, *149*, 97. i) Braterman, P.S.; Cross, R.J.; Young, G.B. *J. Chem. Soc. Dalton Trans.* 1977, 1892. j) Komiya, S.; Albright, T.A.; Hoffmann, R.; Kochi, J.K. *J. Am. Chem. Soc.* 1976, *98*, 7255. k) Kuch, P.L.; Tobias, R.S. *J. Organomet. Chem.* 1976, *122*, 429.

4. For recent reviews on C-H oxidative additions see: a) Crabtree, R.H. *Chem. Rev. 1985, 85*, 245. b) Green, M.L.H.; O'Hare, D. *Pure. Appl. Chem.* 1985, *57*, 1897. c) Halpern, J. *Inorg. Chem. Acta* 1985, *100*, 41. d) Bergman, R.G. *Science*, 1984, *223*, 902.

5. a) Jones, W.D.; Foster, G.P.; Putinas, J.M. *J. Am. Chem. Soc.*1987, *109*, 5047. b) Fisher, B.J.; Eisenberg, R. *Organometallics*, 1983, *2*, 764. c) Kunin, A.J.; Eisenberg, R. *Organometallics, 1986, 7*, 2124. d) Kunin, A.J.; Eisenberg, R. *J. Am. Chem. Soc.* 1986, *108*, 535. e) Gordon, E.M.; Eisenberg, R. *J. Mol. Cat.* 1988, *45*, 57.

6. a) Hoyano, J.K.; McMaster, A.D.; Graham. W.A.G.; *J. Am. Chem. Soc.* 1983, *105*, 7190. b) Hackett, M.; Ibers, J.A.; Whitesides, G. *J. Am. Chem. Soc.*, 1988, *110*, 1436. c) Hackett, M.; Whitesides, G. *J. Am. Chem. Soc.*, 1988, *110*, 1449.d) Baker, M.V.; Field, L.D. *J. Am. Chem. Soc. 1986, 108*, 7433; 7436. e) Antberg, M.; Dahlenberg, L. *Angew. Chem. Int. Ed. Engl.* 1986, *25*, 260. f) Jones, W.D.; Feher, F.J. *J. Am. Chem. Soc.* 1985, *107*, 620. g) Periana, R.A.; Bergman, R.G. *Organometallics* 1984, *3*, 508. h) Ghosh, C.K.; Graham, W.A.G. *J. Am.Chem. Soc.* 1987, *109*, 4726. i) Ghosh, C.K.; Rodgers, D.P.S. Graham, W.A.G. *J. Chem. Soc., Chem. Commun.* 1988, 1511. j) Janowicz, A.H.; Bergman, R.G. *J. Am. Chem. Soc.* 1982, *104*, 352; 1983, *105*, 3929. k) Ittel, S.D.; Tolman, C.A.; English,A.D.; Jesson, J.P. *J. Am. Chem. Soc. 1976, 98*, 6073.

7. a) Werner, H. Gotzig, J. *Organometallics* 1983, *2*, 547. b) Werner, H.; Werner, R. *J. Organomet. Chem.* 1981, *209*, C60. c) Rathke, J.W.; Muetterties, E.L. *J. Am. Chem. Soc. 1975, 97*, 3272. d) Karsch, H.H.; Klein, H.-F.; Schmidbaur, H. *Angew. Chem. Int. Ed. Engl.* 1975, *14*, 637.

8. Slatter, J.A.; Wilkinson, G.; Thornton-Pett, M.; Hursthouse, M.B. *J. Chem. Soc. Dalton Trans.* 1984, 1731.

9. Jones, R.A.; Mayor Real, F.; Wilkinson, G.; Galas, A.M.R.; Hursthouse, M.B.; Malik K.M.A. *J. Chem. Soc. Dalton Trans.* 1980, 551.

10. Hartwig, J.F.; Andersen, R.A.; Bergman, R.G. *J. Am. Chem. Soc.* 1989, *111*, 2717

11. Chapter 4.

12. (a) Bennett, M.A.; Milner, D.L. *J. Am. Chem. Soc.* 1969, *91*, 6983. (b) Tulip, T.H.; Thorn, D.L. *J. Am. Chem. Soc.* 1980, *102*, 6713. (c) Foley, P.; DiCosimo, R.; Whitesides, G.M. *J. Am. Chem. Soc.* 1980, *102*, 6713. For reviews of cyclometallation reactions see: (d) Constable, E.C. *Polyhedron* 1984, *3*, 1037. (e) Webster, D.E. *Adv. Organomet. Chem.* 1977, *15*, 147. (f) Shilov, A.E.; Steinman, A.A. *Coord. Chem. Rev.* 1977, *24*, 97.

13. (a) Pearson, R.G. *Chem. Rev.* 1986, *85*, 41. (b) Crabtree, R.H. *Chem. Rev.* 1985, *84*, 245.

14. Cotton, F.A.; Wilkinson, G. *Advanced Organometallic Chemistry*, John Wiley and Sons, New York, 1980, p. 912.

15. Bergman, R.G.; Buchanan, J.M.; McGhee, W.D.; Periana, R.A.; Seidler, P.F.; Trost, M.K.; Wenzel, T.T. In *Experimental Organometallic Chemistry: A Practicum in Synthesis and Characterization*; Wayda, A.L.; Darensbourg, M.Y., Eds.; ACS Symposium Series 357; American Chemical Society: Washington, DC, 1987, p 227.

16. Statler, J.A.; Wilkinson, G.; Thornton-Pett, M.; Hursthouse, M.B. *J. Chem. Soc., Dalton Trans.* 1984, 1731.

17. Mainz, V.V.; Andersen, R.A. *Organometallics*, 1984, *3*, 675.

Chapter 2

Alkyl, Aryl, Hydrido, and Acetate Complexes of $(DMPM)_2Ru$ [DMPM=*bis*-(dimethylphosphino)methane]: Reductive Elimination and Oxidative Addition of C-H bonds.

Introduction

Transition metal systems that undergo oxidative addition of alkane C-H bonds are typically electron rich, and often have a d^6 or d^8 electron count.[1,2] Although most of these complexes also contain cyclopentadienyl or cyclopentadienyl analogues as ligands,[1d-k] systems which catalytically functionalize hydrocarbons by oxidative addition reactions have possessed labile non-Cp ligands.[3]

Phosphine ligands are strong electron donors, and therefore metal-phosphine systems often undergo oxidative addition reactions.[4] For this reason, transition metal complexes containing phosphines as the only dative ligands have been investigated for their activity in the oxidative addition of C-H bonds.[2a-c,5] Indeed, this type of compound readily adds sp^3 C-H bonds. Often this C-H bonds is from a phosphine ligand, giving rise to products resulting from intra-rather than intermolecular C-H oxidative addition,[5b-i] and in other cases, the C-H bond is from an alkyl or aryl group.[5g-i,6]

It has been known for over 25 years that $(DMPE)_2Ru(H)(naphthyl)$ (DMPE=*bis*-dimethylphosphinoethane) thermally eliminates naphthalene and the resulting intermediate (presumably $(DMPE)_2Ru$ or a solvate of this species) is capable of undergoing C-H oxidative addition processes.[5a, 7] Although this ruthenium system forms a dinuclear species upon prolonged thermolysis or photolysis[7b,8] the analogous iron system has been shown to add the C-H bonds of alkane solvent at low temperatures.[2a] The osmium complex $Os(PMe_3)_4(H)(CH_2CMe_3)$ leads to intermediates capable of reacting with methane, but intramolecular reaction with ligand C-H bonds is competitive with the intermolecular reaction pathway.[5f-j]

We have investigated routes to the intermediate (DMPM)Ru (DMPM=*bis*-dimethylphosphinomethane) in the hope that the metal center would be electron rich enough to undergo oxidative addition of C-H bonds, and that the four membered ring of the metal-ligand system would prevent intramolecular C-H additions. During the course of this work, Cole-Hamilton *et al.* reported the reduction of $(DMPM)_2Ru(Cl)_2$ with Na/Hg in benzene to form the product of

solvent C-H bond addition, (DMPM)Ru(H)(Ph), which undergoes exchange with C_6D_6 and toluene solvent.[9] We present here the synthesis of a variety of $(DMPM)_nRu(X)(Y)$ complexes, including the synthesis of dialkyl, dihydride, and alkyl hydride complexes, as well as two routes to generate the intermediate $(DMPM)_2Ru$. The dialkyl complexes are markedly more stable than the analogous $(PMe_3)_4Ru(R)(R')$ complexes with monodentate phosphine ligands, but the alkyl and aryl hydride products are much less stable than those of the L_4Ru, $L_4=(PMe_3)_4$ system.[10]

Results and Discussion

Acetate complexes. The synthesis of DMPM substituted ruthenium acetate complexes is shown in Scheme 1. Exchange of a trialkylphosphine for coordinated triarylphosphines has been used as a route to trialkyl phosphine metal complexes;[11] synthesis of trimethylphosphine ruthenium acetate compounds by the addition of excess PMe_3 to $(PPh_3)_2Ru(OAc)_2$ (**1**) has been described.[12] We found the synthesis of $(DMPM)_2Ru(OAc)_2$ to be less straightforward than that of the PMe_3-substituted compound. Addition of excess DMPM to **1** in benzene solvent led to formation of the *tris*-substituted product $(\eta^1\text{-DMPM})_2(\eta^2\text{-DMPM})Ru(OAc)_2$ (**2**). This complex was characterized by conventional spectroscopic techniques and microanalysis, and is analogous to the $Ru(DMPM)_3(Cl)_2$ complex believed to be formed by the addition of excess DMPM to $(PPh_3)_3Ru(Cl)_2$, but not isolated in pure form or fully characterized.[9] The $^{31}P\{^1H\}$ NMR spectrum of **2** is shown in Figure 1, and indicates both η^1- and η^2-coordination modes for the DMPM ligands. Although the spectrum is second order, there are clearly three resonances of equal intensity. Two are characteristic of DMPM coordinated to ruthenium. However, the resonance at δ -60 is close to the δ -55 chemical shift of free DMPM; therefore one end of a DMPM ligand is not coordinated to the metal center. Moreover, the large coupling between two of the bound phosphorus atoms indicates a trans orientation between them. The ^1H NMR spectrum displays one resonance for two equivalent acetate groups in addition to the DMPM resonances. Mass spectrometry showed a parent ion at *m/e*=569, consistent with loss of

Scheme 1

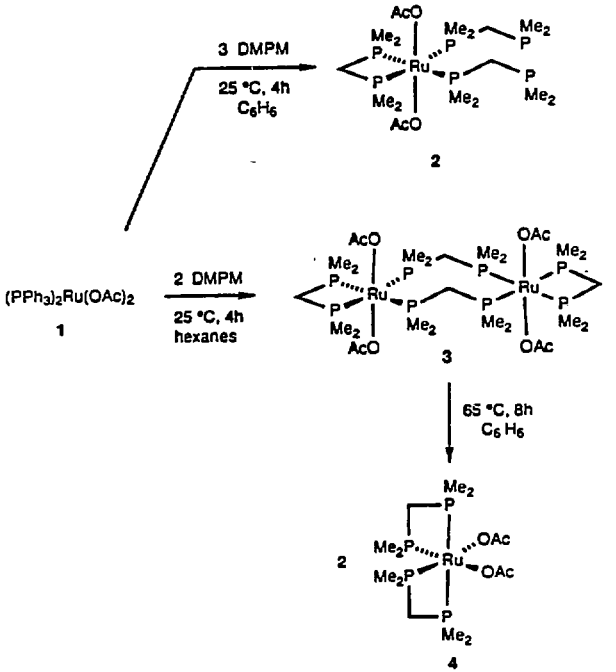
3 DMPM
25 °C, 4h
C6H6
2
(PPh3)2Ru(OAc)2
1
2 DMPM
25 °C, 4h
hexanes
3
65 °C, 8h
C6H6
2
4

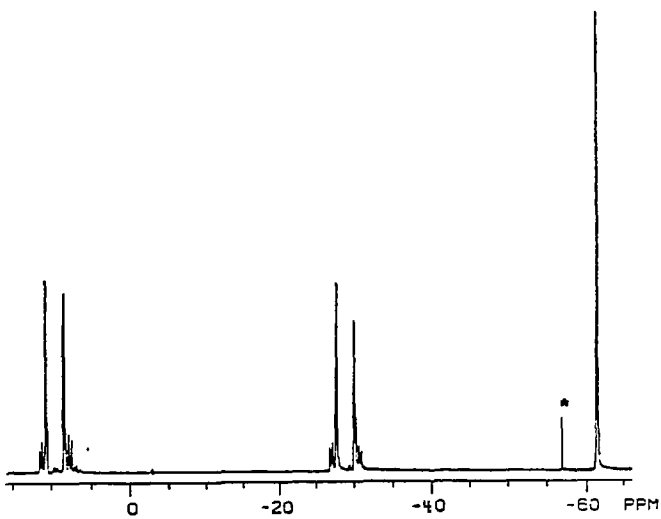

Figure 1. $^{31}P\{^{1}H\}$ NMR spectrum of $(\eta^{1}\text{-DMPM})_2(\eta^{2}\text{-DMPM})Ru(OAc)_2$ (2). The asterisk corresponds to free DMPM.

acetate from the monomer. The stereochemistry shown in Scheme 1 is consistent with all these data.

Addition of two equivalents of DMPM to a suspension of the triphenylphosphine complex **1** in hexane, followed by heating for 4 h at 65 °C, formed the dimeric species $(\eta^2, \mu^2\text{-DMPM})_2(\eta^2, \mu^1\text{-DMPM})_2Ru(\eta^1\text{-OAc})_4$ (**3**) shown in Scheme 1. Compound **3** was also fully characterized by conventional spectroscopic techniques and microanalysis. Again, the $^{31}P\{^1H\}$ NMR spectrum was second order (Figure 2). It displayed two resonances of equal intensity with large trans coupling, and chemical shifts similar to those of coordinated DMPM in **2**. Two types of ligand methyl groups and one type of acetate resonance were observed in the ^1H NMR spectrum. Mass spectrometry showed a parent ion at 984, corresponding to the dimeric structure.

Heating compound **3** in benzene solvent at 110 °C for 8 h led to cleavage of the dimer and formed the monomeric *bis*-DMPM, *bis*-acetate complex $(\eta^2\text{-DMPM})_2Ru(OAc)_2$ (**4**). Compound **4** was characterized by conventional spectroscopic techniques and microanalysis. Four phosphine methyl groups were observed in the ^1H and $^{13}C\{^1H\}$ NMR spectrum of **4**, and two triplets were observed in the $^{31}P\{^1H\}$ NMR spectrum; the phosphorus atoms located trans to the acetate substituents resonated downfield from the mutually trans phosphorus atoms. A monomer parent ion at m/e=492 was observed in the mass spectrum.

Dialkyl and Dihydride complexes. The substitution reactions with **4** to form alkyl and hydride compounds are shown in Scheme 2. Addition of 1/2 equivalent of $LiAlH_4$ at room temperature in ether led to clean formation of the dihydride *cis*-$(DMPM)_2Ru(H)_2$ **5** in 63% isolated yield. Compound **5** was characterized by conventional spectroscopic techniques and microanalysis, and all data were consistent with a cis orientation of the hydride substituents. Two triplet resonances were observed in the $^{31}P\{^1H\}$ NMR spectrum of **5**; the phosphorus atoms located trans to the hydride substituents resonated upfield from the mutually trans phosphorus atoms. Four ligand methyl resonances were observed in the ^1H and $^{13}C\{^1H\}$ NMR spectra. One doublet of quartets hydride resonance at δ-8.24 was observed in the ^1H NMR spectrum, and two hydride absorptions at 1750 cm^{-1} and 1767 cm^{-1} were observed in the IR spectrum.

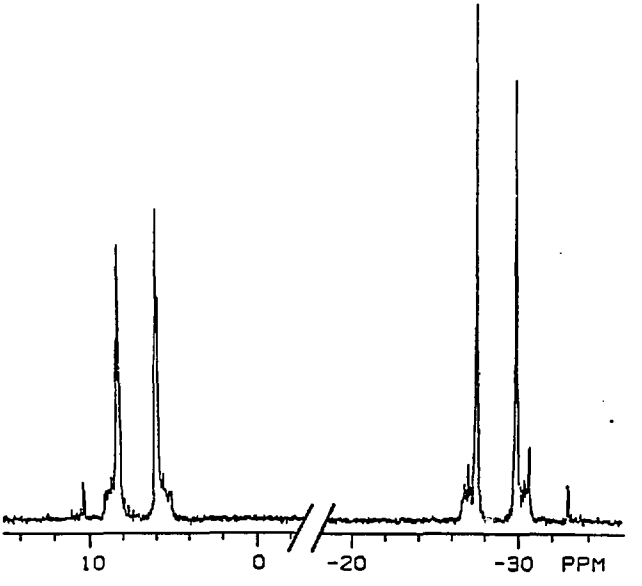

Figure 2. $^{31}P\{^{1}H\}$ NMR spectrum of $(\eta^{1}\text{-DMPM})_2(\eta^{2}\text{-DMPM})_2Ru_2(OAc)_4$ (3).

Scheme 2

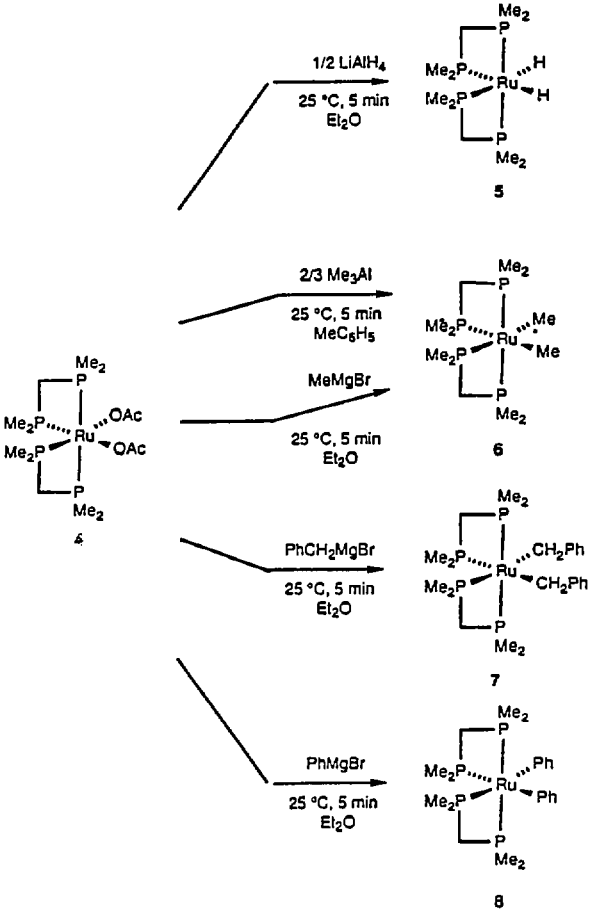
1/2 LiAlH4
25 °C, 5 min
Et2O
2/3 Me3Al
25 °C, 5 min
MeC6H5
MeMgBr
25 °C, 5 min
Et2O
PhCH2MgBr
25 °C, 5 min
Et2O
PhMgBr
25 °C, 5 min
Et2O
4
5
6
7
8

Room temperature addition of 2/3 equivalent of Me_3Al in toluene led to formation of the dimethyl complex *cis*-$(DMPM)_2Ru(Me)_2$ (6) in 87% isolated yield. Two triplets were observed in the $^{31}P\{^1H\}$ NMR spectrum of 6, demonstrating the *cis*-orientation of the methyl groups. The ^1H NMR spectrum displayed a resonance at δ0.21 and the $^{13}C\{^1H\}$ NMR spectrum contained a resonance at δ-8.98 for the metal bound methyl group. The room temperature addition of Grignard reagents also led to alkyl substituted products, but in lower yields than those experienced with aluminum reagents. For example, addition of MeMgBr to 4 led to formation of 6 in 52% yield after extraction with pentane. Similarly, addition of $PhCH_2MgBr$ led to formation of the *bis*-benzyl complex *cis*-$(DMPM)_2Ru(CH_2Ph)_2$ (7)in 22% yield. This compound was identified by its ^1H, $^{31}P\{^1H\}$, and $^{13}C\{^1H\}$ NMR spectra. Two equivalent η^1-bound benzyl groups were observed in the ^1H and $^{13}C\{^1H\}$ NMR spectrum, and two triplets were observed in the $^{31}P\{^1H\}$ NMR spectrum, with chemical shifts similar to those of the dimethyl complex 6, consistent with a cis geometry.

As discovered during the preparation of of alkyl complexes, triaryl aluminum reagents gave higher isolated yields than Grignard reagents. Addition of PhMgBr led to formation of the diphenyl complex $(DMPM)_2Ru(Ph)_2$ (8) in roughly 10% yield after extraction with pentane. However, addition of Ph_3Al led to 8 in 48 % isolated yield. Compound 8 was characterized by ^1H, $^{31}P\{^1H\}$, $^{13}C\{^1H\}$, and IR spectroscopy. Four ligand methyl groups were observed in the ^1H NMR spectrum along with resonances for two equivalent η^1-bound aryl groups. The resonance for the *ipso* carbon of the equivalent aryl rings was observed at δ174, which showed the appropriate doublet of quartets pattern, a large coupling due to the trans phosphorus atom and three smaller, indistinguishable cis couplings.

The dialkyl and diaryl complexes were thermally stable, even at elevated temperatures. Thermolysis of C_6D_6 solutions of 7 or 8 at 110 °C for 8h led to no decomposition of the dialkyl and diaryl complexes. Most notably the complexes were stable toward orthometallation reactions. No evidence for the formation of toluene and $(DMPM)_2Ru(CH_2C_6H_4)$ was observed while monitoring the thermolysis of 7. No evidence for orthometallation of 8 to form benzene and

$(DMPM)_2Ru(C_6H_4)$ or reductive elimination to form biphenyl and products from the intermediate $(DMPM)_2Ru$ (*vide infra*) was observed. Similarly, dimethyl compound **6** was stable toward 5 atm of hydrogen for 24 h at room temperature.

Hydrido methanesulfonate complex. Attempts to synthesize the mixed complexes $(DMPM)_2Ru(R)(OAc)$ (R=Me, H) by the addition of 1/3 equiv. of Me_3Al or 1/4 equiv. $LiAlH_4$ to **4** led to intractable mixtures. However, addition of one equivalent of methanesulfonic acid to dihydride **5** cleanly precipitated the hydrido methanesulfonate complex *trans*-$(DMPM)_2Ru(H)(OSO_2Me)$ (**9**) in 70% yield (Scheme 3). Compound **9** was characterized by ^1H, $^{31}P\{^1H\}$, $^{13}C\{^1H\}$ NMR and IR spectroscopy, as well as microanalysis. The singlet resonance at δ-25.5 in the $^{31}P\{^1H\}$ NMR spectrum and the pentet resonance at δ-20.5 in the ^1H NMR spectrum corresponding to the hydride substituent indicated a trans orientation of the hydride and methanesulfonate groups. It is possible that these two spectra result from rapid dissociation of the weakly coordinating methanesulfonate group, forming a five-coordinate cation which rapidly exchanges phosphine coordination sites. However, cooling a sample of **9** in THF-d_8 to -80 °C led to no change in the ^1H or $^{31}P\{^1H\}$ NMR spectra, suggesting that a trans orientation of the hydride and methanesulfonate groups is the lowest energy structure in solution.

Alkyl and Aryl Hydride complexes. The formation and thermal stabilities of the alkyl and aryl hydride complexes are shown in Scheme 4. Addition of Me_3Al to the hydrido methanesulfonate complex **9** at room temperature in benzene led to formation methane and the phenyl hydride **10**. Initial formation of a methyl hydride complex, followed by reductive elimination of methane to form $(DMPM)_2Ru$ which oxidatively adds the solvent C-H bond, would account for the reaction products. Indeed, the *trans*-methyl hydride intermediate **12** was generated in 46 % NMR yield by addition of Me_3Al at -78 °C to a toluene-d_8 solution of **9**, and was identified by low temperature ^1H, $^{31}P\{^1H\}$, and $^{13}C\{^1H\}$ NMR spectroscopy. The ^1H and $^{13}C\{^1H\}$ NMR spectra demonstrated the presence of a hydride and metal-bound methyl group located trans to each other. The hydride substituent was identified by a pentet resonance at δ-8.14 in the ^1H NMR spectrum. The metal-bound methyl group was observed as a pentet resonance at δ0.27 in the ^1H

Scheme 3

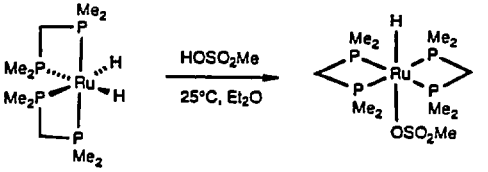
Me2
P
Me2P
Ru
H
Me2P
H
P
Me2
HOSO2Me
25°C, Et2O
H
Me2
Me2
P
P
Ru
P
P
Me2
Me2
OSO2Me

5 **9**

Scheme 4

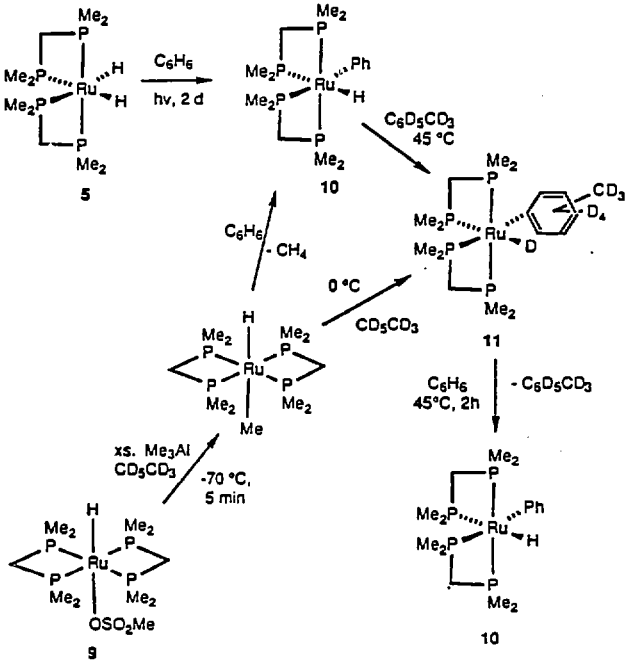
Me2
P
Me2P
Ru
H
Me2P
H
P
Me2
5
C6H6
hv, 2 d
Ph
10
C6D5CD3
45 °C
CD3
D4
D
11
C6H6
- CH4
0 °C
CD3CD3
H
Me
xs. Me3Al
CD3CD3
-70 °C,
5 min
C6H6
45°C, 2h
- C6D5CD3
OSO2Me
9
10

NMR spectrum and at δ-25.11 in the $^{13}C\{^1H\}$ NMR spectrum. A singlet resonance at δ-22.4 was observed in the $^{31}P\{^1H\}$ NMR spectrum, consistent with a trans orientation of the hydride and methyl groups.

Allowing this sample to warm to 0 °C showed the formation of methane (identified by ^1H NMR spectroscopy) and provided ^1H and $^{31}P\{^1H\}$ NMR spectra which were identical to those obtained from a toluene-d_8 solution of phenyl hydride **10** after 8 h (*vide infra*). These data demonstrate that the methyl hydride complex **10** is unstable toward reductive elimination at room temperature, and forms the more stable aryl hydride complexes. Under these conditions, no *cis* (DMPM)Ru(Me)(H) (cis-**12**) was observed. However, previous studies have demonstrated the necessity of a cis orientation for reductive elimination.[13] Therefore, we propose that trans to cis isomerization is the rate determining step in the formation of phenyl hydride **10** from the trans methyl hydride **12**. We propose that isomerization of the trans complex to the cis isomer occurs by dissociation of one end of the DMPM ligand to form a five coordinate species, which undergoes rearrangement and recoordination of the DMPM chelate to form the saturated *cis*-complex. Mechanisms involving 5-coordinate intermediates have been proposed for trans to cis rearrangements.[14]

Irradiation of a benzene-d_6 solution of dihydride **5** for 4 d led to formation of hydrogen (observed by ^1H NMR spectroscopy) and the phenyl-d_5 deuteride complex $(DMPM)_2Ru(C_6D_5)(D)$**10**-d_6 in 48% yield by ^1H NMR spectroscopy. This procedure led to significant decomposition before complete reaction of **5** had occurred, and we were not able to separate the phenyl hydride product from dihydride starting material when the photolysis was run to lower conversion. Therefore, photolysis did not provide a method for obtaining pure samples of **10**. However, addition of trimethylaluminum to a solution of hydrido methanesulfonate (**9**) in benzene solvent, followed by crystallization from a benzene/pentane mixture provided **10** in 19% isolated yield, as material which was pure as determined by $^{31}P\{^1H\}$ NMR spectroscopy. We were able to obtain ^1H, $^{13}C\{^1H\}$, and $^{31}P\{^1H\}$ NMR spectral data on a sample of **10** prepared by this method, although we were not able to obtain analytically pure samples.

Solutions of **10** in benzene-d_6 formed **10**-d_6 after 8 h at room temperature and toluene-d_8 samples of **10** were converted to solutions for which the $^{31}P\{^1H\}$ NMR spectra were nearly identical to those obtained in benzene-d_6 solvent. Removal of the toluene solvent followed by ^2H NMR spectral analysis in C_6H_6 showed three tolyl methyl groups at δ2.35, δ2.31, and δ1.98. Resonances in the aryl region (δ6.9 - δ7.9) were also observed as well as hydride resonances centered at δ-7.75. These data indicated formation of a mixture of three tolyl hydride compounds (**11**)by exchange with toluene-d_8 solvent. The benzene formed by this exchange reaction was analyzed by GC/MS to determine its isotopic distribution. Comparison of the mass spectrum of the benzene byproduct to authentic samples of C_6H_6 and C_6H_5D (prepared by addition of D_2O to PhMgBr) indicated no enrichment of deuterium into this material.

Two mechanisms for arene ring exchanges are displayed in Scheme 5. Path a involves a simple reductive elimination of benzene to form $(DMPM)_2Ru$ (**12**) and oxidative addition of solvent C-D bonds. Path b involves dissociation of one end of the DMPM ligand, followed by oxidative addition to form the ruthenium(IV) intermediate **13**. Intermediate **13** contains a hydride and a deuteride. As a result, path b predicts formation of benzene-d_0 and benzene-d_1 as the organic product. Arene ring exchange in the $(PMe_3)_4Ru(Ph)(H)$[10] system and addition of benzene to $(PMe_3)_4Os(CH_2CMe_3)(H)$[5f,i] were both shown to occur by way of the unsaturated $(PMe_3)_3M(H)(R)$, an intermediate analogous to **13**. In both these cases, incorporation of deuterium from the solvent was observed in the organic byproduct. However, no deuterium enhancement was observed in the benzene byproduct of the $(DMPM)_2Ru(Ar)(H)$ system, supporting a simple reductive elimination and oxidative addition mechanism (path a).

The instability of methyl hydride **12** demonstrates that the (DMPM)Ru(0) intermediate must be generated at low temperature in order to observe formation of alkane C-H activation products. Photolysis of dihydride **5** provides such a method.[2a,d,g,h,j,15] However, monitoring the irradiation of a pentane solution of **5** at -80°C after 2 h and 8 h by low temperature $^{31}P\{^1H\}$ NMR spectroscopy showed only decomposition of **5** and no evidence for an alkyl hydride product.

Scheme 5

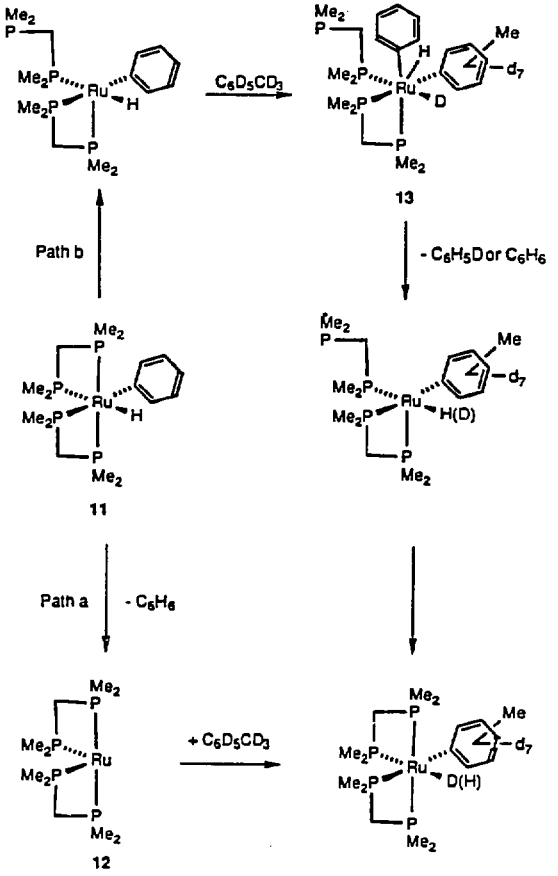
Me2
P
Me2P
Ru
H
Me2P
P
Me2
C6D5CD3
H
Me
d7
D
13
Path b
- C6H5D or C6H6
11
H(D)
Path a
- C6H6
12
+ C6D5CD3
D(H)

Comparison of stabilities to $(PMe_3)_4Ru(R)(R')$, $(PMe_3)_4Ru(H)(R)$, and $(DMPE)_2Ru(R)(R')$.

The dialkyl complexes of this DMPM system are markedly more stable than the analogous compounds containing four η^1-PMe_3 ligands rather than two η^2-DMPM ligands. Addition of two equivalents of $PhCH_2MgBr$ to *trans*-$(PMe_3)_4Ru(Cl)_2$ at room temperature led to formation of toluene and the cyclometallated complex $(PMe_3)_4Ru(\eta^2\text{-}CH_2C_6H_4)$, suggesting that the *bis*-benzyl complex is unstable to orthometallation even at room temperature. The *cis*-$(PMe_3)_4Ru(Ph)_2$ complex is stable under argon, but thermally eliminates benzene to form $(PMe_3)_4Ru(\eta^2\text{-}C_6H_4)$ at 85 °C. In addition, reaction of *cis*-$(PMe_3)_4Ru(Me)_2$ with 1 atm of hydrogen at room temperature for 24 h led to clean formation of *cis*-$(PMe_3)_4Ru(H)_2$.[16] The thermal stability of *cis*-$(DMPM)_2Ru(CH_2Ph)_2$ and *cis*-$(DMPM)_2Ru(Ph)_2$ and the stability of *cis*-$(DMPM)_2Ru(Me)_2$ toward hydrogen suggests that this system, which contains η^2-phosphine ligands, cannot undergo reactions that typically proceed by pathways involving phosphine dissociation.[17] However, isomerization of the *trans*-methyl hydride to the *cis*-isomer before reductive elimination suggests that dissociation of one end of the DMPM ligand occurs even at 0 °C, assuming dissociation of a hydride or methyl group does not occur. Therefore, the rate of recoordination must be faster than the rate of intramolecular C-H oxidative addition or intermolecular H_2 addition to the resulting Ru(II) intermediate.

The synthesis and thermal stabilities of the aryl and alkyl hydride complexes $(DMPE)_2Ru(R)(H)$ have been investigated by several groups,ref [5a,7,8] and we have investigated the thermal reactivity of $(PMe_3)_4Ru(R)(H)$ complexes. The aryl hydride complexes of the DMPE system are stable at room temperature, but reductively eliminate between 45 °C and 85 °C. The alkyl and aryl hydride complexes of the $(PMe_3)_4Ru(R)(H)$ system are even more stable. For example, the methyl[18] and ethyl[19] hydride complexes have been shown to be stable at 65 °C, while the benzyl hydride complex reductively eliminates to form the $(PMe_3)_4Ru$ intermediate over the course of 4 h at 85 °C. The phenyl hydride complex requires heating to 140 °C for 8 h before it eliminates benzene and forms the $(PMe_3)_4Ru$ intermediate.

The electronic properties of DMPE, DMPM, and PMe_3 must be similar since they are essentially trialkyl phophines. We therefore find it surprising that the DMPM complexes display dramatically different stabilities relative to the DMPE and PMe_3 complexes, but offer two explanations for this observation. Steric arguments would predict that the trimethylphosphine system should have a lower barrier to formation of the four-coordinate L_4Ru intermediate from the six-coordinate alkyl hydride $L_4Ru(H)(R)$ starting material because the DMPM system possesses ligands that are pulled away from the alkyl groups. Therefore, a simple steric argument based on the size of the ligand systems in the alkyl hydrides is not adequate to explain the relative stabilities. Our first possible explanation is based on ground state energies, and postulates that the ability of the DMPM ligands to act as strong σ-donors may be reduced by the ring strain in the four-membered ring system necessary to form chelating monomeric complexes. The reduced electron density at the metal center may reduce the strength of the Ru-H and Ru-C bonds. A second explanation involves a possible difference in activation energy due to the reorganization neccessary to adopt the "sawhorse"-type geometry (shown for intermediate **12** in Scheme 5) for C-H reductive eliminations of ML_4 compounds.[20] X-ray structural studies of several $(PMe_3)_4Ru(X)(Y)$ compounds have shown that the two mutually trans phosphine ligands are bent *away* from the other two phosphines and *toward* the two cis, σ-bonded ligands, such that the trans P-Ru-P angle is between 160° and 165°.[16, 21] Therefore the trans phosphines in $(PMe_3)_4Ru(R)(H)$ must bend away from this geometry and increase steric interactions with the two *cis*-PMe_3 ligands to reach the transition state. Perhaps the energy required to adopt this conformation is sufficient to account for the slower reductive elimination of the tetrakis-PMe_3 system relative to its DMPM analogue.

Experimental.

General. Unless otherwise noted, all manipulations were carried out under an inert atmosphere in a Vacuum Atmospheres 553-2 drybox with attached M6-40-1H Dritrain, or by using standard Schlenk or vacuum line techniques.

^1H NMR spectra were obtained on either the 250, 300, 400 or 500 MHz Fourier Transform spectrometers at the University of California, Berkeley (UCB) NMR facility. The 250 and 300 MHz instruments were constructed by Mr. Rudi Nunlist and interfaced with either a Nicolet 1180 or 1280 computer. The 400 and 500 MHz instruments were commercial Bruker AM series spectrometers. ^1H NMR spectra were recorded relative to residual protiated solvent. $^{13}C\{^1H\}$ NMR spectra were obtained at either 75.4, 100.6, or 125.7 MHz on the 300, 400 or 500 MHz instruments, respectively, and chemical shifts were recorded relative to the solvent resonance. ^2H NMR spectra were recorded at 76.4 MHz on the 500 MHz instrument, and chemical shifts were recorded relative to the solvent resonance. Chemical shifts are reported in units of parts per million downfield from tetramethylsilane and all coupling constants are reported in Hz.

IR spectra were obtained on a Nicolet 510 spectrometer equipped with a Nicolet 620 processor using potassium bromide ground pellets, or solution cells as stated. Mass spectroscopic (MS) analyses were obtained at the UCB mass spectrometry facility on AEI MS-12 and Kratos MS-50 mass spectrometers. Elemental analyses were obtained from the UCB Microanalytical Laboratory.

To prepare sealed NMR tubes, the sample tube was attached via Cajon adapters directly to Kontes vacuum stopcocks.[22] Known volume bulb vacuum transfers were accomplished with an MKS Baratron attached to a high vacuum line.

Unless otherwise specified, all reagents, including Grignard and trialkylaluminum reagents, were purchased from commercial suppliers and used without further purification. PMe_3 (Strem) was dried over NaK or a Na mirror and vacuum transferred prior to use; DMPM (strem) was used as received CO was purchased from Matheson. $(PPh_3)_2Ru(OAc)_2$ (1) was prepared by literature methods.[11]

Pentane and hexane (UV grade, alkene free) were distilled from $LiAlH_4$ under nitrogen. Benzene and toluene were distilled from sodium benzophenone ketyl under nitrogen. Ether and tetrahydrofuran were distilled from purple solutions of sodium/benzophenone ketyl. Deuterated

solvents for use in NMR experiments were dried as their protiated analogues but were vacuum transferred from the drying agent.

***cis, trans*(η^1-DMPM)$_2$(η^2-DMPM)Ru(OAc)$_2$ (2).** Ru(PPh$_3$)$_2$(OAc)$_2$ (350 mg, 0.471 mmol) was dissolved in 10 mL of toluene, and an excess of DMPM (300 mg, 2.24 mmol) in 2 mL of toluene was added at room temperature. The bright orange suspension turned pale yellow upon mixing and became homogeneous. The solution was stirred at room temperature for an additional 2 h, after which time the solvent was removed under reduced pressure. The resulting ruthenium complex was very soluble in pentane, precluding simple separation from triphenylphosphine by washing with pentane. Compound **2** was isolated by chromatography in the drybox on alumina III, eluting with ether to remove the triphenylphosphine and then with THF to remove the ruthenium complex. The compound was then crystallized from pentane to yield 88.0 mg (30 %) of **2** as yellow blocks. IR (C_6D_6) 2970, 2908, 1609, 1428, 1372, 1326, 1288, 941, 904; MS (FAB, sulfolane) 569 (M-OAc)H$^+$, 509 (M-2OAc)$^+$; Anal. Calcd. for $C_{19}H_{48}O_4P_6Ru$: C, 46.06; H, 8.54. Found: C, 46.22; H, 8.76.

(η^2, μ^2-DMPM)$_2$(η^2, μ^1-DMPM)$_2$Ru$_2$(η^1-OAc)$_4$ (3). Ru(PPh$_3$)$_2$(OAc)$_2$ (1.18 g, 1.59 mmol) was suspended in 10 mL of hexanes. DMPM (0.432, 3.17 mmol) was added and the suspension was stirred for 4 h at 65 °C, over which time the orange suspension became a pale yellow-green solution containing a white solid. The reaction mixture was cooled to room temperature, the solid was filtered, and the free triphenylphosphine and DMPM was removed by washing three times with a total of 100 mL of pentane to leave 639 mg (82 %) of **3** as a white powder. IR(KBr) 2994, 2968, 2907, 2888, 1589, 1387, 1335, 940, 924, 906; MS (FAB, sulfolane) 984 (MH$^+$), 925 ((M-OAc)$^+$); Anal. Calcd. for $C_{24}H_{56}O_8P_8Ru_2$: C, 34.22; H, 6.97. Found: C, 34.40; H, 6.96.

***cis*-(η^2-DMPM)$_2$Ru(OAc)$_2$ (4).** (η^2, μ^2-DMPM)$_2$(η^2, μ^1-DMPM)$_2$Ru(η^1-OAc)$_4$ (2) (639 mg, 0.651 mmol) was suspended in 50 mL of toluene, and the suspension was placed into a glass reaction vessel equipped with a Kontes vacuum adaptor. The vessel was degassed by two freeze, pump, thaw cycles and heated to 110 °C for 8 h under vacuum. After this time the solution

had become homogeneous. The solvent was then removed under vacuum to provide 512 mg (80.1%) yield of 4 as a white powder, judged pure by ^1H and $^{31}P\{^1H\}$ NMR spectroscopy. A portion of this material was crystalized for microanalysis by diffusing pentane into a toluene solution of 4. IR(KBr) 2967, 2905, 1582, 1407, 1370, 1320, 1280, 927; MS (E.I.) 492 (M^+); Anal. Calcd. for $C_{12}H_{28}O_4P_4Ru$: C, 34.22; H, 6.97. Found: C, 34.48; H, 7.00.

***cis*-(DMPM)$_2$Ru(H)$_2$ (600)** *cis*-(η^2-DMPM)$_2$Ru(OAc)$_2$ (4) (0.578 g, 1.18 mmol) was suspended in 50 mL of ether. To the stirred solution at room temperature was added 0.589 mL (0.589 mmol) of a 1.0 M solution of lithiumaluminumhydride in ether. The yellow solution became white, and was stirred for an additional 10 min. The ether was removed under reduced pressure and the residue was extracted with 100 mL of pentane. The pentane suspension was filtered and the solvent was removed to provide 303 mg (63%) of analytically pure pale yellow powder. IR(KBr) 2959, 2895; 1767, 1750, 1411, 1272, 922; MS (EI) 374 (M^+); Anal. Calcd. for $C_{10}H_{18}P_4Ru$: C, 32.00; H, 8.06. Found: C, 32.21; H, 8.14.

***cis*-(DMPM)$_2$Ru(Me)$_2$ (5).** *cis*-(η^2-DMPM)$_2$Ru(OAc)$_2$ (4) (1.14 g, 2.32 mmol) was dissolved in 75 mL of benzene. To the stirred solution at room temperature was added 0.773 mL (1.55 mmol) of a 2.0 M solution of Me_3Al in toluene. The yellow solution became white, and it was stirred for an additional hour. The benzene was removed under reduced pressure and the residue was extracted with 100 mL of pentane. The pentane suspension was filtered and the solvent was removed to provide 818 mg (87%)of white powder judged pure by ^1H and $^{31}P\{^1H\}$ NMR spectroscopy. A portion of this material was crystallized from pentane at -40 °C for microanalysis. IR(KBr) 2955, 2900, 2892, 2861, 2813, 2774, 1409, 1286, 1272, 1074, 927, 917, 913; Anal. Calcd. for $C_{10}H_{18}P_4Ru$: C, 32.00; H, 8.06. Found: C, 32.21; H, 8.14.

***cis*-(DMPM)$_2$Ru(CH$_2$Ph)$_2$ (7).** *cis*-(η^2-DMPM)$_2$Ru(OAc)$_2$ (314 mg, 0.640 mmol) was dissolved in 10 mL of THF. To the stirred solution at room temperature was added 0.704 mL (1.41 mmol) of a 2.0 M solution of $PHCH_2MgBr$ in THF. The yellow solution became white, and it was stirred for an additional 8 h. The THF was removed under reduced pressure and the residue was extracted with 100 mL of benzene. The benzene suspension was filtered and the solvent was

removed to provide 78.2 mg (22%) of white powder in approximately 95% purity by ^{1}H, $^{31}P\{^{1}H\}$, and $^{13}C\{^{1}H\}$ NMR spectroscopy. Attempts to obtain analytically pure material by crystallization provided material which was of roughly the same purity as the crude material. MS(EI) 465 (M-CH_2Ph)$^+$.

***cis*-(DMPM)$_2$Ru(Ph)$_2$ (8)** *cis*-(η^2-DMPM)$_2$Ru(OAc)$_2$ (4) (250 mg, 0.520 mmol) was dissolved in 10 mL of toluene. To the stirred solution at room temperature was added 99.2 mg (0.382 mmol) of of Ph_3Al as a solid. The solution remained yellow after stirring for 16 h, but $^{31}P\{^{1}H\}$ NMR spectroscopy of an aliquot showed no unreacted *bis*-acetate 4. The toluene was removed under reduced pressure and the residue was extracted with 50 mL of Et_2O. The ether suspension was filtered and the solvent was removed from the filtrate to provide 86.4 mg of off white powder in approximately 95% purity by ^{1}H, $^{31}P\{^{1}H\}$, and $^{13}C\{^{1}H\}$ NMR spectroscopy. Attempts to obtain analytically pure material by crystallization provided material which was of roughly the same purity as the crude material. IR(KBr) 3033, 2979, 2956, 2901, 1561, 1417, 1288, 1274, 1080, 1011, 947, 921.

***trans*-(DMPM)$_2$Ru(H)(OSO$_2$Me) (9)** *cis*-(DMPM)$_2$Ru(H)$_2$ (5) (84.4 mg, 0.225 mmol) was dissolved in 40 mL of THF. To this stirred solution was added, all at once, 54 µL (0.225 mmol) of a 4.17 M solution of $HOSO_2Me$ in THF at room temperature. The hydrido methanesulfonate complex 9 was isolated by concentration of the solution to 5 mL, followed by addition of 50 mL of pentane which precipitated a white solide. This solid was collected by filtration to provide 73.9 mg (70 %) of white powder, judged pure by ^{1}H, $^{31}P\{^{1}H\}$, and $^{13}C\{^{1}H\}$ NMR spectroscopy. Crystalline, analytically pure samples of 9 were obtained from a preparation using 162 mg of starting ruthenium complex, and the crude powder was extracted with 100-150 mL of pentane, concentrated, and cooled to -40 °C to provide 30.0 mg (14.8%) of white needles. IR(KBr) 2962, 2900, 1890, 1420, 1293, 1278, 1207, 1086, 1059, 927; Anal. Calcd. for $C_{11}H_{32}O_3P_4RuS$: C, 28.14; H, 6.87. Found: C, 28.31; H, 6.66.

***cis*-(DMPM)$_2$Ru(Ph)(H) (10)** To a solution of 82.6 mg (0.176 mmol) of 9 in 7 mL of C_6H_6 was added dropwise at room temperture 118 mL (2/3 equiv) of a 1.0 M solution of

trimethylaluminum in toluene. The solution was stirred for 1 h, after which time an oily solid had formed. The solution was decanted from this solid, and the solvent was reduced to 2 mL under reduced pressure. The resulting solution was filtered through a plug of celite and further concentrated to 0.5 mL. Into this solution was vapor diffused 2 mL of pentane, and the resulting solution was cooled to -40°C. The vial continued to be exposed to pentane at -40 °C in a closed system for one week, over which time 14.8 mg (19%) of 10 crystallized as pale yellow needles. IR(KBr): .2898, 2918, 2958, 3031, 1791, 1559, 1417, 1274, 930, 919.

***trans*-(DMPM)$_2$Ru(Me)(H) (11)** *trans*-(DMPM)$_2$Ru(H)(OSO$_2$Me) (9) (24.2 mg, 0.0516 mmol) and 3.1 mg of ferrocene as an internal standard were dissolved in 0.7 mL of toluene-d_8 and placed into an NMR tube equipped with a teflon septum. The tube was cooled to -78 °C and an excess of a 2.0 M solution of Me_3Al (18.5 µL, 0.111 mmol) was added by syringe. The tube was then placed in the NMR probe which had been cooled to -80 °C. ^1H, $^{31}P\{^1H\}$, and $^{13}C\{^1H\}$ NMR spectroscopy showed formation of **11** in 43% yield. The NMR probe was warmed to 0 °C, under which conditions the methyl hydride began to eliminate methane and form (DMPM)$_2$Ru(D)($C_6D_4CO_3$) (**12**-d_8) as determined by comparison of this sample to one obtained by thermolysis of a toluene-d_8 solution of phenyl hydride **10**.

Exchange of *cis*-(DMPM)$_2$Ru(Ph)(H) (10) with toluene-d_8. In 0.3 mL of toluene-d_8 was dissolved 14.8 mg of *cis*-(DMPM)$_2$Ru(Ph)(H) (**10**). The sample was allowed to sit at room temperature for 24 h, after which time the volatile materials were collected by vacuum transfer. GC/MS analysis showed that the benzene byproduct contained no enrichment in C_6H_5D, as determined by comparison of the mass spectrum to an authentic sample of C_6H_6 and C_6H_5D (prepared by addition of D_2O to PhMgBr). ^2H NMR spectroscopy showed resonances in the aromatic region (δ6.9 - δ7.9; 4 hydrogens) in the tolyl region (δ2.35, δ2.31, and δ1.98; 3 hydrogens) and in the deuteride region (δ-7.75; 1 hydrogen), indicating formation of a mixture of tolyl hydride compounds. The resonances in the tolyl region were not well enough resolved to obtain accurate ratios of the three isomers, but the distribution was roughly 4:1:1.

Table 1 ^{1}H NMR spectroscopic data.

Compound	δ(ppm)	multiplicity[1]	J(Hz)	integral	assignment[2]
$(\eta^1$-DMPM)$_2(\eta^2$-DMPM) Ru(OAc)$_2$[3] (2)	3.69	tt	10.6, 1.8	2	$Me_2P\underline{CH_2}PMe_2$
	1.98	s		4	$Me_2P\underline{CH_2}PMe_2$
	1.98	s		6	-OC(O)$\underline{CH_3}$
	1.57	d	7.4	12	$\underline{Me_2}PCH_2P\underline{Me_2}$
	1.30	m		12	$\underline{Me_2}PCH_2P\underline{Me_2}$
	0.98	d	3.5	12	$\underline{Me_2}PCH_2P\underline{Me_2}$
$(\eta^2, \mu^1$-DMPM)$_2(\eta^2, \mu^2$-DMPM) $Ru_2(OAc)_4$[3] (3)	3.71	t	10.5	4	$Me_2P\underline{CH_2}PMe_2$
	2.95	brs		4	$Me_2P\underline{CH_2}PMe_2$
	2.01	s		12	-OC(O)$\underline{CH_3}$
	1.46	d	6.9	24	$\underline{Me_2}PCH_2P\underline{Me_2}$
	1.31	t	3.7	24	$\underline{Me_2}PCH_2P\underline{Me_2}$
$(\eta^2$-DMPM)$_2$Ru(OAc)$_2$[3] (4)	2.91	m		2	$(Me_2P)_2C\underline{H_A}H_B$
	2.31	m		2	$(Me_2P)_2CH_A\underline{H_B}$
	2.29	s		6	-OC(O)$\underline{CH_3}$
	1.76	t	3.5	6	$\underline{Me_2}PCH_2P\underline{Me_2}$
	1.51	t	3.1	6	$\underline{Me_2}PCH_2P\underline{Me_2}$
	1.16	d	10.2	6	$\underline{Me_2}PCH_2P\underline{Me_2}$
	0.83	d	8.3	6	$\underline{Me_2}PCH_2P\underline{Me_2}$
$(\eta^2$-DMPM)$_2$Ru(H)$_2$[3] (5)	3.08	m		2	$(Me_2P)_2C\underline{H_A}H_B$
	2.96	m		2	$(Me_2P)_2CH_A\underline{H_B}$
	1.53	d	6.8	6	$\underline{Me_2}PCH_2P\underline{Me_2}$
	1.46	t	2.7	6	$\underline{Me_2}PCH_2P\underline{Me_2}$
	1.36	d	5.4	6	$\underline{Me_2}PCH_2P\underline{Me_2}$
	1.23	d	1.2	6	$\underline{Me_2}PCH_2P\underline{Me_2}$
	-8.24	dq	78, 22	2	Ru-H
$(\eta^2$-DMPM)$_2$Ru(Me)$_2$[3] (6)	3.02	m		2	$(Me_2P)_2C\underline{H_A}H_B$
	2.73	m		2	$(Me_2P)_2CH_A\underline{H_B}$
	1.25	d	3.8	6	$\underline{Me_2}PCH_2P\underline{Me_2}$
	1.23	d	3.1	6	$\underline{Me_2}PCH_2P\underline{Me_2}$
	1.10	d	2.6	6	$\underline{Me_2}PCH_2P\underline{Me_2}$
	1.03	d	1.4	6	$\underline{Me_2}PCH_2P\underline{Me_2}$
	0.21	m		6	Ru-Me
$(\eta^2$-DMPM)$_2$Ru$(CH_2Ph)_2$[4] (7)	7.20	d	7.7	4	$CH_2\underline{Ph}$
	6.86	t	7.8	4	$CH_2\underline{Ph}$
	6.60	t	7.3	2	$CH_2\underline{Ph}$
	2.99	m		4	$\underline{CH_2}Ph$
	2.38	m		2	$(Me_2P)_2C\underline{H_A}H_B$
	2.05	m		2	$(Me_2P)_2CH_A\underline{H_B}$
	1.60	d	8.0	6	$\underline{Me_2}PCH_2P\underline{Me_2}$
	1.55	d	5.8	6	$\underline{Me_2}PCH_2P\underline{Me_2}$
	1.05	s		6	$\underline{Me_2}PCH_2P\underline{Me_2}$
	0.07	d	2.3	6	$\underline{Me_2}PCH_2P\underline{Me_2}$

Table 1. cont.

$(\eta^2\text{-DMPM})_2Ru(Ph)_2$[4] (8)	7.21	m		4	Ru-Ph
	6.59	t	7.2	4	Ru-Ph
	6.52	t	7.0	2	Ru-Ph
	2.95	m		2	$(Me_2P)_2CH_AH_B$
	2.62	m		2	$(Me_2P)_2CH_AH_B$
	1.61	d	5	6	$Me_2PCH_2PMe_2$
	1.60	s		6	$Me_2PCH_2PMe_2$
	1.23	d	7	6	$Me_2PCH_2PMe_2$
	1.22	s		6	$Me_2PCH_2PMe_2$
$(\eta^2\text{-DMPM})_2Ru(H)(OSO_2Me)$[4] (9)	3.40	m		2	$(Me_2P)_2CH_AH_B$
	3.20	m		2	$(Me_2P)_2CH_AH_B$
	2.48	s		3	$-OSO_2Me$
	1.55	s		12	$Me_2PCH_2PMe_2$
	1.45	s		12	$Me_2PCH_2PMe_2$
	-20.46	pent	20.7	1	Ru-H
cis-$(\eta^2\text{-DMPM})_2Ru(Ph)(H)$[3] (10)	8.08	t	5.9	2	Aromatic
	7.25	t	7.0	2	Aromatic
	7.14	d	6.0	1	Aromatic
	2.80	m		3	$Me_2PCH_2PMe_2$
	2.69	m		1	$Me_2PCH_2PMe_2$
	1.41	d	7.0	3	$Me_2PCH_2PMe_2$
	1.26	m		6	$Me_2PCH_2PMe_2$
	1.16	m		15	$Me_2PCH_2PMe_2$
	-7.72	dq	91, 20	1	Ru-H
$(\eta^2\text{-DMPM})_2Ru(H)(Me)$[5] (11)	3.08	m		2	$(Me_2P)_2CH_AH_B$
	3.01	m		2	$(Me_2P)_2CH_AH_B$
	1.42	s		12	$Me_2PCH_2PMe_2$
	1.28	s		12	$Me_2PCH_2PMe_2$
	0.27	pent	5.8	3	Ru-Me
	-8.14	pent	20.1	1	Ru-H

[1]The multiplicities doublet and triplet, when referring to the DMPM ligands, are apparent splitting patterns and do not necessarily reflect true coupling.
[2]The assignments *cis* and *trans* refer to mutually cis and mutually trans PMe_3 groups.
[3]C_6D_6, 25 °C; [4]THF-d_8, 25 °C; [5]tol-d_8, -40 °C;

Table 2. $^{13}C\{^1H\}$ NMR spectroscopic data.

Compound	δ(ppm)	multiplicity[1]	J(Hz)	assignment[2]
$(\eta^1\text{-DMPM})_2(\eta^2\text{-DMPM})$	177.2	s		-OC(O)Me
$Ru(OAc)_2$ (2)[3]	50.39	tt	22, 4.4	$Me_2PCH_2PMe_2$
	33.70	ddq	31, 15, 4	$Me_2PCH_2PMe_2$
	24.10	s		-OC(O)CH_3
	17.16	dt	15, 2	$Me_2PCH_2PMe_2$
	16.47	ddt	14, 11,4	$Me_2PCH_2PMe_2$
	15.37	td	9, 3	$Me_2PCH_2PMe_2$
$(\eta^2, \mu^1\text{-DMPM})_2(\eta^2, \mu^2\text{-DMPM})$	177.98	s		-OC(O)CH_3
$Ru_2(OAc)_4$[5] (3)	50.67	t	21.9	$Me_2PCH_2PMe_2$
	32.35	s		$Me_2PCH_2PMe_2$
	24.10	s		-OC(O)CH_3
	19.57	d	18.8	$Me_2PCH_2PMe_2$
	16.29	t	9.8	$Me_2PCH_2PMe_2$
$(\eta^2\text{-DMPM})_2Ru(OAc)_2$[5] (4)	176.44	t	3.2	-OC(O)CH_3
	51.73	m		$Me_2PCH_2PMe_2$
	24.37	s		-OC(O)CH_3
	20.32	t	8.8	$Me_2PCH_2PMe_2$
	19.40	m		$Me_2PCH_2PMe_2$
	15.88	t	12.7	$Me_2PCH_2PMe_2$
	12.85	t	10.3	$Me_2PCH_2PMe_2$
$(\eta^2\text{-DMPM})_2Ru(H)_2$[3] (5)	56.90	dt	21, 10	$Me_2PCH_2PMe_2$
	28.09	t	6.7	$Me_2PCH_2PMe_2$
	26.88	t	10	$Me_2PCH_2PMe_2$
	25.69	s		$Me_2PCH_2PMe_2$
	24.95	dt	14, 7	$Me_2PCH_2PMe_2$
$(\eta^2\text{-DMPM})_2Ru(Me)_2$[3] (6)	21.56	m		$Me_2PCH_2PMe_2$
	25.64	dd	6.7, 4.6	$Me_2PCH_2PMe_2$
	22.57	m		$Me_2PCH_2PMe_2$
	16.01	m		$Me_2PCH_2PMe_2$
	9.91	m		$Me_2PCH_2PMe_2$
	-8.98	dq	63, 11	Ru-Me
$(\eta^2\text{-DMPM})_2Ru(CH_2Ph)_2$[4] (7)	166.65	m		CH_2Ph
	130.87	s		CH_2Ph
	130.02	s		CH_2Ph
	122.19	s		CH_2Ph
	54.29	s		$Me_2PCH_2PMe_2$
	21.70	dm	53	CH_2Ph
	23.57	m		$Me_2PCH_2PMe_2$
	21.76	s		$Me_2PCH_2PMe_2$
	21.75	t	3.8	$Me_2PCH_2PMe_2$
	12.15	m		$Me_2PCH_2PMe_2$

Table 2. Cont.

$(\eta^2\text{-DMPM})_2Ru(Ph)_2$[4] (8)	174.05	dq	57.7, 11.8	Ru-Ph
	147.03	s		Ru-Ph
	124.80	s		Ru-Ph
	119.50	s		Ru-Ph
	49.49	tt	21.2, 12.1	$Me_2P\underline{CH_2}PMe_2$
	24.07	d	8.4	$\underline{Me_2}PCH_2P\underline{Me_2}$
	23.03	m		$\underline{Me_2}PCH_2P\underline{Me_2}$
	16.85	s		$\underline{Me_2}PCH_2P\underline{Me_2}$
	11.68	t	6.5	$\underline{Me_2}PCH_2P\underline{Me_2}$
$(\eta^2\text{-DMPM})_2Ru(H)(OSO_2Me)$[4] (9)	57.49	m		$Me_2P\underline{CH_2}PMe_2$
	41.85	s		$-OSO_2\underline{Me}$
	26.48	t	8.6	$\underline{Me_2}PCH_2P\underline{Me_2}$
	19.79	t	4.4	$\underline{Me_2}PCH_2P\underline{Me_2}$
cis-$(\eta^2\text{-DMPM})_2Ru(Ph)(H)$[3] (10)	169.13	dm	56.6	Aromatic
	147.87	m		Aromatic
	124.47	d	4.8	Aromatic
	119.23	s		Aromatic
	54.33	td	18.6, 5.6	$Me_2P\underline{CH_2}PMe_2$
	52.52	td	20.9, 7.0	$Me_2P\underline{CH_2}PMe_2$
	27.02	m		$\underline{Me_2}PCH_2P\underline{Me_2}$
	24.68	dt	8.4, 4.3	$\underline{Me_2}PCH_2P\underline{Me_2}$
	24.25	m		$\underline{Me_2}PCH_2P\underline{Me_2}$
	23.93	d	4.2	$\underline{Me_2}PCH_2P\underline{Me_2}$
	21.47	ddd	6.5, 11, 11	$\underline{Me_2}PCH_2P\underline{Me_2}$
	20.29	m		$\underline{Me_2}PCH_2P\underline{Me_2}$
	16.64	m		$\underline{Me_2}PCH_2P\underline{Me_2}$
	16.25	m		$\underline{Me_2}PCH_2P\underline{Me_2}$
$(\eta^2\text{-DMPM})_2Ru(H)(Me)$[5] (11)	55.44	t	11.7	$Me_2P\underline{CH_2}PMe_2$
	26.44	s		$\underline{Me_2}PCH_2P\underline{Me_2}$
	15.53	s		$\underline{Me_2}PCH_2P\underline{Me_2}$
	-25.11	p	9.5	Ru-Me

[1]The multiplicities doublet and triplet, when referring to the DMPM ligands, are apparent splitting patterns and do not necessarily reflect true coupling.
[2]The assignments *cis* and *trans* refer to mutually cis and mutually trans PMe_3 groups.
[3]C_6D_6, 25 °C; [4]THF-d_8, 25 °C; [5]tol-d_8, -40 °C; [6]CD_2CL_2

Table 3. $^{31}P\{^1H\}$ NMR spectroscopic data.

Compound	δ(ppm)	multiplicity[1]	J(Hz)	integral
$(\eta^1\text{-DMPM})_2(\eta^2\text{-DMPM})$ $Ru(OAc)_2$[3] (2)	9.18	m		1
	-28.81	m		1
	-60.08	m		1
$(\eta^2, \mu^1\text{-DMPM})_2(\eta^2, \mu^2\text{-DMPM})$ $Ru(OAc)_4$[3] (3)	7.0	m		4
	-28.60	m		4
$(\eta^2\text{-DMPM})_2Ru(OAc)_2$[2] (4)	-5.12	t	49.7	2
	-27.45	t		2
$(\eta^2\text{-DMPM})_2Ru(H)_2$[2] (5)	-16.43	t	46.5	2
	-28.87	t		2
$(\eta^2\text{-DMPM})_2Ru(Me)_2$[2] (6)	-18.76	t	39.8	2
	-24.82	t		2
$(\eta^2\text{-DMPM})_2Ru(CH_2Ph)_2$[2] (7)	-23.91	t	37.5	2
	-28.09	t		2
$(\eta^2\text{-DMPM})_2Ru(Ph)_2$[3] (8)	-23.53	t	35.9	2
	-30.29	t		2
$(DMPM)_2Ru(H)(OSO_2Me)$[3] (9)	-25.52	s		4
cis-$(DMPM)_2Ru(H)(Ph)$ (10)[2]	ABCD	δ_A=-19.36	J_{AB}=301.3	
		δ_B=-20.86	J_{AC}=57.9	
		δ_C=-26.81	J_{AD}=-29.8	
		δ_D=-35.20	J_{BC}=28.0	
			J_{BD}=48.1	
			J_{CD}=10.3	
$(\eta^2\text{-DMPM})_2Ru(H)(Me)$[4] (11)	-22.39	s		4

[1] The multiplicities for *cis*-$(DMPM)_2Ru(X)_2$ compounds are apparent splitting patterns. The true spin system for these compounds is AA'BB', even though a pair of triplets was observed in each case.

[2] C_6D_6, 25 °C; [3] THF-d_8, 25 °C; [4] tol-d_8, -40 °C;

Notes and References

1. For recent reviews on C-H oxidative additions see: a) Shilov, A.E. *Activation of Satruated Hydrocarbons by Transition Metal Complexes*; D. Riedel Publishing Co., Dordrecht, 1984. b) Crabtree, R.H. *Chem. Rev. 1985, 85*, 245. c) Green, M.L.H.; O'Hare, D. *Pure. Appl. Chem.* 1985, *57*, 1897. d) Halpern, J. *Inorg. Chem. Acta* 1985, *100*, 41. e) Bergman, R.G. *Science*, 1984, *223*, 902.

2. a) Baker, M.V.; Field, L.D. *J. Am. Chem. Soc. 1986, 108*, 7433; 7436. b) Hackett, M.; Ibers, J.A.; Whitesides, G. *J. Am. Chem. Soc.*, 1988, *110*, 1436. c) Hackett, M.; Whitesides, G. *J. Am. Chem. Soc.*, 1988, *110*, 1449. d) Hoyano, J.K.; McMaster, A.D.; Graham. W.A.G.; *J. Am. Chem. Soc.* 1983, *105*, 7190. e) Ghosh, C.K.; Graham, W.A.G. *J. Am.Chem. Soc.* 1987, *109*, 4726. f) Ghosh, C.K.; Rodgers, D.P.S. Graham, W.A.G. *J. Chem. Soc., Chem. Commun.* 1988, 1511. g) Jones, W.D.; Feher, F.J. *J. Am. Chem. Soc.* 1985, *107*, 620. h) Janowicz, A.H.; Bergman, R.G. *J. Am. Chem. Soc.* 1982, *104*, 352; 1983, *105*, 3929. i) Buchanan, J.M.; Stryker, J.M.; Bergman, R.G. *J. Am. Chem. Soc.*, 1986, *108*, 1537. j) Periana, R.A.; Bergman, R.G. *Organometallics* 1984, *3*, 508. k) Periana, R.A.; Bergman, R.G.; *J. Am. Chem. Soc. 1986, 108*, 7332.

3. a) Jones, W.D.; Foster, G.P.; Putinas, J.M. *J. Am. Chem. Soc.*1987, *109*, 5047. b) Fisher, B.J.; Eisenberg, R. *Organometallics*, 1983, *2*, 764. c) Kunin, A.J.; Eisenberg, R. *Organometallics, 1986, 7*, 2124. d) Kunin, A.J.; Eisenberg, R. *J. Am. Chem. Soc.* 1986, *108*, 535. e) Gordon, E.M.; Eisenberg, R. *J. Mol. Cat.* 1988, *45*, 57. f) Crabtree, R.H.; Mihelcic, J.M.; Quirk, J.M. *J. Am. Chem. Soc.* 1979, *101*, 7738. g) Crabtree, R.H.; Mellea, M.F., Mihelcic, J.M.; Quirk, J.M. *J. Am. Chem. Soc.* 1982, *104*, 107. h) Crabtree, R.H.; Demou, D.C.; Eden, J.M.; Mihelcic, J.M.; Parnell, J.M.; Quirk, J.M.; Morris, G.E. *J. Am. Chem. Soc.* 1982, *104*, 1982.

4. Yamamoto, A . *Organotransition Metal Chemistry*, John Wiley and Sons, Inc., New York, 1986.

5. a) Ittel, S.D.; Tolman, C.A.; English,A.D.; Jesson, J.P. *J. Am. Chem. Soc.* **1976**, *98*, 6073. b) Rathke, J.W.; Muetterties, E.L. *J. Am. Chem. Soc.* **1975**, *97*, 3272. c) Karsch, H.H.; Klein, H.-F.; Schmidbaur, H. *Angew. Chem. Int. Ed. Engl.* **1975**, *14*, 637. d) Antberg, M.; Dahlenberg, L. *Angew. Chem. Int. Ed. Engl.* **1986**, *25*, 260. e) Werner, H.; Werner, R. *J. Organomet. Chem.* **1981**, *209*, C60. f) Werner, H. Gotzig, J. *Organometallics* **1983**, *2*, 547. g) Desrosiers, P.J.; Shinomoto, R.S.; Flood, T.C. *J. Am. Chem. Soc.* **1986**, *108*, 1346. h) Desrosiers, P.J.; Shinomoto, R.S.; Flood, T.C. *J. Am. Chem. Soc.* **1986**, *108*, 7964. i) Harper, T.G.P.; Shinomoto, R.S.; Deming, M.A.; Flood, T.C. *J. Am. Chem. Soc.* **1988**, *110*, 7915. j) Ermer, S.P.; Shinomoto, R.S.; Deming, M.A.; Flood, T.C. *Organometallics* **1989**, *8*, 1377. k) Shinomoto, R.S.; Desrosiers, P.J.; Harper, G.P.; Flood, T.C. *J. Am. Chem. Soc.* **1990**, *112*, 704.

6. Reviews of cyclomtallation reactions include: a) Bruce, M.I. *Angew. Chem. Int. Ed. Engl.* **1977**, *16*, 73. b) Constable, E.C. *Polyhedron*, **1984**, *3*, 1037. Relevant examples include: c) Foley, P.; DiCosimo, R.; Whitesides, G.M. *J. Am. Chem. Soc.* **1980**, *102*, 6713. d) Calabrese, J.C.; Coolton, M.C.; Herskovitz, T.; Klabunde, U.; Parshall, G.W.; Thorn, D.L.; Tulip, T.H. *Annals. New York Acad. Sci.* **1983**, *415*, 302. e) reference 5h.

7. a) Chatt, J.; Davidson, J.M. *J. Chem. Soc.* **1965**, 843. b) Tolman, C.A.; Ittel, S.D.; English, A.D.; Jesson, J.P. *J. Am. Chem. Soc.* **1978**, *100*, 4080

8. Berganini, P.; Sostero, S.; Traverso, C. *J. Organomet. Chem.* **1986**, *299*, C11.

9. Palma-Ramirez, P.; Cole-Hamilton, D.J.; Pogorzelec, P.; Campora, J. *Polyhedron*, **1990**, *9*, 1107.

10. Chapter 1.

11. Armit, P.W.; Boyd, A.S.F.; Stephenson, *J. Chem. Soc., Dalton Trans.* **1975**, 1663.

12. Mainz, V.V.; Andersen, R.A. *Organometallics*, **1984**, *3*, 675.

13. In related systems, reductive elimination has been shown to occur from *cis*- complexes and not from the analogous *trans* isomers: a) Gillie, A.; Stille, J.K. *J. Am. Chem. Soc.*

1980, *102*, 4933. b) Ozawa, F.; Ito, T.; Nakamura, Y.; Yamamoto, A. *Bull. Chem. Soc. Jpn.* 1981, *54*, 1868.

14. (a) Chatt, J.; Hayter, R.G. *J. Chem. Soc.* 1961, 896. (b) Sullivan, B.P.; Meyer, T.J. *Inorg. Chem.* 1982, *21*, 1037. (c) Mezzetti, A.; Delzotto, A.; Rigo, P. *J. Chem. Soc., Dalton Trans.* 1989, 1045; 1990, 2515. (d) Clark, S.F.; Peterson, J.D. *Inorg. Chem.* 1983, *22*, 620.

15. a) Bianotti, C.; Green, M.L.H. *J. Chem. Soc., Chem. Commun.* 1972, 1114. b) Green, M.L.H. Pure Appl. Chem. 1978, *50*, 27. c) Geoffroy, G.L.; Bradley, M.G.; Peirantozzi, R. *Adv. Chem. Ser.* 1978, *167*, 181. d) Pivovarov, A.P.; Gak, Y.V.; Sjul'ga, Y.M.; Makhaev, V.D.; Borisov, A.P. *Izv. Akad,. Nauk. USSR, Ser. Khim.* 1979, 2590, 1207. e) Wrighton, M.S.; Graff. J.L.; Kazlauskas, R.J.; Mitchener, J.C.; Reichel, C.L.; Pure Appl. Chem. *1982 54*, 161. f) Green, M.A.; Huffman, J.C.; Caulton, K.G. *J. Organomet. Chem.* 1983, *243*, C78. g) Wink, D.A.; Ford, P.C. *J. Am. Chem. Soc.* 1986, *108*, 4838.

16. Hartwig, J.F.; Andersen, R.A.; Bergman, R.G., unpublished results.

17. For related studies of cyclometallation and hydrogenation reactions involving phosphine dissociation see: (a) Hartwig, J.F.; Andersen, R.A.; Bergman, R.G. *J. Am. Chem. Soc.* 1989, *111*, 2717. (b) Foley, P.; DiCosimo, R.; Whitesides, G.M. *J. Am. Chem. Soc.* 1980, *102*, 6713. (c) Reamey, R.H.; Whitesides, G.M. *J. Am. Chem. Soc.* 1984, *106*, 81.

18. Statler, J.A.; Wilkinson, G.; Thornton-Pett, M.; Hursthouse, M.B. *J. Chem. Soc., Dalton Trans.* 1984, 1731.

19. Wong, W-K.; Kwok, W.C.; Statler, J.A.; Wilkinson, G. *Polyhedron*, 1984, *3*, 1255.

20. A theoretical study has been conducted on the microscopic reverse, oxidative addition of C-H bonds to d^8 metal centers: Saillard, J.-Y.; Hoffmann, R. *J. Am. Chem. Soc.* 1984, *106*, 2006.

21. (a) Hartwig, J.F.; Andersen, R.A.; Bergman, R.G. *J. Am. Chem. Soc.* **1989**, *111*, 2417. (b) Hartwig, J.F.; Bergman, R.G.; Andersen, R.A. *J. Am. Chem. Soc.* **1990**, *112*, 5670. (c) Chapter 4. (d) Chapter 3.

22. Bergman, R.G.; Buchanan, J.M.; McGhee, W.D.; Periana, R.A.; Seidler, P.F.; Trost, M.K.; Wenzel, T.T. In *Experimental Organometallic Chemistry: A Practicum in Synthesis and Characterization*; Wayda, A.L.; Darensbourg, M.Y., Eds.; ACS Symposium Series 357; American Chemical Society: Washington, DC, 1987, p 227.

Chapter 3

The Structure, Synthesis and Chemistry of $(PMe_3)_4Ru(\eta^2\text{-Benzyne})$. Reactions with Arenes, Alkenes, and Heteroatom-containing Organic Compounds. Synthesis and Structure of a Monomeric Hydroxide Complex.

Introduction

Many organic and main group organometallic reactive intermediates are stable when coordinated to transition metal fragments. The most extensively studied example is probably the transition metal carbene complex.[1] Molecules posessing unstable double or triple bonds have been generated at transition metal centers and have been shown to be stabilized by this interaction: silene[2], disilene[3], ketene[4], benzyne and cycloalkyne[5,6] transition metal complexes are a few examples. In most cases the complexes do not display reactivity similar to that of the free molecule. Yet, studies are beginning to indicate that these complexes display enhanced reactivity over typical M-X bonds. One type of molecule for which the reactivity has been recently developed is the transition metal benzyne complex.

Much of the study of the early metal benzyne complexes has involved addition and insertion reactions involving functionalized organic molecules. These overall transformations cleave a metal-carbon bond of the benzyne complex and form a new metal-nitrogen or metal-oxygen bond in the product, processes which are typically favorable for early metal complexes. In contrast, late transition metal benzyne and cycloalkyne complexes have shown more limited reactivity. They undergo addition reactions with acidic reagents such as alcohols and ketones, but not with amines; they undergo insertion reactions with CO, CO_2, and unsaturated hydrocarbons, but not with ketones, aldehydes, or nitriles.[6b,c] The lack of reactivity of these complexes toward these reagents is consistent with the well established reactivity of late metal alkyl and aryl complexes.[7]

We report the isolation of a benzyne complex of ruthenium which is generated by the same overall transformation used to form early transition metal benzyne complexes,[6f-i] but by a mechanism typical of late transition metal compounds.[7] The ruthenium complex displays reactivity more characteristic of early than late transition metal-carbon bonds; it readily undergoes addition reactions with weak acids and insertion reactions with aldehydes and nitriles, forming ruthenium-oxygen or ruthenium-nitrogen bonds. Thus, this material provides an easily accessible and

versatile starting material for entry into the study of late transition metal heteratom-containing molecules.[8]

Results

Formation of 2, Crystal Structure, and Kinetic Analysis. Synthesis of the ruthenium benzyne complex $(PMe_3)_4Ru(\eta^2\text{-}C_6H_4)$ is shown in Scheme 1. Two methods were developed. Method B was more convenient for preparative scale reactions of 1, while method A allowed for isolation of the intermediate complex $(PMe_3)_4Ru(Me)(Ph)$. A typical preparative scale reaction involved addition of 2.2 equivalents of PhMgBr to 1.5 g of $(PMe_3)_4Ru(Cl)_2$ in ether, followed by heating of the resulting solution at 85 °C for 8h. This provided samples of 1 in 55-70% yield which were pure enough without crystallization for synthetic purposes. Complex 1 was isolated in analytically pure form by crystallization from pentane at -40° C. Alternatively, 1 could be prepared by the addition of PhMgBr to the known $(PMe_3)_4Ru(Me)(Cl)$[11a] to provide $(PMe_3)_4Ru(Me)(Ph)$ (2) in 20% yield after crystallization. Thermolysis of 2 in benzene-d_6 at 110 °C for 12 h provided 1 in 95-100% yield by ^1H NMR spectroscopy. The benzyne complex 1 is a white crystalline solid which is extremely air sensitive but can be stored in a drybox at room temperature for months without decomposition. The ^1H NMR spectrum of 1 showed two broad resonances in the aromatic region at δ7.26 and δ7.31, while the $^{31}P\{^1H\}$ NMR spectrum consisted of a second order A_2B_2 spectrum; this spectrum along with a simulation is shown in Figure 1.

Slow cooling of a pentane solution of 1 provided crystals which were suitable for an X-ray diffraction study. The complex crystallized in space group $P2_1/n$, and showed no unusually short intermolecular contacts. The structure was solved by Patterson methods and refined *via* standard least-squares and Fourier techniques. An ORTEP drawing of 1 is shown in Figure 2; acquisition parameters, intramolecular distances and intramolecular angles are provided in Tables 1-3. The coordination of the ruthenium atom can be described as a trigonal-bipyramid or a distorted octahedron. The atoms P2, P4, Ru, C1, and C2 all lie in a plane with deviations of +/- 0.02 Å. This plane forms an angle of less than 4° to the plane of the benzyne ligand. The angle P1-Ru-P3 is 165° and is bent away from the other two phosphorus atoms. The

Scheme 1

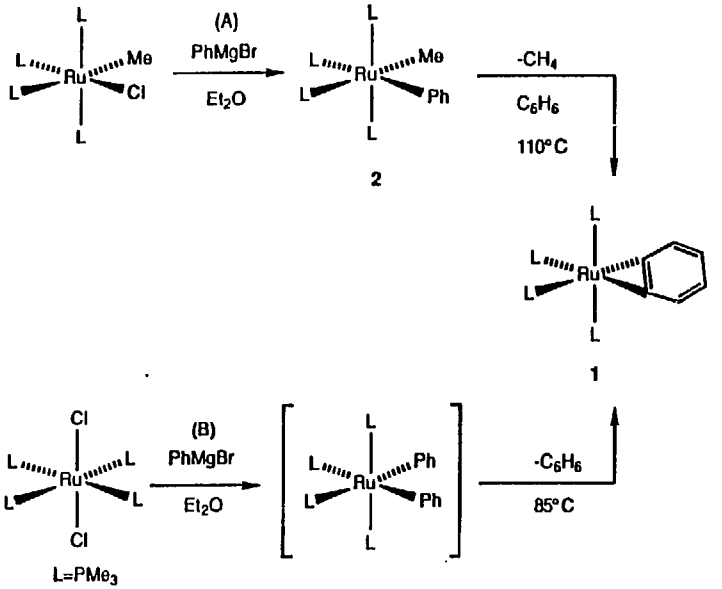

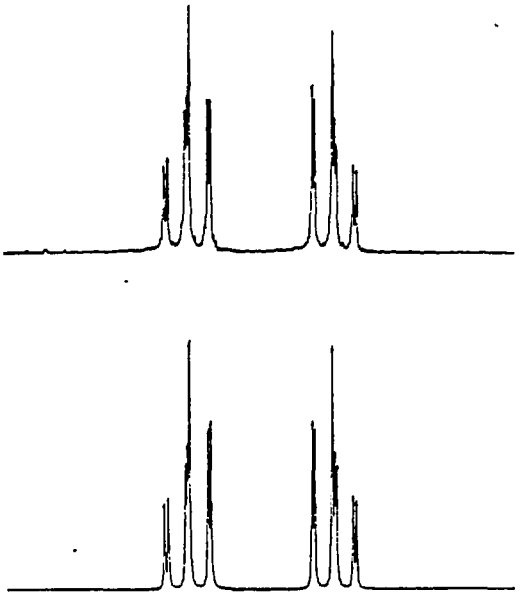

Figure 1. Experimental (top) and calculated (bottom) $^{31}P\{^{1}H\}$ NMR spectra of **1**.

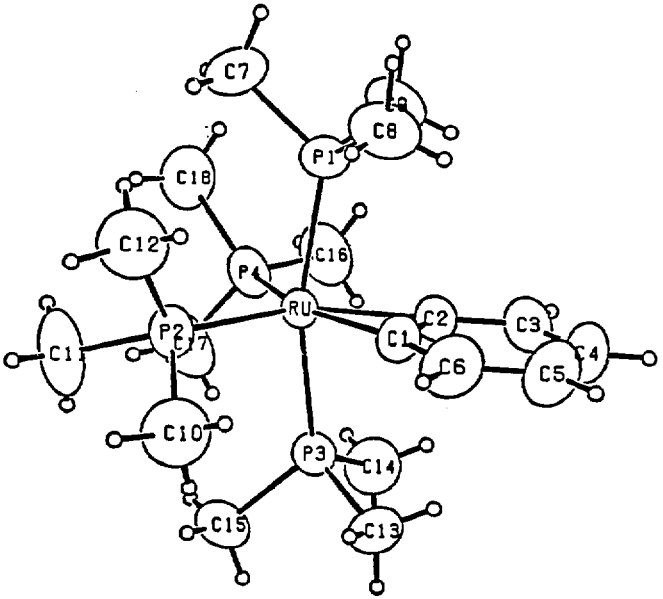

Figure 2. ORTEP drawing of 1.

Table 1. Crystal and Data Collection Parameters.[a]

	1	**9**	**15**
Temperature (°C)	25	-118	-89
Empirical Formula	$RuP_4C_{18}H_{40}$	$RuP_4OC_{18}H_{42}$	$RuP_4NC_{25}H_{45}$
Formula Weight (amu)	481.5	499.5	584.6
Crystal Size (mm)	0.20 x 0.25x 0.50	0.25x 0.29 x 0.30	0.15 x 0.15 x 0.25
Space Group	$P2_1/n$	P1	$P2_12_12_1$
a (Å)	9.4492(10)	8.698(1)	9.722(3)
b (Å)	15.9489(17)	16.423(3)	14.191(6)
c (Å)	16.3007(19)	17.097(3)	20.462(6)
α (°)	90.0	80.858(13)	90.0
β (°)	91.528(9)	84.741(12)	90.0
γ (°)	90.0	88.540	90.0
V ($Å^3$)	2455.7(8)	2400.9(9))	2823.0(0)
Z	4	4	4
d_{calc} (gcm^{-3})	1.30	1.38	1.38
μ_{calc} (cm^{-1})	8.8	9.1	7.8
Reflections Measured	+h, +k, ±l	+h, +k, ±l	+h, +k, +l
Scan Width	$\Delta\theta = 0.65 + 0.35 \tan\theta$	$\Delta\theta = 0.65 + 0.35 \tan\theta$	$\Delta\theta = 1.20 + 0.35 \tan\theta$
Scan Speed (θ, °/m)	6.70	6.70	6.70
Setting Angles (2θ, °)[b]	24-28	24-28	24-28

(a) Parameters common to all structures: Radiation: Mo Kα (λ = 0.71073 Å), except for **1c** λ = 0.70930 Å. Monochromator: highly-oriented graphite (2θ = 12.2°). Detector: crystal scintillation counter, with PHA. 2θ Range: 3-->45°, except for **1c** 2-->45°. Scan Type: θ-2θ. Background: Measured over 0.25(Δθ) added to each end of the scan. Vertical Aperture = 3.0 mm. Horizontal Aperture = 2.0 + 1.0 tanθ mm. Intensity Standards: Measured every hour of x-ray exposure time. Orientation: 3 reflections were checked after every 200 measurements. Crystal orientation was redetermined if any of the reflections were offset from their predicted positions by more than 0.1°. Reorientation was required twice for **1b** and **7a**, and once for **8**. (b) Unit cell parameters and their esd's were derived by a least-squares fit to the setting angles of the unresolved Mo Kα components of 24 reflections with the given 2θ range. In this and all subsequent tables the esd's of all parameters are given in parentheses, right-justified to the least significant digit(s) of the reported value.

Table 2. Intramolecular Distances for 1.

ATOM 1	ATOM 2	DISTANCE
RU	P1	2.354(1)
RU	P2	2.303(1)
RU	P3	2.328(1)
RU	P4	2.319(1)
RU	C1	2.072(2)
RU	C2	2.111(2)
C1	C2	1.355(3)
C1	C6	1.382(3)
C2	C3	1.372(3)
C3	C4	1.411(4)
C4	C5	1.363(4)
C5	C6	1.398(4)
P1	C7	1.854(3)
P1	C8	1.827(3)
P1	C9	1.823(3)
P2	C10	1.840(3)
P2	C11	1.816(3)
P2	C12	1.827(3)
P3	C13	1.820(3)
P3	C14	1.826(3)
P3	C15	1.844(3)
P4	C16	1.831(3)
P4	C17	1.839(3)
P4	C18	1.834(3)

Table 3. Intramolecular Angles for 1.

ATOM 1	ATOM 2	ATOM 3	ANGLE
P1	RU	P2	98.01(2)
P1	RU	P3	165.11(2)
P1	RU	P4	92.18(2)
P2	RU	P3	95.11(2)
P2	RU	P4	103.35(2)
P3	RU	P4	91.57(2)
P1	RU	C1	85.40(6)
P1	RU	C2	83.33(6)
P2	RU	C1	101.79(6)
P2	RU	C2	139.53(6)
P3	RU	C1	85.09(6)
P3	RU	C2	82.15(6)
P4	RU	C1	154.83(7)
P4	RU	C2	117.06(6)
C1	RU	C2	37.78(8)
RU	C1	C2	72.71(13)
RU	C1	C6	164.9(2)
RU	C2	C1	69.52(12)
RU	C2	C3	168.4(2)
C2	C1	C6	122.2(2)
C1	C2	C3	121.8(2)
C2	C3	C4	116.9(3)
C3	C4	C5	121.1(2)
C4	C5	C6	121.1(3)
C1	C6	C5	116.8(3)
RU	P1	C7	123.90(11)
RU	P1	C8	116.23(10)
RU	P1	C9	114.35(10)
C7	P1	C8	98.7(2)
C7	P1	C9	100.4(2)
C8	P1	C9	99.3(2)
RU	P2	C10	113.68(11)
RU	P2	C11	124.15(11)
RU	P2	C12	118.73(11)
C10	P2	C11	99.6(2)
C10	P2	C12	96.7(2)
C11	P2	C12	99.1(2)
RU	P3	C13	116.59(10)
RU	P3	C14	115.35(9)
RU	P3	C15	122.52(9)
C13	P3	C14	98.44(14)
C13	P3	C15	98.93(13)
C14	P3	C15	101.03(13)
RU	P4	C16	115.66(10)
RU	P4	C17	120.99(10)
RU	P4	C18	120.64(11)
C16	P4	C17	99.11(14)
C16	P4	C18	99.02(14)
C17	P4	C18	96.9(2)

angles from the axial to the equatorial phosphorous atoms range from 91.6 ° to 98.0 °, and the P-Ru-P angle in the equatorial plane is 103.4°. The four Ru-P distances are unequal, though they fall into a pattern. The mutually trans phosphorus distances are longer than those trans to the benzyne ligand. The average Ru-P(1,3) distance is 2.341 ± 0.013 Å and the average Ru-P(2,4) distance is 2.311 ± 0.004 Å. The Ru-C distances are different in the solid state, Ru-C(1)=2.072(2) Å and Ru-C(2)=2.111(2) Å, as are the P-Ru-C angles, P(2)-Ru-C(1)=139.53(6) ° and P(4)-Ru-C(2)=117.06(6) °, although no asymmetry is observed in the solution spectroscopy. The source of this asymmetry does not seem to be due to sterric crowding since there are no short intramolecular contacts within the coordination sphere; we are inclined to view that the asymmetry is due to solid state effects and that these two bonds are not chemically different. These two Ru-C bond distances are slightly shorter than the Ru-aryl bond in $(PMe_3)_4Ru(\eta^2\text{-}CH_2C_6H_4)$.[9] The average of the C-C bond distances in the benzyne ligand (1.385 ± 0.015 Å) is close to that found for free benzene (1.392 by x-ray diffraction),[10] as has been the case for the other structurally characterized benzyne complexes.[5] Therefore the sturcture of **1** can be considered to be a Ru(II) complex with two short metal-carbon σ-bonds.

The rate of formation of benzyne complex **1** from the methyl phenyl complex **2** was measured at 110 °C in benzene. The reaction was followed by monitoring the disappearance of the phosphine resonance of **2** at 0.96 ppm in samples containing between 1.70×10^{-3} M and 1.87×10^{-2} M concentrations of phosphine. At all concentrations of phosphine, the reaction displayed clean first order kinetic behavior. The plot of a typical kinetic run (0.0085 M PMe_3) is shown in Figure 3, and a plot of k_{obs} vs 1/[P] is shown in Figure 4, clearly demonstrating an inverse dependence of rate on phosphine concentration.

Addition of C-H, N-H, and O-H bonds. The reactions of **1** with C-H bonds are shown in Scheme 2. Thermolysis of **1** in C_6D_6 provided the deuterated benzyne complex $(PMe_3)_4Ru(\eta^2\text{-}C_6D_4)$, indicating that the formation of the benzyne complex by method B (Scheme 1) is reversible. Complex **1-d_4** was identified by the absence of aromatic resonances in the ^1H NMR spectrum of the reaction mixture and the presence of the benzyne resonances in the

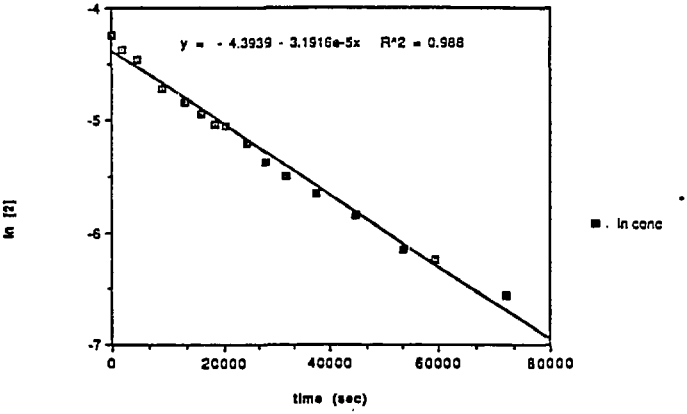

Figure 3. Typical first order plot ([L] = 3.97 mM) for the formation of 1 from 2.

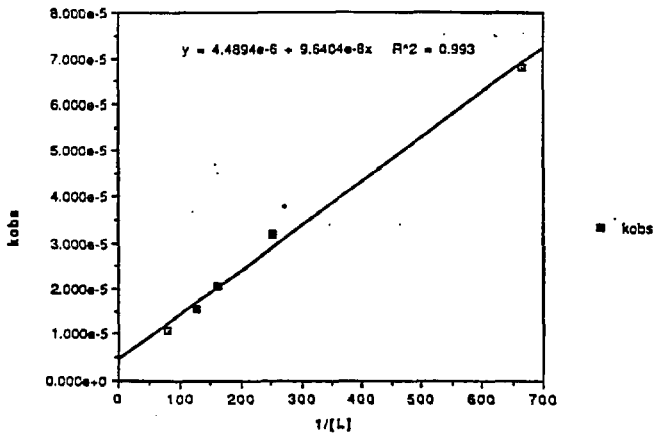

Figure 4. Plot of k_{obs} versus 1/[L] for the formation of **1** from **2**.

Scheme 2

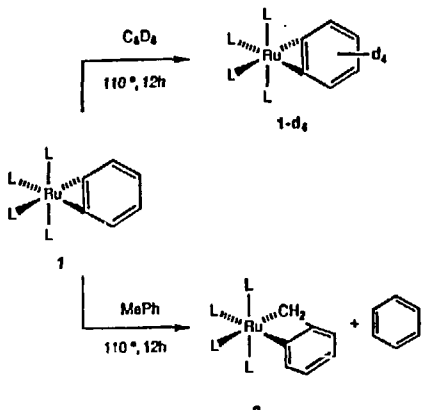

Scheme 3

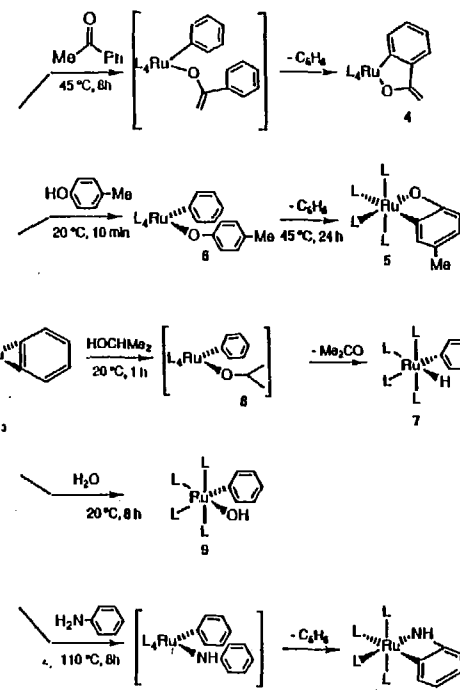

^{2}H NMR spectrum. The appearance of $^{31}P\{^1H\}$ NMR spectrum of the deuterated complex was unchanged from the undeuterated sample. A simulation of the EI mass spectrum of the final reaction mixture showed that the starting complex **1** had been converted to 80-90 % **1-d$_4$**. A more accurate simulation was made difficult by the large number of ruthenium isotopes. Thermolysis of **1** in toluene at 110 °C for 2 d resulted in formation of the known orthometallated benzyl compound **3**[11] in essentially quantitative yield by $^{31}P\{^1H\}$ NMR spectroscopy. Complex **1** was extremely thermally stable in alkane solvents. Thermolysis in pentane at 145 °C for 8 h resulted in no detectable decomposition or reaction with solvent.

Addition reactions of functionalized organic compounds to **1** are shown in Scheme 3. One equivalent of acetophenone reacted with **1** at 45 °C for 8h to form the orthometallated, O-bound, enolate complex **4** in 45% yield. This complex was also the product of the addition of acetone to **1**, a reaction that will be reported in detail in a separate publication. Addition of acetophenone to **1-d$_4$** yielded **4-d$_0$**, as determined by integration of the ^1H NMR spectrum of the product (Scheme 4). Treatment of **1** with one equivalent of *p*-cresol in toluene, followed by heating to 45° C for 24 h, provided the previously reported orthometallated cresolate complex **5**[12] in 70% yield. This reaction was monitored after the addition of the *p*-cresol. *p*-Cresol was added to **1** at room temperature, and the reaction was quickly cooled to -78 °C. ^1H and $^{31}P\{^1H\}$ NMR spectroscopy showed that all of the benzyne complex **1** had reacted to form a complex which was stable at this temperature. This intermediate was not isolated, but the ^1H and $^{31}P\{^1H\}$ NMR spectra were consistent with a compound of structure $(PMe_3)_4Ru(Ph)(OC_6H_4Me)$ (**6**). The formation of **5** from **6** required 24 h at 45 °C.

The qualitative rates of reaction of benzyne complex **1** with p-cresol and of phosphine dissociation from **1** were evaluated. Four equivalents of PMe_3-d_9 were added to **1**, and a $^{31}P\{^1H\}$ NMR spectrum was obtained after 10 min, 2h, and 24 h at 25 °C. After 10 min the ratio of free PMe_3-d_9 to PMe_3-d_0 was 36:1, after 2h the ratio was roughly 2:1, and after 24 h it was 1:1. These results demonstrate that the reaction of p-cresol with **1** to form **6** occured much faster than phosphine dissociation.

Scheme 3

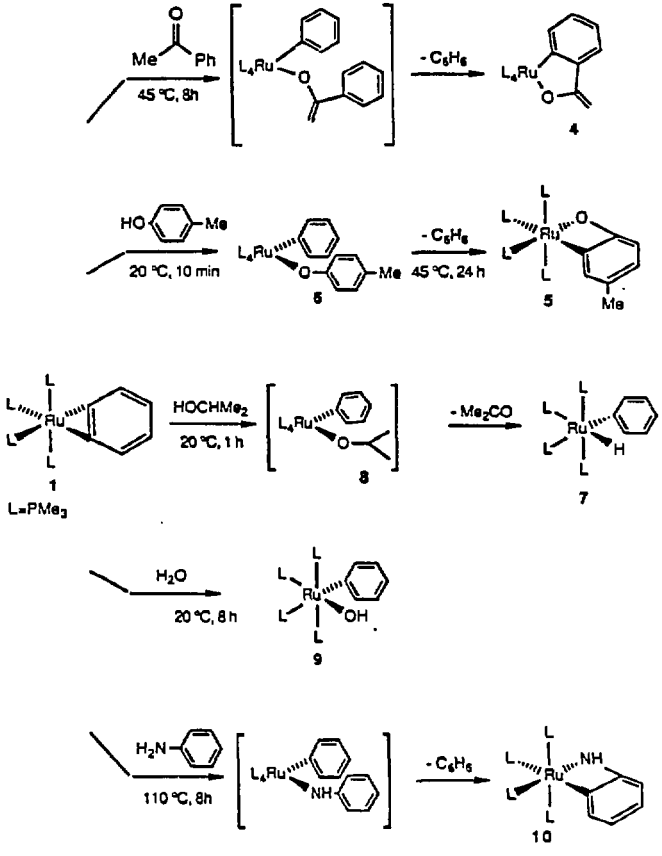
Me
Ph
45 °C, 8h
L4Ru
- C6H6
4
HO
Me
20 °C, 10 min
5
45 °C, 24 h
L
Ru
O
Me
HOCHMe2
20 °C, 1 h
8
- Me2CO
H
7
1
L=PMe3
H2O
20 °C, 8 h
OH
9
H2N
110 °C, 8h
NH
10

Scheme 4

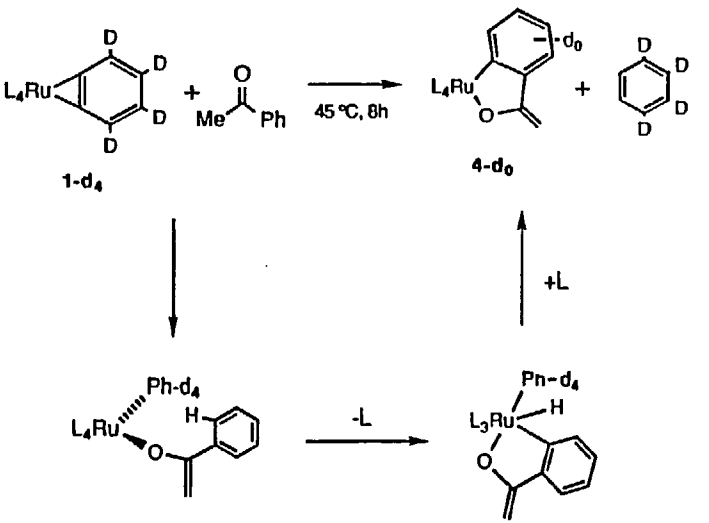
D
D
D
D
L4Ru
+
O
Me
Ph
45 °C, 8h
L4Ru
O
-d0
D
D
D
+
1-d4
4-d0
+L
Ph-d4
H
L4Ru
O
-L
Ph-d4
H
L3Ru
O

Less acidic O-H bonds such as those in isopropanol and water also formally add across the Ru-C bond in **1**. Treatment of **1** with one equivalent of isopropanol led to the phenyl hydride complex **7** in 56% isolated yield. This reaction presumably proceeds by initial addition of the alcohol to **1**, forming a phenyl isopropoxide intermediate **8**, similar to the intermediate observed with the addition of *p*-cresol. Intermediate **8** then leads to **7** by β-hydrogen elimination. Reaction of **1** with water does not afford the possibility of β-hydrogen elimination, and addition of one equivalent of water yielded the phenyl hydroxide complex **9** in 62% yield after crystallization from pentane. Solution spectroscopic analysis of this complex was complicated by broad aryl resonances due to hindered rotation of the phenyl group at room temperature. Therefore, ^{1}H and $^{13}C\{^{1}H\}$ NMR spectra were obtained at -40 °C. At this temperature rotation of the ring was slow, compared to the NMR time scale, and all aryl protons and carbon atoms were inequivalent. The hydroxide moiety was identified by a sharp resonance in the ^{1}H NMR spectrum at δ-4.47 and a sharp band in the solid state infrared spectrum (Nujol) at 3636 cm^{-1}. Similar spectroscopic features are found in related iridium[13] and platinum hydroxide[14] complexes. The structural assignment was confirmed by the $^{31}P\{^{1}H\}$ NMR spectrum, which displayed an A_2BC pattern with one cis phosphine resonating upfield and one resonating downfield from the mutually trans phosphines, indicating that one PMe_3 is located trans to the aryl ring and the other is trans to the hydroxide.

Due to the small number of structurally characterized monomeric hydroxide complexes an X-ray diffraction study was performed on a single crystal of **9**. Suitable crystals were obtained by slow cooling of a pentane solution of **9**. The structure was solved by Patterson methods and refined *via* standard least-squares and Fourier techniques. The crystal contained two molecules in the asymmetric unit; an ORTEP drawing of one of the molecules is shown in Figure 5. Acquisition parameters are included in Table 1; intramolecular distances and angles are provided in Tables 4 and 5. The crystal contained discrete monomers. No hydrogen bonding was observed between the ruthenium complexes, and no water of solvation was observed, confirming that this synthesis is particularly useful since it provides hydroxide complexes which are free of

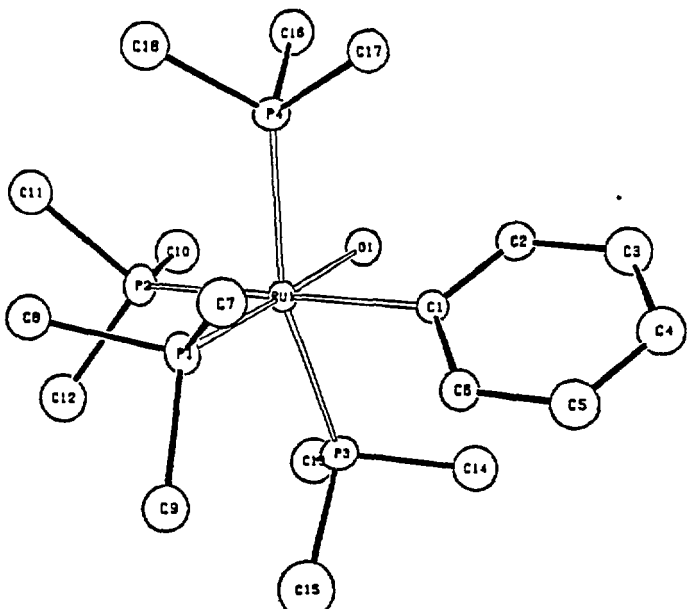

Figure 5 ORTEP drawing of 9. The hydrogen atoms have been removed for clarity.

Table 4. Intramolecular Distances for 9.

ATOM 1	ATOM 2	DISTANCE
RU1	P1	2.286(1)
RU1	P2	2.354(1)
RU1	P3	2.379(1)
RU1	P4	2.332(1)
RU1	O1	2.168(3)
RU1	C1	2.159(5)
C1	C2	1.384(7)
C1	C6	1.426(7)
C2	C3	1.412(7)
C3	C4	1.380(8)
C4	C5	1.414(8)
C5	C6	1.417(7)
P1	C7	1.844(6)
P1	C8	1.851(5)
P1	C9	1.851(6)
P2	C10	1.851(6)
P2	C11	1.866(6)
P2	C12	1.834(6)
P3	C13	1.839(6)
P3	C14	1.834(6)
P3	C15	1.845(7)
P4	C16	1.829(6)
P4	C17	1.833(5)
P4	C18	1.857(6)

Table 5. Intramolecular Angles for 9.

ATOM 1	ATOM 2	ATOM 3	ANGLE
P1	RU1	P2	94.71(5)
P1	RU1	P3	103.82(5)
P1	RU1	P4	91.65(5)
P1	RU1	O1	179.27(10)
P1	RU1	C1	93.37(13)
P2	RU1	P3	93.01(5)
P2	RU1	P4	94.10(5)
P2	RU1	O1	84.58(9)
P2	RU1	C1	171.58(13)
P3	RU1	P4	162.37(5)
P3	RU1	O1	76.07(10)
P3	RU1	C1	82.75(13)
P4	RU1	O1	88.57(10)
P4	RU1	C1	88.03(13)
O1	RU1	C1	87.34(15)
RU1	C1	C2	121.2(4)
RU1	C1	C6	122.5(3)
C2	C1	C6	116.0(4)
C1	C2	C3	123.2(5)
C2	C3	C4	120.5(5)
C3	C4	C5	118.8(5)
C4	C5	C6	119.8(5)
C1	C6	C5	121.7(5)
RU1	P1	C7	117.99(18)
RU1	P1	C8	120.70(18)
RU1	P1	C9	120.82(19)
C7	P1	C8	96.89(25)
C7	P1	C9	99.1(3)
C8	P1	C9	96.24(25)
RU1	P2	C10	114.02(19)
RU1	P2	C11	123.58(19)
RU1	P2	C12	118.58(19)
C10	P2	C11	97.9(3)
C10	P2	C12	102.1(3)
C11	P2	C12	96.6(3)
RU1	P3	C13	116.53(20)
RU1	P3	C14	114.79(20)
RU1	P3	C15	125.45(23)
C13	P3	C14	97.8(3)
C13	P3	C15	98.5(3)
C14	P3	C15	98.9(3)
RU1	P4	C16	111.85(19)
RU1	P4	C17	120.03(18)
RU1	P4	C18	123.86(19)
C16	P4	C17	101.14(25)
C16	P4	C18	95.7(3)
C17	P4	C18	96.23(25)

hydrogen-bound water. The coordination at ruthenium is pseudooctahedral with the phenyl ring and hydroxide group occupying mutually cis sites. The hydrogen atom of the hydroxide moiety was not located. The ruthenium-oxygen distance is 2.168(3) Å, slightly longer than the iridium-oxygen distance of 2.119(5) Å in $[(PMe_3)_4Ir(H)(OH)]PF_6$;[12] the ruthenium aryl distance is 2.159(5) Å, slightly longer than the $(PMe_3)_4Ru$-aryl bonds contained in the metallacycles described in this work and in $(PMe_3)_4Ru(\eta^2\text{-}CH_2C_6H_4)$.[8] The Ru(1)-P(1) bond length, the metal-phosphorus distance corresponding to the ligand located trans to the hydroxide substituent, is significantly shorter than the other ruthenium-phosphorus distances, consistent with a hydroxide ligand having a weak trans influence. The weaker trans influence of the hydroxide substituent in $[(PMe_3)_4Ir(H)(OH)]^+$ relative to that of the hydride or phosphine ligands is also demonstrated by the metal-phosphorus distances, 2.259(2) Å trans to the hydroxide, 2.369(2) Å trans to the hydride, and 2.337 for the mutually trans phosphines.

Addition of aniline to the ruthenium benzyne complex **1** resulted in the formation of the orthometallated anilide complex **10** in 98% yield by ^1H NMR spectroscopy and 68% isolated yield. Complex **10** was identified by conventional spectroscopic techniques and microanalysis. The ^1H NMR spectrum showed four aromatic resonances, and the $^{13}C\{^1H\}$ NMR spectrum contained a doublet of doublet of quartets resonance, corresponding to a quaternary aryl carbon atom, indicating that metallation of the ring had occurred. The $^{31}P\{^1H\}$ NMR spectrum displayed an A_2BC pattern with one phosphine resonating upfield and one downfield of the mutually trans phosphines, similar to the spectrum observed for the phenyl hydroxide complex **9**, and the infrared spectrum contained a stretch at 3336 cm^{-1}.

In light of the results reported for H/D exchange reactions of arylamines with $(PMe_3)_4Ru(D)_2$, which were shown to be catalyzed by trace amounts of water,[15] we were concerned that the addition of aniline to **1** is also catalyzed by amounts of water. As noted above, water adds to **1** to form phenyl hydroxide complex **9**, and addition of aniline to **9** may lead to a phenyl anilide intermediate **11**, as is the case for another ruthenium hydroxide complex.[16] Intermediate **11** could form benzene and **10** by orthometallation as shown in Scheme 5. To

probe this possibility, 1 equiv of aniline was added to phenyl hydroxide **9**, followed by heating to 110 °C for 8h. No formation of **10** was detected. Rather the bridging hydroxide complexes resulting from thermolysis of phenyl hydroxide 9 in the absence of aniline were observed.[17] Although these results suggest that orthometallated anilide **10** does not form directly from **9**, water could be catalyzing this reaction by another mechanism.

The reaction of aniline with 1 takes place at a temperature at which phosphine is rapidly exchanging, and therefore the reaction could proceed by coordination of the amine nitrogen atom to the ruthenium prior to N-H addition. Unfortunately, when monitoring the reaction at 95 °C for 1.5 h in the presence of 5 equivalents of phosphine (0.16 M), the added phosphine appeared to prevent orthometallation of the aryl ring from occurring and led to several reaction products none of which were **10**. These compounds contained resonances between δ -35 and δ -40[18] in the $^{31}P\{^{1}H\}$ NMR spectrum, indicating that cyclometallation of one of the phosphine ligands had occurred to form a metallaphospha-cyclopropane ring (Scheme 5). However, heating this sample for an additional 24 h at 110 °C led to clean formation (81% yield by ^{1}H NMR spectroscopy) of **10**, indicating that these intermediates may be involved in the reactions run in the absence of added phosphine.

Insertion Reactions. The insertion chemistry we have observed with **1** is shown in Scheme 6. Addition of 5-10 equivalents of ethylene to a benzene solution of **1** followed by heating to 85 °C for 8 h resulted in formation of styrene (identified by ^{1}H NMR spectroscopy and GC retention time) and the *bis*-ethylene complex **12**. The organometallic product was independently synthesized by the addition of ethylene to the previously reported complex $(PMe_3)_4Ru(C_2H_4)$[19] and was characterized by conventional spectroscopic techniques. The compound was most clearly identified by its A_2B pattern in the $^{31}P\{^{1}H\}$ NMR spectrum and its two multiplet resonances at δ1.41 and δ1.80 in the ^{1}H NMR spectrum and the two doublet of triplet resonances in the $^{13}C\{^{1}H\}$ NMR spectrum at δ21.14 and δ23.47. The observation of two ethylene resonances in both the ^{1}H and $^{13}C\{^{1}H\}$ NMR spectra is consistent with a rigid structure A in Figure 6, containing two ethylene molecules oriented perpendicular to the axis containing the

Scheme 5

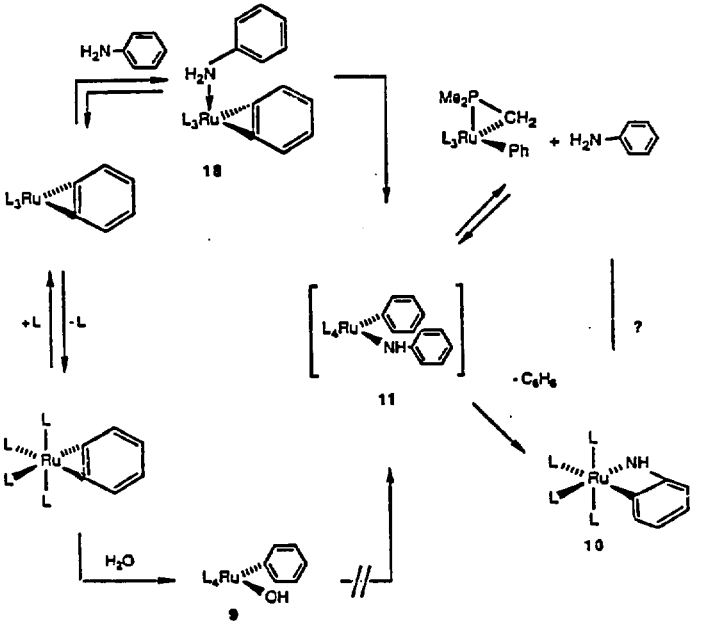
H2N
H2N
L3Ru
18
L3Ru
Me2P
CH2
L3Ru
Ph
+ H2N
+L
-L
L4Ru
NH
11
-C6H6
?
L
L
Ru
L
L
L
L
Ru
NH
L
L
10
H2O
L4Ru
OH
9

Scheme 6

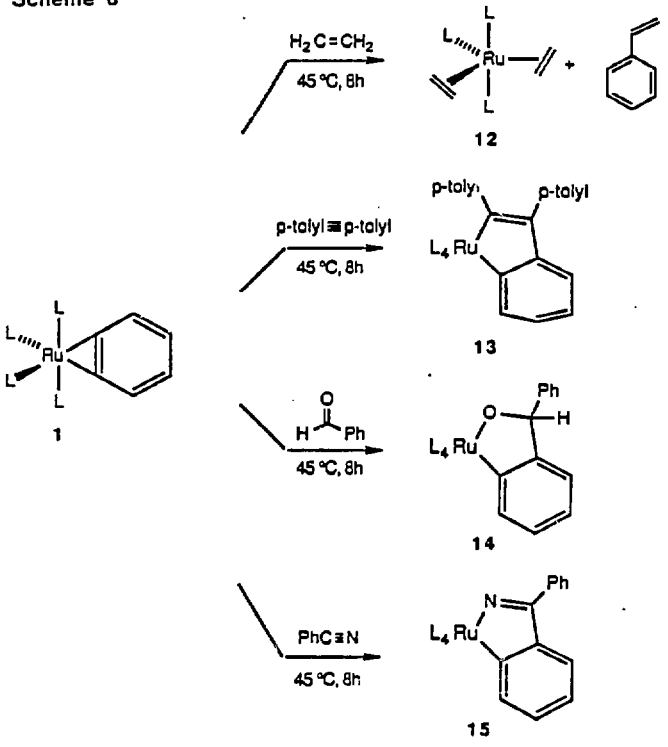
L
L
Ru
L
1
H2C=CH2
45 °C, 8h
12
p-tolyl≡p-tolyl
45 °C, 8h
p-tolyl
p-tolyl
L4Ru
13
O
H
Ph
45 °C, 8h
Ph
O
H
L4Ru
14
PhC≡N
45 °C, 8h
Ph
N
L4Ru
15

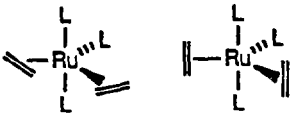

Figure 6. Two possible geometries for $(PMe_3)_3Ru(C_2H_4)_2$ (12).

two trans phosphines, and is inconsistent with structure B, containing two ethylene molecules coordinated parallel to the trans axis.[20] The reaction was run with 5 equivalents of ethylene-1,1-d_2, and a 1:1:1 ratio of the vinylic resonances of the styrene in the final reaction mixture was observed by integration of the ^1H and ^2H NMR spectra of the final reaction mixture.

Insertion of a substituted alkyne would prevent β-hydrogen elimination from occurring. The reaction of one equivalent of di-*p*-tolylacetylene with **1** for 12 h at 85 °C gave rise to the single insertion product **13** in 56% isolated yield. The ^1H and $^{13}C\{^1H\}$ NMR spectra indicated the presence of an *ortho*- substituted aryl ring and two *para*- substituted rings. The $^{31}P\{^1H\}$ NMR spectrum consisted of an A_2BC pattern with both mutually cis phosphine ligands resonating upfield from the mutually trans ones, indicating that they are located trans to two different metal-carbon bonds.

Addition of one equivalent of benzaldehyde to a benzene solution of **1** followed by heating to 45 °C for 8 h led to formation of the single insertion product **14** in 93% yield by ^1H NMR spectroscopy and 32% isolated yield. This product was characterized by conventional spectroscopic techniques and microanalysis. The observation of one ortho-substituted aryl ring in the ^1H and $^{13}C\{^1H\}$ NMR spectra, a resonance at δ5.45 in the ^1H NMR spectrum, and the absence of stretches between 1500 and 1800 cm^{-1} in the infrared spectrum indicated most clearly that **14** was the insertion product. The inequivalence of the mutually trans phosphines in the $^{31}P\{^1H\}$ NMR spectrum was also consistent with this assignment. A second order ABCD pattern was observed, with one of the cis phosphines resonating downfield and one upfield from the mutually trans phosphines, confirming the presence of one ruthenium-oxygen and one ruthenium-carbon bond. The identity of this spin system was confirmed by simulation, which included a trans P-P coupling constant of 332 Hz. The calculated and experimental spectra are shown in Figure 7.

In contrast to these observations, addition of a 5-10 fold excess of pivaldehyde to **1** resulted in no reaction upon heating to 85 °C for 8h, and addition of acetaldehyde did not lead to

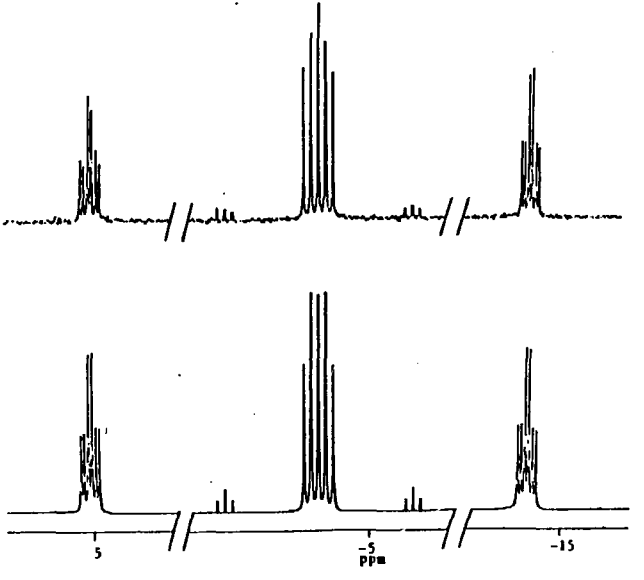

Figure 7. Experimental (top) and calculated (bottom) $^{31}P\{^{1}H\}$ NMR spectra of **14**.

clean reaction. Addition of benzophenone (a ketone without α-hydrogens) did not react with **1** upon heating to 85 °C for 8 h.

Reaction of **1** with one equivalent of benzonitrile did lead cleanly to the insertion product **15** in quantitative yield by ^{1}H NMR spectroscopy and 46% isolated yield. The structure of **15** was inferred from solution NMR and solid state infrared spectroscopy and microanalysis. An infrared absorption band at 1436 cm^{-1} was observed, indicating that insertion had occurred to form a N-metalloimine. Unlike the ^{31}P{^{1}H} NMR spectrum of compound **14**, the spectrum of **15** showed both of the cis phosphine resonances upfield from the resonances corresponding to the mutually trans phosphines, perhaps due the the inability of the metalloimine to act as a π-donor since it is constrained in the metallacycle.

Because of this anomalous ^{31}P{^{1}H} NMR spectrum, the structure of **15** was confirmed by X-ray crystallography. Compound **15** crystallized from pentane in space group $P2_12_12_1$, with no close intermolecular contacts. The structure was solved by Patterson methods and refined *via* standard least-squares and Fourier techniques. An ORTEP drawing of **15** is shown in Figure 8; acquisition parameters are included in Table 1, and metric measure are provided in Tables 6 and 7. The coordination at ruthenium is pseudooctahedral; the ruthenium-carbon bond distance is 2.123 (13)Å, in the range found in other ruthenium aryl compounds,[8] and the metal-nitrogen bond length is 2.108 (13)Å. The metal-phosphine distance trans to the nitrogen is significantly shorter than that trans to the aryl group, as is expected from conventional trans influences.[7]

Addition of other nitriles did not lead to clean reactions. For example, *tert*-butylnitrile did not react with **1** at 85 °C for 12 h, and acetonitrile reacted with **1** under these conditions to yield several products. Several pathways for the reaction of acetonitrile are possible, including exchange of acetonitrile for phosphine ligands, addition of the activated C-H bond, and insertion of the C-N bond. No products were isolated from the reaction with acetonitrile, but ^{31}P{^{1}H} NMR spectroscopy of the crude reaction mixture showed one product with an A_2B pattern and others

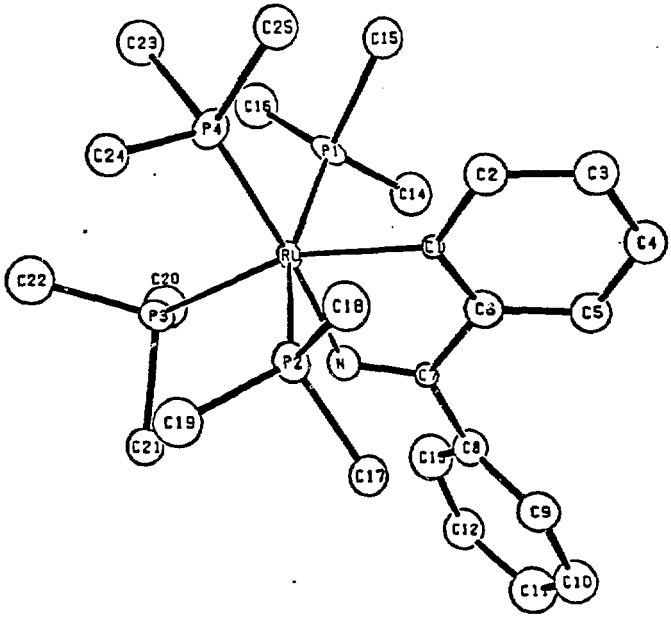

Figure 8. ORTEP drawing of 15. The hydrogen atoms have been removed for clarity.

Table 6. Intramolecular Distances for 15.

ATOM 1	ATOM 2	DISTANCE
RU	P1	2.366(4)
RU	P2	2.323(4)
RU	P3	2.373(4)
RU	P4	2.317(4)
RU	N	2.108(13)
RU	C1	2.123(13)
N	C7	1.26(2)
C1	C2	1.43(2)
C1	C6	1.37(2)
C2	C3	1.41(2)
C3	C4	1.41(2)
C4	C5	1.45(2)
C5	C6	1.42(2)
C6	C7	1.49(2)
C7	C8	1.49(2)
C8	C9	1.38(2)
C8	C13	1.44(2)
C9	C10	1.45(2)
C10	C11	1.47(2)
C11	C12	1.41(2)
C12	C13	1.50(2)
P1	C14	1.845(14)
P1	C15	1.88(2)
P1	C16	1.83(2)
P2	C17	1.836(13)
P2	C18	1.90(2)
P2	C19	1.86(2)
P3	C20	1.86(2)
P3	C21	1.88(2)
P3	C22	1.85(2)
P4	C23	1.86(2)
P4	C24	1.839(15)
P4	C25	1.91(2)

Table 7. Intramolecular Angles for 15.

ATOM 1	ATOM 2	ATOM 3	ANGLE
P1	RU	P2	164.32(15)
P1	RU	P3	98.24(16)
P1	RU	P4	91.28(16)
P1	RU	N	87.7(4)
P1	RU	C1	81.8(4)
P2	RU	P3	96.64(16)
P2	RU	P4	92.19(16)
P2	RU	N	90.4(4)
P2	RU	C1	82.6(4)
P3	RU	P4	95.58(15)
P3	RU	N	78.4(3)
P3	RU	C1	156.7(4)
P4	RU	N	173.7(4)
P4	RU	C1	107.7(4)
N	RU	C1	78.4(5)
RU	N	C7	114.9(10)
RU	C1	C2	128.5(11)
RU	C1	C6	112.8(10)
C2	C1	C6	118.2(14)
C1	C2	C3	120.2(14)
C2	C3	C4	121.3(14)
C3	C4	C5	119.0(14)
C4	C5	C6	117.3(14)
C1	C6	C5	123.9(14)
C1	C6	C7	114.1(15)
C5	C6	C7	121.9(15)
N	C7	C6	119.2(15)
N	C7	C8	120.8(13)
C6	C7	C8	120.0(14)
C7	C8	C9	123.2(15)
C7	C8	C13	114.4(14)
C9	C8	C13	121.5(16)
C8	C9	C10	120.6(16)
C9	C10	C11	120.8(16)
C10	C11	C12	117.2(16)
C11	C12	C13	121.8(16)
C8	C13	C12	117.7(15)
RU	P1	C14	115.7(5)
RU	P1	C15	115.2(5)
RU	P1	C16	126.1(6)
C14	P1	C15	98.2(7)
C14	P1	C16	97.8(7)
C15	P1	C16	99.0(8)
RU	P2	C17	115.8(4)
RU	P2	C18	114.6(5)
RU	P2	C19	125.2(5)
C17	P2	C18	99.7(7)
C17	P2	C19	99.7(7)
C18	P2	C19	97.6(7)
RU	P3	C20	113.5(6)
RU	P3	C21	114.3(5)
RU	P3	C22	125.8(6)
C20	P3	C21	97.6(6)
C20	P3	C22	102.7(8)
C21	P3	C22	98.6(7)
RU	P4	C23	117.1(5)
RU	P4	C24	120.0(5)
RU	P4	C25	122.6(6)
C23	P4	C24	97.3(7)
C23	P4	C25	98.6(8)
C24	P4	C25	96.1(7)

with A_2BC patterns, suggesting that ligand substitution competed with C-H addition and C-N insertion pathways.

In order to determine if phosphine dissociation played a role in the unusual aldehyde and nitrile insertion reactions, these reactions were run in the presence of added phosphine (5 equivalents, 0.16 M). A marked inhibition of the reaction rate for the samples containing added phosphine was observed. The insertion of benzaldehyde was complete after 2.5 h at 45 °C for the sample containing no added phosphine, while the reaction had run to only 28% completion for the reaction run in a 0.16 M solution of PMe_3 in benzene-d_6. Similarly, the nitrile insertion reaction was complete after 2.5 h at 55 °C for the sample containing no added phosphine, but had run to only 57% completion in a 0.16 M solution of PMe_3 in C_6D_6.

Discussion

Mechanism of the Benzyne Formation Reaction. Two possible pathways for the generation of benzyne complex **1** from the methyl phenyl complex **2** are shown in Scheme 7. Pathway A in this scheme is a typical one for orthometallation or γ-elimination reactions of late transition metal complexes,[21] and consists of phosphine dissociation to open a coordination site, followed by oxidative addition of the ortho C-H bond, reductive elimination of methane or benzene, and recoordination of phosphine. Pathway B is the route thought to be followed by early metal systems that form benzyne complexes,[6f-i,22] and presumably would not require phosphine loss; *four-centered addition of the ortho C-H bond across the metal-alkyl bond* would lead directly to product.

The rate laws for these two mechanisms are provided in equations 1 and 2. We observed a linear inverse dependence of k_{obs} on phosphine concentration, consistent with the rate law corresponding to pathway A. Although C-H orthometallation reactions are fairly common, **2** is a rare example of a first metal system to form a benzyne complex by this route. The only other possible example is the rhenium benzyne complex recently prepared.[6d, e] This reaction is favorable, despite generating the unusually reactive organometallic species $(PMe_3)_4Ru(\eta^2\text{-}C_6H_4)$

Scheme 7

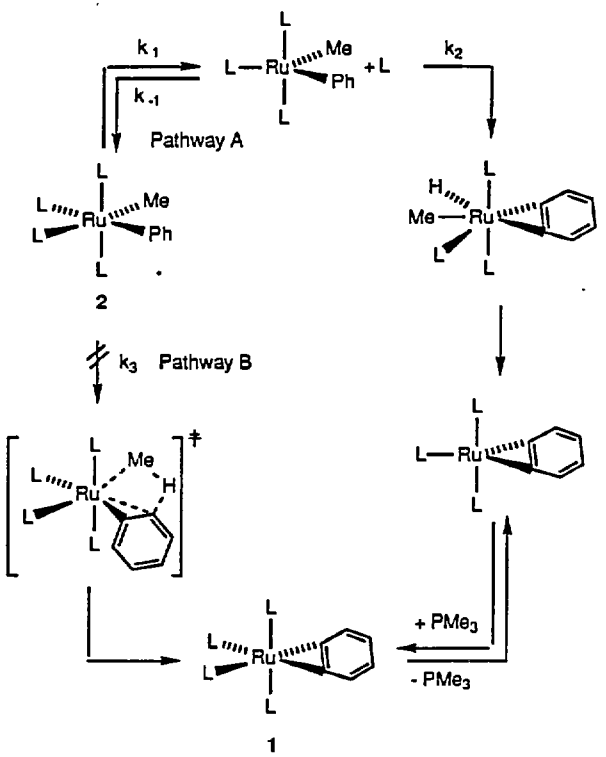

$$\text{Pathway A:}\quad \frac{d[1]}{dt} = \frac{k_1k_2[1]}{k_2 + k_1[L]}\ ;\ k_{obs} = \frac{k_1k_2}{k_2 + k_1[L]} \qquad (1)$$

$$\text{Pathway B:}\quad \frac{d[1]}{dt} = k_3[1]\ ;\ k_{obs} = k_3 \qquad (2)$$

because a strong C-H bond in the methane or benzene byproduct is formed along with **1**. Benzyne or cycloalkyne complexes of other late transition metal systems (i.e in the nickel triad) have been formed by the reduction of a metal halide bound to an *ortho*-halo aryl or α-halo vinyl group.[6b,c]

Mechanism of Addition Reactions. The exchange of the aryl ring in **1** with solvent benzene and the addition of toluene to **1** presumably occurs by the microscopic reverse of the benzyne formation reaction. More specifically, dissociation of phosphine followed by addition of the C-H bond of benzene regenerates diphenyl complex **3** which is the precursor to **1** by method A (Scheme 1). We have no experimental evidence to distinguish between the initial reaction of **1** with a benzylic C-H bond of toluene, followed by orthometallation and initial reaction with the ortho position of the toluene followed by metallation at the benzylic methyl group.

The result of the addition of acetophenone to **1-d$_4$** is consistent with initial addition of the C-H bond of acetophenone or the O-H bond of its enol form. The mechanism in Scheme 4 accounts for the formation of protiated product. Addition of the α-CH bond of the ketone to **1** results in the formation of the O-bound phenyl enolate intermediate.[23] Oxidative addition of the ortho C-H bond followed by reductive elimination of benzene and recoordination of phosphine forms the protiated final product **4**.

In contrast to the aryl C-H addition reactions, the O-H addition reaction with *p*-cresol occurs without prior phosphine dissociation. Reaction of *p*-cresol with the benzyne complex occurred faster than phosphine exchange in **1**, ruling out the possibility (illustrated in Scheme 3) that the unsaturated intermediate resulting from phosphine dissociation undergoes oxidative

addition of the O-H bond in *p*-cresol or that the oxygen of the *p*-cresol forms a complex such as **17** with the unsaturated metal center before addition of the O-H bond. Instead, we propose that reaction of the acidic O-H bond with the highly basic metal center occurs directly to form an intermediate 7-coordinate species **16**. (Scheme 8) This then undergoes reductive elimination to form the phenyl cresolate intermediate **6**, which can be observed by ^1H and $^{31}P\{^1H\}$ NMR spectroscopy. Finally, orthometallation of **6** and reductive elimination of benzene then leads to **5**. Results from the reaction of $(DMPE)_2Fe(H)_2$ (DMPE=1,2-*bis*-dimethylphosphinoethane) with ethanol has shown that even aliphatic alcohols are acidic enough to protonate an L_4M (L=phosphine) metal center. The authors provide low temperature NMR spectroscopic evidence for the ionic species $[(DMPE)_2Fe(H)_2(H)]OEt$.[24]

Although we have not obtained mechanistic data on the reaction of aniline with **1**, it seems likely that this organic substrate is not acidic enough to react with **1** directly. Consistent with this notion, the H/D exchange reactions of arylamines with $(PMe_3)_4Ru(D)_2$ at room temperature were shown to be catalyzed by water.[25] Although addition of aniline to phenyl hydroxide **9** did not lead to formation of orthometallated anilide **10**, an acid catalyst formed under the 110 °C reaction conditions could promote the addition of the aniline N-H bond. Alternatively, initial dissociation of phosphine, coordination of the aniline nitrogen atom to the metal center to form an intermediate such as **18** would enhances the acidity of the N-H proton as shown in Scheme 5, and the reaction of **1** with aniline does occur only at temperatures at which phosphine rapidly dissociates. Coordination of the aniline could promote either direct protonation of the metal-aryl bond, or protonation of the metal center followed by C-H reductive elimination from one side of the benzyne moiety to form the phenyl (anilide) intermediate **11** which gives rise to **10**. Evidence for a similar mechanism was reported for the reaction of phenols with a coordinatively saturated octahedral dialkyl iron compound.[26]

Mechanism of the Reaction of 1 with Ethylene. Two likely pathways for reaction of **1** with ethylene are depicted in Scheme 9. Pathway A involves initial C-H oxidative addition of the C-H bond of ethylene,[27] while pathway B involves initial insertion of ethylene into the M-C

Scheme 8

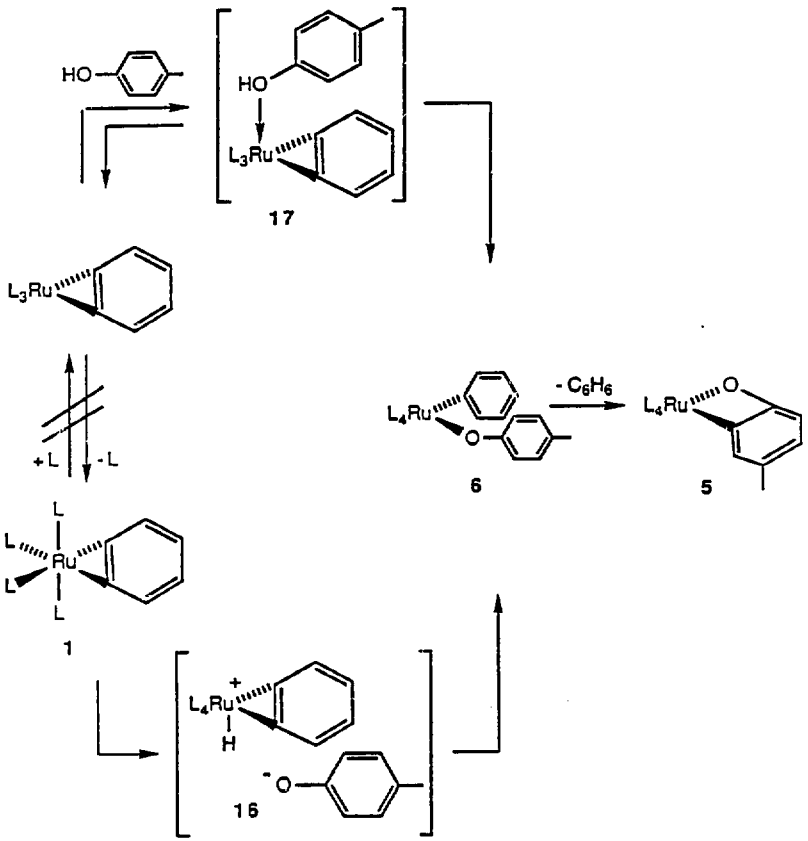

Scheme 9

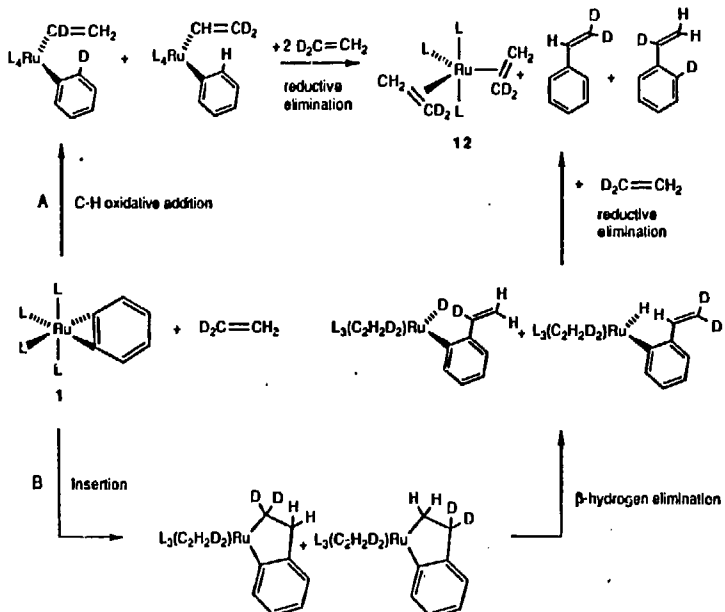
CD=CH2
L4Ru
D
CH=CD2
L4Ru
H
+2 D2C=CH2
reductive elimination
L
Ru
CH2
CD2
CD2
L
12
D
H
D
H
D
H
D
A
C-H oxidative addition
+ D2C=CH2
reductive elimination
L
L
Ru
L
L
1
+ D2C=CH2
L3(C2H2D2)Ru
+ L3(C2H2D2)Ru
B
Insertion
β-hydrogen elimination
L3(C2H2D2)Ru
+ L3(C2H2D2)Ru

bond.[6b,c] The oxidative addition step in pathway A would give rise to a primary isotope effect, and would favor formation of the β, β-d_2-styrene over formation of α, ortho-d_2-styrene. In addition, the rate determining step in a mechanism involving reversible insertion of ethylene would involve cleavage of the β-C-H bond and, again, would give rise to a primary isotope effect. In contrast, *irreversible* insertion of ethylene *via* pathway B would involve cleavage of the C-C double bond in the rate determining step and would give rise to a secondary isotope effect. The observation of a 1:1:1 integrated ratio of vinyl resonances in the ^{1}H NMR spectrum of the reaction mixture is consistent only with pathway B, involving irreversible insertion of ethylene.

We have not investigated the mechanism of the other three insertion reactions in detail, but have obtained qualitative information which indicates that they proceed by initial coordination of the unsaturated substrate, followed by migration of the benzyne carbon to the electrophilic site of the coordinated molecule. This coordination and migration mechanism, which requires initial dissociation of phosphine, would lead to a dependence of rate on phosphine concentration if the phosphine reassociation step is competetive with the addition and migration processes (similar to the kinetic behavior for the benzyne formation reaction). Our observations are consistent with these predictions: each of the insertion reactions proceeds at a rate that is much slower than the rate of phosphine exchange with **1**, and addition of one equivalent of phosphine to the reaction mixture markedly inhibits the rate of the reaction. Although a coordination and migration mechanism are usually invoked for the insertion reactions of carbon monoxide and ethylene into metal alkyl bonds,[7] little mechanistic data is available to support this mechanism for other substrates such as aldehydes and nitriles.

Comparison of Reactivity to other Transition Metal-Carbon Bonds. Benzyne complex **1** displays reactivity which is markedly different from that which has previously been observed for late transition metal-carbon bonds. Addition and insertion reactions with late transition metal-carbon bonds that result in the formation of new M-O or M-N bond are rare.[12,19,28] Transformations such as the reaction of **1** with aniline, which converts a late

transition metal carbon σ-bond to a late metal nitrogen bond of an aryl- or alkylamide substituent, have not previously been observed.[29]

The insertion of benzaldehyde and benzonitrile are also noteworthy. Insertion reactions of aldehydes and ketones with M-C bonds have typically been limited to early transition metal alkyl complexes.[30] Decarbonylation reactions with aldehydes, which proceed by initial addition of the aldehyde C-H bond, are more characteristic of the reactivity of late transition metal complexes.[31] Only recently has the insertion of formaldehyde into a Pt-C bond been observed;[32] prior to this, only insertions involving fluorinated ketones and aldehydes had been reported.[33] The lack of insertion chemistry of aldehyde and ketones with late metal complexes has been attributed to the strong C=O bond strength and formation of a metal alkoxide which would be unstable relative to the starting metal alkyl. To our knowledge, the reaction of **1** with benzonitrile is the first nitrile insertion into a late transition metal alkyl or aryl bond.

Experimental

General. Unless otherwise noted, all manipulations were carried out under an inert atmosphere in a Vacuum Atmospheres 553-2 drybox with attached MO-40-1H Dritrain, or by using standard Schlenk or vacuum line techniques. ^{1}H NMR spectra were obtained on either the 250, 300, 400 or 500 MHz Fourier Transform spectrometers at the University of California, Berkeley (UCB) NMR facility. The 250 and 300 MHz instruments were constructed by Mr. Rudi Nunlist and interfaced with either a Nicolet 1180 or 1280 computer. The 400 and 500 MHz instruments were commercial Bruker AM series spectrometers. ^{1}H NMR spectra were recorded relative to residual protiated solvent. ^{13}C NMR spectra were obtained at either 75.4 or 100.6 MHz on the 300 or 500 MHz instruments, respectively, and chemical shifts were recorded relative to the solvent resonance. Chemical shifts are reported in units of parts per million downfield from tetramethylsilane and all coupling constants are reported in Hz. IR spectra were obtained on a Perkin-Elmer Model 283 infrared spectrometer or on a Perkin-Elmer Model 1550 or 1750 FT-IR spectrometer using potassium bromide ground pellets. Mass spectroscopic (MS) analyses were

obtained at the UCB mass spectrometry facility on AEI MS-12 and Kratos MS-50 mass spectrometers. Elemental analyses were obtained from the UCB Microanalytical Laboratory. Sealed NMR tubes were prepared by fusing Wilmad 505-PP and 504-PP tubes to ground glass joints which were then attached to a vacuum line with Kontes stopcocks or alternatively, the tubes were attached via Cajon adapters directly to Kontes vacuum stopcocks.[34] Known volume bulb vacuum transfers were accomplished with an MKS Baratron attached to a high vacuum line. Unless otherwise specified, all reagents were purchased from commercial suppliers and used without further purification. PMe_3 (Strem) was dried over NaK or a Na mirror and vacuum transferred prior to use. Acetophenone and benzaldehyde were distilled under nitrogen prior to use. Benzyonitrile was purchased from Alpha and used as received. Aniline was dried over a small piece of sodium and distilled under argon. A benzene solution of p-cresol was azeotroped using a Dean-Stark trap, and the p-cresol distilled under argon. Ethylene was purchased from Matheson. Ethylene-1,1-d_2 was purchased from MSD Isotopes and was stated to be 99.6% isotopically pure. Deionized water was degassed by bubbling nitrogen through it for 15 min. PhMgBr and $AlMe_3$ were purchased form Aldrich and used as received. Pentane and hexane (UV grade, alkene free) were distilled from $LiAlH_4$ under nitrogen. Benzene and toluene were distilled from sodium benzopnenone ketyl under nitrogen. Dichloromethane was either distilled under N_2 or vacuum transferred from CaH_2. Deuterated solvents for use in NMR experiments were dried as their protiated analogues but were vacuum transferred from the drying agent.

$(PMe_3)_4Ru(Me)(Cl)$. We found the procedure provided here to be more convenient than the published procedure.[35] In a 250 mL round bottom flask, 1.50g of $(PMe_3)_4Ru(OAc)(Cl)$ was dissolved in 100 mL of toluene. To this stirred solution was added, at room temperature over 3 min, 0.50 mL (0.33 equiv.) of $AlMe_3$ as a 2.0 M solution in toluene. The solution was stirred for 1 h at room temperature over which time a fine white powder formed. The volume of the solution was reduced to 5-10 mL and filtered, while still cold from solvent removal, in order to remove all aluminum salts. The resulting yellow solution was then layered with pentane to yield 0.629 g

(46%) yield of yellow blocks. The supernatant was then cooled to -40 °C to yield an additional 0.246 g (18%) of product.

$(PMe_3)_4Ru(\eta^2\text{-}C_6H_4)$ (1). In a typical preparative scale reaction, a 250 mL flask equipped with a side arm was charged with 1.50 g (3.15 mmol) of $Ru(PMe_3)_4(Cl)_2$[36] and 100 mL of ether and a magnetic stir bar. To a Schlenk tube was added 2.31 mL (2.2 equiv., 6.93 mmol) of PhMgBr as a 3.0 M solution in ether and 5 mL of additional ether. Both vessels were brought out of the drybox, carefully degassed, and charged with argon. It is essential that all solutions be nitrogen free because $Ru(PMe_3)_4(Ph)_2$ forms a complex with nitrogen. The Grignard reagent was added by cannula to the ether slurry of $Ru(PMe_3)_4(Cl)_2$ at room temperature over a 5-10 minute period. The solution was then stirred under argon for ~3 h at room temperature, until no orange, solid $Ru(PMe_3)_4(Cl)_2$ remained. The resulting solution, including magnesium salts, was transferred by cannula to a glass reaction vessel fused to a Kontes vacuum adaptor. The vessel was partially degassed. The vessel was then closed and heated to 85 °C for 8h. The solution turned a dark brown color upon heating; the reaction was complete when the solution became light brown in color while at 85 °C. After this time, the solvent was removed under reduced pressure, and the residue extracted three times with a total of 150 mL of pentane, stirring for 5 min after each addition of pentane. Removal of the pentane solvent provided a pale-yellow or white solid in 55-70% yield which is pure enough (~95%) for synthetic purposes. Crystallization from pentane provided analytically pure samples of 1 in 35-50% yield. IR (Nujol) 2055 (m), 1974 (m), 1931 (m), 1886 (s), 1819, 27.1 (m), 1788 (m), 1767 (m), 1705 (m), 1570 (s), 1523 (m), 1412 (s), 1402 (s), 1316 (s), 1295 (s), 1277 (s), 1188 (m), 1140 (m), 1115 (m), 1070 (m), 1028 (s), 1000 (m), 932 (s), 885 (s), 780 (m), 705 (s), 674 (s), 660 (s), 610 (s); MS (EI) m/e 482(M^+); Anal. Calcd. for $C_{18}H_{40}P_4Ru$: C, 44.90%; H, 8.37%. *Found:* C, 45.17%; H, 8.38%.

X-ray crystal structure determination of 1.

Mounting Procedure. Clear colorless columnar air-sensitive crystals of 1 were obtained by slow crystallization from pentane at -40 °C. End fragments cleaved from some of these crystals were mounted in thin-wall quartz capillaries in an inert-atmosphere glove box, and

then flame sealed. Preliminary precession photographs indicated monoclinic Laue symmetry and yielded approximate cell dimensions.

The crystal used for data collection was transferred to the Enraf-Nonius CAD-4 diffractometer and centered in the beam. Automatic peak search and indexing procedures yielded a monoclinic reduced primitive cell. The final cell parameters and specific data collection parameters for this data set are given in Table 1.

Structure Determination. The 3571 raw intensity data were converted to structure factor amplitudes and their esd's by correction for scan speed, background and Lorentz and posarization effects. Inspection of the intensity standards revealed a gradual reduction in intensity with a sudden jump of about 8% superimposed on it between the 7th and 8th hours of data collection. The data were corrected for this variation. Inspection of the azimuthal scan data showed a variation I_{min}/I_{max} = +/-1% for the average curve. No correction for absorption was applied. Inspection of the systematic absences indicated uniquely space group $P2_1/n$. Removal of systematically absent and redundant data left 3202 unique data in the final data set. The structure was solved by Patterson methods and refined via standard least-squares and Fourier techniques. In a difference Fourier map calculated following the refinement of all non-hydrogen atoms with anisotropic thermal parameters, peaks were found corresponding to the positions of most of the hydrogen atoms. Hydrogen atoms were assigned idealized locations and values of B_{iso} approximately 1.3 (1.2 for bezyne hydrogens) times the B_{eqv} of the atoms to which they were attached. they were included in structure factor calculations, but not refined. Before the final cycles of refinement, eight reflections which appeared to be affected by multiple diffraction were removed from the data set.

The final residuals for 208 variables refined against the 2761 accepted data for which $F^2 > 3\sigma(F^2)$ were R = 2.11%, wR = 2.99% and GOF = 1.542. The R value for all 3194 accepted data was 3.40 %.

The quantity minimized by the least squares program was $\Sigma w(|F_o|-|F_c|)^2$ where w is the weight of a given observation. The p-factor, used to reduce the weight of intense reflections, was

set to 0.03 throughout the refinement. The analytical forms of the scattering factor tables for the neutral atoms were used and all scattering factors were corrected for both the real and imaginary components of anomalous dispersion.

Inspection of the residuals ordered in ranges of $\sin\theta/\lambda$, $|F_o|$, and parity and value of the individual indexes showed no unusual features or trends. The largest peak in the final difference Fourier map had an electron density of 0.36 $e^-/Å^3$. Both were located near the ruthenium atom. There was no indication of secondary extinction in the high-intensity low-angle data.

Positional parameters, thermal parameters of the non-hydrogen atoms, anisotropic thermal parameters, and the positions and thermal parameters of the hydrogen atoms are available as supplementary material.

$(PMe_3)_4Ru(\eta^2\text{-}C_6H_4)$ (**1-d_4**). Unlabeled benzyne complex **1** was dissolved in 1.7 mL of C_6D_6 in a 9" NMR tube. The sample was degassed and the tube sealed. The sample was heated at 110 °C for 3 d in order to provide complete conversion to **1-d_4**. No decomposition products were observed by ^1H or $^{31}P\{^1H\}$ NMR spectroscopy under these conditions. The tube was then opened, the solvent removed, and the residue crystallized from pentane at -40 °C to provide 35.6 mg (54% yield) of **1-d_4**. MS (EI) m/e 486 (M^+).

$Ru(PMe_3)_4(Ph)(Me)$ (2). A round bottom flask was charged in the drybox with 0.708 g (1.55 mmol) of $Ru(PMe_3)_4(Cl)(Me)$ and 100 mL of ether. While stirring this solution, 0.518 mL of a 3.0 M solution of PhMgBr was added at room temperature over 5 min. The solution was stirred for an additional 3 h at room temperature. At this time the solvent was removed under reduced pressure, and the residue was extracted with pentane (3 x 50 mL). The solution was concentrated to a volume of 5-10 mL, and cooled to -40 °C. The material recovered from this crystallization was then recrystallized to yield 153 mg (19.9%) of white crystals of **2** which were analytically pure and suitable for kinetic studies. IR (KBr) 3121 (m), 3101 (m), 3052 (s), 3038 (m), 3025 (s), 2969 (s), 2910 (s), 2471 (w), 2363 (w), 2343 (w), 1967 (w), 1925 (w), 1859 (w), 1637 (w), 1561 (s), 1462 (s), 1429 (w), 1296 (s), 1273 (s), 1237 (w), 1190 (s), 1178 (w), 1058 (w), 1010 (m),

964 (s), 934 (s), 849 (s), 735 (s), 699 (s), 670 (m), 656 (s), 629 (m), 492 (w); MS (EI) m/e 482 (M-CH_4^+); *Anal. Calcd.for* $C_{19}H_{44}P_4Ru$: C, 45.87%; H, 8.91%. *Found:* C, 45.99%; H, 9.05%.

Kinetic evaluation of the thermolysis of $Ru(PMe_3)_4(Ph)(Me)$ in C_6D_6. Into a 5.00 mL volumetric flask was weighed 35.6 mg (0.0716 mmol) $Ru(PMe_3)_4(Ph)(Me)$ and 28 mg of ferrocene as an internal standard. C_6D_6 was added to the flask, making a 0.0143 M solution. In a typical experiment, 0.700 mL of this solution was added by syringe to a thin walled, 9" NMR tube. The tube was degassed, the appropriate amount of PMe_3 was added by vacuum transfer and the tube was flame sealed to give a length of 8.5". The tubes were heated at 110 °C in a factory-calibrated Neslab Exocal Model 251 constant temperature bath filled with Dow Corning 200 silicone Fluid, and frozen rapidly in ice water after removal from the bath. All reactions were monitored to greater than 3 half-lives by ambient-temperature ^1H NMR spectrometry by integrating the PMe_3 resonance of the starting material at 0.99 vs. the ferrocene internal standard. The spectra were taken with a single acquisition and double checked with a second acquisition after a delay of at least 10 T_1. All kinetic plots displayed excellent linearity with correlation coefficients of 0.98 or better. A plot of k_{obs} vs. 1[L] is shown in Figure 4 and displays a correlation coefficient of 0.99.

$Ru(PMe_3)_4(\eta^2\text{-}OC(CH_2)C_6H_4)$ (4). Into a glass reaction vessel fused to a Kontes vacuum adaptor was weighed 31.6 mg (0.0656 mmol) of **1**. Benzene (5 mL) was added, and to the resulting solution was added 7.9 mg (1 equiv) of acetophenone. The vessel was heated to 45 °C for 8h, after which time the initial clear solution had turned yellow. The solvent was then removed and the product was crystallized from a pentane/toluene (10:1) solvent mixture to yield 13.6 mg (39.5%) of yellow product. An alternative preparation of this compound from the reaction of acetone and **1**, along with a determination of its structure by X-ray diffraction, will be reported in a separate publication.[37] *IR* (KBr) 3103 (m), 3050 (s), 3043 (s), 3028 (m), 2969 (s), 2903 (s), 1977 (w), 1934 (w), 1624 (w), 1569 (s), 1548 (m), 1431 (s), 1395 (s), 1338 (s), 1316 (s), 1298 (s), 1279 (s), 1262 (s), 1238 (m), 1122 (s), 1021 (m), 990 (s), 938 (s), 854 (s), 841 (s), 784 9s), 736 (s), 712 (s), 700 (s), 662 (s), 647 9(s), 634 (m), 498 (m); MS (FAB) m/e 525 (MH^+).

$Ru(PMe_3)_4(\eta^2\text{-}OC_6H_3Me)$ (5). Into a small vial with a stir bar was placed 20.4 mg of **1**, 7 mg of ferrocene and 1.0 mL of C_6D_6. This solution was divided into two equal portions. One sample was placed into an NMR tube. To the other sample was added 2.3 mg (1 equiv.) of *p*-cresol in 0.4 mL of C_6D_6 while stirring. The solution, which immediately turned from clear to orange/yellow, was quickly transferred to an NMR tube. ^1H and $^{31}P\{^1H\}$ NMR spectra obtained within 10 min after the addition showed that all of **1** had reacted, and that it had been converted to at least two intermediates. The NMR tube was then brought into the drybox, equipped with a vacuum adaptor, and sealed. Heating the tube for 24 h at 45 °C provide conversion of the intermediates to $Ru(PMe_3)_4(\eta^2\text{-}OC_6H_3Me)$ in 70% yield by ^1H NMR spectroscopy, as determined by comparison of integrated ratios of the PMe_3 resonances in the starting material and product to the ferrocene internal standard.

Low temperature observation of $Ru(PMe_3)_4(Ph)(OC_6H_4Me)$ (6). In the drybox, 15.1 mg of **1** was dissoved in 0.7 mL of toluene-d_8 in an NMR tube equipped with a vacuum adaptor. To this stirred solution was added 3.4 mg (1 equiv) of *p*-cresol in 0.2 mL toluene. Immediately after addition the sample was brought out of the drybox and cooled in a -78 °C bath. The tube was sealed and placed into the probe of the NMR spectrometer which had been pre-cooled to -60 °C. $^{31}P\{^1H\}$ and ^1H NMR spectra were taken at this temperature and indicated clean conversion to the phenyl cresolate intermediate.

$Ru(PMe_3)_4(Ph)(H)$ (7). To a solution of 300 mg (0.627 mmol) of $Ru(PMe_3)_4(\eta^2\text{-}C_6H_4)$ in 5 mL pentane was added 47.7 µL (0.627 mmol) isopropanol in 0.5 mL pentane at room temperature. After allowing the mixture to react for 1 h, the volume was reduced under vacuum to 1 mL and cooled to -40 °C to yield 145 mg (48.2 %) white crystals. IR 3060 (m), 2981 (m), 2966 (m), 1859 (M-H, s), 1561 (m), 1424 (m), 1419 (m), 1295 (s), 1278 (m); 940 (s); MS (EI) *m/e* 406 ($M\text{-}C_6H_6$), 330 ($M\text{-}C_6H_6\text{-}PMe_3$); Anal. Calcd. for $C_{18}H_{42}P_4Ru$: C, 44.71; H, 8.62. Found: C, 44.82; H, 8.83.

$Ru(PMe_3)_4(Ph)(OH)$ (9). In the drybox, 78.6 mg of **1** and 1 mL of benzene was added to a glass vessel fused to a Kontes vacuum adaptor. The vessel was brought out of the drybox and 3.0 μL (1 equiv.) of water was added by syringe to the vessel on a Schlenk line. The solution was allowed to react for 8 h at room temperature, after which time the solvent was removed and the residue extracted with 25 mL of pentane. The clear solution was concentrated to 5-10 mL and cooled to -40 °C to provide 43.6 mg (54 %) of product. IR (Nujol) 3636 (w), 1974 (w), 1933 (w), 1853 (w), 1562 (s), 1553 (m), 1523 (m), 1436 (s), 1423 (s), 1297 (s), 1279 (s), 1241 (m), 1180 (m), 1147 (m), 1060 (m), 1014 (s), 942 (s), 855 (s), 795 (s), 731 (s), 709 (s), 662 (s), 634 (m); MS (FAB) m/e 482 ($MH-H_2O^+$), 406 ($M-OH_2-PMe_3^+$); Anal. Calcd.for $C_{18}H_{42}OP_4Ru$: C, 43.28; H, 8.48. Found: C, 43.02; H, 8.39.

$Ru(PMe_3)_4(\eta^2\text{-}NHC_6H_4)$ (10). Into a vial was placed 80.2 mg (0.167 mmol) of **1**, 17.06 mg (1.1 equiv) of aniline and 2 mL of benzene. The solution was then placed in a 9" NMR tube which was degassed and sealed. The sample was heated to 110 °C for 8 h. Upon cooling, 56.4 mg (58.2%) of **3** had crystallized from the reaction solution and all of the starting material had been consumed as determined by $^{31}P\{^1H\}$ NMR spectroscopy. The material that crystallized from solution was pure by ^1H NMR spectroscopy, but a portion of this sample was crystallized from ether for microanalysis. IR (KBr) 3337 (w) 3019(m), 2989 (m), 2969 (m), 2906 (s), 1594 (m), 1560 (m), 1534 (m), 1435 (s), 1425 (s), 1297 (m), 1281 (m), 1266 (m), 942 (s), 705 (s), 665 (s); Anal Calcd. for $C_{18}H_{41}NP_4Ru$: C, 43.55; H, 8.32; N, 2.82. Found: C, 43.35; 8.15; N, 2.82.

Addition of Aniline to 9. Into an NMR tube was placed a C_6D_6 solution containing 10.2 mg of **9**. To this solution was added 1 equiv. of aniline. The tube was degassed and sealed. Heating of the sample to 110 °C for 2 h led to formation of bridging hydroxide complexes which are formed from **9** in the absence of aniline.[16] No formation of **10** was detected.

$Ru(PMe_3)_3(C_2H_4)_2$ (12). A 100 mL round bottom flask was charged with 505 mg (1.06 mmol) of $Ru(PMe_3)_4(Cl)_2$ and 25 mL of ether. To this suspension was added 2.2 equiv of C_2H_5MgCl as a 1.5 M solution in ether. The reaction was stirred at room temperature until the all

orange $Ru(PMe_3)_4(Cl)_2$ had reacted and the suspension was a milky white (2-3 h). At this time the ether was removed under vacuum and the residue was extracted with pentane (3 x 20 mL). The volume of the extract was reduced to 5 mL and placed in a glass vessel fused to a Kontes vacuum adaptor. Ethylene (2.1 equiv) was condensed into the vessel, and the resulting solution was heated for 24 h at 85 °C. At this point the volume of the solution was reduced under vacuum to 2 mL and filtered through a plug of celite. Reducing the volume to 1 mL and cooling to -40 °C provided 244 mg (59.7 %) yield of clear blocks. IR(KBr) 3027 (m) 2964 (m), 2903 (m), 2896 (m), 1424 (m), 1298 (m), 1293 (m), 1279 (s), 1132 (s), 941 (s), 845 (m), 711 (m),l 699 (m), 660 (s).

Reaction of ethylene with 1. Into an NMR tube was placed 6.9 mg (0.0143 mmol) of 1 and 0.7 mL of benzene-d_6. The sample was degassed and 10 equiv. of ethylene were added by vacuum transfer. The tube was sealed and heated to 85 °C for 1.5 d, at which point the ^1H NMR spectrum of the final reaction mixture showed the formation of styrene (confirmed by GC/MS) in 70% yield. The ^1H and $^{31}P\{^1H\}$ NMR spectra showed the formation of $(PMe_3)_3Ru(C_2H_4)_2$ in 68% yield by comparison with the independently prepared sample.

Reaction of ethylene-1,1-d_2 with 1. Into an NMR tube was placed 8.0 mg (0.0143 mmol) of 1 and 0.7 mL of benzene-d_6. The sample was degassed and 7 equivalents of ethylene-1,1-d_2 were added by vacuum transfer. The tube was sealed and heated to 85 °C for 16 h. The ^1H NMR spectrum of the final reaction mixture showed a 1:1:1 ratio of the vinylic resonances (to within the roughly 10% error of integration), indicating a 1:1 ratio of the two isomers, β, β-d_2-styrene and α, 2-d_2-styrene. The experiment was conducted a second time following a similar procedure, except the reaction was run in benzene-d_0 and the final reaction mixture was analyzed by ^2H NMR spectroscopy. Again, within the accuracy of the integration (roughly 10%), a 1:1:1 ratio of vinylic resonances was observed.

$Ru(PMe_3)_4(\eta^2$-C(p-tolyl)C(p-tolyl)$C_6H_4)$ (13). Into a glass reaction vessel fused to a Kontes vacuum adaptor was placed 121 mg (0.252 mmol) of 1 and 5 mL toluene. To this solution was added 5 equivalents of di-p-tolylacetylene. The reaction vessel was partially degassed by one freeze-pump-thaw cycle and heated to 85 °C for 24 h. After this time the

solution was concentrated under vacuum and filtered. Layering of the solution with pentane and cooling to -40 °C provided 79.4 mg (46 %) of product which was pure by ^{1}H NMR spectroscopy. This material was recrystallized from toluene/pentane vapor diffusion for microanalysis. IR(KBr) 2972 (m), 2911 (s), 1437 (m),1434 (m), 1420 (m), 1298 (m), 965 (m), 942 (s), 855 (m), 728 (m), 701 (m), 662 (m); Anal. Calcd. For $C_{34}H_{54}P_4Ru$: C, 59.38; H, 7.91. Found: C, 59.28; H, 8.04.

$Ru(PMe_3)_4(\eta^2\text{-}OC(H)(Ph)C_6H_4)$ (14). Into a glass reaction vessel fused to a Kontes vacuum adaptor was placed 80.0 mg of 1, along with the minimum amount of pentane (~2 mL) necessary to dissolved the material. To this solution was added 17.6 mg (1 equiv) of benzaldehyde at room temperature. The vessel was then heated to 45 °C for 1.5 d, during which period the solution turned dark brown. (When the reaction was run in tetrahydrofuran the reaction solution turned green.) Upon cooling to room temperature the product crystallized from the reaction solution as green blocks (31.8 mg, 32.6%). MS (FAB) m/e 589 (MH^+); IR (KBr) 3078 (m), 3044 (m), 3025 (m), 2970 (s) 2906 (s), 2815 (m), 2708 (m), 2661 (m), 2504 (m), 1597 (m), 1578 (m), 1566 (m), 1542 9m), 1505 (m), 1490 (m), 1431 (m), 1397 (m), 1351 (s), 1298 (s), 1279 (s), 1233 (m), 1059 (s), 1042 (m), 1027 (m), 1017 (m), 964 (s), 941 (s), 854 9s), 763 (m), 736 9s), 702 (s), 664 (s), 629 (m); Anal. Calcd. for $C_{25}H_{46}OP_4Ru$: C, 51.10; H, 7.89. Found: C, 50.97; H, 7.95.

$Ru(PMe_3)_4(\eta^2\text{-}NC(Ph)C_6H_4)$ (15). Into a glass reaction vessel fused to a Kontes vacuum adaptor was placed 158 mg (0.328 mmol) of 1 and 8 mL benzene. To this solution was added 5 equiv of benzonitrile. The reaction vessel was partially degassed by one freeze-pump-thaw cycle and heated to 85 °C for 24 h. After this time the solvent was removed under reduced pressure. The residue was extracted with toluene, and the extracts were filtered, concentrated under vacuum, and crystallized by layering the toluene solution with pentane and cooling to -40 °C to provide 88.6 mg (46 %) yellow blocks suitable for microanalysis and X-ray crystal structure analysis.

X-ray crystal structure determination of complexes 9 and 15.

The procedure used in the determination of the structure of **1** was employed with the following modifications:

(a) Mounting Procedure: Orange, air-sensitive crystals of **15** were obtained by layering a toluene solution of **15** with pentane. Clear, air sensitive crystals of **9** were obtained by cooling a pentane solution of **9**. End fragments cleaved from some of these crystals were mounted in a viscous oil. The final cell parameters and specific data collection parameters for the data set for **9** and **15** are given in Table 1.

(b) Structure Determination: For **9**, 2135 raw intensity data were collected and for **15**, 6274 were collected. These data were converted to structure factor amplitudes and their esd's by correction for scan speed, background and Lorentz and polarization effects. Inspection of the azimuthal scan data showed a variation I_{min}/I_{max} = +/-1% for the average curve. No correction for absorption was applied. Inspection of the systematic absences indicated space group P1 for **9** and $P2_1/n$ for **15**. Removal of systematically absent and redundant data left 6274 unique data in the final data set for **9** and 2113 for **15**.

Each structure was solved by Patterson methods and refined via standard least-squares and Fourier techniques. The final refinement included anisotropic refinement of the ruthenium and phosphorus atoms and isotropic refinement of the carbon and nitrogen atoms. Hydrogen atoms were not included in the refinement.

The final residuals for the 243 variables for **9** were refined against the 5021 accepted data for which $F^2 > 3\sigma(F^2)$ were R = 5.8%, wR = 9.2% and GOF = 3.86. The R value for all 3194 accepted data was 7.2%. The final residuals for the 150 variables for **15** were refined against the 1462 accepted data for **15** for which $F^2 > 3\sigma(F^2)$ were R = 6.4%, wR = 6.9% and GOF = 1.93. The R value for all 3194 accepted data was 11.0%.

Positional parameters, thermal parameters of the non-hydrogen atoms, and anisotropic thermal parameters are available as supplementary material.

Phosphine Inhibition studies for the reaction of 1 with benzaldehyde and benzonitrile. Into a vial was weighed 40.6 mg of **1** and 10 mg of ferrocene as an internal

standard. Benzene-d_6 (3 mL) was added and the solution was divided into two equal portions. To one of the samples was added 5 equiv of benzaldehyde and to the other, 5 equiv of benzonitrile. Each of these samples was then further divided into two equal portions and placed into NMR tubes to make a total of four samples. Each NMR tube was degassed by three freeze-pump-thaw cycles. To one sample containing benzaldehyde and to another containing benzonitrile was added 5 equiv of PMe_3 by vacuum transfer before all of the tubes were sealed. ^1H and $^{31}P\{^1H\}$ NMR spectra of the solutions were obtained before heating. The two samples containing benzaldeyde were heated to 45 °C for 2.5 h, and the two containing benzonitrile were heated to 55 °C for 2.5 h. Conversions and yields were determined by comparing ^1H and $^{31}P\{^1H\}$ NMR spectra to those obtained before heating. The experiment was conducted twice with similar phosphine inhibition observed during both runs.

Phosphine exchange studies for 1. Into an NMR tube was placed 0.7 mL of a C_6D_6 solution containing 12.4 mg of **1**. The tube was degassed and 4 equiv of PMe_3-d_9 was condensed into the sample. The approximate amounts of phosphine exchange at 5 min, 2 h, and 24 h were determined by integrating the $^{31}P\{^1H\}$ NMR signals for free PMe_3-d_9 and PMe_3-d_0. The ratios were found to be 36:1 after 10 min, 2:1 after 2 h, and 1:1 after 24 h.

Table 8. ^{1}H NMR Spectroscopic Data[a]

Compound	d (ppm)	multiplicity	J (Hz)	Integral	assignment
$(PMe_3)_4Ru(\eta^2\text{-}C_6H_4)$ (1)[b]	0.78	t	4.4	18	*trans*-PMe_3
	1.28	d	2.6	18	*cis*-PMe_3
	7.26	br, s		2	Aromatic
	7.31	br, s		2	
$(PMe_3)_4Ru(\eta^2\text{-}C_6D_4)$ (1-d_4)[b]	0.78	t	4.4	18	*trans*-PMe_3
	1.28	d	2.6	18	*cis*-PMe_3
$(PMe_3)_4Ru(Me)(Ph)$ (2)[b]	-0.033	dq	7.7, 3.5	3	Ru-Me
	0.96	t	5.2	18	*trans*-PMe_3
	1.04	d	5.0	9	*cis*-PMe_3
	1.22	d	4.7	9	
	7.13	m		1	Aromatic
	7.19	m		2	
	7.88	br, s		2	
$(PMe_3)_4Ru(\eta^2\text{-}OC(CH_2)C_6H_4)$ (4)[c]	1.02	t	6.0	18	*trans*-PMe_3
	1.42	d	6.9	9	*cis*-PMe_3
	1.45	d	6.0	9	
	3.39	d	1.2	1	$CC(\underline{CH_2})C_6H_4$
	3.95	br, s		1	
	6.61	tq	7.3, 1.0	1	$OC(CH_2)C_6\underline{H_4}$
	6.63	t	7.1	1	
	7.11	dt	7.6, 1.6	1	
	7.46	m		1	
$(PMe_3)_4Ru(\eta^2\text{-}OC_6H_3Me)$ (5)[b]	1.00	d	7.4	9	*cis* PMe_3
	1.09	d	6.0	9	
	1.15	t	5.8	18	*trans* PMe_3
	2.58	s		3	p-Me
	6.06	d	7.6	1	Aromatic
	6.96	d	7.2	1	
	7.30	br, s		1	
$(PMe_3)_4Ru(OC_6H_4Me)(Ph)$ (6)[d]	0.88	t	2.8	18	*trans*-PMe_3
	0.90	d	6.8	9	*cis*-PMe_3
	1.06	d	5.6	9	
	2.49	s		3	*p*-Me
	6.67	d	8.2	2	*p*-cresolate
	7.22	d	8.3	2	
	7.31	m		2	phenyl
	7.45	t	7.0	1	
	7.87	br, s		1	
	8.73	br, d	7.2	1	
$(PMe_3)_4Ru(H)(Ph)$ (7)[e]	-9.50	ddt	92.6, 18.3, 18.3	1	Ru-H
	1.10	t	2.6	18	*trans*-PMe_3
	1.35	d	5.8	9	*cis*-PMe_3
	1.38	d	5.4	9	
	6.60	m		3	Aromatic
	7.45	m		1	
	7.75	m		1	

Table 8 (cont'd.)

$(PMe_3)_4Ru(OH)(Ph)$ (9)[f]	-4.47	m		1	Ru-OH
	1.06	t	5.6	18	*trans*-PMe_3
	1.37	d	7.3	9	*cis*-PMe_3
	1.40	d	6.0	9	
	6.70	m		3	Aromatic
	7.53	t	5.7	1	
	7.97	d	7.1	1	
$(PMe_3)_4Ru(\eta^2\text{-}NHC_6H_4)$ (10)[b]	0.98	d	5.7	9	*cis*-PMe_3
	1.06	d	6.7	9	
	1.13	t	2.5	18	*trans*-PMe_3
	5.85	d	7.4	1	Aromatic
	6.65	t	6.6	1	
	7.12	t	7.3	1	
	7.33	br, s		1	
$(PMe_3)_3Ru(C_2H_4)_2$(12)[b]	0.66	t	2.3	18	*trans*-PMe_3
	1.25	d	6.1	9	*cis*-PMe_3
	1.41	m		4	C_2H_4
	1.80	m		4	
$(PMe_3)_4Ru(\eta^2\text{-}C(p\text{-tolyl})C(p\text{-tolyl})C_6H_4)$ (13)[b]	0.82	d	4.9	9	*cis*-PMe_3
	1.25	d	4.8	9	
	1.17	t	2.7	18	*trans*-PMe_3
	2.14	s		3	p-Me
	2.18	s		3	
	6.91	d	7.8	2	p-tolyl
	7.03	d	7.9	2	
	7.10	d	7.8	2	
	7.30	d	7.9	2	
	7.20	m		3	C_6H_4
	8.07	br, s		1	
$(PMe_3)_4Ru(\eta^2\text{-}OC(H)(Ph)C_6H_4)$ (14)[b]	1.03	dd	4.8, 0.5	9	PMe_3
	1.27	d	4.9	9	
	1.38	d	5.7	9	
	1.45	d	6.6	9	
	5.45	t	3.7	1	$C(\underline{H})(Ph)C_6H_4$
	6.22	d	7.4	1	Aromatic
	6.46	t	7.4	1	
	6.53	td	7.3, 0.7	1	
	7.01	tt	7.1, 1.3	1	
	7.12	t	7.5	2	
	7.22	dd	6.3, 1.4	2	
	7.48	td	5.0, 1.4	1	

Table 8 (Cont'd)

$(PMe_3)_4Ru(\eta^2\text{-}NC(Ph)C_6H_4)$ (15)[b]	0.92	t	2.8	18	*trans*-PMe_3
	1.48	d	5.4	9	*cis*-PMe_3
	1.54	d	5.8	9	
	6.70	m		2	Aromatic
	7.01	dt	7.1, 1.9	1	
	7.11	t	7.3	1	
	7.22	t	5.8	2	
	7.44	d	6.9	2	
	7.70	br, t	6	1	

[a] The multiplicities d and t, when applied to the PMe_3 resonances, refer to apparent splitting patterns. Accordingly, the values reported for J do not reflect true coupling constants. [b] C_6D_5, 20° C. [c] THF-d_8, 20°-C. [d] PhMe-d_8, -60° C. [e] THF-d_8, -55° C. [f] THF-d_8, -45° C.

Table 9. $^{13}C\{^1H\}$ NMR Spectroscopic Data.[a]

Compound	δ (ppm)	multiplicity[b]	J (Hz)	assignment
$(PMe_3)_4Ru(\eta^2\text{-}C_6H_4)$ (1)[b]	21.32	tt	13.1, 3.6	*trans*-PMe_3
	27.64	m		*cis*-PMe_3
	125.09	t	2.4	Aromatic
	126.12	d	4.6	
	142.07	dq	52, 9.7	
$(PMe_3)_4Ru(Me)(Ph)$ (2)[b]	-2.64	dtd	55.5, 13.2, 7.9	Ru-Me
	20.27	t	12.4	*trans*-PMe_3
	23.73	d	17.0	*cis*-PMe_3
	24.89	d	19.9	
	119.92	s		Aromatic
	123.92	s		
	124.95	s		
	143.22	s		
	147.59	d	15.6	
	173.50	dq	75.8, 10	
$(PMe_3)_4Ru(\eta^2\text{-}OC(CH_2)C_6H_4)$ (4)[c]	19.40	td	12.6, 2.6	*trans*-PMe_3
	22.28	dt	17.0, 1.7	*cis*-PMe_3
	25.23	dm	23.6	
	72.90	s		$C(CH_2)C_6H_4$
	120.68	d	1.3	$C(CH_2)C_6H_4$
	122.81	d	1.4	and
	125.23	m		Aromatic
	141.27	m		
	152.86	d	3.1	
	176.60	dm	7.7	
	177.71	dq	65.0, 8.2	
$(PMe_3)_4Ru(\eta^2\text{-}OC_6H_3Me)$ (5)[c]	18.65	td	13.5, 3.0	*trans*-PMe_3
	22.44	dt	18.1, 2.6	*cis*-PMe_3
	25.32	dq	25.0, 3.4	
	21.88	s		p-Me
	105.55	s		Aromatic
	120.44	s		
	122.00	s		
	137.80	s		
	142.69	dtd	65, 16, 6	
	182.41	s		
$(PMe_3)_4Ru(H)(Ph)$ (7)[d]	23.59	t	12.2	*trans*-PMe_3
	24.67	m		*cis*-PMe_3
	27.96	d	18	
	119.69	s		Aromatic
	124.84	s		
	125.32	s		
	146.55	d	8.8	
	153.10	s		
	174.20	m		

Table 9 (Cont'd)

$(PMe_3)_4Ru(OH)(Ph)$ (9)[a]	18.53	td	12.5, 2	*trans*-PMe_3
	22.02	d	17.4	*cis*-PMe_3
	25.54	d	24	
	120.51	s		Aromatic
	124.70	s		
	125.15	s		
	139.83	s		
	145.77	d	8.0	
	174.55	dtd	74.2, 16.1, 10.0	
$(PMe_3)_4Ru(\eta^2\text{-}NHC_6H_4)$ (10)[b]	19.57	tm	11.8	*trans*-PMe_3
	23.36	dt	16.9, 2.2	*cis*-PMe_3
	25.31	dm	21.4	
	105.28	m		Aromatic
	111.12	dt	5.4, 1.8	
	122.78	s		
	136.38	m		
	143.46	dtd	64.2, 15.7, 7.5	
	178.80	q	6.1	
$(PMe_3)_3Ru(C_2H_4)_2$ (12)[b]	14.69	td	11.4, 3.0	*trans*-PMe_3
	23.03	dt	18.3	*cis*-PMe_3
	21.14	dt	10.8, 4.2	C_2H_4
	23.47	dt	8.0, 2.4	
$(PMe_3)_4Ru(\eta^2\text{-}C(p\text{-tolyl})C(p\text{-tolyl})C_6H_4)$ (13)[b]	21.24	tt	12.9, 3.5	*trans*-PMe_3
	24.90	dq	16.0, 2.1	*cis*-PMe_3
	25.71	dq	15.2, 2.6	
	21.16	s		p-Me
	21.28	s		
	121.63	s		Aromatic
	121.73	s		and
	122.73	s		vinyl
	127.88	s		
	128.41	s		
	128.48	s		
	131.28	s		
	133.03	s		
	130.98	s		
	143.01	s		
	143.16	s		
	149.54	s		
	156. 34	s		
	163.31	d	6.6	
	174.40	dm	56.5	
	184.43	dm	57.5	

Table 9 (Cont'd)

$(PMe_3)_4Ru(\eta^2\text{-}OC(H)(Ph)C_6H_4)$ (14)[b]	19.17	ddd	18.3, 7.0, 2.7	PMe_3
	19.88	ddd	16.8, 7.2, 2.9	
	21.60	dt	16.8, 1.4	
	25.25	dt	23.4, 1.5	
	90.12	d	8.5	$OC(H)(Ph)C_6H_4$
	120.48	s		Aromatic
	122.84	s		
	123.73	s		
	125.61	s		
	127.86	s		
	129.64	s		
	139.32	s		
	152.86	s		
	161.22	s		
	178.13	dm	68.8	
$(PMe_3)_4Ru(\eta^2\text{-}NC(Ph)C_6H_4)$ (15)[b]	19.95	t	14.0	*trans*-PMe_3
	22.34	d	17.9	*cis*-PMe_3
	25.92	d	15.7	
	120.20	s		Aromatic
	123.20	s		and
	124.85	s		Imine
	125.84	s		
	127.82	s		
	128.34	s		
	142.84	t	2.0	
	146.37	d	9.1	
	155.20	d	12.6	
	175.46	m		
	187.30	dq	67.8, 6.8	

[a] The multiplicities d and t, when applied to the PMe_3 resonances, refer to apparent splitting patterns. Accordingly, the values reported for J do not reflect true coupling constants. [b] C_6D_6, 20° C. [c] THF-d_8, 20°-C. [d] THF-d_8, -55° C. [e] THF-d_8, -45° C.

Table 10. $^{31}P\{^{1}H\}$ NMR Spectroscopic Data.

Compound	Spin System	d (ppm)	J (Hz)
$(PMe_3)_4Ru(\eta^2\text{-}C_6H_4)$ (1)[b]	A_2B_2	δA=-6.84 δB=-8.15	J_{AB}=31.5
$(PMe_3)_4Ru(Me)(Ph)$ (2)[b]	A_2BC	δA=-2.76 δB=-9.99 δC=-14.82	J_{AB}=25.5 J_{AC}=23.7 J_{BC}=14.0
$(PMe_3)_4Ru(\eta^2\text{-}OC(CH_2)C_6H_4)$ (4)[c]	A_2BC	δA=0.69 δB=-13.71 δC=6.86	J_{AB}=25.3 J_{AC}=32.2 J_{BC}=14.3
$(PMe_3)_4Ru(\eta^2\text{-}OC_6H_3Me)$ (5)[b]	A_2BC	δA=-2.73 δB=15.78 δC=-9.31	J_{AB}=34 J_{AC}=24 J_{BC}=17
$(PMe_3)_4Ru(OC_6H_4Me)(Ph)$ (6)[d]	A_2BC	δA=-4.07 δB=9.03 δC=-13.3	J_{AB}=36.7 J_{AC}=22.0 J_{BC}=21.3
$(PMe_3)_4Ru(H)(Ph)$ (7)[e]	A_2BC	δA=-1.32 δB=-10.59 δC=-17.18	J_{AB}=24.5 J_{AC}=26.7 J_{BC}=18.9
$(PMe_3)_4Ru(OH)(Ph)$ (9)[f]	A_2BC	δA=-3.34 δB=3.97 δC=-11.80	J_{AB}=31.2 J_{AC}=25.2 J_{BC}=16.5
$(PMe_3)_4Ru(\eta^2\text{-}NHC_6H_4)$ (10)[b]	A_2BC	δA=-4.01 δB=6.56 δC=-10.89	J_{AB}=32.7 J_{AC}=23.9 J_{BC}=17.6
$(PMe_3)_3Ru(C_2H_4)_2$ (12)[b]	A_2B	δA=1.80 δB=-0.94	J_{AB}=25.1
$(PMe_3)_4Ru(\eta^2\text{-}C(p\text{-tolyl})C(p\text{-tolyl})C_6H_4)$ (13)[b]	A_2BC	δA=-8.81 δB=-19.23 δC=-21.95	J_{AB}=30.7 J_{AC}=23.1 J_{BC}=9.2
$(PMe_3)_4Ru(\eta^2\text{-}OC(H)(Ph)C_6H_4)$ (14)[b]	ABCD	δA=4.75 δB=-3.46 δC=-4.73 δD=-14.37	J_{AB}=29.0 J_{AC}=30.6 J_{AD}=11.9 J_{BC}=332.1 J_{BD}=29.5 J_{CD}=28.3
$(PMe_3)_4Ru(\eta^2\text{-}NC(Ph)C_6H_4)$ (15)[b]	A_2BC	δA=5.53 δB=-11.57 δC=-13.67	J_{AB}=29.4 J_{AC}=28.0 J_{BC}=9.1

[b] C_6D_6, 20° C. [c] THF-d_8, 20°-C. [d] PhMe-d_8, -60° C. [e] THF-d_8, -55° C. [f] THF-d_8, -45° C.

Notes and References

1. Fischer, E.O *Transition Metal Carbene Complexes* Verlag Chemie: Weinheim, 1983.
2. (a) Randolph, C.L.; Wrighton, M.S. *Organometallics* 1987, *6*, 365. (b) Campion, B.K.; Heyn, R.H.; Tilley, T.D. *J. Am. Chem. Soc.* 1988, 7558. (c) Koloski, T.S.; Carrol, P.J.; Berry, D.H. *J. Am. Chem. Soc.* 1990, *112*, 6405.
3. (a) Pham, E.D.; West R. *J. Am. Chem. Soc.* 1989, 7667. (b) Pham, E.K.; West, R. *Organometallics* 1990, *9*, 1517. (c) Berry, D.H.; Chey, J.H.; Zipin, H.S.; Carrol, P.J. *J. Am. Chem. Soc.* 1990, *112*, 452.
4. (a) Miyashita, A.; Shitara, H.; Nohira, H. *Organometallics* 1985, *4*, 1463. (b) Miyashita, A.; Shitara, H.; Nohira, H *J. Chem. Soc., Chem. Commun.* 1985, 850. (c) Straus, D.A.; Grubbs, R.H. *J. Am. Chem. Soc.* 1982, *104*, 5499. (d) Doherty, N.M.; Fildes, M.J.; Forrow, N.J.; Knox, S.A.R.; Macpherson, K.A. *J. Chem. Soc., Chem. Commun.* 1986, 1355. (e) Cutler, A.R.; Bodnar, T.W. *J. Am. Chem. Soc.* 1983, *105*, 5926.
5. Bennett, M.A.; Schwemlein, H.P. *Angew. Chem. Int. Ed. Engl.* 1989, *28*, 1296.
6. (a) Gowling, E.W.; Kettle, S.F.A.; Sharples, G.M. *J. Chem. Soc., Chem. Comm.* 1968, 21. (b) Bennett, M.A.; Yoshida, T.; *J. Am. Chem. Soc.* 1978, *110*, 1750. (c) Bennett, M.A.; Hambley, T.W.; Roberts, N.K.; Robertson, G.B *Organometallics* 1985, *4*, 1992. (d) Arnold, J.; Wilkinson, G.; Hussain, B.; Hursthouse, M.B. *J. Chem. Soc., Chem. Comm.* 1988, 704. (e) Arnold, J.; Wilkinson, G.; Hussain, B.; Hursthouse, M.B. *Organometallics* 1989, *8*, 415. (f) Buchwald, S.L.; Watson, B.T.; Huffman, J.C. *J. Am. Chem. Soc.* 1986, *108*, 7411. (g) Buchwald, S.L.; Lum, R.T., Dewan, J.C. *J. Am. Chem. Soc.* 1986, *108*, 7441. (h) Buchwald, S.L.; Watson, B.J.; Lum, R.T.; Nugent W.A. *J. Am. Chem. Soc.* 1987, *109*, 7157. (i) Buchwald, S.L.; Sayers, A.; Watson, B.T.; Dewan, J.C. *Tetrahedron Lett.* 1987, *28*, 3245. (j) McLain, S.J.; Schrock, R.R.; Sharp, P.R.; Churchill, M.R.; Youngs, W.J. *J. Am. Chem. Soc.* 1979, *101*, 263. (k) Churchill, M.R.; Youngs, W.J. *Inorg. Chem.* 1979, *18*, 1697. (l) Sarry, V B , Schaffernicht, R.; *Z. Naturforsch* 1981, *86b*, 1238. (m) Sarry, V.B.; Singh, H.; Hahn,

B.; Schaffernicht, R *Z. Anorg. Allg. Chem.* 1979, *456*, 181. (n) Bartlett, R. A.; Power, P.P.; Shoner, S.C. *J. Am. Chem. Soc.* 1988, *110*, 1966. Other d^0 benzyne complexes have been detected by labeling or trapping studies: (o) Masai, H.; Sonogashira, K.; Hagihara, N.; *Bull. Chem. Soc., Japan* 1968, *41*, 750. (p) Dvorak, J.; O'Brien, R.J.; Santo, W. *J. Chem. Soc., Chem. Comm.* 1970, 411. (q) Kolomnikov, I.S.; Gobeeva, T.S.; Gorbachevskaya, V.V.; Aleksandrov, G.G.; Struckhov, Y.T.; Vol'pin, M.E.*J. Chem. Soc., Chem. Comm.* 1971, 972. (r) Boekel, C.P.; Teuben, J.H.; De Liefde Meiger, H.J.; *J. Organomet. Chem.* 1974, *81*, 371; 1975,*102*, 161. (s) Shur, V.B.; Berkovitch, E.G.; Vasiijeve, L.B.; Kudryavtsev, R.V.; Vol'pin, M.E. *J. Organomet. Chem.* 1974, *78*, 127. (t) Erker, G. *J. Organomet. Chem.* 1977, *134*, 189.(u) Erker, G.; Kropp, K. *J. Am. Chem. Soc.* 1979, *101*, 3659. (v) Erker, G.; Czisch, P.; Mynott, R.; Tsay, T-H.; Kruger, C. *Organometallics* 1985, *4*, 1310. (w) Chamberlain, L.R.; Kerschner, J.L.; Rothwell, A.P.; Rothwell, I.P.; Huffman, J.C. *J. Am. Chem. Soc.* 1987, *109*, 6471. (x) Schock, L.E.; Brock, C.P.; Marks, T.J. *Organometallics* 1987, *6*, 232.

7. Yamamoto, A. *Organotransition Metal Chemistry*; Wiley: New York, 1986. Collman, J.P.; Hegedus, L.S.; Norton, J.R.; Finke, R.G. *Principles and Applications of Organotransition Metal Chemistry*; University Science Books: Mill Valley, 1987.
8. Portions of this work have been reported previously in communication form. Hartwig, J.F.; Andersen, R.A.; Bergman, R.G. *J. Am. Chem. Soc.* 1989, *111*, 2717.
9. Calabrese, J.C.; Colton, M.C.; Herskovitz, T.; Klabunde, U.; Parshall, G.W.; Thorn, D.L.; Tulip, T.H. *Annals. New York Acad. Sci.* 1983, *415*, 302. An ORTEP diagram is provided in this reference but bond distances are not provided. The Ru-aryl bond length is 2.118(3) Å, Tulip, T.H., *personal communication.*
10. Recent values are provided in:Jeffrey, G.A.; Ruble, J.R.; McMullan, R.K.; Pople, J.A.*Proc. R. Soc. London, A* 1987, *414*, 47.

11. Statler, J.A.; Wilkinson, G.; Thornton-Pett, M.; Hursthouse, M.B. *J. Chem. Soc., Dalton Trans.* 1984, 1731. (b) Calabrese, J.C.; Cotton, M.C.; Herskovitz, T.; Klabunde, U.; Parshall, G.W.; Thorn, D.L.; Tulip, T.H. *Annals. New York Acad. Sci.* 1983, *415*, 302.

12. Chapter 4.

13. Milstein, D.; Calabrese, J.C.; Williams, I.D. *J. Am. Chem. Soc.* 1986, *108*, 6387.

14. Arnold, D.P.; Bennett, M.A. *J. Organomet. Chem.* 1980, *199*, 119.

15. Chapter 6.

16. Bryndza, H.E.; Fong, L.K.; Paciello, R.A.; Tam, W.; Bercaw, J.E. *J. Am. Chem. Soc.* 1987, *109*, 1444.

17. Hartwig, J.F.; Andersen, R.A.; Bergman, R.G. unpublished results.

18. a) Werner, H. Gotzig, J. *Organometallics* 1983, *2*, 547. b) Werner, H.; Werner, R. *J. Organomet. Chem.* 1981, *209*, C60.

19. Wong, W-K.; Chiu, K.W.; Statler, J.A.; Wilkinson, G.; Motevalli, M.; Hursthouse, M.B. *Polyhedron* 1984, *3*, 1255.

20. A study on the orientation of the ethylene ligands in the related compound $[(PMe_3)_3(C_2H_4)Ir]BF_4$ was recently published: Lundquist, E.G.; Folting, K.; Streib, W.E.; Huffman, J.C.; Eisenstein, O.; Caulton, K.G. *J. Am. Chem. Soc.* 1990, *112*, 855.

21. (a) Bennett, M.A.; Milner, D.L. *J. Am. Chem. Soc.* 1969, *91*, 6983. (b) Tulip, T.H.; Thorn, D.L. *J. Am. Chem. Soc.* 1981, *103*, 2448. (c) Foley, P.; DiCosimo, R.; Whitesides, G.M. *J. Am. Chem. Soc.* 1980, *102*, 6713. For reviews of cyclometallation reactions see: (d) Constable, E.C. *Polyhedron* 1984, *3*, 1037. (e) Webster, D.E. *Adv. Organomet. Chem.* 1977, *15*, 147. (f) Shilov, A.E.; Steinman, A.A. *Coord. Chem. Rev.* 1977, *24*, 97. (g) Ryabov, A.D. *Chem. Rev.* 1990, *90*, 403.

22. For mechanistic studies of cyclometallations and β-hydride eliminations at the Cp_2Zr^{IV} center, see: Buchwald, S.L.; Nielsen, R.B. *J. Am. Chem. Soc.* 1988, *110*, 3171 and references therein.

23. Addition of acetone to the platinum cyclohexyne complex $(Ph_2PCH_2CH_2PPh_2)Pt(\eta^2\text{-}C_6H_8)$ led to formation of the C-bound enolate $(Ph_2PCH_2CH_2PPh_2)Ni(C_6H_9)(CH_2C(O)CH_3)$, ref 6b. We have reported the observation of only the O-bound form for the $(PMe_3)_4Ru$ enolate complexes we have prepared, Hartwig, J.F.; Bergman, R.G.; Andersen, R.A. *J. Am. Chem. Soc.* 1990, *112*, 3234, with the exception of one example which exists as an equilibrium mixture of the O- and C-bound forms Hartwig, J.F.; Andersen, R.A.; Bergman, R.G. *J. Am. Chem. Soc.* 1990, *112*, 5670.

24. Baker, M.V.; Field, L.D.; Young, D.J. *J. Chem. Soc., Chem. Commun.* 1988, 546.

25. Chapter 6.

26. Komiya, S, Tane-ichi, S.; Yamamoto, A.; Yamamoto, T. *Bull. Chem. Soc. Jpn.* 1980, *53*, 673.

27. (a) Faller, J.W.; Smart, C.J. *Organometallics* 1988, *7*, 1670. (b) Stoutland, P.O.; Bergman, R.G. *J. Am. Chem. Soc.* 1988, *110*, 5732. (c) Stoutland, P.O.; Bergman, R.G. *J. Am. Chem. Soc.* 1985, *107*, 1985.

28. Bryndza, H.E.; Tam, W. *Chem. Rev.* 1988, *88*, 1163, and references therin.

29. Examples of addition of arylamide to osmium cluster compounds include (a) Bryan, E.G.; Johnson, B.F.G.; Lewis, J. *J. Chem. Soc., Dalton Trans.* 1977, 1328. (b) Susa-Fink, G. *Z. Naturforsch., B: Anorg. Chem., Org. Chem.* 1980, *35B*, 454. (c) Johnson, B.F.G.; Lewis, J.; Odiaka, T.I.; Raithby, P.R.; *J. Organomet. Chem.* 1981, C56. Examples of N-H addition reactions to Ir(I) include (d) Park, S.; Hedden, D.; Roundhill, D.M. *Organometallics*, 1986, *5*, 2151. (e) Casalnuovo, A.L.; Calabrese, J.C.; Milstein, D. *Inorg. Chem.* 1987, *26*, 973. (f) Casalnuovo, A.L.; Calabrese, J.C.; Milstein, D. *J. Am. Chem. Soc.* 1988, *110*, 6738. Addition of organic amide N-H bonds across a Ru-C has been observed recently (g) Schaad, D.R.; Landis, C.R. *J. Am. Chem. Soc.* 1990, *112*, 1628.

30. (a) Weidmann, B.; Seebach, D. *Angew. Chem. Int. Ed. Engl.* 1983, *22*, 31. (b) Tikkanen, W.R.; Petersen, J.L. *Organometallics* 1984, *3*, 1651.

31. Tsuji, J.; Ohno, K. *Synthesis*, 1969, *157*, 1.

32. Carmona, E.; Gutierrez-Puebla, E.; Marin, J.M.; Monge, A; Paneque, M.; Poveda, M.L.; Ruiz, C. *J. Am. Chem. Soc.* 1989, *111*, 2883.

33. Hayashi, Y.; Komiya, S.; Yamamoto, T.; Yamamoto, A. *Chem. Lett.* 1984, 1363.

34. Bergman, R.G.; Buchanan, J.M.; McGhee, W.D.; Periana, R.A.; Seidler, P.F.; Trost, M.K.; Wenzel, T.T. In *Experimental Organometallic Chemistry: A Practicum in Synthesis and Characterization*; Wayda, A.L.; Darensbourg, M.Y., Eds.; ACS Symposium Series 357; American Chemical Society: Washington, DC, 1987, p 227.

35. Statler, J.A.; Wilkinson, G.; Thornton-Pett, M.; Hursthouse, M.B. *J. Chem. Soc., Dalton Trans.* 1984, 1731.

36. Sellmann, D.; Bohlen, E.; *Z. Naturforsch., Teil B* 1982, *37*, 1026.

37. Hartwig, J.F.; Andersen, R.A.; Bergman, R.G. *unpublished results.*

Chapter 4

A Phosphorus-Carbon Bond Cleavage Reaction of Coordinated Trimethylphosphine in $(PMe_3)_4Ru(OC_6H_4Me)_2$

Introduction

Phosphines are among the most common ligands in coordination and organometallic chemistry, and metal phosphine complexes are often used as homogeneous catalysts[1]. They are important because of their strong electron donating properties[2], and in most cases they are inert toward reactions other than addition of their C-H bonds[3]. However, it has been noted that the cleavage of the P-C bond is a possible decomposition route for some catalysts containing aryl phosphine ligands; products resulting from the cleavage of the P-C bond in aryl phosphine ligands have been isolated[4]. In contrast, evidence for cleavage of the P-C bond in trialkylphosphine compounds has been reported in only a few cases[5]. To our knowledge, no product has been isolated in which a coordinated trialkylphosphine has been structurally changed as a result of P-C bond cleavage. We report such a reaction, in which a trimethylphosphine ligand of $(PMe_3)_4Ru(OAr)_2$ is transformed under mild thermolysis conditions into an orthometallated dimethylarylphosphinite ligand, the result of P-C bond cleavage.

Results and Discussion

The aryloxide compound $(PMe_3)_4Ru(OAr)_2$ (1) was prepared by the addition of two equivalents of p-cresol (p-methylphenol) to $(PMe_3)_4Ru(Me)_2$[6] in toluene to form 1 in 66% isolated yield, as shown in Scheme I. An AA'BB' pattern in the aryl region of the ^1H NMR spectrum of 1 indicates η^1 coordination of the two equivalent p-cresolate substituents, and an A_2B_2 pattern in the $^{31}P\{^1H\}$ NMR spectrum indicates that the complex adopts a cis geometry.

Addition of one equivalent of p-cresol to $(PMe_3)_4Ru(Me)_2$ yielded roughly 50% of 1 and 50% of starting material. However, use of $(PMe_3)_3Ru(\eta^2\text{-}CH_2PMe_2)(Me)$ allowed the selective addition of one equivalent of p-cresol to the ruthenium center (Scheme I). This cyclometallated precursor was synthesized in 40% isolated yield by the thermolysis of $(PMe_3)_4Ru(Me)_2$ in hexane followed by sublimation. Addition of one equivalent of p-cresol to $(PMe_3)_3Ru(\eta^2\text{-}CH_2PMe_2)(Me)$ at room temperature followed by heating to 85 °C for 3 h did not provide the simple addition product, but yielded methane (identified by ^1H NMR spectroscopy) and the orthometallated cresolate complex $(PMe_3)_4Ru(\eta^2\text{-}OC_6H_3Me)$ (2) in 56% isolated yield. The observation of three

Scheme I

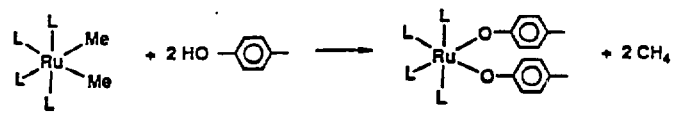

L = PMe_3 1

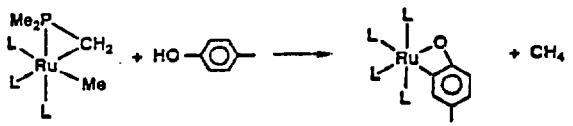

2

aryl resonances in the ^1H NMR spectrum of **2** in a 1:1:1 ratio, as well as an A_2BC pattern in its $^{31}P\{^1H\}$ NMR spectrum, indicated orthometallation of the aryl ring had occurred.

Thermolysis of **1** in benzene for 8 h at 85 ° C or 70 h at 65 °C also produced methane (identified by ^1H NMR spectroscopy) and complex **3**, the product of P-C bond cleavage, in quantitative yield by ^1H NMR spectroscopy and 34% isolated yield, as shown in Scheme II. The $^{31}P\{^1H\}$ NMR spectrum of **3** contained two resonances in the chemical shift range associated with PMe_3 groups coordinated to ruthenium[7] and a deshielded resonance at 172 ppm. The latter resonance is in the range found for coordinated phosphite ligands[8]. The $^{31}P\{^1H\}$ NMR spectrum is an example of an A_2BX spin system. The two equivalent phosphorus nuclei appear as a doublet of doublets centered at δ-1.69 with J_{AB}=24.3 Hz and J_{AX}=37.2 Hz. The other PMe_3 resonance appears as a doublet of triplets centered at δ-19.2 with J_{AB}=24.3 Hz and J_{BX}=9.0 Hz. The X nucleus appears as a doublet of triplets at δ172.3. The coupling constants are consistent with a geometry in which equivalent phosphines P_A are trans to each other and are cis to P_B and P_X. The ^1H NMR spectrum shows a phosphine methyl group ratio of 18:9:6, indicating that one of the phosphines assigned to P_x contains only two methyl substituents. The ^1H NMR spectrum requires the presence of two types of p-cresolate ligands, one of which shows an AA'BB' pattern for the ring protons, similar to that found in **1**. The other cresolate shows an ABC pattern for the ring protons similar to those found in **2**, consistent with ring metallation in the *ortho*-position. Two isomers, **A** and **B**, shown in Figure 1 are consistent with the spectroscopic observations, and we could not distinguish between them spectroscopically, though both contain coordinated dimethyl phosphinite ligands of two different types. A few coordinated dialkylphosphinites have been described and their $^{31}P\{^1H\}$ NMR chemical shifts are in the range of δ140 to 160[9].

X-ray crystallography shows that **A** is the correct structure. Compound **3** crystallized from a toluene/pentane solution at -40 ° C. The structure was solved by Patterson methods and refined *via* standard least squares and Fourier techniques. The space group is $P2_1/n$ with two crystallographically independent but chemically identical molecules in the asymmetric unit. The structure contained no abnormally short intermolecular distances. An ORTEP diagram of one of

Scheme II

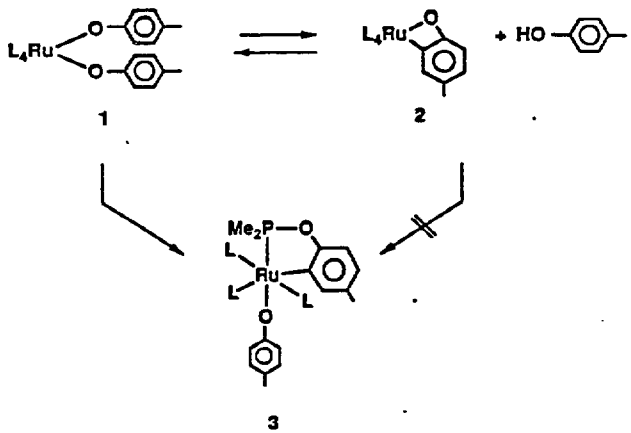

L = PMe_3

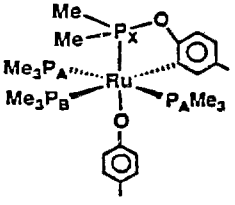

A

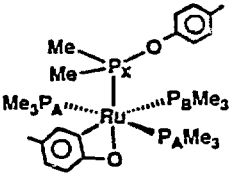

B

Figure 1. Two structures consistent with spectroscopic data for 3.

the two molecules is shown in Figure 2. Intramolecular bond distances and angles for this molecule are given in Tables 1 and 2, crystal and data collection parameters are given in Table 3. The geometry of the complex is based upon six coordinate Ru(II) with two mutually trans PMe_3 ligands, a PMe_3 trans to the metallated aryl ring of the phosphinite ligand, and an η^1-cresolate ligand trans to the phosphorus of the phosphinite ligand.

The Ru-P(2, 4) distances of 2.357(2) Å and 2.366(2) Å are in the range found in related alkylphosphine derivatives of Ru(II) in six coordination[7,10]. The lengths of the mutually trans phosphine-ruthenium bonds range from 2.2 to 2.4 Å. The Ru-P(3) distance of 2.381(2) Å is in the region found for Ru-P (*ca.* 2.32 Å) trans to a carbon ligand[7a, c, g]. The Ru-P(1) bond length of 2.199(2) Å is the shortest Ru-P distance in the structure. Since values for metal-dialkylphosphinite bonds are not known, we must use other comparisons to see if this value is unusual, that is, if M-P(OR)$_x$(R)$_{3-x}$ distances are typically shorter than those for M-PR_3. In structurally similar d^6 compounds, $(CO)_5Cr$-P(OPh)$_3$ and (CO)Cr-PPh_3[11], $BrMn(CO)_3(P(OMe)_2Ph)_2$[12] and $BrMn(CO)(PPh_3)$[13], and in *trans*-[$(PhO)_3P$][Ph_3P]$Cr(CO)_4$[14], the metal-phosphite or -phosphonite bond lengths are shorter than the metal-phosphine bond lengths by 0.1 to 0.16 Å. The difference is usually rationalized in terms of the stronger π-accepting character of the phosphite and phosphonite ligands. Thus, the shorter distance for the ruthenium-dimethylphosphinite bond seems to agree with previous results. The π-accepting nature of the $Me_2P(OAr)$ ligand and the π-donating ability of the aryloxide ligand which is located trans to it may lead to the shorter Ru-P(3) distance.

The P-C cleavage product **3** was also obtained by the addition of p-cresol to the orthometallated cresolate complex **2** followed by heating under the same conditions as the thermolysis of **1**. Moreover, when the thermolysis of **1** or **2** and cresol was stopped before completion (16 h at 65 °C), a mixture of starting complex **1**, orthometallated cresolate complex **2**, and P-C cleaved product **3** was observed as shown in Scheme II. From these data it cannot be determined if **1** or **2** gives rise to the P-C cleavage reaction, since these two complexes interconvert at a rate which is faster than the formation of **3**. Addition of phenol, rather than p-

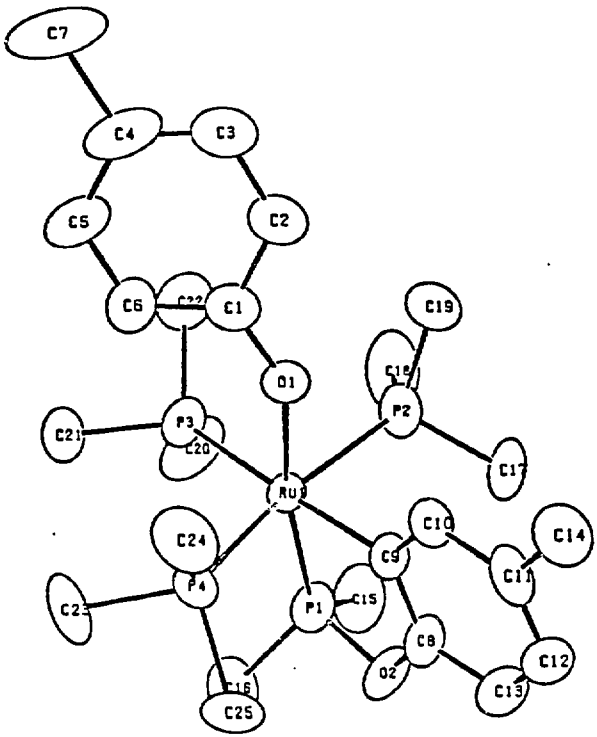

Figure 2. ORTEP Diagram of Complex 3. The hydrogen atoms are omitted for clarity.

Table 1

Crystallographic Data for Complex 3

Empirical formula: $Ru\ P_4\ O_2\ C_{36}\ H_{44}$

A)Crystal Parameters at T = 25°C [a,b]

a = 11.8875(11) Å	Space Group: $P2_1/n$
b = 36.000(4) Å	Formula weight = 603.6 amu
c = 14.1207(13) Å	Z = 8
α = 90.0 °	d(calc) = 1.33 g cm^{-3}
β = 90.428(8) °	
γ = 90.0 °	μ(calc) = 7.4 cm^{-1}

V = 6042.7(18) $Å^3$

Size: 0.10x0.20x0.29 mm

B) Data Measurement Parameters [8]

Radiation : Mo Kα (λ = 0.71073 Å)

Monochromator : Highly-oriented graphite (2θ = 12.2)

Detector : Crystal scintillation counter, with PHA.

Reflections measured : + H, + K, +/-L

2θ range: 3 -> 45 deg Scan Type: θ-2θ

Scan width: Δθ = 0.60 + 0.60 tanθ

Scan speed: 0.72 -> 6.70 (θ, deg/min)

Background: Measured over 0.25*(Δθ) added to each end of the scan.

Vert. aperture = 3.0 mm Horiz. aperture = 2.0 + 1.6 tanθ mm

No. of reflections collected: 8048

No. of unique reflections: 7642

Table 2

Intramolecular Distances

ATOM 1	ATOM 2	DISTANCE
RU1	P1	2.199(2)
RU1	P2	2.357(2)
RU1	P3	2.381(2)
RU1	P4	2.366(1)
RU1	O1	2.161(4)
RU1	C9	2.092(8)
P1	C15	1.811(7)
P1	C16	1.861(7)
P1	O2	1.667(4)
P2	C17	1.857(7)
P2	C18	1.868(7)
P2	C19	1.856(7)
P3	C20	1.851(8)
P3	C21	1.836(7)
P3	C22	1.839(7)
P4	C23	1.865(6)
P4	C24	1.825(6)
P4	C25	1.859(6)
O1	C1	1.327(10)
C1	C2	1.419(13)
C1	C6	1.439(10)
C2	C3	1.401(19)
C3	C4	1.389(15)
C4	C5	1.373(13)
C4	C7	1.576(16)
C5	C6	1.384(12)
O2	C8	1.371(11)
C8	C9	1.426(12)
C8	C13	1.421(9)
C9	C10	1.376(12)
C10	C11	1.435(10)
C11	C12	1.421(18)
C11	C14	1.527(12)
C12	C13	1.380(18)

Table 3

Intramolecular Angles

ATOM 1	ATOM 2	ATOM 3	ANGLE
P1	RU1	P2	92.67(7)
P1	RU1	P3	97.91(6)
P1	RU1	P4	92.09(6)
P1	RU1	O1	167.00(11)
P1	RU1	C9	81.6(3)
P2	RU1	P3	93.34(6)
P2	RU1	P4	162.59(6)
P2	RU1	O1	83.98(11)
P2	RU1	C9	83.61(16)
P3	RU1	P4	102.58(6)
P3	RU1	O1	94.83(11)
P3	RU1	C9	176.88(17)
P4	RU1	O1	87.65(11)
P4	RU1	C9	80.53(16)
O1	RU1	C9	85.5(3)
RU1	P1	O2	106.62(16)
RU1	P1	C15	125.7(3)
RU1	P1	C16	122.81(23)
RU1	P2	C17	115.90(23)
RU1	P2	C18	122.7(3)
RU1	P2	C19	113.52(22)
RU1	P3	C20	117.2(3)
RU1	P3	C21	123.47(25)
RU1	P3	C22	116.4(3)
RU1	P4	C23	123.46(23)
RU1	P4	C24	113.27(22)
RU1	P4	C25	118.59(24)
C15	P1	O2	99.2(3)
C16	P1	O2	100.9(3)
C15	P1	C16	97.0(3)
C17	P2	C18	99.1(3)
C17	P2	C19	100.2(3)
C18	P2	C19	102.0(4)
C20	P3	C21	97.3(4)
C20	P3	C22	100.4(4)
C21	P3	C22	97.7(3)
C23	P4	C24	100.5(3)
C23	P4	C25	97.6(3)
C24	P4	C25	99.3(3)

cresol, to 2 yielded a mixture of P-C cleaved products due presumably to rapid scrambling of the aryloxide ligands, and provided no insight into this problem.

Careful monitoring of the reaction by ^1H NMR spectroscopy provided evidence that it is the *bis*-cresolate complex 1 that gives rise to the P-C cleaved product. The appearance of product was followed at 65 ° C for 2.5 half lives using three different NMR tubes: one containing only 1, one containing equivalent concentrations of 3 and p-cresol, and one containing the equilibrium concentrations of all three reactants. Identical linear first order plots for disappearance of total metal complex vs. time were obtained in all three cases ($k_{obs} = 8.7x10^{-6}$ sec^{-1}) for the data points collected after an initial period during which time equilibrium was established (5 h). The data collected over this time were not accurate enough to extract rate constants for the approach to equilibrium, but it was clear that the sample containing only 1 reacted at a faster initial rate than the equilibrium mixture, while the sample containing 2 and p-cresol reacted more slowly than the equilibrium mixture and showed an initial induction period as displayed in Figure 3. In all three cases, the formation of 3 was strongly inhibited by the addition of PMe_3 to the reaction solution. No product was observed after 3 d for the tubes containing added PMe_3, while reaction was complete for the samples containing no added PMe_3. However, the equilibrium was established at roughly the same rate for the tubes containing added phosphine as for those containing no added phosphine. Although we have no direct mechanistic information about the fundamental phosphorus-carbon bond cleavage step, we suggest that dissociation of phosphine precedes oxidative addition of the P-C bond (Scheme III), as has been proposed[4] for the decomposition of aryl phosphine ligands. Migration of the aryloxide ligand to the phosphido substituent of the intermediate formed by this process followed by orthometallation would form 3.

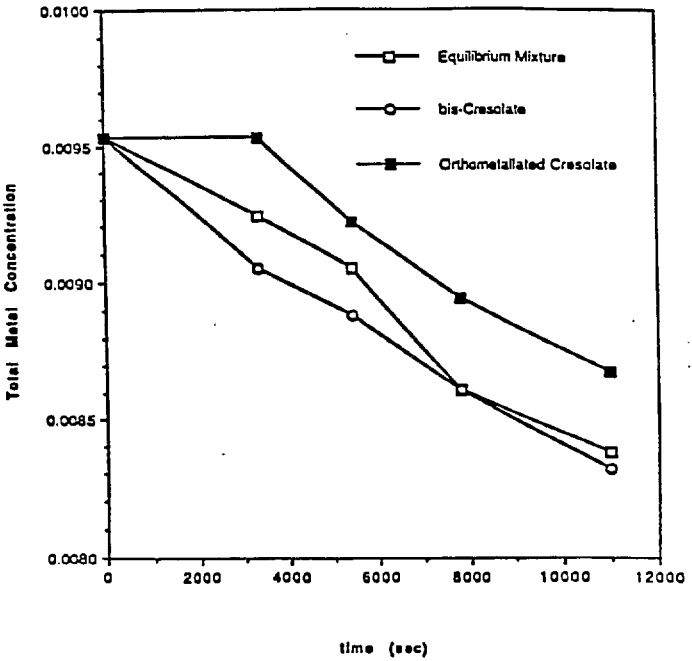

Figure 3. A comparison of the rate of formation of **3** from samples containing only *bis*-cresolate complex **1**, orthometallated cresolate complex **2** and the equilibrium mixture of the two.

Scheme III

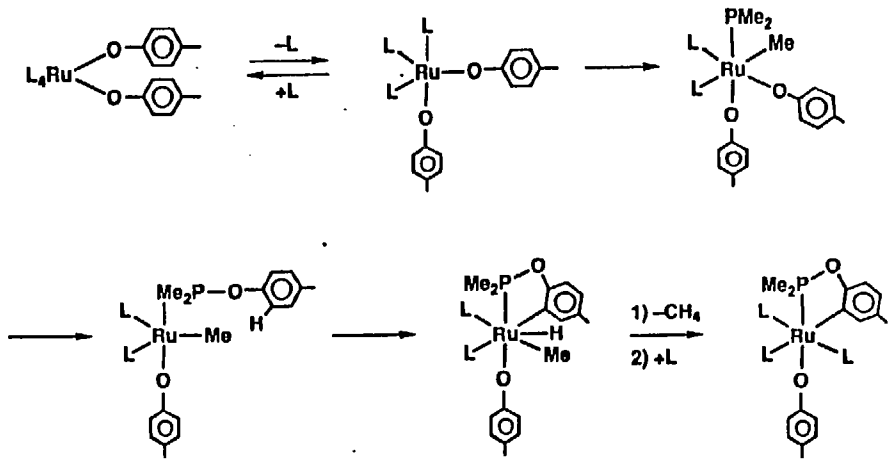
L4Ru
O
O
-L
+L
L
L
L
Ru
O
O
PMe2
Me
L
L
Ru
O
O
Me2P
O
H
L
L
Ru
Me
O
Me2P
O
L
L
Ru
H
Me
O
1) -CH4
2) +L
Me2P
O
L
L
Ru
L
O

Experimental.

General. *Unless otherwise noted, all manipulations were carried out under an inert* atmosphere in a Vacuum Atmospheres 553-2 drybox with attached M6-40-1H Dritrain, or by using standard Schlenk or vacuum line techniques.

^{1}H NMR spectra were obtained on either the 250, 300, 400 or 500 MHz Fourier Transform spectrometers at the University of California, Berkeley (UCB) NMR facility. The 250 and 300 MHz instruments were constructed by Mr. Rudi Nunlist and interfaced with either a Nicolet 1180 or 1280 computer. The 400 and 500 MHz instruments were commercial Bruker AM series spectrometers. ^{1}H NMR spectra were recorded relative to residual protiated solvent. ^{13}C NMR spectra were obtained at either 75.4 or 100.6 MHz on the 300 or 500 MHz instruments, respectively, and chemical shifts were recorded relative to the solvent resonance. Chemical shifts are reported in units of parts per million downfield from tetramethylsilane and all coupling constants are reported in Hz.

IR spectra were obtained on a Perkin-Elmer Model 283 infrared spectrometer or on a Perkin-Elmer Model 1550 or 1750 FT-IR spectrometer using potassium bromide ground pellets. Mass spectroscopic (MS) analyses were obtained at the UCB mass spectrometry facility on AEI MS-12 and Kratos MS-50 mass spectrometers. Elemental analyses were obtained from the UCB Microanalytical Laboratory.

Sealed NMR tubes were prepared by fusing Wilmad 505-PP and 504-PP tubes to ground glass joints which were then attached to a vacuum line with Kontes stopcocks or alternatively, the tubes were attached via Cajon adapters directly to Kontes vacuum stopcocks[15]. Known volume bulb vacuum transfers were accomplished with an MKS Baratron attached to a high vacuum line.

Unless otherwise specified, all reagents were purchased from commercial suppliers and used without further purification. PMe_3 (Strem) was dried over NaK or a Na mirror and vacuum transferred prior to use. Ferrocene (Aldrich) was sublimed prior to use. p-Cresol was dried by refluxing a solution in benzene using a Dean-Stark trap followed by distillation under argon.

Pentane and hexane (UV grade, alkene free) were distilled from $LiAlH_4$ under nitrogen. Benzene, toluene, and tetrahydrofuran were distilled from sodium benzophenone ketyl under nitrogen. Dichloromethane was either distilled under N_2 or vacuum transferred from CaH_2. Deuterated solvents for use in NMR experiments were dried as their protiated analogues but were vacuum transferred from the drying agent.

$Ru(\eta^2\text{-}CH_2PMe_2)(Me)(PMe_3)_3$. $Ru(PMe_3)_4(Me)_2$[5] (1.12 g, 2.57 mmol) was dissolved in 100 mL of hexane in a closed glass vessel of 1 l volume to accommodate the methane produced by the reaction. The solution was degassed and heated to 150° C for 20 h, over which time the solution turned dark brown. The solvent was removed and the residue was sublimed (85 ° C, 10^{-3} torr) to yield 435 mg (40.3 %) of a slightly pink solid. MS (EI): 420 (M^+), 405 (M-Me^+), 344 (M-PMe_3^+); Anal. Calcd. for $C_{13}H_{38}P_4Ru$: C, 37.22; H, 9.13. Found: C, 37.19; H, 9.32.

$(PMe_3)_4Ru(OC_6H_4Me)_2$ **(1).** To a stirring solution of $(PMe_3)_4Ru(Me)_2$ (82.4 mg, 0.189 mmol) in 10 mL of toluene, 2.2 equiv. of p-methylphenol (49.2 mg) in 1 mL of toluene was added by pipette at room temperature in the drybox. Evolution of gas was observed over a period 2 h and the solution turned orange. After a period of 8 h, blocks of 1 crystallized from the reaction solution. The supernatant was decanted and then layered with 5 mL pentane and cooled to -40 ° C for 8 h to yield 66.2 mg (56.8 %) of 1 as yellow blocks. For microanalysis and kinetic studies, a portion of this material was recrystallized by vapor diffusion of pentane into a solution of 1 in toluene. IR (KBr) 3064 (m), 3042 (m), 3001 (m), 2974 (s), 2909 (s), 2854 (m), 1602 (s), 1547 (m), 1504 (s), 1494 (s), 1327 (s), 1303 (s), 1294 (s), 1277 (s), 1161 (m), 971 (s), 942 (s); Anal. Calcd. for $C_{28}H_{50}O_2P_4Ru$: C, 50.40; H, 8.13. Found: C, 50.55; H, 8.17.

$(PMe_3)_4Ru(\eta^2\text{-}OC_6H_3Me)$ **(2).** To a stirred solution of $(PMe_3)_4Ru(\eta^2\text{-}PMe_2CH_2)(Me)$ (421 mg, 1.00 mmol) in toluene (15 mL), one equiv of p-methylphenol (108 mg) in 1 mL toluene was added dropwise by pipette at room temperature. The clear solution turned yellow/orange upon addition of the phenol. The solution was then transferred to a sealed glass reaction vessel, degassed and heated to 85° C for 3 h. After this time the reaction was allowed to cool to room temperature at which point pale yellow blocks of 2 crystallized from the reaction mixture. The

supernatant was decanted and then layered with 5 mL pentane followed by cooling to -40° C to provide 322 mg of **2** (61 % total yield) as yellow blocks. IR: 3029 (m), 2968 (m), 2902 (s), 2852 (m), 1439 (s), 1426 (m), 1297 (m), 1280 (m), 1250 (m), 1231 (m), 1219 (m), 1190 (m), 970 (m), 941 (s), 857 (m), 712 (m), 665 (m), 542 (m); Anal. Calc. for $C_{19}H_{42}OP_4Ru$: C, 44.61; H, 8.28. Found: C, 44.80; H, 8.41.

$(PMe_3)_3(\eta^2\text{-}PMe_2OC_6H_3{}^tRu(OC_6H_4Me)$ (**3**) A solution of 120 mg (0.194 mmol) **1** in toluene (70 ml) was heated for 8 h at 100 ° C in an evacuated, sealed glass vessel. No significant color change occurred in the initial yellow solution. After this time the solvent was removed under reduced pressure. The resulting solid was dissolved in a minimum amount of toluene (1.5 ml), and vapor diffusion of pentane into the toluene solution at room temperature for 24 h yielded 40.8 mg (34.0 %) of **3** as yellow blocks. IR: 2996, (m), 2988 (m), 2969 (m), 2958 (m), 2907 (m), 1601 (m), 1409 (s), 1498 (s), 1441 (m), 1323 (s), 1303 (m), 1293 (m), 1282 (m), 1180 (m), 946 (s), 935 (s), 933 (s), 858 (s), 816 (s), 716 (s); Anal. Calcd. for $C_{25}H_{46}O_2P_4Ru$: C, 49.67; H, 7.67. Found: C, 49.87; H, 7.43.

Crystal and Molecular Structure Determination of **3**. Pale, clear yellow plate-like crystals of the compound were obtained by slow cooling to -30° C from pentane/toluene. Fragments cleaved from some of these crystals were mounted on glass fibers using polycyanoacrylate cement. The X-ray structure determination was carried out by Dr. F.J. Hollander of the UC Berkeley X-ray Diffraction Facility (CHEXRAY). Preliminary precession photographs indicated monoclinic Laue symmetry and yielded approximate cell dimensions.

The crystal used for data collection was then transferred to our Enraf-Nonius CAD-4 diffractometer[16] and centered in the beam. Automatic peak search and indexing procedures yielded the monoclinic reduced primitive cell. The final cell parameters and specific data collection parameters for this data set are given in Table 3. Due to some errors on set-up, the data collection parameters were not ideal, and a significant number of data suffered from overlap of neighboring data.

The 8048 raw intensity data were converted to structure factor amplitudes and their esd's by correction for scan speed, background and Lorentz and polarization effects. Inspection of the intensity standards revealed a variation of +/- 1.5% of the original intensity. No correction for crystal decomposition was necessary. Inspection of the azimuthal scan data showed a variation I_{min}/I_{max}=0.91 for the average curve. An empirical correction based on the observed variation was applied to the data (T_{max}=1.0, T_{min}=0.91). Removal of systematically absent data left 7877 unique data in the final data set. Further rejection of a rough cone of data which showed themselves to be severely affected by overlap left a final total of 7642 acceptable data.

The structure was solved by Patterson methods and refined via standard least squares and Fourier techniques. Following refinement of all atoms with anisotropic thermal parameters, data suffering from extreme overlap were removed from the data set as noted above. However, it is certain that other data suffer likewise, but were simply not obvious. In a final difference Fourier map peaks were found corresponding to the positions of only a few of the expected hydrogen atoms. No hydrogens were included in the calculation of structure factors for the last cycles of least squares.

The final residuals for 557 variables refined against the 5406 data for which $F^2 > 3\sigma(F^2)$ were R = 5.93%, wR = 7.75%, and GOF = 3.00. The R value for all 1392 data points was 13.2%.

The quantity minimized by the least squares program was $\Sigma w(|F_o|-|F_c|)^2$ where w is the weight of intense reflections, was set to 0.03 throughout the refinement. The analytical forms of the scattering factor tables for the neutral atoms were used and all scattering factors were corrected for both the real and imaginary components of anomalous dispersion.

Inspection of the residuals ordered in ranges of $\sin(\theta)/\lambda$, $|F_o|$, and parity and value of the individual indexes showed no features or trends not previously noted. The largest peak in the final difference Fourier map had an electron density of 0.76 $e^-/Å^3$ and the lowest excursion -0.61$e^-/Å^3$. There was no indication of secondary extinction in the high-intensity low angle data.

Kinetic analysis. Two stock solutions were prepared. Into a 3 mL volumetric flask was weighed 14.7 mg (0.0287 mmol) of 3 and 3.1 mg (0.0287) of p-cresol, followed by addition of

toluene-d_8 to give a 0.00957 M solution of both reagents. Into a 2 mL volumetric flask was weighed 11.9 mg of **1** (0.0193 mmol) followed by addition of toluene to give a 0.00964 M solution. To one 9" NMR tube was added 0.70 mL of the solution of **1**, to another tube was added 0.70 mL of the solution of **1** and p-methylphenol, and to a third tube was added 0.40 mL of the solution of **1** and 0.30 mL of the solution of **3** and p-cresol. To each tube was added 2-3 mg ferrocene as an internal standard. Each tube was freeze pump thawed through three cycles and sealed to give a tubes of equal length. The tubes were heated at 65 ° C in a factory-calibrated Neslab Exocal Model 251 constant temperature bath filled with Dow Corning 200 silicone fluid, and cooled in a room temperature water bath after removal from the 65° C bath. All three reactions were monitored to 2.5 half-lives by ambient-temperature ^{1}H NMR spectrometry by integrating the methyl protons of the p-methylphenol group vs. the ferrocene internal standard. An infinity point was obtained experimentally by heating the three tubes to 85 for 8 h and obtaining ^{1}H NMR spectra after this time. All spectra were taken with a single acquisition and double checked with a second acquisition after a delay of at least 10 T_1. All three kinetic plots displayed excellent linearity with correlation coefficients of 0.985 or better, and the yield of each reaction was greater than 98 %.

Dependence of reaction on PMe_3 concentration. Four NMR tubes were prepared. Two were prepared exactly as the tubes described in the kinetic analysis section containing only **1**, except that 10 equivalents (0.0675 mmol) PMe_3 was added to one of these tubes to give a concentration of 0.0964 M PMe_3. Two other tubes were prepared in the same manner except the solution of **3** and p-cresol was used instead of the solution of **1**. The tubes were heated to 65° C for 3 d and monitored periodically by ^{1}H and ^{31}P NMR spectrometry. The addition of PMe_3 had no effect on the rate at which equilibrium was established. However no product was observed after 3 d at for the tubes containing added PMe_3, while reaction was complete for the samples containing no additional PMe_3.

Acknowledgements

We thank Dr. Thomas H. Tulip for providing us with crystallographic details on the structure of $(PMe_3)_4Rh(\eta^2\text{-}CH_2C_6H_4)$.

Table 4. ^{1}H NMR Spectroscopic Data

Compound	d (ppm)	multiplicity	J (Hz)	integral	assignment
$(PMe_3)_3Ru(\eta^2\text{-}CH_2PMe_2)Me$	-0.41	dddd	7.7, 7.7, 7.5,3.6	3	Me
	-0.58	m		1	CH_2PMe_2
	-0.24	m		1	
	1.10	d	5.3	9	PMe_3
	1.21	dd	7.9,3.3	9	
	1.24	dd	7.0, 1.8,	9	
	1.18	dd	9.0, 5.3	3	CH_2PMe_2
	1.28	dd	8.9, 2.4	3	
$(PMe_3)_4Ru(OC_6H_4Me)_2$ (1)	0.96	d	7.7	18	*cis* PMe_3
	1.14	N[a]	6.2	19	*trans* PMe_3
	2.40	s		6	p-Me
	7.04	d	8.4	4	Aromatic
	7.22	d	8.4	4	
$(PMe_3)_4Ru(\eta^2\text{-}OC_6H_3Me)$ (2)	1.00	d	7.4	9	*cis* PMe_3
	1.09	d	6.0	9	
	1.15	N	5.8	18	*trans* PMe_3
	2.58	s		3	p-Me
	6.06	d	7.6	1	Aromatic
	6.96	d	7.2	1	
	7.30	br, s		1	
$(PMe_3)_3(\eta^2\text{-}PMe_2OC_6H_3)Ru$-$(OC_6H_4Me)$ (3)	0.92	N	6.2	18	*trans* PMe_3
	1.06	d	5.5	9	*cis* PMe_3
	1.29	d	6.4	6	Me_2POAr
	2.42	s		3	p-Me
	2.43	s		3	
	6.89	d	7.4	2	OC_6H_4Me
	7.04	d	7.8	2	
	6.67	dd	6.4, 2	1	$ArOPMe_2$
	7.04	dd	7.8, 2	1	
	8.10	br, s		1	

[a] The value of N refers to the separation between the two outermost lines. See Harris, R.K.; Hayter, R.G. *Can. J. Chem.* 1964, *42*, 2282. Harris, R.K. *Can. J. Chem.*1964, *42*, 2275.

Table 5. $^{13}C\{^1H\}$ NMR Spectroscopic Data.

Compound	δ (ppm)	multiplicity[b]	J (Hz)	assignment
$(PMe_3)_3Ru(\eta^2\text{-}PMe_2CH_2)Me$	24.73	dd	18.0, 7.5	PMe_3
	24.57	d	15.4	
	22.10	dq	20.1, 2.6	
	15.36	td	9.3, 3.5	$\underline{P}Me_2PCH_2$
	5.78	dd	7.7, 6.6	
	-1.27	dq	54.1, 11.7	Me
	-10.57	m		$PMe_2\underline{P}CH_2$
$(PMe_3)_4Ru(OC_6H_4Me)_2$ (1)	18.65	t	12.6	*trans* PMe_3
	22.57	m		*cis* PMe_3
	20.75	s		p-Me
	118.36	s		Aromatic
	120.66	s		
	129.68	s		
	169.41	s		
$(PMe_3)4Ru(\eta^2\text{-}OC_6H_3Me)$ (2)	18.65	td	13.5, 3.0	*trans* PMe_3
	22.44	dt	18.1, 2.6	*cis* PMe_3
	25.32	dq	25.0, 3.4	
	21.88	s		*p-Me*
	105.55	s		Aromatic
	120.44	s		
	122.00	s		
	137.80	s		
	142.69	dtd	65, 16, 6	
	182.41	s		
$(PMe_3)_3(\eta^2\text{-}PMe_2OC_6H_3)Ru$-$(OC_6H_4Me)$ (3)	18.40	t	13.4	PMe_3 and
	23.89	d	18.1	$\underline{Me_2}POAr$
	27.39	d	30	
	20.72	s		p-Me
	21.49	s		
	112.86	dd	13, 0.6	Aromatic groups
	120.79	s		
	123.51	s		
	126.73	t	2	
	131.48	dd	4.2	
	132.41	s		
	140.61	s		
	162.72	dq	43, 12	
	165.80	dq	11.1, 2.2	
	172.81	d	1.8	

[b]The symbols d and t, when applied to the PMe_3 resonances are observed patterns, not true multiplicity patterns. Accordingly, the values reported as coupling constants for these resonances are the separation between lines and do not necessarily reflect the true coupling constants.

Table 6. $^{31}P\{^{1}H\}$ NMR Spectroscopic Data.

Compound	Spin System	d (ppm)	J (Hz)
$(PMe_3)_3Ru(\eta^2\text{-}PMe_2CH_2)Me$	ABCD	δA=5.76	J_{AB}= 0
		δB=0.64	J_{AC}=27
		δC=-7.61	J_{AD}=231
		δD=-37.93	J_{BC}=24
			J_{BD}=38
			J_{CD}=24
$(PMe_3)_4Ru(OC_6H_4Me)_2$ (1)	A_2B_2	δA=14.89	J_{AB}=31.8
		δB= -0.98	
$(PMe_3)4Ru(\eta^2\text{-}OC_6H_3Me)$ (2)	A_2BC	δA=-2.73	J_{AB}=34
		δB=15.78	J_{AC}=24
		δC=-9.31	J_{BC}=17
$(PMe_3)_3(\eta^2\text{-}PMe_2OC_6H_3)Ru(OC_6H_4Me)$ (3)	A_2BC	δA= -1.69	J_{AX}=37.2
		δB= -19.24	J_{AB}=24.3
		δX=172.29	J_{BX}= 9.0

References

1 McAuliffe, S.A. *Transition Metal Complexes of Phosphorus, Arsenic and Antimony Ligands* Wiley: New York, 1973. McAuliffe, C.A.; Levason, W. *Phosphine, Arsine , and Stibine Complexes of the Transition Elements* Elsevier: Amsterdam, 1979.

2 a) C.A. Tolman, *Chem. Rev.* 77 (1977) 313. b) Rahman, Md. M; Hong-Ye, L.; Eriks, K.;Prock, A.; Giering, W.P. *Organometallics* 1989, *8*, 1.

3 a) Crabtree, R.H. *Chem. Rev.* 1985, 245. b) Derosiers, P.J.; Shinomoto, R.S.; Flood, T.C. *J. Am. Chem. Soc.* 1986, *108*, 7964.

4 a) P.E. Garrou, *Chem. Rev.* 1985, *85*, 171. b) Doherty, N.M.; Hogarth, G.; Knox, S.A.R.; Macpherson, K.S.; Melchior, F.; Orpen, A.G. *J. Chem. Soc., Chem. Commun.* 1986, 540. c) Doel, G.R.; Feasey, N.D.; Knox, S.A.R.; Orpen, A.G.; Webster, J. *J. Chem. Soc., Chem. Commun.* 1986, 542. d) Benlaarab, H.; Chaudret, B.; Dahan, F.; Poilblanc, R. *J. Organomet. Chem.* 1987, *320*, C51. e) McGhee, W.D.; Foo, T.; Hollander, F.J.; Bergman, R.G. *J. Am. Chem. Soc.* 1988, *110*, 8543.

5 a) A. Gillie, J.K. Stille, *J. Am. Chem. Soc.* 102 (1980) 4933. b) K. Kikukawa, T. Yamane, Y. Ohibe, M. Takagi, T. Matsuda, *Bull. Chem. Soc. Jpn.* 52 (1979) 1187. c) K. Kikukawa, M. Takage, T. Matsuda, *Bull. Chem. Soc. Jpn.* 52 (1979) 1493. d) J.V. Ortiz, Z. Havlas, R. Hoffmann, *Helv. Chim. Acta.* 67 (1984) 1.

6 Andersen, R.A.; Jones, R.A.; Wilkinson, G. *J. Chem. Soc. Dalton Trans.* 1978, 446.

7 a) W.K. Wong, K.W. Chiu, J.A. Slatter, G. Wilkinson, M. Motevalli, M.B. Hursthouse *Polyhedron* 1984, *3*, 1255. b) Slatter, J.A.; Wilkinson, G.; Thornton-Pett, M.; Hursthouse, M.B. *J. Chem. Soc., Dalton Trans.* 1984, 1255. c) Calabrese, J.C.; Colton, M.C.; Herskovits, T.; Klabunde, U.; Parshall, G.W.; Thorn, D.L.; Tulip, T.H. *N.Y. Acad. Sci.* 1983, *415*, 302. An ORTEP is provided in this reference, but no distances are given. The Ru-P bond lengths are 2.343(1), 2.347(1), (mutually trans PMe_3 groups) 2.321(1), 2.321(1) (mutually cis PMe_3 groups). *private communication.* d) Antberg, M.; Dahlenburg, L.; Frosin, K.M.; Höck, N.

Chem. Ber. 1988, *121*, 859. e) Dahlenburg, L.; Frosin, K.M. *Chem. Ber.* 1988, *121*, 864. f) Hartwig, J.F.; Andersen, R.A.; Bergman, R.G. *J. Am. Chem. Soc.* 1989, *111*, 2717.

8 a) Nixon, J.F.; Pidcock, A. *Ann. Rev. NMR Spectroscopy*, 1969, *2*, 345. b) Verkade, J.M.; Quin, L.D. eds. *Phosphorus-31 NMR Spectroscopy in Stereochemical Analysis*; VCH Publishers: New York, 1987.

9 Sime, W.J.; Stephenson, T.A. *J. Chem. Soc., Dalton Trans.*, 1978, 1647. b) reference 7b p. 500.

10 An ORTEP is provided in reference 7c, but no bond distances are given. The Ru-P bond lengths are 2.343(1), 2.347(1), (mutually trans PMe_3 groups) 2.321(1), 2.321(1) (mutually cis PMe_3 groups), private communication.

11 Plastas, H.J.; Stewart, J.M.; Grim, S.O. *J. Am. Chem. Soc.* 1969, *91*, 4326.

12 Kruger, M.J.; Heckroodt, R.O.; Reimann, R.H.; Singleton, E. *J. Organomet. Chem.* 1975, *87*, 323.

13 Vahrenkamp, H. *Chem. Ber.* 1971, *104*, 449.

14 Workulich, M.J.; Atwood, J.L.; Canada, L.; Atwood, J.D. *Organometallics*, 1985, *4*, 867.

15 Bergman, R.G.; Buchanan, J.M.; McGhee, W.D.; Periana, R.A.; Seidler, P.F.; Trost, M.K.; Wenzel, T.T. In *Experimental Organometallic Chemistry: A Practicum in Synthesis and Characterization*; Wayda, A.L.; Darensbourg, M.Y., Eds.; ACS Symposium Series 357; American Chemical Society: Washington, DC, 1987, p 227.

16 For a description of the X-ray diffraction and analysis protocols used, see (a) Hersh, W.H.; Hollander, F.J.; Bergman, R.G. *J. Am. Chem. Soc.* 1983, *105*, 5834. (b) Roof, R.B., Jr. *A Theoretical Extension of the Reduced-Cell Concept in Crystallography*; Publication LA-4038, Los Alamos Scientific Laboratory: Los Alamos, NM 1969. (c) Cromer, D.T.; Waber, J.T. *International Tables for X-ray Crystallography*; Kynoch Press: Birmingham, England, 1974; Vol IV, Table 2.2B.

Chapter 5

Insertion Reactions of CO and CO_2 with Ruthenium Benzyl, Arylamido, and Aryloxide Complexes: A Comparison of the Reactivity of Ruthenium-Carbon, Ruthenium-Nitrogen, and Ruthenium-Oxygen Bonds.

Introduction

Transition metal-carbon, -oxygen, and -nitrogen bonds are involved in many homogeneous and heterogeneous catalytic processes.[1] Although late transition metal-carbon bonds have been carefully studied for many years, examples of late transition metal-oxygen and -nitrogen linkages have only recently been actively investigated.[2] It has been thought that late transition metal alkoxide and amide complexes would be unstable due to matching a soft metal system with a traditionally hard ligand.[3] Yet, several monomeric alkoxide and amide complexes have now been isolated in 16 electron square planar complexes,[4] as well as 18 electron octahedral and pseudooctahedral geometries.[5]

Reactions such as reductive elimination and migratory insertion, which are well understood with metal-carbon bonds, have been observed with only a few systems containing late transition metal-oxygen and -nitrogen bonds.[4b-h, 5a,6 ,7] Insertion of carbon monoxide, carbon dioxide, and alkenes into transition metal alkyl bonds have attracted the most attention, and recently the insertion of these substituents into late transition metal alkoxide and amide linkages has been observed. Examples of insertion reactions involving platinum alkoxide and amide linkages exist,[6,7] as do insertions into both 16-electron and 18-electron iridium and rhodium alkoxide bonds.[4d-f, 5a] Some kinetic[5a, 6f] and labelling[6g] data have been obtained for these reactions, and complexes which may model reaction intermediates have been isolated or observed.[4f, 7] Nevertheless, the little information that is available on these reactions has not led to a clear mechanistic picture. Some authors have proposed ionic mechanisms, while others have proposed concerted ones.[5a, c] In our laboratories we observed what may be a model for an intermediate in CO_2 insertion reactions, the direct product of the addition of *tert*-butylisocyanate to an azairidacylobutane.[8]

In addition to these mechanistic questions, the factors that control selectivity of unsaturated organic compounds toward insertion into the metal-carbon, - nitrogen, and -oxygen bonds are not well understood. The mismatch of a soft late transition metal center and a hard amide or alkoxide substituent has led to the expectation that late metal heteroatom

bonds should react preferentially over metal-carbon bonds. This has been the result with some systems,[6a, b, f, g, i] but another system shows preferential M-C over M-O insertion of carbon monoxide.[4b,-c] Often the question of whether the products obtained are kinetically or thermodynamically controlled has been ignored. One problem in understanding the migratory aptitudes of these substituents has been the lack of metal-ligand systems in which a series of compounds containing metal-carbon, -oxygen, and -nitrogen bonds can be directly and systematically compared.

We report here the reactions of a series of compounds containing ruthenium-carbon, ruthenium-oxygen, and ruthenium-nitrogen bonds to the same L_4Ru ($L=PMe_3$) fragment. Their insertion reactions with carbon monoxide and carbon dioxide are selective for the metal-carbon bond in some cases and the metal-heteroatom bond in other cases. We have been able to obtain mechanistic data for the insertion reactions of CO_2, including the observation of probable reaction intermediates.

Results

The synthesis of the orthometallated benzyl compound, $L_4Ru(\eta^2\text{-}CH_2C_6H_4)$ ($L=PMe_3$) (1) (Scheme I) was reported by Wilkinson in 1984.[9] We have described the analogous orthometallated aryloxide complex $L_4Ru(OC_6H_3Me)$ (2) (Scheme II)[10] and have reported the preparation of the orthometallated arylamide complex $L_4Ru(NHC_6H_4)$ (3) (Scheme III)[11] and $L_4Ru(NHC_6H_3CMe_3)$ (4) in communication form.[5d] For the purpose of reference, the ^1H, $^{31}P\{^1H\}$, and $^{13}C\{^1H\}$ NMR spectral data for compounds 1-3 are included in Tables 1-3. In this paper we describe the insertion reactions of these three compounds with CO and CO_2.

Insertion Reactions of the Orthometallated Benzyl Complex, $L_4Ru(\eta^2\text{-}CH_2C_6H_4)$. The products of reaction of the known orthometallated benzyl complex 1 with CO and CO_2 are shown in Scheme I. The reaction of 1 with 2 atm of carbon monoxide in benzene led to formation of 5, the result of insertion into the metal aryl bond and substitution

Table 1. ^{1}H NMR Spectroscopic Data[a]

Compound	d (ppm)	multiplicity	J (Hz)	Integral	assignment[b]
$(PMe_3)_4Ru(\eta^2\text{-}CH_2C_6H_4)$ (1)[g]	0.93	d	5	9	*cis*-PMe_3
	1.17	d	5	9	
	1.03	t	3	18	*trans*-PMe_3
	1.35	m		2	CH_2
	6.61	d	7	1	Aromatic
	7.11	t	7	1	
	7.20	t	7	1	
	7.52	d	7	1	
$(PMe_3)_3(CO)Ru(\eta^2\text{-}CH_2C_6H_4C(O))$ (5)[f]	1.14	t	3.1	18	*trans*-PMe_3
	1.49	d	6.7	9	*cis*-PMe_3
	2.65	td	7.6, 4.4	2	CH_2
	6.84	td	13.8, 0.7	1	Aromatic
	7.04	td	7.4, 1.3	1	
	7.09	d	7.6	1	
	7.35	d	7.5	1	
$(PMe_3)_4Ru(\eta^2\text{-}OC(O)C_6H_4CH_2)$ (6)[d]	0.81	d	7.4	9	*cis*-PMe_3
	1.10	d	5.9	9	
	0.97	t	2.7	18	*trans*-PMe_3
	2.44	m		2	CH_2
	7.15	m		1	Aromatic
	7.20	t	7.2	1	
	7.43	d	7.3	1	
	8.84	d	7.6	1	
$(PMe_3)_3Ru(\eta^4\text{-}OC(O)C_6H_4CH_2)$ (7)[e]	0.35	d	8.1	9	PMe_3
	1.13	d	9.7	9	
	1.14	d	6.8	9	
	1.69	m		1	CH_2
	2.43	m		1	
	6.86	t	6.8	1	Aromatic
	7.00	m		2	
	8.43	m		1	
$(PMe_3)_4Ru(\eta^2\text{-}OC_6H_3Me)$ (2)[f]	1.00	d	7.4	9	*cis* PMe_3
	1.09	d	6.0	9	
	1.15	N	5.8	18	*trans* PMe_3
	2.58	s		3	p-Me
	6.06	d	7.6	1	Aromatic
	6.96	d	7.2	1	
	7.30	br, s		1	
$(PMe_3)_3(CO)Ru(\eta^2\text{-}OC_6H_3(Me)C(O))$ (8)[d]	0.97	t	5.2	18	*trans*-PMe_3
	1.17	d	7.7	9	*cis*-PMe_3
	2.28	s		3	Me
	7.13	d	9.2	1	Aromatic
	7.27	d	9.3	1	
	7.74	br,s		1	

Table 1. ^1H NMR Spectroscopic Data (cont.)

$(PMe_3)_4Ru$ (η^2-$OC_6H_3(Me)C(O)O$) (9)[c]	1.24	t	3.1	18	*trans*-PMe_3
	1.37	d	2.14	9	*cis*-PMe_3
	1.39	d	2.31	9	
	2.11	s		3	Me
	6.42	d	8.3	1	Aromatic
	6.76	dd	8.2, 2.5	1	
	7.71	d	2.4	1	
$(PMe_3)_4Ru(\eta^2$-$NHC_6H_4)$) (3)	0.98	d	5.7	9	*cis*-PMe_3
	1.06	d	6.7	9	
	1.13	t	2.3	18	*trans*-PMe_3
	1.28	br, s		1	NH
	5.84	d	7.4	1	Aromatic
	6.65	t	6.5	1	
	7.11	t	7.3	1	
	7.33	br, s		1	
$(PMe_3)_3(CO)Ru(\eta^2$-$NHC_6H_4C(O))$ (10)[d]	0.93	t	3.3	18	*trans* PMe_3
	1.23	d	8.1	9	*cis* PMe_3
	3.12	br, s		1	NH
	6.37	m		1	Aromatic
	6.64	dd	21.4, 8.3	1	
	7.07	m		1	
	7.81	t	7.6	1	
$(PMe_3)_4Ru(\eta^2$-$OC(O)NHC_6H_4)$ (11)[c]	0.93	d	6.6	9	*cis*-PMe_3
	1.07	d	5.8	9	
	0.94	t	2.9	18	trans-PMe_3
	6.43	d	7.7	1	Aromatic
	6.76	t	7.0	1	
	6.96	t	7.2	1	
	7.25	m		1	
	7.48	br, s		1	NH
$(PMe_3)_4Ru(\eta^2$-$NHC_6H_4C(O)O)$ (13)[c]	1.25	t	2.8	18	*trans*-PMe_3
	1.33	d	7.6	9	*cis*-PMe_3
	1.40	d	7.6	9	
	2.35	br, s		1	NH
	5.85	t	7	1	Aromatic
	6.21	d	8	1	
	6.65	t	7	1	
	7.77	d	8	1	

Table 1. ^{1}H NMR Spectroscopic Data (cont.)					
$(PMe_3)_4Ru(\eta^2\text{-}C(O)C_6H_3NH_2)$ (17)	1.06	t	2.7	18	*trans*-PMe_3
	1.43	d	7.3	9	*cis*-PMe_3
	1.46	d	6.0	9	
	5.88	s		2	NH
	6.11	d	1	7.6	Aromatic
	6.72	t	1	7.4	
	6.82	m	1		

[a] The symbols d and t, when applied to the PMe_3 resonances are observed patterns, not true multiplicity patterns. Accordingly, the values reported as coupling constants for these resonances are the separation between lines and do not necessarily reflect the true coupling constants.

[b] The assignments of cis and trans for the PMe_3 ligands refers to the mutually cis and mutually trans PMe_3 sites.

[c] CD_2Cl_2, 25 °C; [d] C_6D_6, 25 °C; [e] $C_6H_5Me\text{-}d_8$, -10° C; [f] THF-d_8, 25 °C

Table 2. $^{13}C\{^1H\}$ NMR Spectroscopic Data.[a]

Compound	δ (ppm)	multiplicity[b]	J (Hz)	assignment[c]
$(PMe_3)_4Ru(\eta^2\text{-}CH_2C_6H_4)$ (1)[d]	-3.5	dq	51, 8	CH_2
	19.7	tt	13, 4	*trans*-PMe_3
	24.5	dm	14	*cis*-PMe_3
	26.1	dm	12	
	120.2	s		Aromatic
	122.9	s		
	124.1	s		
	138.0	s		
$(PMe_3)_3(CO)Ru(\eta^2\text{-}CH_2C_6H_4C(O))$ (5)[f]	18.93	td	15, 3	*trans*-PMe_3
	21.56	d	22.1	*cis*-PMe_3
	21.06	dt	48.8, 10.1	CH_2
	117.94	s		Aromatic
	123.58	s		
	129.44	s		
	130.00	d	6.9	
	153.75	d	2.3	
	162.04	s		
	206.15	m		M-CO
	274.50	m		
$(PMe_3)_4Ru(\eta^2\text{-}OC(O)C_6H_4CH_2)$ (6)[d]	16.08	dq	53.7, 9.2	CH_2
	19.18	t	12.21	*trans*-PMe_3
	21.98	d	17.4	*cis*-PMe_3
	23.43	d	26.3	
	122.70	s		Aromatic
	127.69	s		
	132.67	s		
	132.74	s		
	139.64	s		
	152.65	s		
	171.08	s		OC(O)
$(PMe_3)_3Ru(\eta^4\text{-}OC(O)C_6H_4CH_2)$ (7)[e]	19.70	d	26.3	PMe_3
	20.45	d	21.2	
	21.25	d	37.8	
	37.30	d	25.8	CH_2
	102.47	d	4.3	Aromatic
	118.09	s		
	121.05	s		
	130.37	s		
	132.14	s		
	137.29	s		
	169.54	s		OC(O)

Table 2. $^{13}C\{^1H\}$ NMR Spectroscopic Data (cont.)

$(PMe_3)_4Ru(\eta^2\text{-}OC_6H_3Me)$ (2)[f]	18.65	td	13.5, 3.0	*trans* PMe_3
	22.44	dt	18.1, 2.6	*cis* PMe_3
	25.32	dq	25.0, 3.4	
	21.88	s		p-Me
	105.55	s		Aromatic
	120.44	s		
	122.00	s		
	137.80	s		
	142.69	dtd	65, 16, 6	
	182.41	s		
$(PMe_3)_3(CO)Ru(\eta^2\text{-}OC_6H_3(Me)C(O)$ (8)[d]	17.16	t	14.5	*trans* PMe_3
	20.50	d	30.0	*cis* PMe_3
	20.48	s		Me
	118.53	s		Aromatic
	120.07	s		
	120.32	s		
	133.44	s		
	139.34	s		
	177.90	s		
	202.68	s		M-CO
	265.38	m		
$(PMe_3)_4Ru(\eta^2\text{-}OC_6H_3(Me)C(O)O)$ (9)[c]	17.52	t	12.7	*trans*-PMe_3
	21.09	d	30.3	*cis*-PMe_3
	21.37	d	27.40	
	20.33	s		Me
	119.59	s		Aromatic
	121.38	s		
	123.84	d	4.6	
	132.18	s		
	133.79	s		
	168.86	s		
	170.61	s		OC(O)
$(PMe_3)_4Ru(\eta^2\text{-}NHC_6H_4)$ (3)[c]	19.57	tt	12.9, 1.8	*trans*-PMe_3
	23.37	dt	16.8, 2.2	*cis*-PMe_3
	25.32	dm	20.0	
	105.28	m		Aromatic
	111.09	m		
	122.78	s		
	136.38	m		
	142.97	dtd	64.3, 15.9, 7.5	
	178.84	d	4.0	

Table 2. $^{13}C\{^1H\}$ NMR Spectroscopic Data (cont.)

$(PMe_3)_3(CO)Ru(\eta^2\text{-}NHC_6H_4C(O))$ (10)[d]	17.93	t	14.7	*trans*-PMe_3
	20.57	d	27.6	*cis*-PMe_3
	109.20	s		Aromatic
	115.50	d	4.6	
	120.94	s		
	131.97	s		
	134.02	s		
	169.11	s		
	202.77	m		M-CO
	205.39	m		
$(PMe_3)_4Ru(\eta^2\text{-}OC(O)NHC_6H_4)$ (11)[c]	19.17	td	13.0, 1.8	*trans* PMe_3
	21.53	d	18.3	*cis* PMe_3
	24.48	d	25.8	
	113.49	s		Aromatic
	118.27	s		
	122.11	s		
	145.95	d	0.9	
	148.18	s		
	150.27	dm	73.6	
	157.57	s		OC(O)
$(PMe_3)_4Ru(\eta^2\text{-}NHC_6H_4C(O)O)$ (14)[c]	18.05	t	12.9	*trans*-PMe_3
	21.09	d	25.0	*cis*-PMe_3
	22.00	d	27.4	
	107.63	s		Aromatic
	115.43	s		
	121.08	d	5.1	
	129.86	s		
	134.72	s		
	160.36	s		
	170.68	s		
$(PMe_3)_4Ru(\eta^2\text{-}OC(O)C_6H_3NH_2)$ (15)[c]	18.63	td	13.2,2.4	*trans*-PMe_3
	22.29	dt	20.3, 1.8	*cis*-PMe_3
	24.99	dtd	25.9, 4.0, 1.8	
	109.19	s		Aromatic
	124.56	d	2.7	
	129.00	dd	3.7, 1.7	
	129.64	dd	4.4, 1.6	
	148.86	s		
	181.76	dtd	70.8, 14.9, 7.9	
	183.50	d	10.0	OC(O)

[a] The symbols d and t, when applied to the PMe_3 resonances are observed patterns, not true multiplicity patterns. Accordingly, the values reported as coupling constants for these resonances are the separation between lines and do not necessarily reflect the true coupling constants.

[b] The assignments of cis and trans for the PMe_3 ligands refers to the mutually cis and mutually trans PMe_3 sites.

[c] CD_2Cl_2; [d] C_6D_6; [e] $C_6H_5Me\text{-}d_8$, -10C; [f] $THF\text{-}d_8$

Table 3. $^{31}P\{^{1}H\}$ NMR Spectroscopic Data.

Compound	Spin System	d (ppm)	J (Hz)
$(PMe_3)_4Ru(\eta^2\text{-}CH_2C_6H_4)$ (1)[b]	A_2BC	δA=-5.6 δB=-10.4 δC=-10.7	J_{AB}=27 J_{AC}=27 J_{BC}=13
$(PMe_3)_3(CO)Ru(\eta^2\text{-}CH_2C_6H_4C(O))$ (5)[d]	A_2B	δA=-4.01 δB=-15.49	J_{AB}=27.0
$(PMe_3)_4Ru(\eta^2\text{-}OC(O)C_6H_4CH_2)$ (6)[b]	A_2BC	δA=-1.34 δB=14.12 δC=-14.00	J_{AB}=35.5 J_{AC}=24.6 J_{BC}=15.1
$(PMe_3)_3Ru(\eta^4\text{-}OC(O)C_6H_4CH_2)$ (7)[c]	ABC	δA=24.80 δB=17.34 δC=-10.81	J_{AB}=43.4 J_{AC}=6.6 J_{BC}=28.2
$(PMe_3)_4Ru(\eta^2\text{-}OC_6H_3(Me))$ (2)[b]	A_2BC	δA=-2.73 δB=15.78 δC=-9.31	J_{AB}=34 J_{AC}=24 J_{BC}=17
$(PMe_3)_3(CO)Ru(\eta^2\text{-}OC_6H_3(Me)C(O))$ (8)[b]	A_2B	δA=-2.57 δB= 7.54	J_{AB}=30.8
$(PMe_3)_4Ru(\eta^2\text{-}OC_6H_3(Me)C(O)O)$ (9)[a]	A_2BC	δA=1.14 δB=11.35 δC=14.35	J_{AB}=17 J_{AC}=17 J_{BC}=17
$(PMe_3)_4Ru(\eta^2\text{-}NHC_6H_4)$ (3)[b]	A_2BC	δA=-4.01 δB=6.56 δC=-10.89	J_{AB}=32.7 J_{AC}=23.9 J_{BC}=17.6
$(PMe_3)_4Ru(\eta^2\text{-}^{15}NHC_6H_4)$ (3-^{15}N)[b]	A_2BC	δA=-4.01 δB=6.42 δC=-10.89	J_{AB}=32.6 J_{AC}=24.1 J_{BC}=17.6 J_{BX}=30.7
$(PMe_3)_3(CO)Ru(\eta^2\text{-}NHC_6H_4C(O))$ (10)[b]	A_2B	δA=-1.35 δB= -4.79	J_{AB}=31.4
$(PMe_3)_4Ru(\eta^2\text{-}OC(O)NHC_6H_4)$ (11)[b]	A_2BC	δA=-2.81 δB=10.39 δC=-14.50	J_{AB}=34.1 J_{AC}=24.5 J_{BC}=14.9

Table 3. $^{31}P\{^{1}H\}$ NMR Spectroscopic Data (cont.)

$(PMe_3)_4Ru(\eta^2\text{-}NHC_6H_4C(O)O)$ (14)[a]	A_2BC	δA=14.11 δB=1.80 δC=14.11	J_{AB}=29.1 J_{AC}=33.2 J_{BC}=28.8
$(PMe_3)_4Ru(\eta^2\text{-}NHC_6H_4C(O)O)$ (15)	A_2BC	δA=-2.27 δB=9.23 δC=-14.57	J_{AB}=34.8 J_{AC}=25.2 J_{BC}=16.1

[a]CD_2Cl_2; [b]C_6D_6; [c]$C_6H_5Me\text{-}d_8$, -10C; [d]$THF\text{-}d_8$

Scheme I

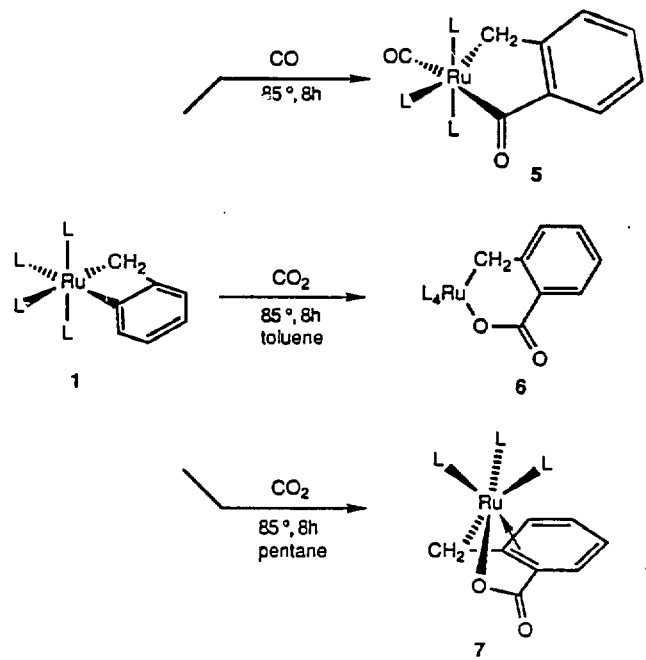
CO
85 °, 8h
L
CH2
OC
Ru
L
L
O
5
L
L
Ru
CH2
L
L
1
CO2
85 °, 8h
toluene
CH2
L4Ru
O
O
6
CO2
85 °, 8h
pentane
L
L
L
Ru
CH2
O
O
7

of carbon monoxide for a phosphine ligand. Both the ^{1}H and $^{13}C\{^{1}H\}$ NMR spectrum showed a doublet of triplets pattern for the benzylic CH_2 group, due to coupling to one trans and three cis phosphorus nuclei, similar to that observed for starting complex 1. The large ^{31}P-^{13}C coupling constant (J=48.8) indicated that a phosphine was located trans to the CH_2. Since the other phosphines are located trans to each other (A_2B pattern in the $^{31}P\{^{1}H\}$ NMR spectrum), the coordinated CO must be located trans to the inserted CO.The aryl carbon atom which was metal bound in the starting material and exhibited a doublet of quartets pattern in the $^{13}C\{^{1}H\}$ NMR spectrum due to ^{31}P-^{13}C coupling, was observed as a singlet in the product.

Reaction of 1 with one equivalent of carbon dioxide in benzene led predominantly (90-95%) to formation of 6, the product of insertion into the metal aryl bond. Isolation of this product in crystalline form was achieved by cooling a solution of 6 which contained excess trimethylphosphine. The structure of 6 was assigned on the basis of ^{1}H, $^{31}P\{^{1}H\}$, $^{13}C\{^{1}H\}$ NMR spectral analysis in a sealed tube containing two equivalents of added phosphine. It was necessary to conduct solution spectroscopic analysis in the presence of added PMe_3 because of the lability of the phosphine ligands (*vide infra*). Elemental and mass spectral analysis for 6 were unsatisfactory, presumably due to this istability.

The $^{31}P\{^{1}H\}$ NMR chemical shifts of the phosphine ligands reflect the nature of the substituent which is located trans to it,[12] and this property is particularly useful in identifying $L_4Ru(X)(Y)$ compounds. Many complexes with the formula, *cis*-$(PMe_3)_4Ru(X)(Y)$ X, Y=alkyl or hydride, have been synthesized,[5d, 11, 13] and the $^{31}P\{^{1}H\}$ NMR spectrum of all of these complexes show chemical shifts for the phosphine ligands trans to the alkyl or hydride which are upfield from the chemical shift of the two mutually trans phosphines. When X or Y correspond to π-donors such as chloride[9, 11] or acetate,[14] the chemical shift of the phosphine ligand trans to it is observed downfield from the chemical shift of the mutually trans phosphines. These trends in chemical shift are due to the high trans influence of the alkyl group and the low trans-influence of the halide substituent relative to the phosphine

ligand.[12] The $^{13}C\{^1H\}$ NMR spectrum contained a resonance at 171.06 ppm, corresponding to the carbonyl carbon, and showed a doublet of quartets pattern for the methylene carbon.

The $^{31}P\{^1H\}$ NMR spectrum of **6** displayed an A_2BC pattern with P_B resonating upfield and P_C resonating downfield from P_A, indicating that a reaction had occurred to form a ruthenium-oxygen bond. The ^1H NMR spectrum of **6** displayed a multiplet corresponding to the benzylic CH_2 group at δ2.65 ppm, compared to δ1.35 in the starting complex, consistent with protons located in the α-position to a carbonyl group in the product.

When the reaction was conducted for 2 d at 85° C in *n*-pentane instead of an arene solvent, a single product **7**, containing three rather than four phosphine ligands, crystallized from solution. This compound was observed as the minor product in the reaction of **1** with CO_2 in arene solvent, and was observed in all solutions of **6** without added phosphine, as the product of ligand dissociation.

Determination of the structure of **7** by spectroscopic means was complicated due to its fluctional nature (vide infra), so an X-ray structure analysis was obtained to determine the bonding mode. The complex crystallized in space group $P2_1/n$; an ORTEP drawing of the molecule is given in Figure 1. There are no unusually short inter-molecular contacts. Data collection parameters are given in Table 4, and metric measures of the molecule in Tables 5 and 6.

The Ru-P3 distance is longer than the other two by a significant amount. The organic ligand is bonded such that the Ru-O1 and Ru-C1 contacts are short, apparently normal metal-X bonds,[5d, 9, 15] while the contacts to C2 and C3 are much longer than the Ru-O1 and -C1 distances, but in the range which would be regarded as bonding. If the arene is considered η^2-bound, then the complex is an 18 electron, octahedral complex with PMe_3 groups occupying three sites and the organic ligand occupying the three other sites. The bond distances in the ligand show a significant shortening of bonds C4-C5 and C6-C7, compared to the other aryl bond distances, including the coordinated aryl bond, C2-C3. The C-O bond distances are typical for a carboxylate group. The C1-C2 bond is long for a C=C bond and

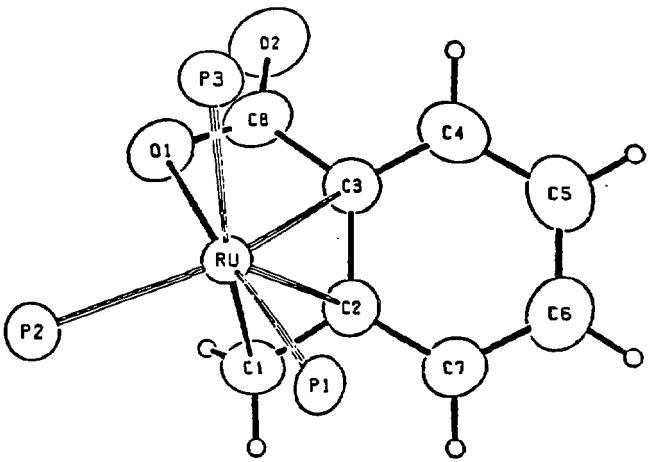

Figure 1. ORTEP drawing of 7. The methyl groups of the PMe_3 ligand have been omitted for clarity.

Table 4. Crystal and Data Parameters for 7

Empirical formula: $Ru P_2 O_2 C_{37} H_{33}$

A) Crystal Parameters at T = 25°C

a = 9.0279(13) Å	Space Group: $P\bar{1}$
b = 9.1509(13) Å	Formula weight = 463.4 amu
c = 14.5300(21) Å	Z = 2
α = 79.753(12) °	d(calc) = 1.44 g cm^{-3}
β = 83.175(12) °	
γ = 64.915(11) °	μ(calc) = 9.5 cm^{-1}
V = 1068.5(3) Å^3	

Size: 0.20x0.20x0.20 mm

B) Data Measurement Parameters

Radiation : Mo Kα (λ = 0.71073 Å)

Monochromator : Highly-oriented graphite (2θ = 12.2)

Detector : Crystal scintillation counter, with PHA.

Reflections measured : + H, +/-K, +/-L

2θ range: 3 -> 45 deg Scan Type: θ-2θ

Scan width: Δθ = 0.55 + 0.35 tanθ

Scan speed: 0.66 -> 6.70 (θ, deg/min)

Background: Measured over 0.25*(Δθ) added to each end of the scan.

Vert. aperture = 3.0 mm Horiz. aperture = 2.0 + 1.0 tanθ mm

No. of reflections collected: 2796

No. of unique reflections: 2796

Table 5. Intramolecular Distances for 7

ATOM 1	ATOM 2	DISTANCE
RU	P1	2.262(1)
RU	P2	2.245(1)
RU	P3	2.340(1)
RU	O1	2.170(1)
RU	C1	2.171(2)
RU	C2	2.319(2)
RU	C3	2.411(2)
RU	C8	2.698(2)
C1	C2	1.449(3)
C2	C3	1.436(2)
C2	C7	1.426(3)
C3	C4	1.412(3)
C4	C5	1.356(3)
C5	C6	1.403(3)
C6	C7	1.355(3)
C3	C8	1.500(3)
C8	O1	1.288(2)
C8	O2	1.230(2)
P1	C9	1.828(2)
P1	C10	1.831(2)
P1	C11	1.813(2)
P2	C12	1.812(2)
P2	C13	1.824(2)
P2	C14	1.829(2)
P3	C15	1.823(2)
P3	C16	1.831(2)
P3	C17	1.826(2)

Table 6. Intramolecular Angles for 7

ATOM 1	ATOM 2	ATOM 3	ANGLE
O1	RU	P1	173.26(4)
O1	RU	P2	92.65(4)
O1	RU	P3	86.11(4)
O1	RU	C1	78.47(6)
C1	RU	P1	98.85(5)
C1	RU	P2	92.72(5)
C1	RU	P3	161.45(5)
P1	RU	P2	93.66(2)
P1	RU	P3	95.32(2)
P2	RU	P3	98.28(2)
RU	C1	C2	76.81(10)
RU	O1	C8	99.42(10)
C1	C2	C3	120.74(16)
C1	C2	C7	122.15(16)
C3	C2	C7	116.97(16)
C2	C3	C4	118.14(17)
C2	C3	C8	120.79(16)
C4	C3	C8	119.68(16)
C3	C4	C5	122.60(18)
C4	C5	C6	119.64(19)
C5	C6	C7	119.88(18)
C2	C7	C6	122.65(17)
O1	C8	C3	113.63(15)
O2	C8	C3	120.10(20)
O1	C8	O2	126.23(19)
RU	P1	C9	114.69(7)
RU	P1	C10	117.89(7)
RU	P1	C11	121.43(6)
C9	P1	C10	101.55(10)
C9	P1	C11	100.01(10)
C10	P1	C11	98.00(9)
RU	P2	C12	109.73(8)
RU	P2	C13	124.25(7)
RU	P2	C14	117.38(7)
C12	P2	C13	100.58(10)
C12	P2	C14	101.26(10)
C13	P2	C14	100.24(11)
RU	P3	C15	113.00(8)
RU	P3	C16	115.64(8)
RU	P3	C17	124.82(7)
C15	P3	C16	100.44(11)
C15	P3	C17	99.72(12)
C16	P3	C17	99.47(11)

indicates mostly single-bond character. Although η^3-benzyl groups have been observed,[16] they have not been reported in such a ring system.

The NMR spectra of **7** are temperature dependent. The ^1H (Figure 2a, THF-d_8 solvent) and $^{31}P\{^1H\}$ NMR spectra of **7** at 30° C display broad resonances. At -10 °C, the ^1H (shown in Figure 2b), $^{13}C\{^1H\}$, and $^{31}P\{^1H\}$ NMR spectra sharpened and were consistent with the solid state structure. However, further cooling to -50° C caused only the trimethylphosphine resonance at δ0.77 in the ^1H NMR spectrum to broaden (Figure 2c). The $^{31}P\{^1H\}$ NMR spectrum does not show such pronounced differences presumably due to the larger chemical shift difference and slower time scale; the resonances in the room temperature spectrum are slightly broadened, and sharpen upon cooling to -10° C, but do not show any temperature dependence between -10° C and -80° C. It appears from the ^1H NMR spectra that at least two different fluxional processes are occurring. Unfortunately it is not possible to determine if either of these processes involves phosphine dissociation, since addition of labelled phosphine leads to formation of the tetrakis phosphine complex **6**. Moreover, limitations on the temperature range of the variable temperature NMR experiments prevented observation of the rapid and slow exchange regimes for either process, so we do not fully understand the structural changes that cause these variable spectra.

Insertion Reactions of the Orthometallated Ruthenium Cresolate Complex $L_4Ru(\eta^2\text{-}OC_6H_3Me)$. The insertion reactions of the orthometallated cresolate complex **2** are shown in Scheme II. The reaction of $L_4Ru(\eta^2\text{-}OC_6H_3Me)$ **2** with 2 atm of carbon monoxide at 85 °C for 8 h formed compound **8** in 51 % isolated yield, resulting from insertion of carbon monoxide into the metal carbon bond and substitution of carbon monoxide for the phosphine ligand trans to the inserted carbon monoxide. There was no evidence for any other products when the reaction was monitored in a sealed NMR tube.

The $^{13}C\{^1H\}$ NMR spectrum of the starting material **2** contained an aryl resonance which was observed as a doublet of doublet of triplets pattern at δ142.7 for the metal-bound carbon.[10] The product **8** contained only singlets in the aryl region, indicating that the Ru-C

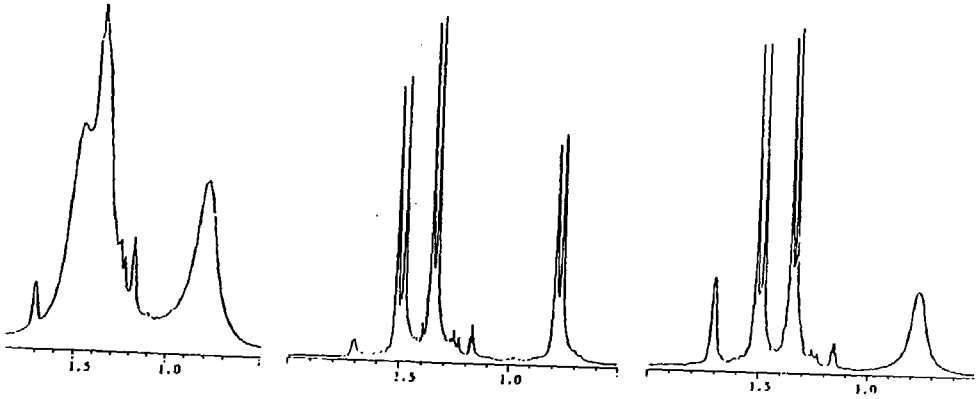

Figure 2. The PMe_3 region of the ^1H NMR spectrum of 7 in THF-d_8 at (a) 30° C, (b) -10° C, (c) -50° C

Scheme II

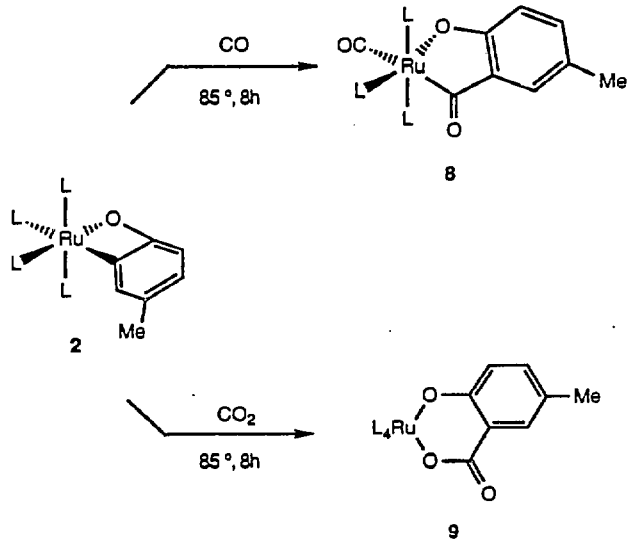

linkage, not the Ru-O linkage had been broken. The $^{13}C\{^1H\}$ NMR resonance corresponding to the inserted carbon monoxide (δ265.38) was observed as a multiplet, indicating that this carbon was bound to ruthenium, but small P-C coupling constants were observed, indicating that the inserted carbon monoxide was bound trans to the coordinated carbon monoxide, not trans to a phosphine. The chemical shifts in the $^{31}P\{^1H\}$ spectrum were also consistent with this assignment. The spectrum of 8 displayed an A_2B pattern, with P_B resonating downfield from P_A, consistent with P_B being coordinated trans to the ruthenium-oxygen bond.

Reaction of **2** with 1 equivalent of carbon dioxide at 85 °C in a closed vessel led to formation of compound **9**, again resulting from reaction with the metal carbon bond. Crystals of the product **9** formed from the reaction solution in 58 % yield, and they were characterized by conventional spectroscopic techniques and combustion analysis. The aryl region of the $^{13}C\{^1H\}$ NMR spectrum of the product showed only singlet and doublet (δ123.84 ppm, J_{PC}=4.6 Hz) resonances, indicating that the metal bound aryl carbon in starting material **2** (observed at δ142.7 as a doublet of doublet of triplets pattern) was no longer bound to ruthenium. The $^{31}P\{^1H\}$ NMR spectrum of **9** further supported this assignment. It consisted of an A_2BC pattern; δB and δC were both observed downfield from δA, indicating that P_B and P_C are coordinated trans to ruthenium-oxygen bonds.

The rate of the insertion reaction showed a marked dependence on phosphine concentration. The reaction of CO_2 (5 equiv.) with **2** was conducted in two NMR tubes, side by side, one tube containing no additional phosphine and one tube containing 3 equivalents of added phosphine (0.029 M). Monitoring the reactions at 85° C showed that the half life for the sample containing no added phosphine was on the order of 45 min, while that for the sample containing three eqivalents of phosphine was roughly 18 h.

Insertion Reactions of Orthometallated Ruthenium Anilide Complex $L_4Ru(\eta^2\text{-}NHC_6H_4)$. Insertion reactions of the orthometallated anilide complex $(PMe_3)_4Ru(\eta^2\text{-}NHC_6H_4)$ **3** are shown in Scheme III. Reaction of **3** with 2 atm carbon monoxide at 85 °C in benzene led to the formation of compound **10**, the product of insertion

Scheme III

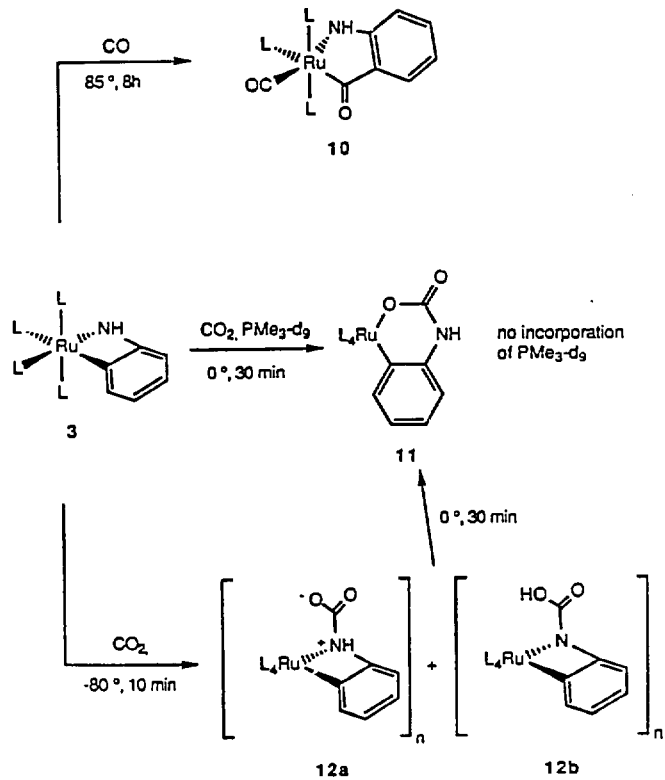
CO
85 °, 8h
10
3
CO_2, PMe_3-d_9
0 °, 30 min
11
no incorporation of PMe_3-d_9
0 °, 30 min
CO_2
-80 °, 10 min
12a
12b

into the ruthenium carbon bond, and substitution of CO for the phosphine trans to the metal-nitrogen bond. The product was isolated by crystallization from pentane at -40 °C in 60 % yield. The $^{13}C\{^1H\}$ NMR spectrum showed all aryl resonances as singlets or doublets (J<5 Hz), indicating that insertion had occurred into the metal-aryl bond. The $^{31}P\{^1H\}$ NMR spectrum, an A_2B pattern with δB resonating upfield from δA, indicated that P_B was trans to the inserted CO. Therefore, unlike the product of CO with **2**, the best π-acceptor CO is located trans to the better π-donor in **10**, the nitrogen of the ruthenium anilide.[17]

In contrast to reactions of **1** and **2**, the reaction of complex **3** with one equivalent of carbon dioxide for 20 min at 25 °C yielded **11**, the product of a formal insertion into the metal nitrogen bond. The white product crystallized from the reaction solution in 57 % yield, and was characterized by conventional spectroscopic techniques. Compound **11** was insoluble in aromatic hydrocarbon and ether solvents, and decomposed in methylene chloride over the period of days, precluding the isolation of crystals suitable for elemental analysis. The $^{13}C\{^1H\}$ NMR spectrum of the product showed an aryl resonance at δ150.3 with a large ^{31}P-^{13}C coupling constant (J=73.6), similar to that observed for the metal-bound aryl resonance in the starting material **3** at δ 143.0 ppm. Moreover, the $^{31}P\{^1H\}$ NMR spectrum of the product consisted of an A_2BC pattern with P_B resonating upfield and P_C resonating downfield from P_A, indicating that in this case a ruthenium carbon bond was retained in the product.

When this reaction was monitored at low temperature by NMR spectroscopy, a complex but well resolved set of spectra was observed which indicated the presence of several of reaction intermediates. The reaction of 5 eqiv of CO_2 with compound **3** in toluene-d_8 was monitored in the spectrometer probe initially at 0° C, and two intermediates, attributed to **12a** and **12b**, were observed. The resonances in the $^{31}P\{^1H\}$ NMR spectrum observed after 5 min at 0° C, displayed A_2BC patterns in the $^{31}P\{^1H\}$ NMR spectrum with δB resonating downfield and δC resonating upfield from δA, indicating one ruthenium-oxygen or ruthenium-nitrogen bond and one ruthenium-carbon bond in the structure. Two broad singlets

corresponding to OH and NH linkages (vide infra) were observed at 14.3 and 11.9 ppm in the ^1H NMR spectrum under these conditions.

The reaction was monitored by ^1H NMR spectroscopy at 10° intervals between 0 and -80° C. At these temperatures a broad doublet resonance was observed at 1.38 ppm at 0 °C which split into two resonances at -30 °C and separated into five different resonances at -60° C (Figure 3). In addition, the two resonances observed between 9 and 15 ppm separated into five singlet resonances upon cooling to -80° C, consistent with at least five intermediates with either NH or OH protons. A stacked plot of the spectra obtained between 0° C and -60° C for the δ9 to δ15 region is shown in spectra b-h of Figure 4. These five intermediates displayed nearly superimposable $^{31}P\{^1H\}$ NMR spectra indicating similar connectivity at ruthenium. The $^{13}C\{^1H\}$ NMR spectrum of the reaction of 3 with $^{13}CO_2$ was also consistent with the existence of five intermediates at this temperature. Five $^{13}CO_2$ resonances were observed between 157 and 165 ppm (Figure 5a). Upon warming the sample to 30° C for 0.5 h, all five resonances in the $^{13}C\{^1H\}$ NMR and ^1H NMR spectra disappeared and were replaced by only the signals corresponding to the resonances of product 11, indicating that this set of five intermediates gives rise to the single product. No reaction was detected between the final insertion product 11 and 5 equivalents of CO_2 at room temperature or below.

Information concerning the connectivity of these intermediates was obtained by the use of ^{15}N labelled starting material. Synthesis of ^{15}N labelled 3 was performed in the same manner as the synthesis of the unlabeled compound, by the addition of ^{15}N labelled aniline to the ruthenium benzyne complex $(PMe_3)_4Ru(\eta^2\text{-}C_6H_4)$ (Equation 1.). The $^{31}P\{^1H\}$ NMR spectrum of the labelled material displayed the A_2BC part of an A_2BCX spectrum, ($X=^{15}N$), with a trans $^{31}P\text{-}^{15}N$ coupling of 30.7 Hz but unresolved cis $^{31}P\text{-}^{15}N$ couplings.

The reaction of 3-^{15}N with 5 equivalents of CO_2 was monitored at -80 °C, following a similar procedure used during the reaction of 3 with CO_2. Again, five intermediates were observed, as demonstrated by the appearance of chemical shifts in the ^1H NMR spectrum identical to those observed in the reaction of 3 with 5 equivalents of CO_2 at -80 °C (spectrum

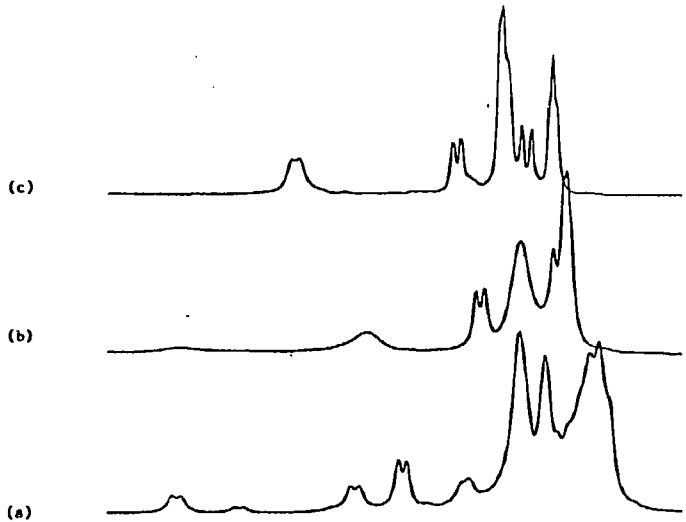

Figure 3. Variable temperature ^1H NMR spectra of the PMe_3 region for 3 + CO_2 (a) -60°C (b)-30°C (c) 0°C.

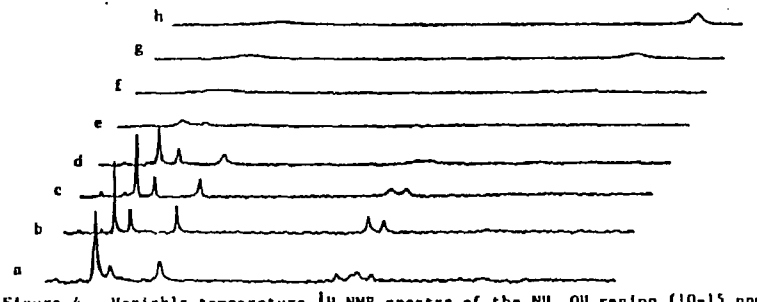

Figure 4. Variable temperature ^{1}H NMR spectra of the NH, OH region (10-15 ppm) for 3 + CO_2 (a)-60°, ^{15}N labelled (b)-60°C (c)-50°C (d)-40°C (e)-30°C (f)-20°C (g)-10°C (h)0°C.

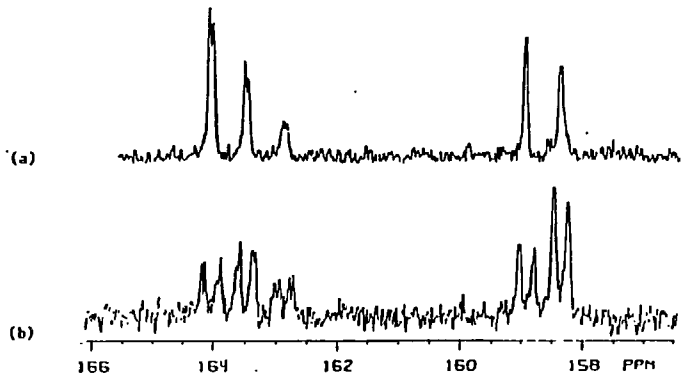

Figure 5. $^{13}C\{^{1}H\}$ NMR spectrum of (a) $^{13}CO_2$ + **3** and (b) $^{13}CO_2$ + **3**-^{15}N in the δ156.6-166 region. The smallest splittings are due to $^{2}J_{C\text{-}H}$ coupling with the NH and OH protons.

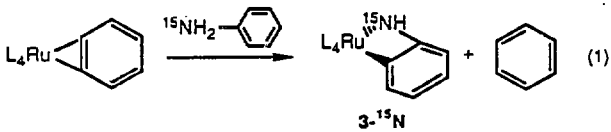

(1)

3-^{15}N

(a) of Figure 4). However, the pattern of the two farthest upfield resonances in the 9 to 15 ppm range now appeared as doublets, due to coupling with ^{15}N (J_{NH}=19 Hz for both),[18] thus assigning these resonances to N-H protons. The three furthest downfield resonances remained singlets in the ^{15}N labelled case, consistent with assignment as O-H protons. The reaction of **3**-^{15}N with $^{13}CO_2$ was performed under identical conditions, and five resonances in the $^{13}C\{^1H\}$ NMR spectrum were observed at -80 °C, all of which showed coupling to ^{15}N, with J_{CN} ranging from 18 to 19 Hz (Figure 5),[18] confirming the N-CO_2 connectivity.

We do not have a definite structural proposal for all five interconverting reaction intermediates, but based on the spectroscopic data, we propose that they fall into two categories of structures, **12a** and **12b** (Scheme III), which are tautomers. The ^{15}N labelling experiment clearly demonstrates that all five intermediates contain an N-CO_2 linkage, while three of the intermediates contain OH linkages and two contain NH linkages. The chemical shifts of the $^{31}P\{^1H\}$ NMR spectra of these intermediates indicate that the metal-aryl bond remains intact in all five. Therefore, we are left with the connectivity shown in structures **12a** and **12b**, the existence of rotamers or aggregates of these isomers would explain the observation more than two intermediates.

To determine qualitatively whether the rate of phosphine dissociation in **3** was competitive with the rate of the insertion reaction, the addition of ten equivalents of CO_2 to **3** was conducted at 0° C and 20° C in the presence of 4 eq of PMe_3-d_9. Over the course of 2h at 20° C, both the reaction to form **11** and the exchange of labelled free phosphine with unlabeled coordinated phosphine occurred.[19] However, at 0° C, the formation of intermediates **12a** and **12b** as well as their conversion to the final product **11** occurred without any exchange of the free deuterated phosphine with coordinated undeuterated phosphine. Thus, insertion of CO_2 must occur without dissociation of the PMe_3 ligands, consistent with direct attack of CO_2 at the nitrogen atom to form **12a** and **12b**.

We independently synthesized the opposite insertion product in the amide case, i.e. the formal insertion product of CO_2 into the metal-carbon bond, $(PMe_3)_4Ru(\eta^2$-

$OC(O)C_6H_4NH$) **13**, (Scheme IV) with the objective of determining whether the thermodynamic insertion product is **11** or **13**, by observing rearrangement of one to the other. Addition of anthranilic acid (2-aminobenzoic acid) to the previously reported compound $(PMe_3)_4Ru(\eta^2\text{-}CH_2PMe_2)(PMe_3)_3$ (**14**) followed by heating to 85° C for 8 h led to **13**, which crystallized from the reaction mixture in 73% yield. Alternatively, this complex was prepared in 76% isolated yield by room temperature addition of the dianion of anthranilic acid to the acetate chloride complex $(PMe_3)_4Ru(OAc)(Cl)$ in THF. The aryl region of the $^{13}C\{^1H\}$ NMR spectrum of this product contained no resonances with large $^{31}P\text{-}^{13}C$ couplings, indicating that the aryl ring is not bound to the metal center, and the $^{31}P\{^1H\}$ NMR spectrum displayed an A_2BC pattern with P_B and P_C resonating downfield from P_A, consistent with these two phosphorus atoms being located trans to ruthenium-oxygen and ruthenium-nitrogen bonds, respectively.

Both **11** and **13**, containing six membered metallacycles, were stable at the conditions under which the conversion of **3** to **11** occurs. Even at higher temperatures, no interconversion of **11** and **13** is observed. Instead both complexes were cleanly converted to products resulting from ring contraction. Heating the direct insertion product **11** to 120 °C for 2 h formed the carboxamide complex $(PMe_3)_4Ru(N(Ph)C(O)O)$ (**15**) as shown in Scheme V. Compound **15** has been independently prepared by the addition of phenylisocyanate to the oxametallacyclobutane $(PMe_3)_4Ru(OC(Me)(Ph)CH_2)$ during the course of another study and was fully characterized.[20] The carbonate complex $(PMe_3)_4Ru(CO_3)$ (**16**)[20] was the major product when a THF-d_8 solution of **11** was heated under these conditions in the presence of added water.

Rearrangement of **13** required prolonged heating at these temperatures. Thermolysis of THF solutions of **13** at 125 °C for 3 d led to formation of a 5.7 ± 0.6 :1 mixture of the O, and C bound anthranilate, $(PMe_3)_4Ru(\eta^2\text{-}OC(O)C_6H_3NH_2)$ **17** and starting material **13** (96% total yield, ^1H NMR spectroscopy, Cp_2Fe internal standard), as shown in Scheme VI. Neither the direct insertion product **11**, nor its thermolysis product, carboxamide **15** was

Scheme IV

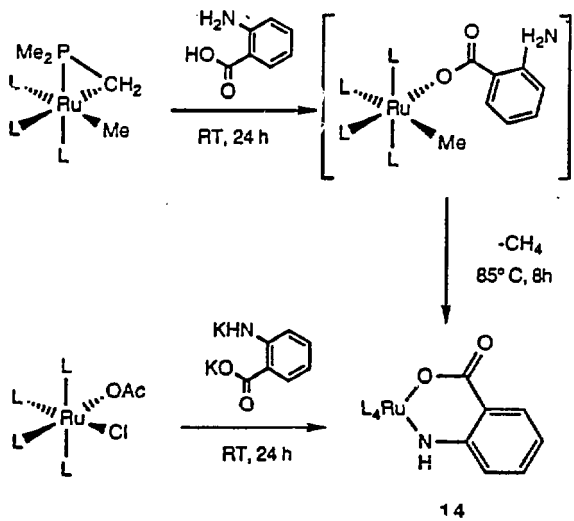
Me2P
CH2
Ru
Me
L
H2N
HO
O
RT, 24 h
H2N
-CH4
85° C, 8h
OAc
Cl
KHN
KO
L4Ru
N
H

14

Scheme V

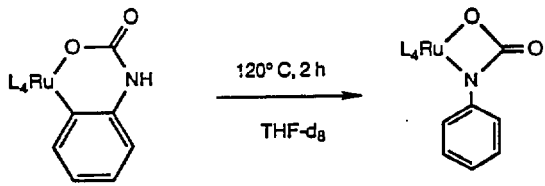

11 13

Scheme VI

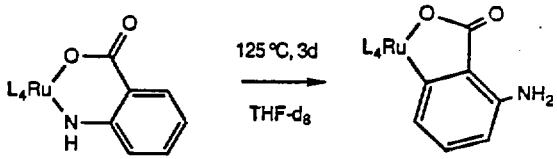

14 15

observed during the course of the reaction. Compound **17** could not be isolated in pure form; roughly the same ratio of **13** and **17** was obtained after crystallization. However, the connectivity of this compound could be determined by ^{1}H, $^{31}P\{^{1}H\}$, and $^{13}C\{^{1}H\}$, NMR, as well as infrared spectroscopy of the mixture since the data of pure **13** had been obtained. The $^{31}P\{^{1}H\}$ NMR spectrum displayed an A_2BC pattern, with one resonance upfield and one resonance downfield of the mutually trans phosphine, indicating one Ru-X, X=O or N and one Ru-C bond. An NH_2 resonance was observed in the ^{1}H NMR spectrum at δ5.88, and integrated to twice the intensity of each of the three aryl resonances observed between δ6.11 and δ6.82. Consistent with these data, the $^{13}C\{^{1}H\}$ NMR spectrum displayed three quarternary resonances and three C-H resonances in the aromatic region, as determined by a DEPT pulse sequence. The infrared spectrum contained a strong absorption at 1584 cm^{-1} corresponding to the carboxylate carbonyl, similar to the frequency of analogous absorptions of **6** and **9**. Two sharp N-H bands were observed at 3384 and 3281 cm^{-1}.

Complete conversion of **13** to **17** was never observed, and it was not straightforward to determine if the 5.7:1 distribution of isomers was an equilibrium ratio. Obtaining samples of **13** and **17** which contained significantly more **17** than the 5.7:1 mixture would have allowed us to clearly demonstrate that this is an equilibrium distribution by observing increasing amounts of **13**. Unfortunately, all samples we obtained by crystalliztion contained between 3.7:1 and 5.7:1 ratios of the **17** to **13**. However, results of kinetic studies on the conversion of **13** to **17** provide evidence that the 5.7:1 mixture is an equilibrium ratio. A first order plot of the disappearance of **13** showed significant curvature after 2 half-lives for each of several runs, whereas first order plots for approach to equilibrium showed good linearity. The kinetic experiments were conducted with three concentrations of added phosphine. The rate constants decreased slightly with increasing phosphine concentration (see experimental section for phosphine concentrations and rate constants), although our data do not clearly demonstrate the role of added phosphine in this rearrangement. In addition, the crystallized sample of **13** and **17** obtained as a 1:3.7 ratio was heated to 120 °C for 24 h, and ^{1}H NMR

spectroscopy again showed a 1:5.6 ratio of the two compounds, providing convincing evidence that this ratio reflects an equilibrium distriubution and that it does not result from decomposition of a trace catalyst.

We attempted to synthesize the insertion products opposite to those observed with CO_2 and **1** and **2**. Addition of phenylacetic acid to **12** led to formation of $(PMe_3)_4Ru(Me)(OC(O)CH_2Ph)$ (equation 2). However, this complex remained stable for 2 d at 135 °C; no formation of methane and the desired orthometallated product was observed. The addition of $KOC(O)OC_6H_4Me$ to $(PMe_3)_4Ru(Me)Cl$ led to decarboxylation before orthometallation and formed $(PMe_3)_4Ru(Me)(OC_6H_4Me)$[21] (equation 3).

Discussion

Mechanism. Many mechanistic studies have been conducted concerning the insertion of CO into metal-carbon bonds.[22] These investigations have demonstrated that such reactions normally proceed by initial coordination of the small organic molecule followed by migration of the alkyl or aryl substituent. Our observations on the CO insertion reactions of **1**, **2**, and **3** are consistent with this mechanism. Although these are coordinatively saturated, 18 electron complexes, an open coordination site is readily available by dissociation of phosphine, as demonstrated by the complete exchange of coordinated with uncoordinated phosphine over two hours at room temperature with compound **3**.

Less mechanistic information is available concerning insertion reactions of CO_2.[23, 24] Studies on the reactions of anionic transition metal alkyl complexes with CO_2 have shown insertion rates which are faster than that of ligand dissociation, precluding a mechanism involving coordination of the CO_2 and migration of the alkyl group. Yet, mechanistic information on CO_2 deinsertion reactions from formate complexes to form the metal hydride and free CO_2 provide evidence that these processes involve coordinated CO_2 on the reaction pathway.[25]

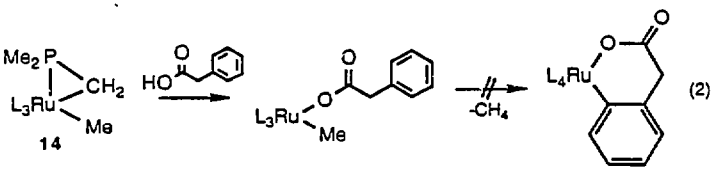
Me2P
CH2
L3Ru
Me
14
HO
O
L3Ru
O
Me
-CH4
L4Ru
O
O

(2)

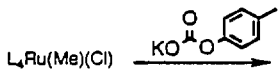
L4Ru(Me)(Cl)
KO
O
O
25 °C, 24 h
L4Ru(Me)(OC6H4-p-Me) + CO2

(3)

A coordination and migration mechanism for the insertion of CO_2 into **2** is shown in Scheme VII. The rate expression for a direct insertion mechanism which would not require phosphine dissociation is shown in equation 4.The marked decrease in rate observed for samples containing added phosphine is inconsistent with this rate law. Rather, it is consistent with equation 5, derived for the mechanism in Scheme VII involving a reversible dissociation of phosphine preceeding the rate determining step of the reaction. This suggests that coordination of CO_2 to form intermediate **18**, followed by migration of the aryl group, leads to the final product.

In contrast to the insertion and deinsertion of CO_2 into the metal-aryl bonds, the reaction of **3** with CO_2 must occur without phosphine dissociation, and low temperature NMR studies suggest that it is intermediates **12a** and **12b** which are first formed by direct reaction of CO_2 at the nitrogen atom; these species then rearrange to the final product **11**. Thus the formal insertion of CO_2 into the metal-nitrogen bond in the orthometallated anilide complex **9** proceeds by a pathway different from the coordination/migration mechanism which appears to operate for the metal-carbon bond insertion reactions.

Selectivities. The migratory aptitudes of various alkyl groups toward coordinated CO have been well studied,[26] and in general benzyl groups undergo migratory insertion reactions slower than aryl groups. Much less studied is a comparison of the relative rates of the migration of alkoxide and amide groups versus aryl and alkyl groups. The tetrakis (phosphine) ruthenium system provides a unique spectrum of substituents on the metal center that can be used to address this question. In addition to the reactions of the four-membered metallacycles reported in this paper, we have recently generated another four membered metallacycle, an oxaruthenacyclobutane complex. Upon addition of carbon monoxide, this complex undergoes insertion of CO into the metal-carbon bond rather than the metal-oxygen bond.[27] Thus, in all the $(PMe_3)_4Ru(X)(Y)$ compounds that we have examined, the metal-oxygen and metal-nitrogen bonds are remarkably inert toward insertion of carbon monoxide; in all cases, migration of the alkyl or aryl substituent is faster than migration of the heteroatom containing substituent.

Scheme VII

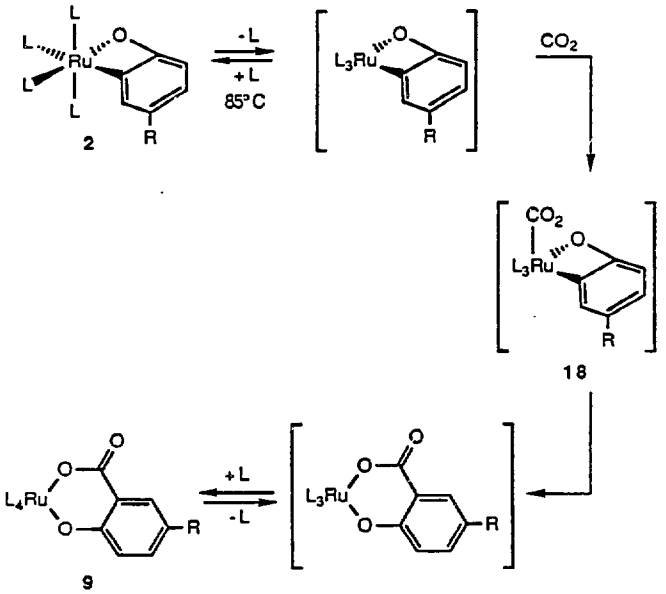
L
L
L
Ru
O
L
2
R
-L
+L
85°C
L3Ru
O
R
CO2
CO2
O
L3Ru
R
18
O
O
L4Ru
O
R
9
+L
-L
O
O
L3Ru
O
R

Scheme VIII

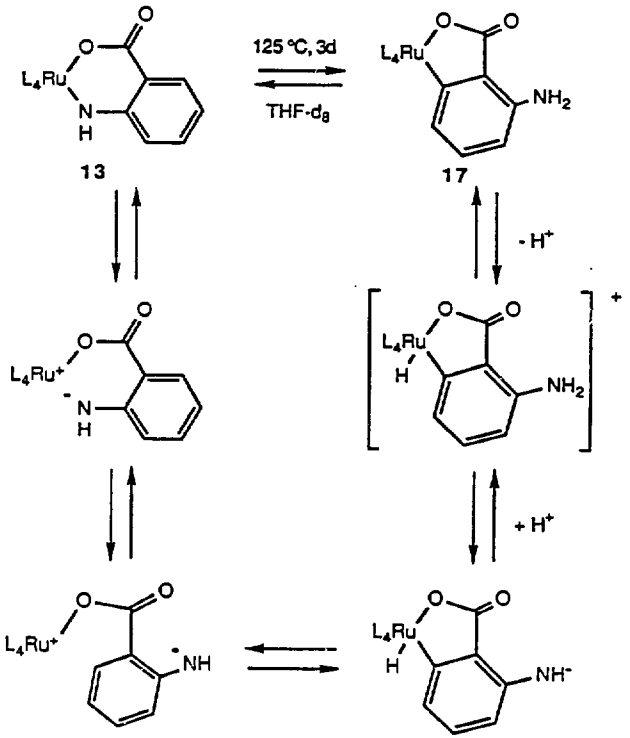

In contrast, carbon dioxide shows different reactivity toward aryloxide and amide substituents. CO_2 reacts with the metal-carbon bond in the cyclometallated cresolate **2**, and with the metal-nitrogen bond in cyclometallated anilide **3**. Our experiments suggest that insertion of CO_2 into the metal-carbon bonds proceeds by initial coordination to the metal center, followed by migration of the aryl substituent, and reaction with **9** proceeds by direct attack of the anilide nitrogen atom on CO_2. It appears that the relatively high nucleophilicity of the anilide nitrogen atom relative to the aryloxide oxygen atom accounts for the mechanistic and selectivity differences with these two compounds.

Rearrangements. Several of the six membered heterometallacycles prepared in this study rearrange thermally to isomers containing smaller ring systems. Compound **6** dissociates phosphine to form the tris phosphine complex **7**, which crystallizes from the reaction solution when run in alkane solvent. When the reaction was run in arene solvents, the ratio of **6** to **7** was roughly 9:1, implying that the formation of **6** in alkane solvents is driven by the insolubility of **7**.

We believe that the rearrangements of **11** and **13**, each containing 6-membered rings, are driven by the thermodynamic stability of 4- and 5-membered ring systems in the products. Our qualitative kinetic results have demonstrated that the rearrangement of **13** is not catalyzed by water. Instead, we propose that the reaction proceeds by a mechanism such as the one shown in Scheme VIII. Dissociation of the arylamide portion of the metallacycle provides a site of unsaturation. Rotation of the resulting η^1-bound organic ligand allows the proper geometry to add the aromatic C-H bond, and proton transfer forms the final rearrangement product. Because it appears that compounds **13** and **17** are in equilibrium, each step in Scheme VIII must be reversible. Therefore, if the proton transfer from the metal center to the uncoordinated nitrogen atom occurs directly, the reverse process (transfer of the N-H proton to the metal center) must also occur directly. It seems likely that trace acid catalysts may facilitate these steps, although water does not appear to be acidic enough to affect the reaction rates.

The conversion of **11** to **13** may also involve proton transfer processes. Although protonolyisis of the metal aryl bond by the amide N-H would form **13**, such a direct reaction seems

$$\frac{d[2]}{dt} = k_1[2][CO_2] \quad (4)$$

$$\frac{d[2]}{dt} = \frac{k_2k_3[2][CO_2]}{k_2[L] + k_3} \quad (5)$$

unlikely since the amide N-H bond and the ruthenium-aryl bond are located on opposite sides of the ring. Proton transfer by an acid catalyst formed under the 120 °C reaction conditions may assist this transformation.

Experimental

General. Unless otherwise noted, all manipulations were carried out under an inert atmosphere in a Vacuum Atmospheres 553-2 drybox with attached M6-40-1H Dritrain, or by using standard Schlenk or vacuum line techniques.

^{1}H NMR spectra were obtained on either the 250, 300, 400 or 500 MHz Fourier Transform spectrometers at the University of California, Berkeley (UCB) NMR facility. The 250 and 300 MHz instruments were constructed by Mr. Rudi Nunlist and interfaced with either a Nicolet 1180 or 1280 computer. The 400 and 500 MHz instruments were commercial Bruker AM series spectrometers. ^{1}H NMR spectra were recorded relative to residual protiated solvent. ^{13}C NMR spectra were obtained at either 75.4 or 100.6 MHz on the 300 or 500 MHz instruments, respectively, and chemical shifts were recorded relative to the solvent resonance. Chemical shifts are reported in units of parts per million downfield from tetramethylsilane and all coupling constants are reported in Hz.

IR spectra were obtained on a Perkin-Elmer Model 283 infrared spectrometer or on a Perkin-Elmer Model 1550 or 1750 FT-IR spectrometer using potassium bromide ground pellets. Mass spectroscopic (MS) analyses were obtained at the UCB mass spectrometry facility on AEI MS-12 and Kratos MS-50 mass spectrometers. Elemental analyses were obtained from the UCB Microanalytical Laboratory.

Sealed NMR tubes were prepared by fusing Wilmad 505-PP and 504-PP tubes to ground glass joints which were then attached to a vacuum line with Kontes stopcocks or alternatively, the tubes were attached via Cajon adapters directly to Kontes vacuum stopcocks.[28] Known volume bulb vacuum transfers were accomplished with an MKS Baratron attached to a high vacuum line.

Unless otherwise specified, all reagents were purchased from commercial suppliers and used without further purification. PMe_3 (Strem) was dried over NaK or a Na mirror and vacuum

transferred prior to use. CO and CO_2 (bone dry) were purchased from Matheson. Anthranilic acid was dried by azeotroping with benzene using a Dean-Stark trap, and then purified by sublimation.

Pentane and hexane (UV grade, alkene free) were distilled from $LiAlH_4$ under nitrogen. Benzene and toluene were distilled from sodium benzophenone ketyl under nitrogen. Dichloromethane was either distilled under N_2 or vacuum transferred from CaH_2. Deuterated solvents for use in NMR experiments were dried as their protiated analogues but were vacuum transferred from the drying agent.

$Ru(PMe_3)_3(CO)(\eta^2\text{-}CH_2C_6H_4C(O))$ (5). To a glass reaction vessel fused to a Kontes vacuum adaptor was added 82.8 mg (0.167 mmol) of $Ru(PMe_3)_4(\eta^2\text{-}CH_2C_6H_4)$ (**1**)[11] in 12 mL of toluene. The vessel was degassed by two or three freeze-pump-thawing cycles and 450 torr of CO was added with the vessel submerged in liquid nitrogen. This procedure results in addition of ~2 atm CO at 25° C. The vessel was heated to 85° C for 20 min, over which time the solution turned from clear to yellow. The toluene was removed and the residue was crystallized from pentane at -40° C to yield 59.4 mg (74.8%) of product. IR: 2982 (m), 2969 (m), 2907 (m), 1910 (s), 1594 (m), 1556 (s), 1528 (m), 942 (s); MS (EI): 476 (M^+), 448 ($M\text{-}CO^+$); Anal. Calcd. for $C_{18}H_{33}O_2P_3Ru$: C, 45.47; H, 7.00; Found: C, 45.62; H, 7.06.

$Ru(PMe_3)_4(\eta^2\text{-}OC(O)C_6H_4CH_2)$ (6). Into a glass reaction vessel fused to a Kontes vacuum adaptor was placed 250 mg (0.505 mmol) of $Ru(PMe_3)_4(\eta^2\text{-}CH_2C_6H_4)$ (**1**)[11] in 20 mL of benzene. The vessel was degassed by two or three freeze-pump-thawing cycles, and CO_2 (1.5 eq, 0.25 mmol) was added by vacuum transfer. The vessel was heated to 85° C for 16 h. After this time the benzene was removed under reduced pressure. Toluene (~ 2 mL) and PMe_3 (0.2 mL) were added and the vessel was heated to 85° C to dissolve the compound and convert any of **7** present to **6**. Upon cooling to -40° C for 12 h, and then -80° C for 24 h, white crystals of **6** formed. These crystals were collected to yield 128 mg (47.0%) of product. When the crystals were dissolved in toluene, the solution rapidly turned yellow, indicating some conversion of **6** to **7** had occurred. All solution spectra of **6** were therefore taken in the presence of 2 eq of PMe_3. Due to the lability of the phosphine ligand, satisfactory mass spectral and microanalytical analyses were

not obtained. IR (KBr): 2970 (m), 2910 (m), 1599 (s), 1582 (s), 1551 (s), 1425 (m),1358 (m), 1300 (m), 1279 (m), 942 (s).

$Ru(PMe_3)_3(\eta^4\text{-}OC(O)C_6H_4CH_2)$ (7). To a glass reaction vessel fused to a Kontes vacuum adaptor was added 88.0 mg (0.178 mmol) $Ru(PMe_3)_4(\eta^2\text{-}CH_2C_6H_4)$ (1)[11] in a 7 mL of pentane. The vessel was degassed by two or three freeze-pump-thawing cycles, and CO_2 (1.5 eq. 0.267 mmol) was added by vacuum transfer. The vessel was heated to 85° C for 3 d. The clear solution turned yellow, and over the course of the 3 d, yellow crystals formed. The crystals were collected to yield 79.0 mg (96.0%)of analytically pure 7. IR (KBr): 2965 (m), 2907 (m), 2851 (m), 1625 (s), 1604 (m), 1428 (m), 1323 (m) 1299 (m), 1279 (m), 957 (m), 941 (s); MS (FAB, sulfolane) 465 (MH^+), 389 ($MH\text{-}PMe_3^+$); Anal. Calcd. for $C_{17}H_{33}O_2P_3Ru$: C, 44.06; H, 7.18. Found: C, 44.22; H, 7.27.

Crystal and Molecular Structure Determination of 7. The X-ray structure determination was carried out by Dr. F.J. Hollander of the UC Berkeley X-ray Diffraction Facility (CHEXRAY). Clear yellow plate-like crystals of the compound were obtained from the pentane reaction mixture. Some of these crystals were mounted on glass fibers using polycyanoacrylate cement. They were then coated with epoxy to retard air oxidation. Preliminary precession photographs indicated triclinic Laue symmetry and yielded approximate cell dimensions.

The crystal used for data collection was then transferred to our Enraf-Nonius CAD-4 diffractometer[29] and centered in the beam. Automatic peak search and indexing procedures yielded a triclinic reduced primitive cell. The final cell parameters and specific data collection parameters for this data set are given in Table 4.

The 2796 unique raw intensity data were converted to structure factor amplitudes and their esd's by correction for scan speed, background and Lorentz and polarization effects. Inspection of the Azimuthal scan data showed a variation I_{min}/I_{max} =0.95 for the average curve. An empincal correction based on the observed variation was applied to the data. The choice of the centric space group P1 was confirmed by the successful solution and refinement of the structure.

The structure was solved by Patterson methods and refined via standard least squares and Fourier techniques. A difference Fourier map was calculated following the refinement of all non-hydrogen atoms with anisotropic thermal hydrogen atoms. Hydrogen atoms were assigned idealized locations and values of B_{iso} approximately 1.2 times the B_{eqv} of the atoms to which they were attached. They were included in structure factor calculations, but not refined.

The final residuals for 209 variables refined against the 2637 data for which $F^2 > 3\sigma(F^2)$ were R = 1.77%, wR = 3.19%, and GOF = 1.84. The R value for all 1392 data points was 2.11%. In the final cycles of refinement a secondary extinction parameter was included (maximum correction : 7% of F).

The quantity minimized by the least squares program was $\Sigma w(|F_o|-|F_c|)^2$, where w is the weight of intense reflections, was set to 0.03 throughout the refinement. The p-factor, used to reduce the weight of intense reflections, was set to 0.03 throughout the refinement. The analytical forms of the scattering factor tables for the neutral atoms were used and all scattering factors were corrected for both the real and imaginary components of anomalous dispersion.

Inspection of the residuals ordered in ranges of $\sin(\theta)/\lambda$, $|F_o|$, and parity and value of the individual indexes showed no unusual features or trends. The largest peak in the final difference Fourier map had an electron density of $0.24e^-/Å^3$ and the lowest excursion $-0.21e^-/Å^3$.

Crystal and data collection parameters, intramolecular distances and intramolecular angles are given in Tables 4-6. Tables of positional parameters, anisotropic thermal parameters, root-mean-square amplitudes of anisotropic displacement, torsion angles and least squares planes are available as supplementary material.

$Ru(PMe_3)_3(CO)(\eta^2\text{-}OC_6H_3(Me)C(O))$ (8). To a glass reaction vessel fused to a Kontes vacuum adaptor was added 100 mg (0.196 mmol) of $Ru(PMe_3)_4(\eta^2\text{-}OC_6H_3(Me))$ (2)[12] in 20 mL of toluene. The vessel was degassed by freeze-pump-thawing through either two or three cycles and 450 torr of CO was added with the vessel submerged in liquid nitrogen. This procedure results in addition of ~2 atm CO at 25° C. The vessel was then heated to 85° C for 8 h, over which time the solution turned darker yellow. The toluene was removed and the residue was

crystallized from a toluene/pentane (1:1) solution at -40° C to yield 54.1 mg (51.3%) of product. IR: 2968 (m), 2911 (m), 1947 (s), 1605 (s), 1551 (s), 1475 (s), 1284 (s), 947 (s); MS (EI): 492 (M^+), 464 ($M-CO^+$), 436 ($M-2CO^+$); Anal. Calcd. for $C_{18}H_{33}O_3P_3Ru$: C, 43.99; H, 6.77; Found: C, 43.80; H, 6.75.

$Ru(PMe_3)_4(\eta^2\text{-}OC_6H_3(Me)C(O)O)$ (9). To a glass reaction vessel fused to a Kontes vacuum adaptor was added 100 mg (0.196 mmol) of $Ru(PMe_3)_4(\eta^2\text{-}OC_6H_3(Me))$ (2)[12] in 5 mL of toluene (not all of the ruthenium complex dissolved in this amount of solvent) The vessel was degassed by freeze-pump-thawing through either two or three cycles, and CO_2 (1.5 equiv, 0.29 mmol) by vacuum transfer. The vessel was then heated to 85° C for 8h over which time period the solution turned clear. Upon cooling, white analytically pure crystals formed and these crystals were collected to yield 62.5 mg (57.5%) of product. IR: 2972 (m), 2911 (m), 1614 (s), 1567 (s), 1479 (s), 1410 (s), 1329 (s), 944 (s); MS (FAB, p-nitrobenzyl alcohol): 557 (MH^+), 481 ($MH-PMe_3^+$) Anal. Calcd. for $C_{20}H_{42}O_3P_4Ru$: C, 43.24; H, 7.62. Found: C, 42.92; H, 7.41.

Reaction of 3 with CO_2 in the presence of added phosphine. In a small vial was weighed 10.0 mg (0.0196 mmol) of **3**, which was then dissolved in 1.2 mL of C_6D_6. An equal amount of the solution was added to two NMR tubes. One of these tubes was degassed by three freeze-pump-thaw cycles, 5 equiv (0.0489 mmol) of CO_2 was added by vacuum transfer, and the tube was sealed. The other tube was degassed, and 5 equiv of CO_2 was added, followed by 3 equiv. (0.0294 mmol) of PMe_3 to give a concentration of 0.049 M. The samples were heated at 85° C, and monitored by ^1H NMR spectroscopy at 0.5, 2, and 18 h. The half life for the reaction with no added phosphine was roughly 0.5 h, while that for the sample containing added phosphine was on the order of 18 h.

$Ru(PMe_3)_3(CO)(\eta^2\text{-}NHC_6H_3(Me)C(O))$ (10). To a glass reaction vessel fused to a Kontes vacuum adaptor was added 80.6 mg (0.163 mmol) of $Ru(PMe_3)_4(\eta^2\text{-}NHC_6H_4)$ (3)[5d] in 5 mL of toluene. The vessel was degassed by freeze-pump-thawing, and CO (2 atm) was added by exposing the vessel, submerged in liquid nitrogen, to 450 torr of CO. The vessel was then heated to 85° C for 16 h, over which time the initial yellow solution turned orange. The solvent

was removed under reduced pressure, and the residue was crystallized from a pentane/toluene (10:1) solvent mixture at -40° C to yield 46.2 (59.7%) yield of orange crystals. IR (KBr): 3323 (m), 1922 (s), 1599 (s)1582 (s), 1538 (s)1479 (s), 1463 (s); MS (EI): 477 (M^+), 449 (M-CO^+), 421 (M-$2CO^+$); Anal. Calcd. for $C_{17}H_{32}NO_2P_3Ru$: C, 42.85; H, 6.77; N, 2.94. Found: C, 42.56; H, 6.72; N, 2.96.

$Ru(PMe_3)_4(\eta^2\text{-}OC(O)NHC_6H_4)$ (11). Into a glass reaction vessel fused to a Kontes vacuum adaptor was added 82.0 mg (0.165 mmol) $Ru(PMe_3)_4(\eta^2\text{-}NHC_6H_4)$ (3)[5d] in a minimum amount of toluene (~3 mL). The vessel was degassed by freeze-pump-thawing, and CO_2 (1.5 eq. 0.25 mmol) was added by vacuum transfer. The yellow solution rapidly turned clear and over the course of 4 h clear needles of **11** formed. The vessel was then cooled to -40° C for 12 h to yield 50.5 mg (56.6%) of product. IR (KBr): 3293 (m), 3187 (m), 2972 (m), 2910 (m), 1639 (s), 1575 (m), 1559 (m), 1490 (m) 1407 (m), 1368 (s), 1300 (m), 1279 (m), 944 (s).

$Ru(PMe_3)_4(\eta^{2\text{-}15}NHC_6H_4)$ (3-N^{15}). Into a vial was placed 82.6 mg (0.172 mmol) of **1**, 17.1 mg (1.1 equiv) of aniline-^{15}N and 2 mL of benzene. The solution was then placed in a 9" NMR tube which was degassed and sealed. The sample was heated to 110 °C for 8 h. Upon cooling, 58.2 mg (68.3%) of **3-^{15}N** had crystallized from the reaction solution and all of the starting material had been consumed as determined by $^{31}P\{^1H\}$ NMR spectroscopy The material which had crystallized from solution was pure by ^1H NMR spectroscopy. IR (KBr) 3329 (w), 2968 (m), 2907 (m) 1591 (m), 1559 (m), 1433 (s), 1303 (m), 1282 (s), 943 (s).

Variable Temperature Study on the reaction of 3 and 3-^{15}N with CO_2. The ruthenium complex $Ru(PMe_3)_4(\eta^2\text{-}NHC_6H_4)$ (3)[5d] or $Ru(PMe_3)_4(\eta^{2\text{-}15}NHC_6H_4)$ (3-^{15}N) (15.5 mg, 0.0313 mmol) was dissolved in 0.7 mL of toluene-d_8, and transferred to a 9" medium walled NMR tube. The sample was freeze-pump-thawed through two cycles and 5 equiv (0.156 mmol) of CO_2 was added by vacuum transfer. The tube was sealed to give a final length of 8". The sample was thawed at -78° C and was placed in the NMR probe, which had been pre-cooled to at least -30° C After acquiring the data for the temperature range 0 to -80° C, the sample was warmed to 30-35° C and the conversion of **12a** and **12b** to product **11** was observed over the course of 0.5h.

Thermolysis of 11. A sample of **11** (2.4 mg, 0.0044 mmol), prepared as described above, was dissolved in tetrahydrofuran-d_8 in an NMR tube equipped with a vacuum adaptor, and 1 mg of mesitylene was added as an internal standard. The sample was degassed, sealed, and heated to 120 °C for 2 h. ^1H and $^{31}P\{^1H\}$ NMR spectrometry showed that **15** was the only product formed.

$(PMe_3)_4Ru(\eta^2\text{-}NHC_6H_4C(O)O)$ (13). (a) Addition of anthranilic acid to $(PMe_3)_2Ru(\eta^2\text{-}CH_2PMe_2)(Me)$ (**14**). To a small vial was added 78.2 mg of $(PMe_3)_2Ru(\eta^2\text{-}CH_2PMe_2)(Me)$ (**14**) and 2 mL of benzene. To this solution was added 38.4 mg (1.5 equiv) of anthranilic acid (2-aminobenzoic acid) as a solid. The suspension was stirred for 2h, after which time ^1H NMR spectroscopy showed that a metal-bound methyl group remained. The solution was then placed into a 9" NMR tube, which was equipped with a vacuum adaptor, degassed and sealed. The sample was heated to 65° C for 3 h, over which time 74.6 mg (74%) of orange/yellow crystals precipitated from the reaction solution. A portion of the recovered material was recrystallized by vapor diffusion of ether into a tetrahydrofuran solution of **13**. IR (KBr) 3364 (w), 2992 (m), 2972 (m), 2910 (m), 1599 (s), 1560 (s), 1521 (m), 1519 (m), 1473 (s), 1453 (s), 1365 (m), 1355 (m), 1262 (s), 941 (s), 731 (m), 717 (m), 700 (m), 666 (m); Anal. Calcd. for $C_{19}H_{41}NOP_4Ru$: C, 42.22; H, 7.65; N, 2.59. Found: C, 42.27; H, 7.73; N, 2.50.

(b) To a solution of 356 mg (0.713 mmol) of $(PMe_3)_4Ru(OAc)(Cl)$ in 10 mL of tetrahydrofuran was added 232 mg (1.5 equiv) of the potassium salt of the dianion of anthranilic acid, $K_2OC(O)C_6H_4NH$, prepared by addition of KH to anthranilic acid in tetrahydrofuran and isolated by filtration. The solution was stirred for 24 h. After roughly 0.5 h the initial pale yellow slurry turned a darker orange/yellow and after an additional 0.5 h it turned back to a paler yellow. Both the anthranilic acid salt and the ruthenium anthranilate product are only sparingly soluble in THF. The tetrahydrofuran solvent was removed under reduced pressure, and the residue was extracted with CH_2Cl_2 and filtered through a plug of celite. Removal of CH_2Cl_2 under reduced pressure provided 292 mg (76%) of product which was pure enough (~95%) for preparation of the thermolysis product **17**.

$(PMe_3)_4Ru(\eta^2\text{-}OC(O)C_6H_3NH_2)$ (17). (a) Preparative Scale: Into a glass reaction vessel equipped with a Kontes vacuum adaptor was placed a suspension of 252 mg (0.467 mmol) of anthranilate **13** in 15 mL of tetrahydrofuran. The vessel was frozen in liquid nitrogen and exposed to vacuum before thermolysis at 135 °C for 16 h. At this temperature, the solution is initially yellow and homogeneous. The product is also yellow, but is very soluble in THF. The solution volume was reduced to 1 mL *in vacuo*, layered with ether, and cooled to -40 °C to provide 64.6 mg (25.6%) of a mixture of **13** and **17** as yellow crystals. ^1H, $^{31}P\{^1H\}$, and $^{13}C\{^1H\}$ NMR spectroscopy of this recovered material showed only O- and N-bound anthranilate starting material and the O- and C-bound product in a 1:3.7 ratio. Thermolysis of 2.1 mg of this crystallized material in 0.6 mL of THF-d_8 at 125 °C for 24 h provided a 5.6:1 ratio of **17** to **13**. IR (KBr) 3384 (m), 3281 (w), 2971 (m), 2906 (s), 1584 (s), 1556 (s), 1523 (s), 1430 (m), 1344 (m), 1299 (m), 1279 (m), 970 (m), 942 (s).

(b) Thermolysis with internal standard: Into an NMR tube was placed 0.7 mL of a THF-d_8 solution of 10.6 mg (0.0196 mmol) of **13** and 4 mg of ferrocene as an internal standard. The tube was degassed and sealed. An ^1H NMR spectrum was obtained before thermolysis. The NMR tube was submerged in an oil bath heated to 115° C, and NMR spectra taken periodically over the course of three days showed that **13** was converted to a 5.7±6.0:1 ratio of **11**:**13** in 96% overall yield.

Approach to Equilibrium Kinetics for 13 and 17. Into a 5.00 mL volumetric flask was weighed 18.5 mg (0.0343 mmol) of anthranilate **13** and 4.5 mg of mesitylene as internal standard. Tetrahydrofuran-d_8 was added to the flask to make 3.00 mL of solution which was 7.5 mM concentration of mesitylene. A stirbar was added and the solution was stirred for 8 h. Not all of **13** dissolved, so a typical experiment involved addition of 0.700 mL of the supernatant of this solution by syringe to a thin walled, 9" NMR tube to provide homogeneous samples of **13** and mesitylene. The tube was degassed, PMe_3 was added by vacuum transfer to provide 0.026, 0.099 and 0.143 M solutions, and the tube was flame sealed to give a length of 8.5". The concentration of **13** and added phosphine was determined by integrating versus the known

concentration of mesitylene internal standard. The tubes were heated at 125 °C in a factory-calibrated Neslab Exocal Model 251 constant temperature bath filled with Dow Corning 200 silicone Fluid. All reactions were monitored by ambient-temperature ^{1}H NMR spectrometry by integrating mutually trans PMe_3 resonance of the starting material versus the mesitylene internal standard. The spectra were taken with a single acquisition and double checked with a second acquisition after a delay of at least 10 T_1. All first order kinetic plots displayed excellent linearity over the first two half lives with correlation coefficients of 0.99 or better. However, after 2 to 2 1/2 halflives the first order plot deviated from linearity, and the reaction stopped in all three cases at 85% converstion. However, when the data were plotted as a first order approach to equilibrium (using the 5.7:1 ratio as the infinity point) good linearity ($r^2 \geq 0.98$) was observed for each run. The rates obtained for the three concentrations of phosphine ($2.7 \pm 0.3 \times 10^{-5}$ for 0.026 M, $1.1 \pm 0.1 \times 10^{-5}$ for 0.099 M, and $1.2 \pm 0.1 \times 10^{-5}$ for 0.143 M) did not indicate a strong dependence of reaction rate on phosphine concentration.

Acknowledgements. We gratefully acknowledge support for this work from the National Institutes of Health (Grant no. GM-25459). The crystal structure analysis was performed by Dr. F.J. Hollander, staff crystallographer at the UC Berkeley X-ray crystallographic facility (CHEXRAY).

Notes and References

1. Masters, C *Homogeneous Transition-Metal Catalysis*, Chapman and Hall, New York, 1981.

2. Bryndza, H.E.; Tam, W. *Chem. Rev.* 1988, *88*, 1163.

3. (a) Pearson, R.G. *J. Am. Chem. Soc.* 1963, *85*, 3533. (b) Pearson, R.G. *J. Chem. Educ.*, 1968, *45*, 643. (c) Hartley, F.R. *The Chemistry of Platinum and Palladium*; Wiley: New York, 1976; p 169. (d) Lappert, M.F.; Power, P.P.; Sanger, A.R.; Srivastava, R.C. *Metal and Metalloid Amides*; Ellis Harwood: Chinchester, 1980.

4. (a) Bryndza, H.E.; Fong, L.K.; Paciello, R.A.; Tam, W.; Bercaw, J.E. *J. Am. Chem. Soc.* 1987, *109*, 1444. (b) Kim, Y-J.; Osakada, K.; Sugita, K.; Yamamoto, T.; Yamamoto, A. *Organimetallics*, 1988, *7*, 2182. (c) Komiya, S.; Akai, Y.; Tanaka, K.; Yamamoto, T.;

Yamamoto, A *Organometallics*, 1985, *4*, 1130. (d) Yoshida, T.; Okano, T.; Ueda, Y.; Otsuka, S. *J. Am. Chem. Soc.* 1981, *103*, 3411. (e) Rees, W.M.; Churchill, M.R.; Fettinger, J.C.; Atwood, J.D. *Organometallics*, 1985, *4*, 2179. (f) Rees, W.M. Atwood, J.D. *Organometallics*, 1985, *4*, 402. (g) Cowan, R.L.; Trogler, W.C. *J. Am. Chem. Soc.* 1989, *111*, 4750. (h) Bugro, C.D.; Pasquali, M.; Leoni, P.; Subatino, P.; Braga, D. *Inorg. Chem.* 1989, *28*, 1390.

5. (a) Newman, L.J.; Bergman, R.G. *J. Am. Chem. Soc.* 1985, *107*, 5314. (b) Milstein, D.; Calabrese, J.C.; Williams, I.D. *J. Am. Chem. Soc.* 1986, *108*, 6387. (c) Darensbourg, D.J.; Sanchez, K.M.; Rheingold, A.L. *J. Am. Chem. Soc.* 1987, *109*, 290. (d) Hartwig, J.F.; Andersen, R.A.; Bergman, R.G. *J. Am. Chem. Soc.* 1989, *111*, 2717.
6. (a) Bennett, M.A.; Yoshida, T. *J. Am. Chem. Soc.* 1978, *100*, 1750. (b) Arnold, D.P.; Bennett, M.A.; Crisp, G.T.; Jeffery, J.C. *Adv. Chem. Ser.*, 1982, *No. 196*, 195. (c) Michelin, R.A.; Napoli, M.; Ros, R. *J. Organomet. Chem.* 1979, *175*, 239. (d) Bennett, M.A. *J. Organomet. Chem.* 1986, *300*, 7. (e) Bennett, M.A.; Rokicki, A. *J. Organomet. Chem.* 1979, *175*, 239. (f) Bryndza, H.E. *Organometallics* 1985, *4*, 1686. (g) Bryndza, H.E.; Calabrese, J.C.; Reford, S.S. *Organometallics* 1984, *3*, 1603. (h) Bryndza, H.E.; Kretchmer, S.; Tulip, T.H. *J. Chem. Soc., Chemm. Commun.* 1985, 977. (i) Bryndza, H.E.; Fultz, W.C.; Tam, W.; *Organometallics* 1985, *4*, 939.
7. Bryndza, H.E. *Organometallics*, 1985, *4*, 406.
8. Klein, D.P.; Hayes, J.C.; Bergman, R.G. *J. Am. Chem. Soc.* 1988, *110*, 3704.
9. Statler, J.A.; Wilkinson, G.; Thornton-Pett, M.; Hursthouse, M.B. *J. Chem. Soc., Dalton Trans.*, 1984, 1731.
10. Chapter 4.
11. Chapter 3.
12. A trans influence series is given in Appleton, T.G.; Clark, H.C.; Manger, L.E. *Coord. Chem. Rev.* 1973, *10*, 335. Discussion of correlations between trans influence and ^{31}P chemical shifts is found in: (a) Nixon, G.F.; Pidcock, A. *Ann. Rev. NMR Spectroscopy*, 1969, *2*, 345.

(b) Verkade, J.M.; Quin, eds., *Phosphorus-31 NMR Spectroscopy in Stereochemical Analysis*, VCH Publishers: New York, 1987. (c) Meek, D.W.; Mazanec, T.J. *Acc. Chem. Res.* **1981**, *14*, 266.

13. (a) Andersen, R.A.; Jones, R.A.; Wilkinson, G. *J. Chem. Soc., Dalton Trans.* **1978**, 446. (b) Wong, W-K.; Chiu, K.W.; Statler, J.A.; Wilkinson, G.; Motevalli, M.; Hursthouse, M.B. *Polyhedron*, **1984**, *3*, 1255.
14. Mainz, V.V.; Andersen, R.A. *Organometallics* **1984**, *3*, 675.
15. (a)Wong, W.K.; Chiu, K.W.; Statter, J.A.; Wilkinson, G.; Motevalli, M.; Hursthouse, M.B. *Polyhedron*, **1984**, *3*, 1255. (b) Calabrese, J.C.; Colton, M.C.; Herskovits, T.; Klabunde, U.; Parshall, G.W.; Thorn, D.L.; Tulip, T.H. *Proc. N.Y. Acad. Sci.*, **1983**, *415*, 302. (c) Antberg, M.; Dahlenburg, L.; Frosin, K.M.; Höck, N. *Chem. Ber.*, **1988**, *121*, 859. (d) Dahlenburg, L.; Frosin, K.M. *Chem. Ber.* **1988**, *121*, 864.
16. For a recent reference on an η^3-benzyl compound see: Brookhart, M.; Buck, R.C.; Danielson, E., III *J. Am. Chem. Soc.* **1989**, *111*, 567. An extensive list of such compounds is provided in this reference.
17. Collman, J.P.; Hegedus, L.S.; Norton, J.R.; Finke, R.G. *Principles and Applications of Organotransition Metal Chemistry*; University Science Books: Mill Valley, 1987; p. 37, 56.
18. For a review of ^{15}N NMR spectroscopy which includes values of ^{1}H-^{15}N, and ^{13}C-^{15}N coupling constants in organic molecules see: Philipsborn, W -n.; Muller, R. *Angew. Chem. Int. Ed. Engl.* **1986**, *25*, 383.
19. Free PMe_3 and free PMe_3-d_9 can be easily distinguished due to their large isotopic shift in the $^{31}P\{^{1}H\}$ NMR spectrum.
20. (a) Chapter 9. (b) Hartwig, J.F.; Bergman, R.G.; Andersen, R.A. *J. Am. Chem. Soc.* **1990**, *112*, 3234.
21. Hartwig, J.F.; Andersen, R.A.; Bergman, R.G. unpublished results.
22. Yamamoto, A. *Organotransition Metal Chemistry*; Wiley: New York, 1986.

23. Darensbourg, D.J.; Kudaroski, R.A. *Adv. Organomet. Chem.* **1983**, *22*, 129. (b) Behr, A. *Angew. Chem. Int. Ed. Engl.* **1988**, *27*

24. (a) Darensbourg, D.J.; Hanckel, R.K.; Bauch, C.G.; Pala, M.; Simmons, D.; White, J.N. *J. Am. Chem. Soc.* **1985**, *107*, 7463. (b) Grötsch, G.; Darensbourg, D.J. *J. Am. Chem. Soc.* **1985**, *107*, 7473.

25. See for example, (a) Darensbourg, D.J.; Wiegreffe, P.; Riordan, C.G. *J. Am. Chem. Soc.* **1990**, *112*, 5759. (b) Darensbourg, D.J.; Fischer, M.B.; Schmidt, R.E., Jr.; Baldwin, B. *J. Am. Chem. Soc.* **1981**, *103*, 1297. (c) Merrifield, J.H.; Gladysz, J.A. *Organometallics*, **1983**, *2*, 782.

26. Alexander, J.J. *The Chemistry of the Metal-Carbon Bond*; Hartley, F.R., Ed.; Wiley: New York, 1985; vol 2, chapter 5.

27. Hartwig, J.F.; Bergman, R.G.; Andersen, R.A *J. Am. Chem. Soc.* **1990**, *112*, 3234.

28. Bergman, R.G.; Buchanan, J.M.; McGhee, W.D.; Periana, R.A.; Seidler, P.F.; Trost, M.K.; Wenzel, T.T. In *Experimental Organometallic Chemistry: A Practicum in Synthesis and Characterization*; Wayda, A.L.; Darensbourg, M.Y., Eds.; ACS Symposium Series 357; American Chemical Society: Washington, DC, 1987, p 227.

29. For a description of the X-ray diffraction and analysis protocols used, see (a) Hersh, W.H.; Hollander, F.J.; Bergman, R.G. *J. Am. Chem. Soc.* **1983**, *105*, 5834. (b) Roof, R.B., Jr. *A Theoretical Extension of the Reduced-Cell Concept in Crystallography*; Publication LA-4038, Los Alamos Scientific Laboratory: Los Alamos, NM 1969. (c) Cromer, D.T.; Waber, J.T. *International Tables for X-ray Crystallography*; Kynoch Press: Birmingham, England, 1974; Vol. IV, Table 2.2B.

Chapter 6

Synthesis and Chemistry of Ruthenium Hydrido Aryloxides and Arylamides. An Investigation of Structure, N-H and O-H Elimination Processes, Proton-Catalyzed Exchange Reactions, and Relative Ru-X Bond Strengths.

Introduction.

Processes such as reductive elimination and oxidative addition, although well studied for the formation and cleavage of C-H bonds at transition metal centers,[1] remain relatively unexplored for the formation and cleavage of N-H and O-H bonds. In fact, few monomeric complexes have been prepared which contain both a metal hydride and an η^1-metal-OR or metal-NHR (R=alkyl or aryl) linkage. Examples of such compounds in the late transition metal series include $Cp^*Ir(PPh_3)(H)(OEt)$,[2] *trans*-$(PR_3)_2Pt(H)(XAr)$ where X=O and NH,[3] $(PEt_3)Pd(H)(OPh)$,[4] and $[(PMe_3)_4Ir(H)(OMe)]PF_6$.[5] Early metal examples include $Cp_2Hf(H)(XR)$ where X=NH and O,[6] and $Cp^*_2Th(H)(OR)$.[7]

Most of the late transition metal examples have been prepared by the metathetical replacement of a late transition metal-halide or -pseudohalide by an alkalai metal-amide or -alkoxide. Although the preparation of aryloxide complexes has been achieved by the reaction of phenols or substituted phenols with late metal complexes,[8] few hydrido alkoxides or amides have been achieved by this route.[3a, 5] The formation of transition metal amides by addition of the N-H bond of alkyl or aryl amines is less common than reactions with the fairly acidic O-H bond of phenols or alcohols. Reaction of amines to provide monomeric late transition metal alkyl or aryl amides has been reported in only a few cases.[9] Rather, addition of these unactivated N-H bonds has been reported with trinuclear osmium compounds, with a monomeric iridium complex to form products with bridging amides, and with an iridium complex containing a chelated amine.[10]

A study of ligand-induced O-H reductive elimination of ethanol from the ethoxy hydride $Cp^*Ir(PPh_3)(OEt)(H)$[2] was reported from this laboratory. This work has recently been extended to include the N-H reductive elimination of aniline from $Cp^*Ir(PPh_3)(NHPh)(H)$.[11] Only a few other cases of N-H and O-H reductive elimination reactions have been observed, all of them ligand *induced*.[3b, 4, 12]

We have investigated the reactions of an electron-rich ruthenium system with N-H and O-H bonds in the hope that such a metal system would favor oxidative addition of these bonds as it does for the oxidative addition of C-H bonds. Formation of the hydrido aryloxide and arylamide

complexes by these processes has allowed a comparison of the stability of these compounds with the analogous hydrido benzyl complex.[13] In addition, the reversible addition of hydrogen to these compounds has provided both mechanistic information and relative thermodynamic stabilities of the M-O, M-N, and M-H linkages in these compounds. Finally, substitution of the poor σ-donating and strong π-accepting ligand CO for one of the σ-donating phosphine ligands has allowed us to determine the solid state structure and the solution state reactivity changes that occur when the electron density at the metal center is reduced.

Results

$(PMe_3)_4Ru(H)(NHPh)$. The synthesis of compounds $(PMe_3)_4Ru(H)(NHPh)$ (**1**) and $(PMe_3)_4Ru(H)(OC_6H_4\text{-}p\text{-}Me)$ (**2**) is summarized in Scheme 1. Addition of aniline to the ethylene complex (**3**)[14] followed by heating to 135 °C for 24h led to clean formation of the hydrido anilide complex **1** in 66% isolated yield. Addition to the cyclometallated hydride $(PMe_3)_3Ru(CH_2PMe_2)(H)$ (**4**)[15] followed by heating to 110 °C for 24h led to **1** in 93% yield by ^1H NMR spectroscopy. These reaction conditions reliably led to formation of **1**, but during some preparations from ethylene complex **3**, the reaction rate was markedly faster; heating to 110 °C for 3-12 h often gave complete conversion. Compound **1** was characterized by ^1H, $^{31}P\{^1H\}$, $^{13}C\{^1H\}$, and IR spectroscopy, as well as microanalysis and X-ray diffraction (*vide infra*). The A_2BC pattern in the $^{31}P\{^1H\}$ NMR spectrum indicated a cis configuration of the σ-bound ligands. The other possible geometry, a trans relationship between the hydride and anilide substituents, would result in a singlet resonance in the $^{31}P\{^1H\}$ NMR spectrum. The doublet of quartets hydride resonance (one large trans coupling and three nearly identical cis couplings) at δ-7.69 confirms this assignment. The Ru-H linkage was confirmed by an infrared absorption at 1845 cm^{-1}. The N-H proton was observed at δ1.71 in the ^1H NMR spectrum and at 3370 cm^{-1} in the infrared spectrum. The aryl region of the ^1H NMR spectrum contained five inequivalent resonances between δ6.43 and δ7.38, and the $^{13}C\{^1H\}$ NMR spectrum displayed five inequivalent C-H resonances between δ107.39 and δ129.83 and one quaternary resonance at δ161.83. These

Scheme 1

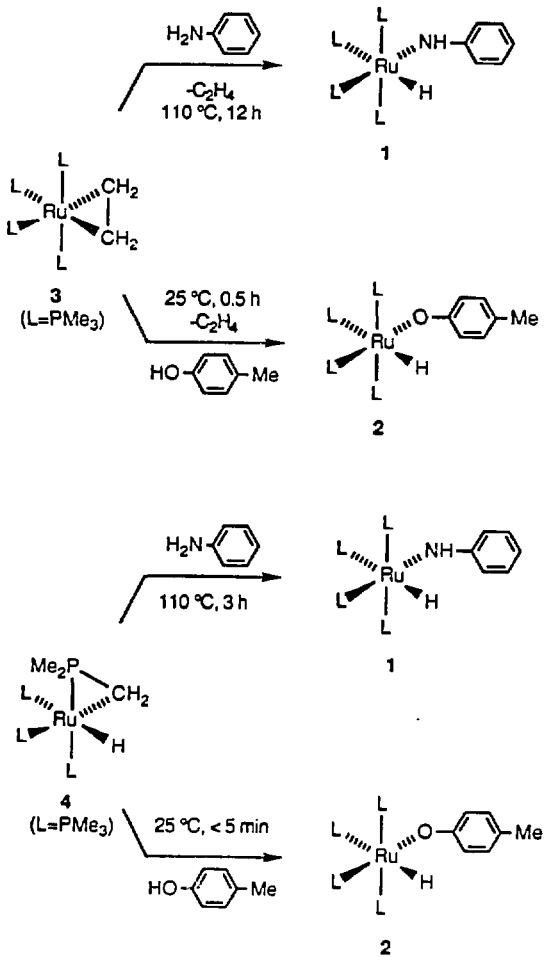
H2N
-C2H4
110 °C, 12 h
L
Ru
NH
H
1
CH2
3
(L=PMe3)
25 °C, 0.5 h
-C2H4
HO
Me
O
2
110 °C, 3 h
Me2P
4
(L=PMe3)
25 °C, < 5 min

signals fall in the region of normal, uncomplexed aryl rings; the inequivalence of the two sides of the ring indicate that it is not rotating on the NMR time scale.

The addition of aniline was conducted with and without added PMe_3. No rate inhibition was observed for the sample with added phopshine. Rather, qualitative studies showed that samples containing added PMe_3 reacted 10-20% faster than for those with no added phosphine. In addition, the reaction of rigorously dried (*vide infra*) *p*-chloroaniline was run in the presence and absence of added water. The sample containing added water reacted at two to three times the rate as the sample containing no added water.

The dideuterated analogue of **1** was prepared in 38% yield by the addition of 0.25 equivalents of lithiumaluminumdeuteride to a THF solution of the complex $(PMe_3)_4Ru(OAc)(Cl)$, followed by addition of the deuterated lithiumanilide, LiNDPh. No hydride or anilide resonance was observed in the ^1H NMR spectrum for a 0.06 M sample, indicating at least 95% isotopic purity. The deuteride resonance was observed at δ-7.67, and the anilide deuterium was observed at δ1.66 in the ^2H NMR spectrum; no other resonances were observed. An infrared absorption band at 2497 cm^{-1} was assigned to the N-D stretch, and a shoulder at 1326 corresponded to the Ru-D stretch.

Thermolysis of the labelled compound at 125 °C for 4 h led to scrambling of the deuterium into the phosphine and aryl groups, (determined by ^2H NMR spectroscopy) preventing useful mechanistic results from deuterium labelling experiments. When N,N-d_2-aniline was added to cyclometallated hydride **4** at 110 °C (the conditions used for formation of **1**) and the fate of the deuterium label was determined by ^2H NMR spectroscopy, signals were observed not only in the hydride and anilide N-H position, but in the aromatic and phosphine regions as well. Reversible cyclometallation of the anilide substituent would account for incorporation of deuterium into these positions, and orthometallation of the anilide substituent would account for the presence of aryl resonances.

$(PMe_3)_4Ru(H)(OC_6H_4\text{-}p\text{-}Me)$. Addition of one equivalent of *p*-cresol to the ethylene complex **3** at room temperature led to rapid formation of ethylene and $(PMe_3)_4Ru(H)(OC_6H_4\text{-}p\text{-}$

Me) (2) in 64% isolated yield. Addition of *p*-cresol to the cyclometallated hydride 4 also occurred rapidly at room temperature and provided (1) in 62% isolated yield. Again, 3 proved to be the more convenient starting material. Compound 2 was characterized by ^1H, $^{31}P\{^1H\}$, $^{13}C\{^1H\}$, and IR spectroscopy, as well as microanalysis. As observed for compound 2, the $^{31}P\{^1H\}$ NMR spectrum displayed an A_2BC pattern, and the ^1H NMR spectrum contained a doublet of quartets pattern for the hydride resonance, indicating a *cis* orientation of the hydride and aryloxide ligands. The Ru-H infrared absorption was observed at 1836 cm^{-1}. In contrast to the anilide substituent in 1, the two sides of the aryl ring in the cresolate substituent of 2 were equivalent by ^1H and $^{13}C\{^1H\}$ NMR spectroscopy (an AA'BB' pattern of the aryl region of the ^1H NMR spectrum, and two CH resonances in the aryl region of the $^{13}C\{^1H\}$ NMR spectrum). Therefore, the aryl ring of 1 is either located in the plane of the two mutually trans phosphine ligands and the oxygen atom of the aryloxide substituent, or it is freely rotating on the NMR time scale. X-ray diffraction shows that the ring is located in the plane of the hydride, ruthenium, and oxygen atoms in the solid state (*vide infra*), suggesting that the two sides of the ring are inequivalent in the lowest energy conformation in solution, but are rapidly exchanging on the NMR time scale.

$(PMe_3)_3(CO)Ru(H)(OC_6H_4$-p-Me) Addition of carbon monoxide (2 atm) to compound 2 at 65 °C for 8 h led to formation of the CO ligand substitution product $(PMe_3)_3(CO)Ru(H)(OC_6H_4$-p-Me) (5), in which the poor σ-donor and strong π-acceptor CO[16] is located *trans* to the aryloxide substituent (Equation 1). Compound 5 was characterized by ^1H, $^{31}P\{^1H\}$, $^{13}C\{^1H\}$, IR spectroscopy, microanalysis, and X-ray diffraction (*vide infra*). Again, $^{31}P\{^1H\}$ and ^1H NMR spectroscopy demonstrated the stereochemistry. A doublet of triplets resonance with a large trans H-P coupling constant on the order of that observed for 2 (117.8 Hz versus 102.8 for 2) was observed at δ-5.92 for the hydride substituent, indicating that a phosphine ligand is located trans to it. Moreover, an A_2B pattern in the $^{31}P\{^1H\}$ NMR spectrum with P_B resonating upfield from P_A is consistent with P_B being located trans to a substituent with a stronger trans influence than phosphine.[17]

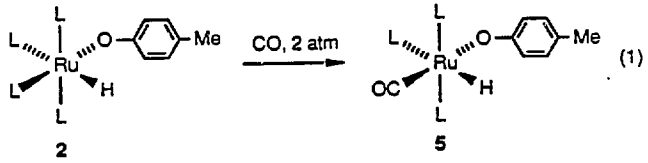

2 **5** (1)

X-ray Structural Analyses. A suitable single crystal of **1** was obtained by allowing a refluxing hexane solution to cool slowly to room temperature. The compound crystallized in space group P1 bar with two independent molecules in the asymmetric unit. Crystal and data collection parameters are provided in Table 1; intramolecular bond distances and angles are displayed in Tables 2 and 3. An ORTEP drawing of the molecule is shown in Figure 1. Compound **2** crystallized in space group $P2_1/n$ with 2 crystallographically independent molecules in the asymmetric unit by cooling a solution of **1** in pentane to -40 °C. An ORTEP drawing of the molecule is provided in Figure 2. Crystal and data collection parameters are included in Table 1; intramolecular distances and angles are provided in Tables 4 and 5. A suitable single crystal of **5** (space group Cmca) was obtained by slow cooling of a toluene/pentane (1:100) solution to -40 °C. An ORTEP drawing of the molecule is shown in Figure 3. Crystal and data collection parameters are included in Table 1; intramolecular bond distances and angles are displayed in Tables 6 and 7. The structures were solved by Patterson methods and refined by least squares and Fourier techniques.

All three structures are distorted octahedra, with a hydride ligand occupying the vacant site of molecules **1** and **5**; the hydrides were not located on the Patterson map for these two compounds. To simplify the discussion, the distances and angles for one of the two independent molecules of **1** and **2** will be used; the two molecules are chemically equivalent in both cases. The Ru-N bond length in **1** is 2.160(6)Å, and the aryl ring is located in the plane of the ruthenium, hydride, and nitrogen atoms, consistent with the inequivalence of the two sides of the aryl ring in the ^1H and $^{13}C\{^1H\}$ NMR spectra. The Ru-O bond length of **2** is 2.152(3)Å. Although a slightly shorter M-O distance may be expected, simply based on the smaller ionic radius of oxygen versus nitrogen, the difference in these two bond lengths is not statistically significant. Similarly, the O-C bond length in the aryloxide substituent of **2** (1.308(7)) is slightly shorter than the N-C bond length (1.340(9)) in **1**. As observed for **1**, the aryl ring is located in the plane of the hydride, ruthenium, and oxygen atoms. As noted in the previous section, the ring must be freely rotating

Table 1. Crystal and Data Collection Parameters.[a]

	1	**2**	**8**
Temperature (°C)	-90	25 °C	-89
Empirical Formula	$RuP_4NC_{18}H_{43}$	$RuP_4OC_{19}H_{44}$	$RuP_3O_2C_{17}H_{35}$
Formula Weight (amu)	498.5	513.5	465.5
Crystal Size (mm)	0.20 x 0.21 x 0.36	0.20x 0.25 x 0.50	0.10 x 0.20 x 0.25
Space Group	P1 bar	$P2_1/n$	C_{mca}
a (Å)	12.364(4)	13.539(2)	13.300(2)
b (Å)	13.951(6)	13.771(2)	14.088(3)
c (Å)	15.062(5)	29.302(2)	24.950(3)
α (°)	103.79(3)	90.0	90.0
β (°)	96.10(2)	102.50(2)	90.0
γ (°)	90.02(3)	90.0	90.0
V ($Å^3$)	2507.9(3)	5310.2(3)	4676.9(3)
Z	4	8	8
d_{calc} (gcm^{-3})	1.32	1.28	1.32
μ_{calc} (cm^{-1})	8.7	8.8	8.7
Reflections Measured	+h, +k, ±l	+h, +k, ±l	+h, +k, +l
Scan Width	Δθ = 0.70 + 0.35 tanθ	Δθ = 0.70 + 0.35 tanθ	Δθ = 0.80 + 0.35 tanθ
Scan Speed (θ, °/m)	6.70	6.70	6.70
Setting Angles (2θ, °)[b]	24-28	24-28	22-26

(a) Parameters common to all structures: Radiation: Mo Kα (λ = 0.71073 Å), except for **1c** λ = 0.70930 Å. Monochromator: highly-oriented graphite (2θ = 12.2°). Detector: crystal scintillation counter, with PHA. 2θ Range: 3-->45°, except for **1c** 2-->45°. Scan Type: θ-2θ. Background: Measured over 0.25(Δθ) added to each end of the scan. Vertical Aperture = 3.0 mm. Horizontal Aperture = 2.0 + 1.0 tanθ mm. Intensity Standards: Measured every hour of x-ray exposure time. Orientation: 3 reflections were checked after every 200 measurements. Crystal orientation was redetermined if any of the reflections were offset from their predicted positions by more than 0.1°. Reorientation was required twice for **1b** and **7a**, and once for **8**. (b) Unit cell parameters and their esd's were derived by a least-squares fit to the setting angles of the unresolved Mo Kα components of 24 reflections with the given 2θ range. In this and all subsequent tables the esd's of all parameters are given in parentheses, right-justified to the least significant digit(s) of the reported value.

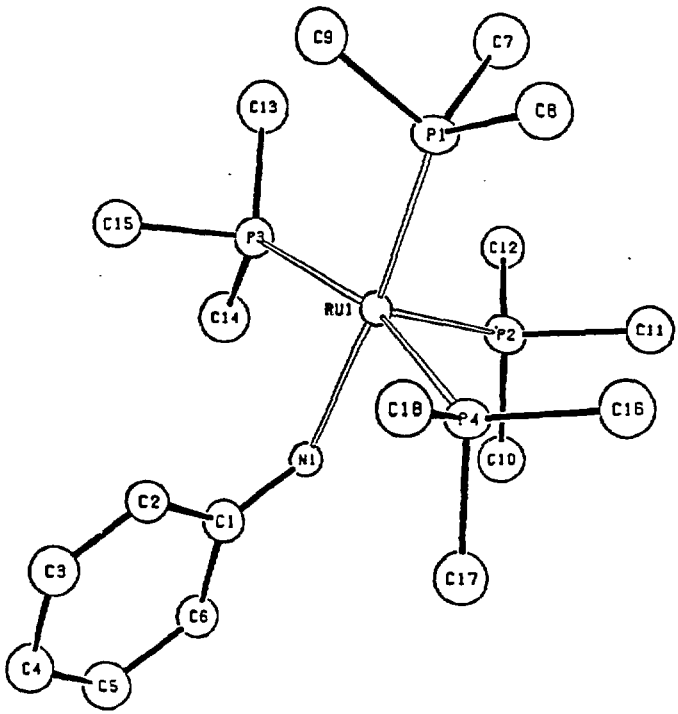

Figure 1. ORTEP drawing of 1. The ruthenium-bound hydrogen was not located.

Table 2. Selected intramolecular bond distances for 1.

ATOM 1	ATOM 2	DISTANCE
RU1	P1	2.268(2)
RU1	P2	2.363(2)
RU1	P3	2.325(2)
RU1	P4	2.331(2)
RU1	N1	2.160(6)
RU2	P5	2.354(2)
RU2	P6	2.271(2)
RU2	P7	2.318(2)
RU2	P8	2.345(2)
RU2	N2	2.163(6)
N1	C1	1.340(9)
C1	C2	1.475(10)
C1	C6	1.475(10)
C2	C3	1.324(10)
C3	C4	1.417(11)
C4	C5	1.376(10)
C5	C6	1.403(10)
N2	C21	1.355(8)
C21	C22	1.431(10)
C21	C26	1.438(9)
C22	C23	1.353(10)
C23	C24	1.392(11)
C24	C25	1.482(11)
C25	C26	1.326(10)
P1	C7	1.838(9)
P1	C8	1.858(8)
P1	C9	1.845(8)
P2	C10	1.861(8)
P2	C11	1.856(8)
P2	C12	1.877(8)
P3	C13	1.858(9)
P3	C14	1.844(9)
P3	C15	1.831(8)
P4	C16	1.865(9)
P4	C17	1.844(8)
P4	C18	1.806(8)
P5	C27	1.861(8)
P5	C28	1.844(8)
P5	C29	1.858(8)
P6	C30	1.875(9)
P6	C31	1.865(9)
P6	C32	1.834(9)
P7	C33	1.853(9)
P7	C34	1.851(8)
P7	C35	1.861(8)
P8	C36	1.834(9)
P8	C37	1.825(9)
P8	C38	1.841(8)

Table 3. Selected intramolecular bond angles for 1.

ATOM 1	ATOM 2	ATOM 3	ANGLE
P1	RU1	P2	98.37(7)
P1	RU1	P3	94.24(7)
P1	RU1	P4	95.87(7)
P1	RU1	N1	172.09(15)
P2	RU1	P3	96.18(7)
P2	RU1	P4	97.88(7)
P2	RU1	N1	88.72(15)
P3	RU1	P4	161.27(8)
P3	RU1	N1	81.44(16)
P4	RU1	N1	86.57(16)
P5	RU2	P6	97.93(7)
P5	RU2	P7	99.09(7)
P5	RU2	P8	94.52(7)
P5	RU2	N2	90.69(16)
P6	RU2	P7	95.38(8)
P6	RU2	P8	95.11(8)
P6	RU2	N2	170.93(16)
P7	RU2	P8	161.48(8)
P7	RU2	N2	85.97(16)
P8	RU2	N2	81.34(16)
RU1	N1	C1	134.1(5)
RU2	N2	C21	135.6(5)
N1	C1	C2	125.4(6)
N1	C1	C6	119.4(6)
C2	C1	C6	115.1(6)
C1	C2	C3	118.5(7)
C2	C3	C4	128.1(7)
C3	C4	C5	114.1(7)
C4	C5	C6	123.9(7)
C1	C6	C5	120.0(7)
N2	C21	C22	122.4(6)
N2	C21	C26	123.7(6)
C22	C21	C26	113.9(6)
C21	C22	C23	122.6(7)
C22	C23	C24	123.5(8)
C23	C24	C25	115.0(7)
C24	C25	C26	120.5(7)
C21	C26	C25	124.4(7)

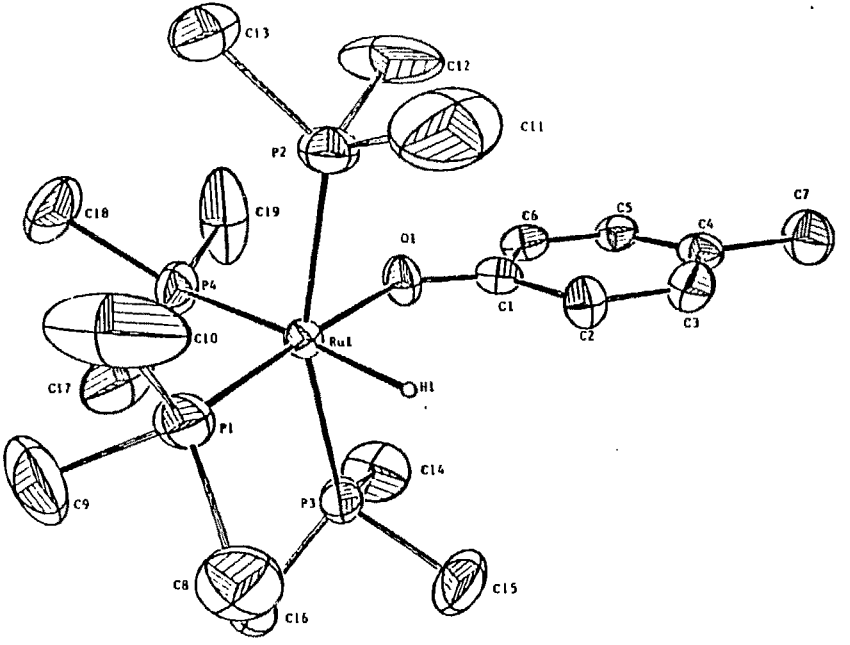

Figure 2. ORTEP drawing of 2. The ruthenium bound hydrogen was located but not refined. Most of the other hydrogen atoms were also located but have been omitted for clarity.

Table 4. Selected intramolecular bond distances for **2**.

ATOM 1	ATOM 2	DISTANCE
RU1	P1	2.229(2)
RU1	P2	2.327(2)
RU1	P3	2.329(2)
RU1	P4	2.364(2)
RU1	O1	2.152(3)
RU1	H1	1.734(1)
P1	C8	1.803(8)
P1	C9	1.831(10)
P1	C10	1.791(8)
P2	C11	1.828(7)
P2	C12	1.802(7)
P2	C13	1.841(7)
P3	C14	1.825(8)
P3	C15	1.781(8)
P3	C16	1.811(10)
P4	C17	1.820(8)
P4	C18	1.803(9)
P4	C19	1.794(8)
O1	C1	1.388(7)
C1	C2	1.413(7)
C1	C6	1.399(7)
C2	C3	1.375(8)
C3	C4	1.364(7)
C4	C5	1.384(7)
C4	C7	1.524(9)
C5	C6	1.387(8)

Table 5. Selected intramolecular bond angles for 2.

ATOM 1	ATOM 2	ATOM 3	ANGLE
P1	RU1	P2	94.48(6)
P1	RU1	P3	96.16(6)
P1	RU1	P4	99.49(7)
P1	RU1	O1	176.96(11)
P1	RU1	H1	76.31(6)
P2	RU1	P3	168.97(7)
P2	RU1	P4	96.97(6)
P2	RU1	O1	83.47(10)
P2	RU1	H1	82.44(4)
P3	RU1	P4	96.76(7)
P3	RU1	O1	85.21(10)
P3	RU1	H1	84.82(5)
P4	RU1	O1	83.01(10)
P4	RU1	H1	175.68(5)
O1	RU1	H1	101.15(9)
RU1	P1	C8	117.2(3)
RU1	P1	C9	119.4(3)
RU1	P1	C10	121.4(3)
C8	P1	C9	96.8(4)
C8	P1	C10	99.2(4)
C9	P1	C10	98.0(5)
RU1	P2	C11	114.46(22)
RU1	P2	C12	115.18(22)
RU1	P2	C13	125.15(22)
C11	P2	C12	99.4(4)
C11	P2	C13	98.9(3)
C12	P2	C13	99.6(3)
RU1	P3	C14	125.5(3)
RU1	P3	C15	114.4(3)
RU1	P3	C16	115.0(3)
C14	P3	C15	98.2(4)
C14	P3	C16	100.2(4)
C15	P3	C16	99.2(6)
RU1	P4	C17	121.05(23)
RU1	P4	C18	120.58(25)
RU1	P4	C19	115.2(3)
C17	P4	C18	96.7(4)
C17	P4	C19	98.8(4)
C18	P4	C19	100.3(5)
RU1	O1	C1	133.3(3)
O1	C1	C2	118.6(4)
O1	C1	C6	125.4(4)
C2	C1	C6	116.0(5)
C1	C2	C3	121.2(5)
C2	C3	C4	122.9(4)
C3	C4	C5	116.5(5)
C3	C4	C7	122.7(4)
C5	C4	C7	120.8(5)
C4	C5	C6	122.5(5)

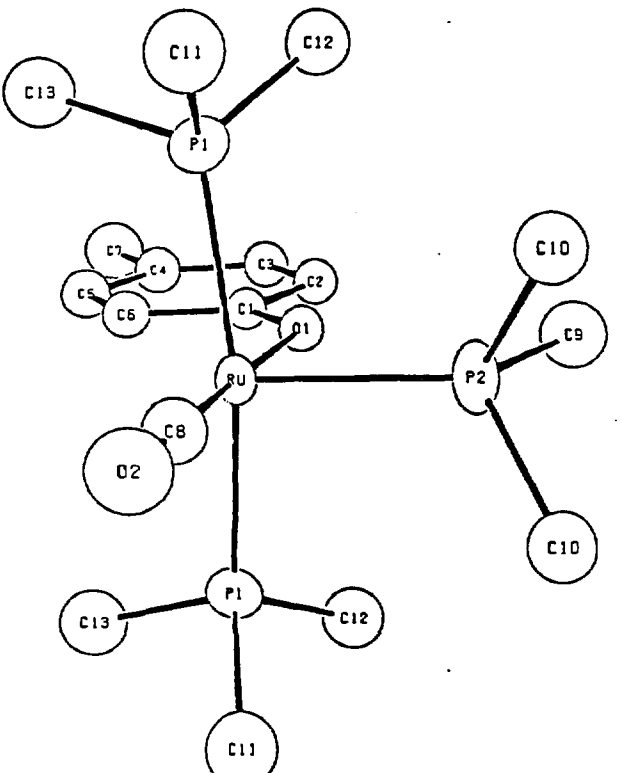

Figure 3. ORTEP drawing of 5. The ruthenium-bound hydrogen was not located.

Table 6. Selected intramolecular bond distances for 8.

ATOM 1	ATOM 2	DISTANCE
RU	P1	2.334(2)
RU	P2	2.396(3)
RU	O1	2.108(6)
RU	C8	1.783(10)
C8	O2	1.201(11)
O1	C1	1.333(10)
C1	C2	1.429(12)
C1	C6	1.409(13)
C2	C3	1.387(13)
C3	C4	1.399(12)
C4	C5	1.367(13)
C4	C7	1.621(15)
C5	C6	1.370(13)
P1	C11	1.860(8)
P1	C12	1.822(7)
P1	C13	1.827(7)
P2	C9	1.853(11)
P2	C10	1.839(8)

Table 7. Selected intramolecular bond angles for 8.

ATOM 1	ATOM 2	ATOM 3	ANGLE
P1	RU	P1	163.60(9)
P1	RU	P2	96.43(5)
P1	RU	O1	85.60(5)
P1	RU	C8	94.52(6)
P2	RU	O1	86.21(17)
P2	RU	C8	94.8(3)
O1	RU	C8	179.0(4)
RU	C8	O2	177.9(9)
RU	O1	C1	132.9(5)
O1	C1	C2	117.1(7)
O1	C1	C6	125.5(8)
C2	C1	C6	117.4(8)
C1	C2	C3	119.3(8)
C2	C3	C4	121.8(9)
C3	C4	C5	118.5(9)
C3	C4	C7	119.1(9)
C5	C4	C7	122.4(9)
C4	C5	C6	121.7(9)
C1	C6	C5	121.4(9)
RU	P1	C11	117.9(3)
RU	P1	C12	115.3(3)
RU	P1	C13	114.1(3)
C11	P1	C12	104.0(3)
C11	P1	C13	101.3(3)
C12	P1	C13	102.0(3)
RU	P2	C9	114.1(4)
RU	P2	C10	117.70(24)
C9	P2	C10	102.1(3)
C10	P2	C10	100.6(5)

on the NMR time scale if this structure also corresponds to the lowest energy configuration in solution.

The Ru-P distances of both structures reflect the weaker trans influence properties of the aryloxide and arylamide ligands relative to those of the hydride or phosphine ligands.[20] The Ru-P distance for the phosphine located trans to the aryloxide in **2** is 2.229(2) Å and the distance for the phosphine located trans to the arylamide in **1** is 2.268(2)Å. The Ru-P distances for the mutually trans phosphine ligands range from 2.327(2) Å to 2.343(2)Å for the two structures, and the two Ru-P distances trans to the hydride substituents are 2.364(2) Å for **2** and 2.363(2)Å for **1**. The shorter distances for the phosphines located trans to the *p*-cresolate and trans to the anilide are consistent with the weaker trans influence of heteroatom containing substituents as compared to phosphine and hydride ligands.[15] The Ru-O-C angle in **2** is 133.3(3)° and the Ru-N-C angle is 134.1(5)° for **1**, indicating that this angle is not particularly sensitive to the difference in π-donating abilities of the aryloxide and aryl amide ligands.

In contrast to the similarity of **1** and **2**, CO substituted compound **5** has a Ru-O bond length of 2.108(6), which is significantly shorter than that in **2**. The O-C(aryl) bond distance in the aryloxide ligand of **5** (1.333(10) Å) is not significantly longer than that of **2**, 1.308(7), and the Ru-O-C bond angle of 132.9(5)° is also similar to that in **2**, 133.3(3)°. The difference in Ru-O bond distances in **1** and **5** may be attributed to the propensity of the aryloxide ligand in **5** to donate π-electron density into the π-accepting CO ligand trans to it.

A similar trend in bond lengths was observed for the Pt(II)-chloride distances in a series of square planar complexes. X-Ray structural analyses have been performed for compounds with the general formula $LL'PtCl_2$, where L is a phosphine and L' is a π-accepting ligand such as CO or an isocyanide. When L is triethylphosphine and L' is CO, the Pt-Cl bond distance trans to PEt_3 was longer (2.368(3) Å) than trans to CO (2.296(4) Å).[18] When L is PEt_2Ph and L' is ethylisocyanide, the Pt-Cl bond distance trans to the phosphine was longer (2.390(8) Å) than trans to the isocyanate (2.314(10) Å).[19] The Pt-Cl distance trans to the phosphine in $(PEt_3)(PhNC)PtCl_2$ was 2.333(12) Å.[20] Therefore, whether the difference in bond lengths

among these platinum and ruthenium compounds is largely caused by changes in the π-accepting or σ-donating properties of the dative ligands, the bonding of the aryloxide ligands in the ruthenium complexes in this study mimics the bonding in simple Pt(II) complexes.

Variable temperature NMR Spectra. The room temperature NMR spectra of **1** and **2** indicate that the donating properties of the heteroatom can have a significant effect on the barrier to rotation of the aryl ring, and variable temperature NMR experiments indicate that the ancillary ligands have a measurable effect on the double bond character of the aryloxide O-C linkage. The O-C(aryl) linkage in the all phosphine complex **2** appears to contain slightly more double bond character than the CO substituted product **5**, as determined from the lower barrier to rotation in **5**. A stacked plot of the aryl region of the ^{1}H NMR spectrum of **2** in the temperature range -9 °C to -88 °C is shown in Figure 4. At -88 °C, four inequivalent resonances are observed, indicating that rotation of the ring is slow on the NMR time scale. The same region in the ^{1}H NMR spectra of the CO substitution product **5** between -79 °C and -105 °C is shown in Figure 5. Even at -105 °C, only one of the aryl resonances of **5** has broadened, and it has not begun to separate into two inequivalent resonances, indicating values of ΔG for the barrier to rotation which are lower than observed for **2**. ^{1}H NMR spectroscopy of the sterically similar benzyl hydride complex[15] showed no change in the aryl region, even at -105 °C, indicating that the slow rotation of the ring in complex **1** at room temperature and complex **2** at -88 °C is a result of electronic rather than steric factors. We did not expect the substitution of CO to cause a significant perturbation in the steric interactions of the cresolate substituent, since the substitution occurs trans to it. Indeed, the X-ray diffraction study shows that the M-O-C angle for **2** and **5** are almost identical. Although differences in σ-donating properties appears to have a larger effect on the M-O bond lengths in **2** and **5**, the difference in π-accepting ability of the ligand trans to the cresolate does have a measurable effect on the rotational barriers of these two compounds, presumably due to differences in π-donation of the oxygen lone pair.

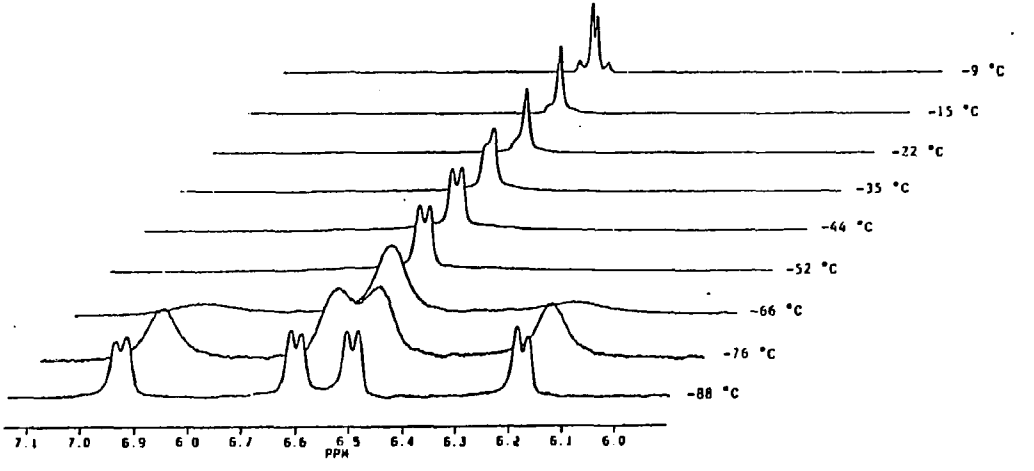

Figure 4. Variable temperature ^{1}H NMR spectra of the aryl region of 2.

H/D exchange reactions with $(PMe_3)_4Ru(H)_2$ (6). Addition of 20 equivalents of N,N-d_2-aniline to the dihydride $(PMe_3)_4Ru(H)_2$[21] (6) at 25 °C for 1 h led to H/D exchange, forming the dideuteride $(PMe_3)_4Ru(D)_2$. This assignment was based on the absence of hydride signals in the ^1H NMR spectrum, the presence of the corresponding resonances in the ^2H NMR spectrum, and the additional coupling in the $^{31}P\{^1H\}$ NMR spectrum. To ensure that the exchange occurred only between the hydride substituents and the NH protons of aniline, the dideuteride $(PMe_3)_4Ru(D)_2$ was treated with 20 equivalents of protiated aniline, leading to formation of the dihydride and incorporation of deuterium into the N-H bonds of the aniline, as determined by the presence of only an N-D signal in the ^2H NMR spectrum of this mixture. Similarly, addition of N,N-d_2-aniline to the cyclometallated hydride complex 4 at room temperature led to incorporation of deuterium into the hydride position.

When attempting to qualitatively determine the basicity of the metal center, the importance of trace amounts of water became evident (Scheme 2). When dideuteride **6-d_2** was treated with 20 equivalents of cyclopentadiene (pKa~16),[22] ^2H NMR spectroscopy showed no detectable resonance for the diene after 4 h; only a resonance for the hydride of starting material **5-d_2** was observed. Similarly, no exchange with the sterically more accessible but less acidic C-H bond of *tert*-butylacetylene (pKa=~22)[23] was observed after 5 h; dideuteride **6-d_2** was treated with 20 equivalents of *tert*-butylacetylene at room temperature and ^2H NMR spectroscopy showed no propargyl C-D resonance. In contrast, the O-H proton of *tert*-butyl alcohol (pKa~16) exchanged with **6-d_2**. After 10 min at room temperature, solutions of **6-d_2** and 20 equivalents of *tert*-butyl alcohol showed only signals in the ^2H NMR spectrum corresponding to the O-D substituent of the organic reagent.

Exchange with diphenylamine (pKa~22) was slower than exchange with N-methylaniline or aniline, and led to roughly 50% exchange after 20 to 30 min at room temperature. However, when **6-d_2** was treated with 20 equivalents of diphenylamine, which had been dried by benzene azeotropic distillation using a Dean-Stark trap and isolated by sublimation, *no* exchange was observed after 2 h at room temperature. We attempted to stop the H/D exchange with the parent

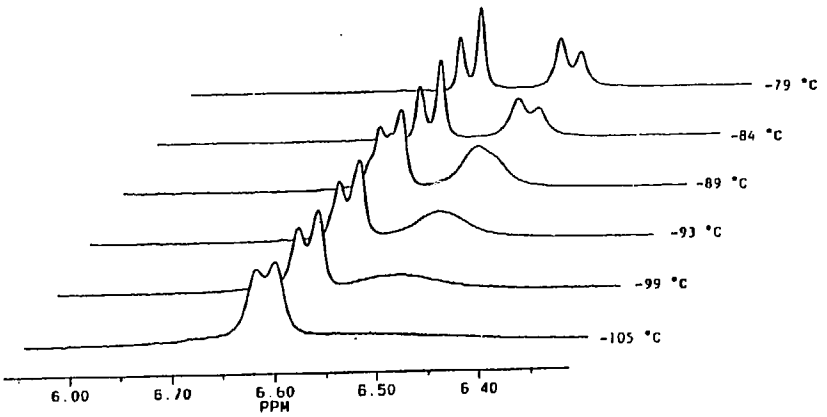

Figure 5. Variable temperature ^{1}H NMR spectra of the aryl region of 8.

Scheme 2

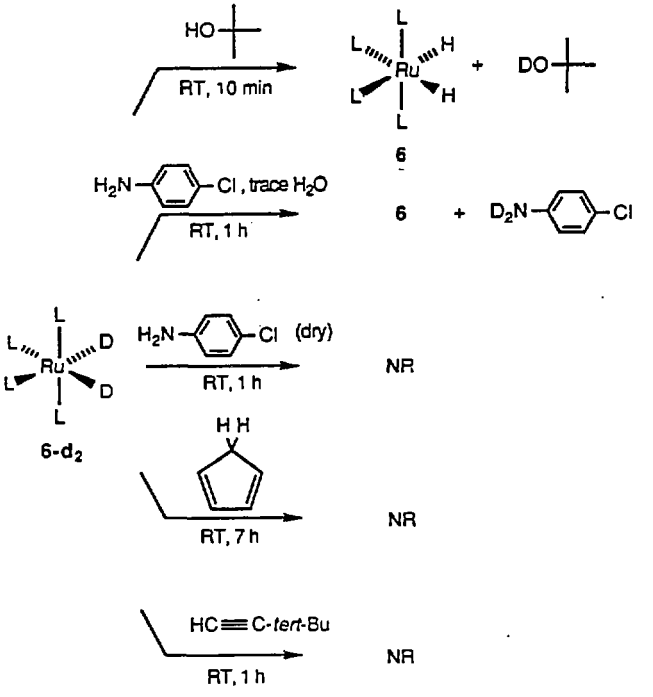
HO
RT, 10 min
L
L
H
Ru
H
L
L
+
DO
6
H2N
Cl, trace H2O
RT, 1 h
6
+
D2N
Cl
L
L
D
Ru
D
L
6-d2
H2N
Cl
(dry)
RT, 1 h
NR
H H
RT, 7 h
NR
HC≡C-tert-Bu
RT, 1 h
NR

aniline by exhaustive drying with vacuum distillation from sodium or CaH_2, or by azeotropic distillation with benene. However, exchange of the aniline N-H with the ruthenium deuteride still occurred over the course of 10 min. To insure that exchange in the case of aniline was a result of the difficulty in obtaining dry arylamine which is a liquid, and not due to a steric difference between aniline and diphenylamine, *p*-chloroaniline, which is a solid, was dried using the same method employed for diphenylamine. Indeed, *no* exchange was observed by ^2H NMR after 0.5 h at room temperature, and addition of 0.1 μL of water to this sample led to complete exchange after 15 min. These results demonstrate that this metal center is capable of rapid uncatalyzed exchange with alcohol O-H bonds, but exchange with less acidic N-H bonds at room temperature requires catalysis by trace amounts of water.

A qualitative comparison of the H/D exchange rate and the phosphine dissociation rate was performed to determine whether exchange also requires the formation of an intermediate resulting from phosphine dissociation. Dihydride **6** was treated with 4 equivalents of PMe_3-d_9 at 25 °C. $^{31}P\{^1H\}$ NMR spectra were obtained after 1 h and 24 h at room temperature, and in both cases only resonances for **6**-d_2 and free PMe_3-d_9 were observed. No free PMe_3-d_0 was formed, indicating that phosphine dissociation was significantly slower than H/D exchange.

Another possible intermediate in both the formation of **1** from **3** and in the H/D exchange reactions is $(PMe_3)_4Ru$ (**7**). If the exchange occurs by way of this intermediate, D_2 must be incorporated into **6** at the same or faster rate than the acidic substrates. However, exchange with D_2 was much slower than it was with the amines or alcohols. Addition of 19 atm (>2000 equiv.) of D_2 to the dihydride complex was conducted at 25 °C for 24 h. After this time, only partial incorporation of deuterium into the hydride position had occurred. A deuteride signal was observed in the ^2H NMR spectrum, but a hydride signal was also observed in the ^1H NMR spectrum.

To probe the intermediacy of **6** in the formation of **1**, benzyl hydride compound $(PMe_3)_4Ru(CH_2Ph)(H)$ (**8**) was heated to 75 °C for 2 h in the presence of one equivalent of aniline at the concentrations used to synthesize **1**. We have reported previously that intermediate **7** is

generated by thermally induced reductive elimination of $(PMe_3)_4Ru(CH_2Ph)(H)$ (**8**), and forms **4** by addition of a ligand C-H bond.[22] These thermolysis conditions provided roughly 45% conversion of **8** to cyclometallated hydride **4**. Only small amounts (*ca.* 5%) of anilide hydride were observed. Heating for an additional 16 h led to complete disappearance of **7** and formation of a 3:1 ratio of **4** and hydrido anilide **1**, undoubtedly formed from **4**.

CO Induced Reductive Elimination. Addition of carbon monoxide to **1**, followed by heating to 85 °C for 8 h, led to reductive elimination of aniline in 94% yield by ^1H NMR spectroscopy, as shown in Scheme 3. Addition of CO to **2**, followed by heating to 135 °C for 5 d, led to formation of *p*-cresol in 98% yield by ^1H NMR spectroscopy (Scheme 3). The organometallic product was $(PMe_3)_2Ru(CO)_3$ (**10**) in both cases and was formed in 79% yield for elimination of aniline and 89% yield for elimination of *p*-cresol. Compound **9** was independently prepared by successive photolysis and thermolysis of $Ru_3(CO)_{12}$ and PMe_3 during the course of a separate study,[24] and was characterized by ^1H, $^{13}C\{^1H\}$, $^{31}P\{^1H\}$ NMR, and IR spectroscopy. The NMR data are provided in Tables 8-10. The stoichiometry was confirmed by observing a quartet in the $^{31}P\{^1H\}$ NMR spectrum of the complex containing ^{13}CO. Monitoring the reductive elimination reaction of **2** showed that the reaction first formed CO substituted product **5**, but a *bis*-CO substituted complex $(PMe_3)_2(CO)_2Ru(H)(OC_6H_4\text{-}p\text{-}Me)$ (**9**) was not observed.

Anilide and Cresolate Exchange Reactions. Addition of 3 equivalents of *p*-cresol to the anilide hydride complex **1** at 25 °C led to complete reaction of this compound in less than 20 min to form the cresolate hydride **2**. One equivalent of free aniline was observed, along with 2 equivalents of free *p*-cresol (Scheme 4).

Scheme 3

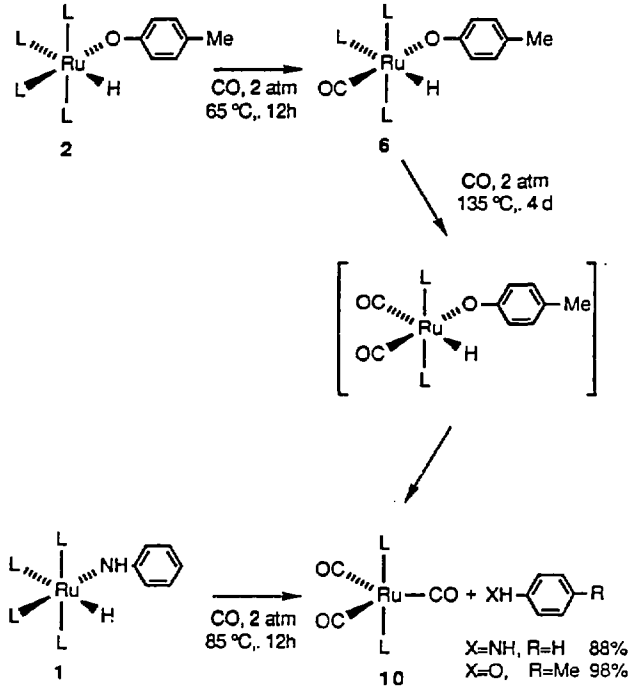
L
L
Ru
O
Me
L
H
L
2
CO, 2 atm
65 °C,. 12h
OC
6
CO, 2 atm
135 °C,. 4 d
[
]
1
NH
CO, 2 atm
85 °C,. 12h
CO + XH
R
10
X=NH, R=H 88%
X=O, R=Me 98%

Scheme 4

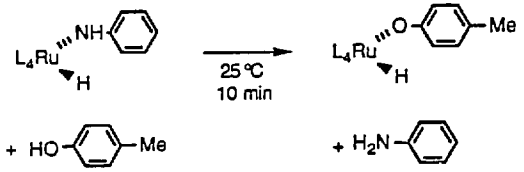

Discussion.

Aniline addition reactions. Several possible mechanisms for the H/D exchange reactions are shown in Scheme 5. One mechanism, pathway a, involves reversible addition of a proton to the metal center, leading to a cationic metal complex. The structure of the cation is written as Ru(IV), though it may exist as a Ru(II)-(η^2-H_2) compound since several related ruthenium hydrogen complexes are known.[25] Pathway b postulates H_2 reductive elimination to form the L_4Ru intermediate, which oxidatively adds N,N-d_2-aniline to form the anilide deuteride **1**-d_2, and reacts with the extruded hydrogen to reform the H/D scrambled product. Two other mechanisms involve initial dissociation of phosphine. In pathway c, the anilide nitrogen atom coordinates to the resulting vacant coordination site, enhancing the acidity of the aniline N-H bond (analogous to the enhanced acidity of coordinated water in aqua ions[26]). In pathway d, the unsaturated intermediate undergoes N-H oxidative addition to form a trihydride intermediate.

Our results are consistent only with the proton transfer pathway a. The rate of H/D exchange is significantly faster than the rate of phosphine dissociation from dihydride **6**, ruling out the possibility of reaction by pathways c and d. Pathway b is ruled out by the failure of D_2 to incorporate into the dihydride **6** on the time scale of the H/D exchange with aniline. Our results with a range of weak acids demonstrates that the metal center is not basic enough to exchange with weak carbon acids such as *tert*-butyl acetylene and cyclopentadiene, but is basic enough to exchange rapidly with *tert*-butanol. Moreover, our ability to significantly slow the H/D exchange process of arylamines by obtaining rigorously dry samples of solid amines indicates that exchange with these substrates occurs by a water catalyzed process. Based on our observations with *tert*-butanol we propose that the catalysis operates by reversible protonation of the metal center with water, and H/D exchange between water and aniline to the incorporate deuterium into the anilide N-H position.

Mechanisms similar to those for the H/D exchange can be invoked for the formation of anilide hydride **1** from cyclometallated hydride **4**. The lack of phosphine inhibition (despite rapid phosphine dissociation at these temperatures) indicates that reaction does not occur by pathways

Scheme 5

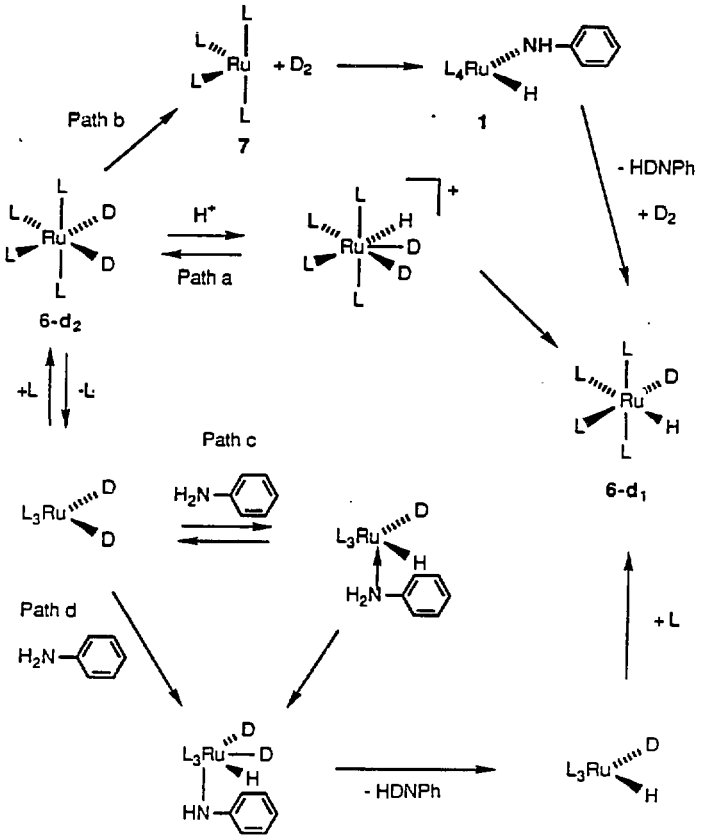
Path b
+ D2
7
L4Ru NH
H
1
- HDNPh
+ D2
H+
Path a
6-d2
+L
-L
Path c
H2N
L3Ru D
D
H
H2N
Path d
H2N
6-d1
+L
L3Ru D
H
HN
- HDNPh
L3Ru D
H

involving phosphine dissociation. Our results do not rigorously rule out reaction by way of intermediate $(PMe_3)_4Ru$ (**7**) to form **1** by direct oxidative addition of the aniline N-H bond. Independent generation of **7** from benzyl hydride **8** demonstrated that intramolecular C-H oxidative addition with this intermediate is faster than reaction with aniline, disfavoring formation of **1** by oxidative addition of the aniline N-H bond to intermediate **7**. However, our data do not rigorously rule out the possibility that intermediate **7** is formed reversibly from cyclometallated hydride **4** and eventually reacts with aniline to form the thermodynamic product **1**.

The results of the H/D exchange study suggest that trace amounts of water are likely to be important if a mechanism for formation of **1** from **4** involves proton transfer processes. The lack of a dramatic rate increase for reaction of rigorously dried *p*-chloroaniline with **4** in the presence of added water, suggest that water catalyzed proton transfer is not as important in the formation of **4** as it is in the H/D exchange. This may reflect a rate determining step which does not involve proton transfer. Consistent with this hypothesis, addition of aniline-d_2 to **4** led to H/D exchange with the hydride substituent at 25 °C, a much lower temperature than required for formation of **1**. We tentatively propose that this N-H addition reaction proceeds by a proton transfer mechanism, in analogy to the H/D exchange processes and the cresol addition reaction, although we have no clearcut means to rule out N-H oxidative addition to the $(PMe_3)_4Ru$ intermediate **7**.[27] We hope that future studies with this compound and others will help clarify the role proton transfer processes play in N-H addition reactions to transition metal centers.

Addition of *p*-cresol. We have reported that addition of *p*-cresol to the benzyne complex $(PMe_3)_4Ru(\eta^2\text{-}C_6H_4)$ occurs faster than phosphine dissociation, implying direct protonation of the electron rich metal center by this acidic substrate, followed by C-H reductive elimination to form the observed phenyl aryloxide intermediate $(PMe_3)_4Ru(Ph)(OC_6H_4\text{-}p\text{-}Me)$.[28] Addition of *p*-cresol to either **3** or **4** also occurs rapidly at room temperature (< 5 min.), suggesting that protonation by the cresol occurs to form cationic intermediate **11** (Scheme 6), followed by reductive elimination to form the ethyl cresolate $(PMe_3)_4Ru(Et)(OC_6H_4\text{-}p\text{-}Me)$ (**12**) and β-hydrogen elimination to form the product **2**. Protonation of **4** followed by C-H reductive

elimination and ion-pair collapse would form **2** directly. Moreover, the reaction of $(PMe_3)_4Ru(C_2H_4)$ with *p*-cresol cannot occur *via* the Ru^0 intermediate **7** because ethylene dissociation is much slower than the cresol addition. The addition of one equivalent of ethylene-d_4 to **3** was monitored over the course of 12h at 25° C. After this time no resonance for free ethylene was observed in the ^1H NMR spectrum, and the chemical shift of bound ethylene did not change, indicating that dissociation of ethylene from **3** does not occur on this time scale.[29] Field has reported the addition of alcohols to the iron dihydride $(DMPE)_2Fe(H)_2$ to form a cationic complex containing three metal-bound hydrogen atoms,[30] an intermediate analogous to the one involved in the protonation of **3**.

CO-Induced Reductive Elimination. Reductive elimination of aniline from **1** is markedly faster than elimination of *p*-cresol from **2**. However, we were not able to observe or isolate the *bis*-CO adduct $(PMe_3)_2(CO)_2Ru(H)(OC_6H_4\text{-}p\text{-}Me)$, the precursor to the O-H elimination reaction, and so the marked difference in rates for the reductive elimination of aniline from **1** and *p*-cresol from **2** may reflect conditions necessary for a second CO substitution reaction rather than a difference in rates of the two reductive elimination processes.

However, it is evident that substitution of the poor σ-donor and strong π-acceptor CO for the strong σ-donor PMe_3, at least kinetically, favors reductive elimination over the all PMe_3 substituted compound. In addition the organometallic product $(PMe_3)_2Ru(CO)_3$ is formed irreversibly, suggesting that an electron rich metal center is crucial to the thermodynamic stability of anilide and cresolate hydride compounds **1** and **2**.

Qualitative Thermodynamic Results. This ruthenium system constitutes a rare example of a series of compounds which undergo C-H, N-H, and O-H reductive elimination reactions. No evidence for direct reductive elimination from **1** or **2** was obtained; only upon addition of CO or H_2 was elimination of aniline or *p*-cresol observed. As reported earlier, thermolysis of the benzyl hydride complex $(PMe_3)_4Ru(H)(CH_2Ph)$ (**8**) at 85 °C for 4 h leads directly to reductive elimination of toluene and formation of the $(PMe_3)_4Ru^0$ intermediate **7** which undergoes activation of ligand C-H bonds and forms cyclometallated hydride **4**. As illustrated in

Scheme 6

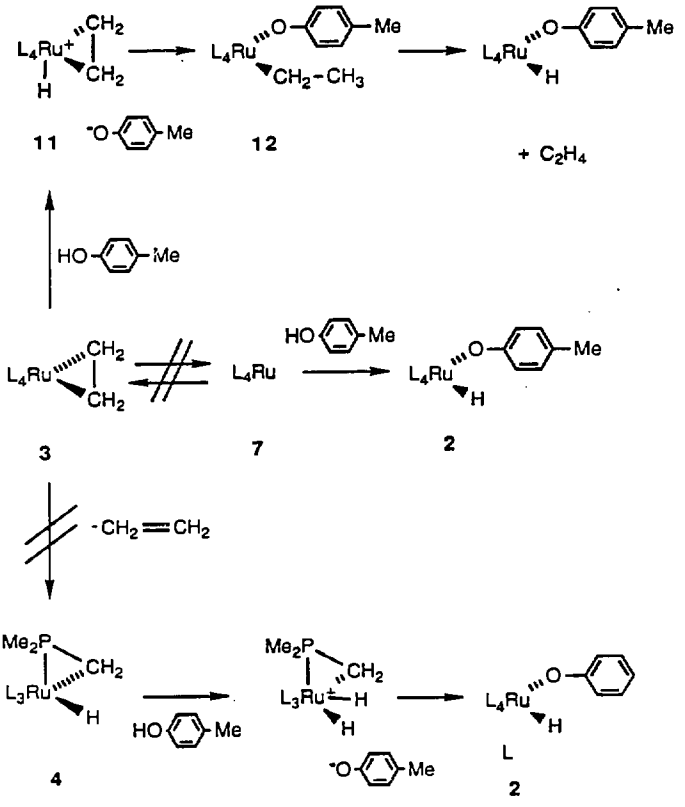
L4Ru+
CH2
CH2
H
11
-O
Me
L4Ru
O
Me
CH2-CH3
12
L4Ru
O
Me
H
+ C2H4
HO
Me
L4Ru
CH2
CH2
3
L4Ru
7
HO
Me
L4Ru
O
Me
H
2
-CH2=CH2
Me2P
CH2
L3Ru
H
4
HO
Me
Me2P
CH2
L3Ru
H
H
-O
Me
L4Ru
O
H
L
2

Scheme 7, these results demonstrate a dramatic contrast between the thermodynamic stabilities of benzyl hydride **8** and heteroatom substituted compounds **1** and **2**. Compounds **1** and **2** are formed by the addition of cresol and aniline to **4**, the product of reductive elimination from **8**. Because the benzyl C-H bond of toluene (88.0 ±1 kcal/mol) is comparable to the strength of the O-H bond of cresol (86.5 ± 2 kcal/mol for phenol) and the N-H bond of aniline (88.0 ± 2 kcal/mol), the Ru-O and Ru-N linkages in **1** and **2** must be stronger than the Ru-C linkage in **8**.[31] Moreover, because dihydrogen has been shown to react with **1** and **2** to form the dihydride **6** and either aniline or *p*-cresol,[32] the Ru-H bond must be at least 16 kcal stronger (the difference between the corresponding H-H and N-H bonds) than either the Ru-N or Ru-O bonds. Similarly, the reaction of *p*-cresol with the anilide hydride **1** to form free aniline and the cresolate hydride **2** shows that the Ru-O linkage is stronger than the Ru-N bond for these two compounds. The following trend in bond strength then results: $L_4(H)Ru\text{-}H > L_4(H)Ru\text{-}OAr > L_4(H)Ru\text{-}NHPh > L_4(H)Ru\text{-}CH_2Ph$.

Scheme 7

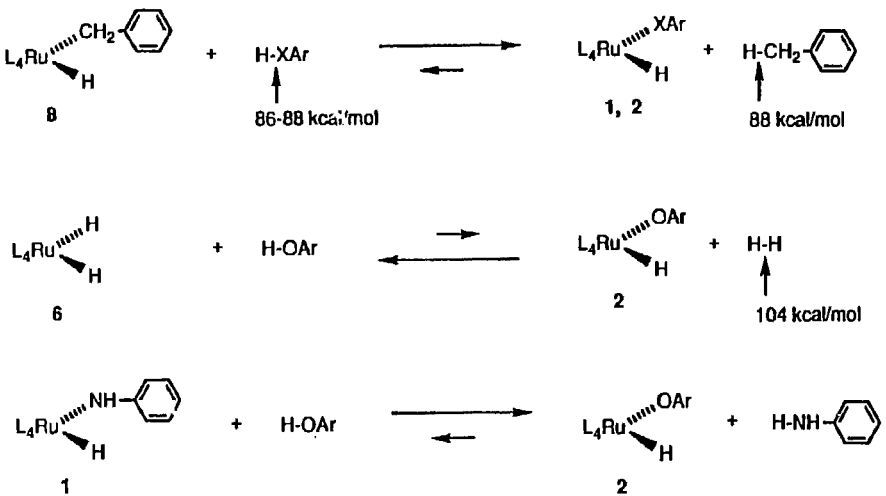

Relative Bond Strengths: $L_4Ru\text{-}H > L_4Ru\text{-}OAr > L_4Ru\text{-}NHPh > L_4Ru\text{-}CH_2Ph$

Table 8 ^{1}H NMR spectroscopic data

	δ (ppm)	multiplicity[a]	J (Hz)	integration	assignment[b]
$(PMe_3)_4Ru(H)(OC_6H_4\text{-}p\text{-}Me)$ (1)[c]	7.18	d	8.6	2	Aromatic
	7.14		8.5	2	
	2.37	s		3	
	1.18	t	2.8	18	*trans*-PMe_3
	1.14	d	5.5	9	*cis*-PMe_3
	0.98	d	7.5	9	
	-7.65	dq	102.8, 27.5	1	Ru-H
$(PMe_3)_4Ru(H)(NHC_6H_5)$ (2)[c]	6.43	t	6.8	1	Aromatic
	6.59	d	8.0	1	
	7.20	t	7.5	1	
	7.35	m		2	
	1.71	d	7.3	1	NH
	1.81	t	2.6	18	*trans*-PMe_3
	1.03	d	6.8	9	*cis* -PMe_3
	0.96	d	4.9	9	
	-7.69	dq	99.0, 26.4	1	Ru-H
$(PMe_3)_3(CO)Ru(H)(OC_6H_4\text{-}p\text{-}Me)$ (5)[c]	7.16	d	8.3	2	Aromatic
	7.03	d	8.3	2	
	2.36	s		3	*p*-Me
	1.16	t	2.6	18	*trans*-PMe_3
	1.08	d	6.4	9	*cis*-PMe_3
	-5.92	dt	117.8, 26.5	1	Ru-H
$(CO)_3Ru(PMe_3)_2$[c] (9)	1.20	t	3.7		PMe_3

[a]The multiplicities reported for the PMe_3 resonances are aparent splittings and do not necessarily reflect true coupling constants. [b]The assignments, *cis*-PMe_3 and *trans*-PMe_3 refer to mutually cis and mutually trans PMe_3 ligands. [c]C_6D_6, 20 °C.

Table 9. $^{13}C\{^1H\}$ NMR spectroscopic Data.

	δ (ppm)	multiplicity[a]	J (Hz)	assignment[b]
$(PMe_3)_4Ru(H)(OC_6H_4\text{-}p\text{-}Me)$ (1)[c]	20.55	d	15.4	*cis*-PMe_3
	27.22	d	23.4	
	22.89	td	12.8, 3.8	*trans*-PMe_3
	20.93	s		*p*-Me
	118.26	s		Aromatic
	120.34	s		
	129.77	s		
	169.13	d	4.5	
$(PMe_3)_4Ru(H)(NHC_6H_5)$ (2)[c]	21.52	dm	14.2	*cis*-PMe_3
	27.44	dm	24.1	
	23.27	td	12.9, 4.0	*trans*-PMe_3
	107.39	s		Aromatic
	114.64	s		
	117.78	d	4.1	
	128.91	s		
	129.45	s		
	161.83	t	3.2	
$(PMe_3)_3(CO)Ru(H)(OC_6H_4\text{-}p\text{-}Me)$ (5)[c]	17.84	d	18	*cis*-PMe_3
	20.45	td	14.6, 3.0	*trans*-PMe_3
	20.83	s		*p*-Me
	119.30	s	10.3	Aromatic
	119.40	s		
	129.79	s		
	168.40	d	4.9	
	204.78	td	14.2, 8.8	CO
$(CO)_3Ru(PMe_3)$[c] (9)	22.69	t	16.3	PMe_3
	210.93	t	16.5	CO

[a]The multiplicities reported for the PMe_3 resonances are apparent splittings and do not necessarily reflect true coupling constants. [b]The assignments, *cis*-PMe_3 and *trans*-PMe_3 refer to mutually cis and mutually trans PMe_3 ligands. [c]C_6D_6, 20 °C.

Table 10. $^{31}P\{^{1}H\}$ NMR spectroscopic data (C_6D_6, 20 °C).

	spin system	δ(ppm)	J(Hz)
$(PMe_3)_4Ru(H)(OC_6H_4\text{-}p\text{-}Me)$ (1)	A_2BC	δ_A=1.54	J_{AB}=32.5
		δ_B=14.92	J_{AC}=27.1
		δ_C=-12.62	J_{BC}=15.9
$(PMe_3)_4Ru(H)(NHC_6H_5)$ (2)	A_2BC	δ_A=-0.98	J_{AB}=26.4
		δ_B=-14.55	J_{AC}=30.8
		δ_C=5.14	J_{BC}=19.0
$(PMe_3)_3(CO)Ru(H)(OC_6H_4\text{-}p\text{-}Me)$ (7)	A_2B	δ_A=0.23	J_{AB}=25.1
		δ_B=-15.77	
$(CO)_3Ru(PMe_3)$ (8)	A_3	2.20	

Experimental

General. Unless otherwise noted, all manipulations were carried out under an inert atmosphere in a Vacuum Atmospheres 553-2 drybox with attached M6-40-1H Dritrain, or by using standard Schlenk or vacuum line techniques.

^{1}H NMR spectra were obtained on either the 250, 300, 400 or 500 MHz Fourier Transform spectrometers at the University of California, Berkeley (UCB) NMR facility. The 250 and 300 MHz instruments were constructed by Mr. Rudi Nunlist and interfaced with either a Nicolet 1180 or 1280 computer. The 400 and 500 MHz instruments were commercial Bruker AM series spectrometers. ^{1}H NMR spectra were recorded relative to residual protiated solvent. ^{13}C NMR spectra were obtained at either 75.4 or 100.6 MHz on the 300 or 500 MHz instruments, respectively, and chemical shifts were recorded relative to the solvent resonance. ^{2}H NMR spectra were recorded at 76.4 MHz on the 500 MHz instrument, and chemical shifts were recorded relative to the solvent resonance. Chemical shifts are reported in units of parts per million downfield from tetramethylsilane and all coupling constants are reported in Hz.

IR spectra were obtained on a Nicolet 510 spectrometer equipped with a Nicolet 620 processor using potassium bromide ground pellets, Nujol mull, or solution cells as stated. Mass spectroscopic (MS) analyses were obtained at the UCB mass spectrometry facility on AEI MS-12 and Kratos MS-50 mass spectrometers. Elemental analyses were obtained from the UCB Microanalytical Laboratory.

To prepare sealed NMR tubes, the sample tube was attached via Cajon adapters directly to Kontes vacuum stopcocks.[33] Known volume bulb vacuum transfers were accomplished with an MKS Baratron attached to a high vacuum line.

Unless otherwise specified, all reagents were purchased from commercial suppliers and used without further purification. PMe_3 (Strem) was dried over NaK or a Na mirror and vacuum transferred prior to use. CO was purchased from Matheson. *p*-Cresol was dried by azeotroping with benzene using a Dean-Stark trap, followed by vacuum distillation. Dry diphenylamine and *p*-chloroaniline were obtained by refluxing a benzene solution using a Dean-Stark trap, and

subliming at 60 °C. Aniline was either vacuum distilled from sodium or calcium hydride, or was refluxed in benzene using a Dean-Stark trap and then vacuum distilled. Dry cyclopentadiene was obtained by heating cyclopentadiene dimer to 170 °C over CaH_2, and the monomer was collected by distillation. *tert*-Butylacetylene was stored under vacuum over P_2O_5, and was used by vacuum transfer. $(PMe_3)_3Ru(H)(CH_2PMe_2$(4) was prepared by the method of Werner,[16] $(PMe_3)_4Ru(C_2H_4)$ was prepared by the addition of EtMgBr to $(PMe_3)_4Ru(Cl)_2$,[15] and $(PMe_3)_4Ru(OAc)(Cl)$ was prepared by the method of Anderson and Mainz.[34]

Pentane and hexane (UV grade, alkene free) were distilled from $LiAlH_4$ under nitrogen. Benzene and toluene were distilled from sodium benzophenone ketyl under nitrogen. Ether and tetrahydrofuran were distilled from purple solutions of sodium/benzophenone ketyl. Deuterated solvents for use in NMR experiments were dried as their protiated analogues but were vacuum transferred from the drying agent.

$(PMe_3)_4Ru(H)(NHC_6H_5)$ (1). (a) Addition of aniline to $(PMe_3)_4Ru(C_2H_4)$. The ruthenium complex $(PMe_3)_4Ru(C_2H_4)$ (3) (350 mg, 0.804 mmol) was dissolved in a minimum amount of hexane (10 mL). It was important to run this reaction in alkane solvent; thermolysis of 3 in benzene led to formation of predominantly $(PMe_3)_4Ru(H)(Ph)$. To this solution was added 1.5 equiv (116 mg) of aniline. The solution was transferred to a glass reaction vessel fused to a Kontes vacuum adaptor, and partially degassed by exposing to vacuum for 2-3 seconds. The vessel was heated to 135 °C for 24 h, over which time the clear solution turned yellow. Upon cooling to room temperature, 266 mg (66.3 %) of product, which was judged to be pure by ^1H NMR spectroscopy, crystallized from the reaction mixture as pale yellow blocks. A portion of the material was recrystallized for microanalysis and an X-ray diffraction study by allowing a refluxing solution of 1 in hexane to cool slowly to room temperature. IR (KBr) 3370 (w), 2967 (s), 2906 (s), 1845 (s), 1586 (s), 1484 (s), 1463 (m), 1426 (m), 1338 (s), 1297 (m), 1276 (m), 942 (s); Anal. Calc'd. for $C_{18}H_{43}NP_4Ru$: C, 43.37; H, 8.69; N, 2.81. Found: C, 43.18; H, 8.73; N, 2.65.

(b) Addition of aniline to $(PMe_3)_3Ru(CH_2PMe_2)(H)$ (4). The ruthenium complex $(PMe_3)_4Ru(H)(CH_2PMe_2)$ (12.6 mg, 0.0311 mmol) was dissolved in 0.7 mL of C_6D_6 and

2 μL of mesitylene as an internal standard was added. A ^{1}H NMR spectrum was obtained on the sample. To the solution was then added 2.9 μL (1.0 equiv) of aniline. The NMR tube was attached to a Kontes vacuum adaptor, degassed by two freeze, pump, thaw cycles and sealed. The sample was heated to 110 °C for 24 h, after which time ^{1}H NMR spectroscopy showed formation of **1** in 93% yield as determined by comparison to the spectrum before heating.

Addition of aniline to 4 in the presence of PMe_3. Ruthenium complex $(PMe_3)_4Ru(H)(CH_2PMe_2)$ (**4**) (14.6 mg, 0.0359 mmol) was dissolved in 1.2 mL of C_6D_6 and 2 μL of mesitylene as an internal standard was added. To the solution was then added 16.8 μL (5.0 equiv.) of aniline. The sample was divided into two NMR tubes. One NMR tube was attached to a Kontes vacuum adaptor, degassed by two freeze, pump, thaw cycles and sealed. To the other tube was added 4.0 equiv (0.24 M) of PMe_3 before sealing by the same method. The reaction was monitored at 1 h intervals at 110 °C for 4 h, and showed that the rates for the sample containing PMe_3 was *ca* 10-20 % faster than the sample containing no PMe_3. Integration versus the mesitylene internal standard showed yields for the two samples which were within 10 %.

Addition of *p*-chloroaniline to 4 in the presence of H_2O. Ruthenium complex $(PMe_3)_4Ru(H)(CH_2PMe_2)$ (**4**) (11.9 mg, 0.0294 mmol) was dissolved in 1.2 mL of C_6D_6. To the solution was then added 38 mg (10 equiv.) of *p*-chloroaniline. The sample was divided into two NMR tubes. One NMR tube was attached to a Kontes vacuum adaptor, degassed by two freeze, pump, thaw cycles and sealed. To the other tube was added 0.1 μL of H_2O (0.006 mmol, 0.4 equiv, 0.009 M) before sealing by the same method. The reaction was monitored at 1 h intervals at 85 °C for 4 h, and showed that the rates for the sample containing H_2O was about twice that for the sample containing no PMe_3.

$(PMe_3)_4Ru(D)(NDC_6H_5)$ (1-d_2). To a stirred solution of $(PMe_3)_4Ru(OAc)(Cl)$ (202 mg, 0.404 mmol) in 8 mL of THF was added 1/4 equiv (4.2 mg) of lithium aluminum deuteride as a slurry in THF. The resulting pale yellow, cloudy solution was filtered, and to the resulting clear yellow solution was added 1.5 equiv of LiNDPh, generated by addition of *n*-BuLi (379 μL, 1.6 M in hexanes) to an ether (2 mL) solution of D_2NPh (57.6 mg). The pale yellow color became darker

upon addition of the lithium anilide. After stirring for 2 h the solution was filtered, and the solvent removed from the filtrate under reduced pressure. The resulting yellow solid was extracted with toluene. The toluene solution was reduced in volume to 1-2 mL, layered with hexanes, and cooled to -40 °C to provide 76.2 mg (38%) of **1-d_2** which was pure by ^{1}H and ^{31}P{^{1}H} NMR spectroscopy, showed no hydride or N-H resonance in the ^{1}H NMR spectrum, and only a hydride and N-H resonance in the ^{2}H NMR spectrum. ^{2}H NMR: δ1.66 (br,s), -7.67 (m); IR (KBr) 2967 (s), 2906 (s), 2497 (w, N-D), 1588 (s), 1484 (s), 1463 (m), 1426 (m), 1340 (s), 1326 (shoulder, Ru-D), 1298 (m), 1276 (m), 949 (s).

$(PMe_3)_4Ru(H)(OC_6H_4$-p-Me) (2). (a) Addition of cresol to $(PMe_3)_4Ru(C_2H_4)$. The uthenium complex $(PMe_3)_4Ru(C_2H_4)$ (702 mg, 1.61 mmol) was dissolved in a minimum amount of pentane (15 mL). To this solution was added at room temperature one equiv (174 mg) of *p*-cresol in 3 mL of pentane. The clear solution turned yellow, and gas evolution (presumably ethylene) was observed. Over the course of 12 h, 527 mg (63.7 %) of product, which was pure by ^{1}H NMR spectroscopy crystallized from the reaction mixture as pale yellow blocks. A portion of this material was recrystallized for microanalysis by vapor diffusing pentane into a solution of **2** in toluene. IR (KBr) 2968 (s), 2908 (s), 1836 (s), 1600 (s), 1501 (s), 1498 (s), 1425 (m), 1323 (s)1310 (s), 1301 (s), 1290 (s), 1281 (s), 1156 (m), 943 (s); Anal. Calc'd. for $C_{19}H_{44}OP_4Ru$: C, 44.44; H, 8.63. Found: C, 44.56; H, 8.53.

(b) Addition of *p*-cresol to $(PMe_3)_3Ru(CH_2PMe_2)(H)$ (4). Ruthenium complex $(PMe_3)_3Ru(CH_2PMe_2)(H)$ (98.8 mg, 0.244 mmol) was dissolved in 5 mL of toluene. One equiv (26.3 mg) of *p*-cresol in 0.5 mL of toluene was added at room temperature. The clear solution turned yellow. Removal of toluene under vacuum, followed by crystallization from pentane at -40 °C provided 77.6 mg (62.0 %) of **2** which was judged pure by ^{1}H NMR spectroscopy.

$(PMe_3)_3(CO)Ru(H)(OC_6H_4$-p-Me) (5). To a 125 mL glass reaction vessel fused to a Kontes vacuum adapter was added 15 mL of a C_6H_6 solution of 252 mg (0.491 mmol) of $(PMe_3)_4Ru(H)(OC_6H_4$-p-Me) (**2**). The entire reaction vessel was cooled in liquid nitrogen and 430 torr of CO (calculated to be 2 atm at 20 °C) was added. The vacuum adaptor was closed and the

vessel was warmed to room temperature. The reaction was then heated to 85 °C for 12h, after which time the volatile materials were removed under vacuum, leaving a pale yellow residue. This residue was crystallized from pentane:toluene (100:1) at -40 °C to yield 77.2 mg (33.8 %) of analytically pure white product containing crystals suitable for an X-ray diffraction study. IR (KBr) 2981 (m), 2971 (m), 2911(m), 2901 (m), 1906 (s), 1852 (m), 1600 (m), 1501 (s), 1429 (m), 1423 (m), 1312 (s), 1301 (s), 943 (s); Anal. Calc'd. for $C_{17}H_{35}O_2P_3Ru$: C, 43.87; H, 7.58. Found: C, 43.59; H, 7.56.

$(PMe_3)_4Ru(D)_2$ (6-d_2). To a solution of $(PMe_3)_4Ru(OAc)(Cl)$ (302 mg, 0.605 mmol) in 10 mL of ether was added at room temperature, 16 mg of $LiAlD_4$ (0.60 equiv) as a solid. The suspension was stirred for 1 h after which time the initial pale yellow solution became clear; a white solid precipitate was also observed. The solvent was removed under reduced pressure, and the resulting white solid was extracted 3 times with a total of 25 mL of pentane. The pentane solution was concentrated to 1-2 mL and cooled to -40 °C to provide 79.1 mg (32%) of 6-d_2 which was pure by ^1H and $^{31}P\{^1H\}$ NMR spectroscopy. ^2H NMR δ-9.75 (m); $^{31}P\{^1H\}$ NMR δ-0.19 (tm, J=26.2 Hz, 2P), δ-8.07(tt, 26.2, 5.8, 2P); IR (KBr) 1309 cm^{-1} (Ru-D).

H/D exchange reactions:

Addition of N,N-d_2-Aniline to $(PMe_3)_4Ru(CH_2PMe_2)(H)$ (4). To a solution of 4 (15.6 mg) in 0.7 mL of C_6H_6 was added 68 µL (20 equiv) of N,N-d_2-aniline. After 1 h, the solution was transferred to an NMR tube. ^2H NMR spectroscopy showed that complete exchange had occurred. A ratio of the deuteride resonance of 4 to the N-D resonance of aniline was roughly 1:40.

Addition of N,N-d_2-Aniline to $(PMe_3)_4Ru(H)_2$ (6). A solution of 21 mg of $(PMe_3)_4Ru(H)_2$ (6) in 0.6 mL of C_6H_6 was added to 96 mg (20 equiv) of N,N-d_2-aniline. The resulting solution was placed in an NMR tube, and ^2H NMR spectroscopy showed a resonance for the dideuteride (6-d_2), and for the N-D of aniline in a ratio of roughly 1:20. A similar procedure, except using C_6D_6 solvent was used for monitoring the reaction by ^1H NMR spectroscopy. After 1 h at room temperature, no hydride resonance was observed for starting material 6.

Addition of aniline to $(PMe_3)_4Ru(D)_2$ (6-d_2). A solution of 16.8 mg of $(PMe_3)_4Ru(D)_2$ (6-d_2) in 0.6 mL of C_6H_6 was added to 76 mg (20 equiv) of aniline. The resulting solution was placed in an NMR tube, and ^2H NMR spectroscopy after 6 h showed only a resonance for the N-D of aniline.

Addition of *p*-chloroaniline to $(PMe_3)_4Ru(D)_2$ (6-d_2). A solution of 15.2 mg of $(PMe_3)_4Ru(D)_2$ (6-d_2) in 0.6 mL of C_6H_6 was added to 95 mg (20 equiv) of *p*-chloroaniline. The resulting solution was placed into an NMR tube equipped with a rubber septum, and ^2H NMR spectroscopy after 30 min showed only a hydride resonance. After this time, 0.10 μL (0.15 equiv) of H_2O was added by syringe. The reaction was monitored at 5 min intervals by ^2H NMR spectroscopy and showed only an N-H resonance after 15 min.

Addition of wet diphenylamine to $(PMe_3)_4Ru(D)_2$ (6-d_2). A solution of 14.8 mg of $(PMe_3)_4Ru(D)_2$ (6-d_2) in 0.6 mL of C_6D_6 was added to 122 mg (20 equiv) of diphenylamine. The resulting solution was placed into an NMR tube, and ^1H NMR spectroscopy after 5 min showed that little exchange had occurred. After 20--30 min, ^1H NMR spectroscopy showed roughly 50% exchange as determined by integration of the hydride resonance in the ^1H NMR spectrum relative to the phosphine resonances. After 24 h at room temperature the C_6D_6 solvent was removed under reduced pressure and replaced with C_6H_6. The benzene solution was then placed into an NMR tube, and ^2H NMR spectroscopy showed only a resonance for the N-H proton of the amine.

Addition of dry diphenylamine to $(PMe_3)_4Ru(D)_2$ (6-d_2). To a solution of 10.2 mg of 6-d_2 in C_6H_6 was added 84.3 mg (20 equiv.) of dry diphenylamine. The reaction was monitored by ^2H NMR spectroscopy, and after 2 h at room temperature, no NH resonance was observed, indicating that exchange did not occur.

Addition of Cyclopentadiene to $(PMe_3)_4Ru(D)_2$ (6-d_2). A solution of 15.2 mg of $(PMe_3)_4Ru(D)_2$ (6-d_2) in 0.6 mL of C_6H_6 was added to 49 mg (20 equiv) of cyclopentadiene monomer. The resulting solution was placed in an NMR tube, and ^2H NMR spectroscopy after 6 h showed only the deuteride resonance of 6-d_2; no resonances were observed for the

cyclopentadiene. A similar procedure, except using C_6D_6 solvent was used for monitoring the reaction by ^1H NMR spectroscopy. After 6 h at room temperature, no hydride resonance was observed for starting material **6-d$_2$**.

Addition of *tert*-butylacetylene to (PMe$_3$)$_4$Ru(D)$_2$ (6-d$_5$). A solution of 15.2 mg of (PMe$_3$)$_4$Ru(D)$_2$ (**6-d$_2$**) in 0.6 mL of C_6H_6 was placed into an NMR tube. The sample was degassed by two freeze-pump-thaw cycles. To it was added 20 equiv of *tert*-butylacetylene by vacuum transfer. The resulting solution was placed into an NMR tube, and ^2H NMR spectroscopy after 6 h showed only the deuteride resonance of **6-d$_2$**; no propargyl C-D resonance was observed.

Addition of D$_2$ to (PMe$_3$)$_4$Ru(H)$_2$ (6) Into a Fischer-Porter bottle was placed a solution of 8.2 mg of **6** in 4 mL of C_6H_6. The solution was exposed to 19 atm of H_2 (*ca.* 2000 equiv) for 24 h. After this time the solution was concentrated to 0.6 mL and placed into an NMR tube for analysis by ^2H NMR spectroscopy. Only a resonance for the deuteride position of **6** was observed. The solvent was then removed under reduced pressure and replaced with C_6D_6 for ^1H NMR spectroscopic analysis. A hydride resonance for **6** was observed in addition to the two phosphine signals.

Addition of PMe$_3$-d$_9$ to 6-d$_2$. A solution of 8.8 mg of **6-d$_2$** in C_6D_6 was placed into an NMR tube equipped with a Kontes vacuum adaptor. The sample was degassed by two freeze-pump-thaw cycles, and to the sample was added 4 equivalents of PMe$_3$-d$_9$. The $^{31}P\{^1H\}$ NMR spectra obtained after 1 h and 24 h showed only resonances for **6-d$_2$** and PMe$_3$-d$_9$. No free PMe$_3$-d$_0$ was observed.

Addition of *p*-cresol to 1. To a solution of 6.4 mg of anilide hydride **1** in 0.6 mL of C_6D_6 was added 4 mg of *p*-cresol. The solution was placed into an NMR tube and ^1H NMR spectroscopy showed the presence of only one equivalent of free aniline, two equivalents of *p*-cresol, and one equivalent of cresolate hydride **2**.

CO Induced Reductive Elimination of aniline from $(PMe_3)_4Ru(H)(NHC_6H_5)$ (1). To a 9" NMR tube was added a solution of 10.2 mg (0.205 mmol) of 1 and 2 μL of mesitylene as an internal standard in 0.7 mL C_6D_6. A ^1H NMR spectrum of the initial solution was obtained. The NMR tube was then attached to a Kontes vacuum adaptor and the sample was degassed by two freeze, pump, thaw cycles. The tube was cooled in liquid nitrogen and exposed to 440 torr of CO. The tube was sealed at the level of the liquid nitrogen to provide a tube of 8.5" length. The sample was heated to 85 °C for 24 h, and ^1H NMR spectroscopy showed a 94% yield of aniline (identified by comparison to an authentic sample) and 79% yield of $(CO)_3Ru(PMe_3)_2$ (10) (identified by comparison to an independently prepared sample[27]), as determined by comparison to the initial solution.

CO Induced Reductive Elimination of *p*-cresol from $(PMe_3)_4Ru(H)(OC_6H_4$-p-Me) (2). To a 9" NMR tube was added a solution of 10.2 mg (0.205 mmol) of 2 and 2 μL of mesitylene as an internal standard in 0.7 mL C_6D_6. A ^1H NMR spectrum of was obtained on the initial solution. The NMR tube was then attached to a Kontes vacuum adaptor and the sample was degassed by two freeze, pump, thaw cycles. The tube was cooled in liquid nitrogen and was exposed to 440 torr of CO. The tube was sealed at the level of the liquid nitrogen to provide a tube of 8.5" length. The sample was heated to 85 °C for 24 h, and ^1H NMR spectroscopy showed 98% yield of *p*- cresol (identified by comparison to an authentic sample) and 89% yield of $(CO)_3Ru(PMe_3)_2$ (10) (identified by comparison to an indenpendently prepared sample[27]), as determined by comparison to the initial solution.

X-ray crystal structure determination of complexes 1,2 and 5.

(a) Mounting Procedure: Pale yellow, air-sensitive crystals of 1 were obtained by allowing a refluxing solution of 1 in hexanes to cool to room temperature. Clear, air sensitive crystals of 2 were obtained by slowly cooling a pentane solution of 2 to -40 °C. Clear, air sensitive crystals of 5 were obtained by cooling a toluene/pentane (1:100) solution to -40 °C. End fragments cleaved from some of these crystals were mounted in a viscous oil, and then placed in the X-ray beam.

The final cell parameters and specific data collection parameters for the data set for **1**,**2** and **5** are given in Table 1.

(b) Structure Determination: For **1**, 6540 raw intensity data were collected; for **2**, 7384 were collected, and for **5**, 1732 were collected. These data were converted to structure factor amplitudes and their esd's by correction for scan speed, background and Lorentz and polarization effects. Inspection of the azimuthal scan data showed a variation I_{min}/I_{max} = +/-1% for the average curve. No correction for absorption was applied for compounds **1** and **5**, but was applied for **2**. Inspection of the systematic absences indicated space group P1 for **1** and $P2_1/n$ for **2**, and Cmca for **5**. Removal of systematically absent and redundant data left 6540 unique data in the final data set for **1**, 6686 for **2** and 1608 for **5**.

Each structure was solved by Patterson methods and refined via standard least-squares and Fourier techniques. The final refinement for **1** and **5** included anisotropic refinement of the ruthenium and phosphorus atoms and isotropic refinement of the carbon and nitrogen atoms. Hydrogen atoms were not included in the refinement. The final refinement for **2** included isotropic refinement of all non-hydrogen atoms.

The final residuals for the 243 variables for **1** were refined against the 4632 accepted data for which $F^2 > 3\sigma(F^2)$ were R = 8.0%, wR = 10.8% and GOF = 4.19. The R value for all 6540 accepted data was 10.6%. The final residuals for the 451 variables for **2** were refined against the 4589 accepted data for **2** for which $F^2 > 3\sigma(F^2)$ were R = 4.1%, wR = 6.3% and GOF = 2.76. The R value for all 6686 accepted data was 10.7%. The final residuals for the 71 variables for **5** were refined against the 1094 accepted data for **5** for which $F^2 > 3\sigma(F^2)$ were R = 5.1%, wR = 6.7% and GOF = 2.47. The R value for all 1608 accepted data was 10.7%.

The positional parameters, thermal parameters of the non-hydrogen atoms, and anisotropic thermal parameters for compounds **1**, **2**, and **5** are available as supplementary material.

1. Collman, J.P.; Hegedus, L.S.; Norton, J.R.; Finke, R.G. *Principles and Applications of Organotransition Metal Chemistry*, University Science Books: Mill Valley, 1987, chapter 5.

2. Newman, L.J.; Bergman, R.G. *J. Am. Chem. Soc.* 1985, *107*, 5314.

3. (a) Fornies, T.; Green, M.; Spencer, J.L.; Stone, F.G.A. *J. Chem. Soc., Dalton Trans.* 1977, 1006. (b) Cowan, R.L.; Trogler, W.C. *J. Am. Chem. Soc.* 1989, *111*, 475.

4. Brugo, C.D.; Pasquali, M.; Leoni, P.; Subatino, P.; Braga, D. *Inorg. Chem.* 1909, *28*, 1390.

5 Milstein, D.; Calabrese, J.C.; Williams, I.D. *J. Am. Chem. Soc.* 1986, *108*, 6387.

6. (a) Hillhouse, G.L.; Bercaw, J.E. *Organometallics*, 1982, *1*, 1025. (b) Wolczanski, P.T.; Bercaw, J.E. *Acc. Chem. Res.* 1980, *13*, 121.

7 Fagan, P.J.; Moloy, K.G.; Marks, T.J. *J. Am. Chem. Soc.* 1981, *103*, 6959.

8. Bryndza, H.E.; Tam, W. *Chem. Rev.* 1988, *88*, 1163, and references therin.

9. Casalnuovo, A.L.; Calabrese, J.C.; Milstein, D. *J. Am. Chem. Soc.* 1988, *110*, 6738.

10. Examples with osmium cluster compounds include (a) Bryan, E.G.; Johnson, B.F.G.; Lewis, J. *J. Chem. Soc , Dalton Trans.* 1977, 1328. (b) Susa-Fink, G. *Z. Naturforsch., B: Anorg. Chem., Org. Chem.* 1980, *35B*, 454. (c) Johnson, B.F.G.; Lewis, J.; Odiaka, T.I.; Raithby, P.R.; *J. Organomet. Chem.* 1981, C56. Examples with Ir(I) include (d) Park, S.; Hedden, D.; Roundhill, D.M. *Organometallics*, 1986, *5*, 2151. (e) Casalnuovo, A.L.; Calabrese, J.C.; Milstein, D. *Inorg. Chem.* 1987, *26*, 973. Examples with activated NH bonds include (f) Roundhill, D.M. *Inorg. Chem.* 1970, *9*, 254. (g) reference 3a. (h) Hedden, D.; Roundhill, D.M.; Fultz, W.C.; Rheingold, A.L. *J. Am. Chem. Soc.* 1984, *106*, 5014. (i) Schaad, D.R.; Landis, C.R. *J. Am. Chem. Soc.* 1990, *112*, 1628.

11. Glueck, D.S.; Newman, L.J.; Bergman, R.G. submitted for publication.

12. Yamamoto, T.; Sano, K.; Yamamoto, A. *Chem. Lett.* 1982,907.

13. Chapter 1.

14. Wong, W-K.; Chiu, K.W.; Statler, J.A.; Wilkinson, G.; Motavelli, M.; Hursthouse, M.B. *Polyhedron* **1984**, *3*, 1255.

15. Werner, H.; Werner, R. *J. Organomet. Chem.* **1981**, *209*, C60.

16. Cotton, F.A.; Wilkinson, G. *Advanced Inorganic Chemistry, 4thed.*, John Wiley and Sons: New York, 1980, p 82.

17. A trans influence series is given in: Appleton, T.G.; Clark, H.C.; Manger, L.E. *Coord. Chem. Rev.* **1973**, *10*, 335. Discussion of correlations between trans influence and ^{31}P chemical shifts is found in: a) J.F. Nixon, A. Pidcock, *Ann. Rev. NMR Spectroscopy* **1969**, *2*, 345. b) J.M. Verkade, L.D. Quin, eds., *Phosphorus-31 NMR Spectroscopy in Stereochemical Analysis*; VCH Publishers: New York, 1987.

18. Manojlovic-Muir, L.J.; Muir, K.W.; Solomon, T. *J. Organomet. Chem.* **1977**, *142*, 265.

19. Manojlovic-Muir, L.J.; Muir, K.W. *Inorganica Chimica Acta* **1974**, *10*, 47.

20. Badley, E.M.; Chatt, J.; Richards, R.L.; Sim, G.A. *J. Chem. Soc., Chem. Comm.* **1969**, 1322. Badley, E.M. *D. Phil. Thesis,* University of Sussex, 1969.

21. Statler, J.A.; Wilkinson, G.; Thornton-Pett, M.; Hursthouse, M.B. *J. Chem. Soc., Dalton Trans.* **1984**, 1731.

22. Streitweiser, A., Jr.; Nebenzahl, L.L. *J. Am. Chem. Soc.* **1976**, *98*, 2188.

23. Streitweiser, A. Jr.; Reuben, D.M.E. *J. Am. Chem. Soc.* **1971**, *93*, 1794.

24 Burn, M.J.; Andersen, R.A.; Bergman, R.A. unpublished results.

25. See for example: (a) Morris, R.H.; Sawyer, J.F.; Shiralian, M.; Zubkowski, J.D. *J. Am. Chem. Soc.* **1985**, *107*, 5581. (b) Bautista, M.; Kelly, A.E.; Morris, R.H.; Sella, A. *J. Am. Chem. Soc.* **1987**, *109*, 3780. (c) Crabtree, R.H.; Hamilton, D.G. *J. Am. Chem. Soc.* **1986**, *108*, 3124

26 Burgess, J. *Metal Ions in Solution*; Horwood-Wiley: New York, 1978.

27. In a recent study, heating the compound $(DMPE)_2Ru(naphthyl)(H)$ in the presence of aniline was reported to yield no reaction (ref. 10i), although previous studies with this ruthenium compound implied addition of the aniline aromatic C-H bonds occurs.

28. (a) Hartwig, J.F.; Andersen, R.A.; Bergman, R.G *J. Am. Chem. Soc.* **1989**, *111*, 2717. (b) Chapter 3.

29. Burn, M.J.; Hartwig, J.F.; Andersen, R.A.; Bergman, R.G. *unpublished results.*

30. Baker, M.V.; Field, L.D.; Young, D.J.; *J. Chem. Soc., Chem. Commun.* **1988**, 546.

31. Bond dissociation energies are taken from McMillen, D.F.; Golden, D.M. *Ann. Rev. Phys. Chem.* **1982**, *33*, 493.

32. Chapter 7.

33. Bergman, R.G.; Buchanan, J.M.; McGhee, W.D.; Periana, R.A.; Seidler, P.F.; Trost, M.K.; Wenzel, T.T. In *Experimental Organometallic Chemistry: A Practicum in Synthesis and Characterization*; Wayda, A.L.; Darensbourg, M.Y., Eds.; ACS Symposium Series 357; American Chemical Society: Washington, DC, 1987, p 227.

34. Mainz, V.V.; Andersen, R.A. *Organometallics* **1984**, *3*, 675.

Chapter 7

Hydrogenolysis of Ruthenium-Heteroatom Bonds: Evidence for an Autocatalytic Metal-Oxygen Bond Cleavage Mechanism

Introduction.

The addition of dihydrogen to transition-metal alkyl complexes has been extensively studied[1] because it is involved in homogeneous and heterogeneous catalytic processes such as hydrogenation of alkenes, termination of ethylene polymerization, and hydroformylation.[2] In contrast, studies involving the reaction of H_2 with transition metal-oxygen and -nitrogen bonds are rare,[3] and little mechanistic information is available on this process, even though it has been proposed as a primary step in several catalytic processes.[2,4] We report the reaction of dihydrogen with ruthenium-cresolate and -anilide complexes *cis*-$(PMe_3)_4Ru(H)(XAr)$, (1: X=NH, Ar=*Ph*; 2: X=O, Ar=*p*-tol) to form aniline and *p*-cresol, respectively, along with the ruthenium dihydride *cis*-$(PMe_3)_4Ru(H)_2$ (3). Mechanistic studies have revealed that reaction of the cresolate occurs by an autocatalytic mechanism in which a product, p-cresol, catalyzes dissociation of the cresolate ligand, while hydrogenolysis of the anilide complex appears to occur predominantly by initial loss of phosphine rather than aniline or anilide ion.

Results and Discussion.

The ruthenium hydrido anilide (1) and cresolate (2) complexes were prepared by the route shown in Scheme 1.[5] Treatment of compound 1 with 2 atm of dihydrogen led to formation of $(PMe_3)_4Ru(H)_2$ (3) and free aniline, both in quantitative yield by ^1H NMR spectroscopy. Analysis of the reaction of H_2 with 2 was not as straightforward. The $^{31}P\{^1H\}$ NMR spectrum of the product mixture at room temperature was identical to that of dihydride 3, and the trimethylphosphine groups in the ^1H NMR spectrum of the product resonated at the same chemical shift as those of dihydride 3. However, the hydride signal was broad at room temperature. Variable temperature NMR analysis of the reaction mixture revealed the occurrence of exchange processes (Figure 1) which were identical to those observed for a solution of independently prepared dihydride containing one equivalent of *p*-cresol and 2 atm of dihydrogen (Figure 2). In addition, the temperature dependent behavior of the $^{31}P\{^1H\}$ NMR spectra for the hydrogenation reaction and independently prepared sample of 3 and *p*-cresol were identical as shown in Figures 3 and 4. We therefore conclude that the overall reaction proceeds analogously

Scheme 1

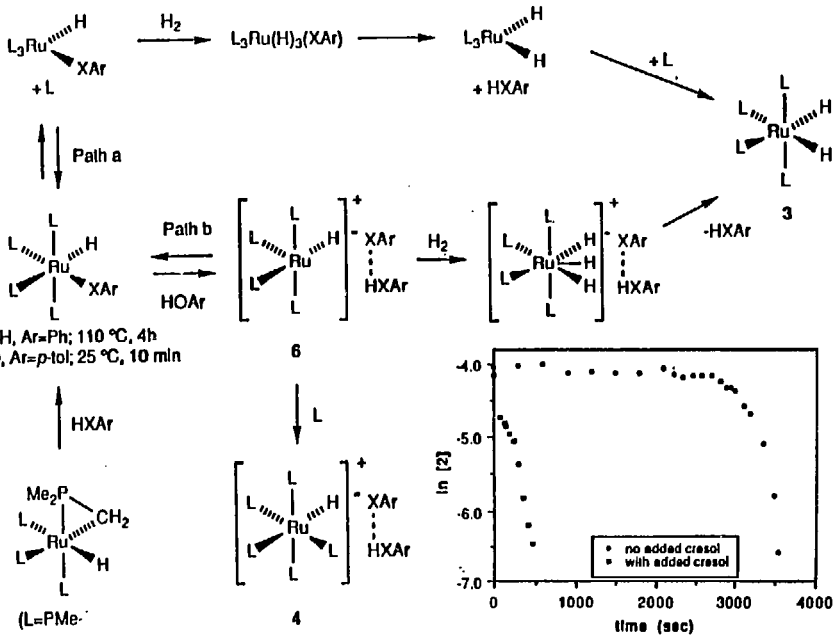
$L_3Ru(H)_3(XAr)$
+ HXAr
+L
-HXAr
3
Path a
Path b
HOAr
H_2
XAr
HXAr
6
4
HXAr
L
1: X=NH, Ar=Ph; 110 °C, 4h
2: X=O, Ar=p-tol; 25 °C, 10 min
Me_2P
CH_2
(L=PMe
ln [2]
time (sec)
no added cresol
with added cresol

to the hydrogenolysis of **1**, and the mixture of dihydride **3** and p-cresol undergoes an interaction in which hydrogen atoms are rapidly exchanged between the phenol and ruthenium center. The lack of significant chemical shift changes relative to those of pure dihydride **3** indicate that this is the predominant species in the mixture. No temperature dependent behavior of mixtures containing dihydride **3** with H_2 alone was observed between 30 °C and -90 °C.

Careful monitoring of the reaction between dihydrogen and cresolate **2** demonstrated that the rate reproducibly *increased* with time, as shown in Scheme 1 for an experiment at 28 °C. Suspecting that this behavior was due to autocatalysis, we repeated the reaction with small quantities (<1 equiv) of *p-cresol added to samples of* **2**. *Addition of* H_2 *in this case led to* complete reaction in less than 5 min (data also illustrated in Scheme 1). Similar experiments carried out with dihydride **3** (but no p-cresol) added initially to the hydrogenolysis mixture provided no such acceleration. We therefore conclude that the organic product *p*-cresol catalyzes the hydrogenolysis.

Addition of labelled and unlabeled phosphine provided further mechanistic information. Treatment of cresolate **2** with PMe_3-dg showed that the rate of phosphine exchange was significantly slower than hydrogenolysis; only small amounts (<5%) of labelled phosphine were incorporated into **2** after the 2 h necessary for complete reaction with hydrogen. In the absence of *p*-cresol, adding PMe_3 to the reaction solution inhibited the rate of disappearance of starting material. In the presence of added PMe_3 and *p*-cresol, all of the starting material again reacted within 5 *min*. However, under these conditions the added phosphine diverted the course of reaction from hydrogenolysis product **3** to the formation of a new material. This compound was identified as the salt **4** (see Scheme 1) on the basis of spectroscopic features similar to those of the salt $[(PMe_3)_5Ru(H)]PF_6$ (**5**). The $^{31}P\{^1H\}$ NMR spectrum of **4** in C_6D_6 displayed a PMe_3 region identical to that of **5** in CD_2Cl_2 solvent[6] (all resonances identical to within ±0.05 ppm). Because of the insolubility of **5** in C_6D_6, ^1H NMR spectra (and $^{31}P\{^1H\}$ NMR spectra) were compared by

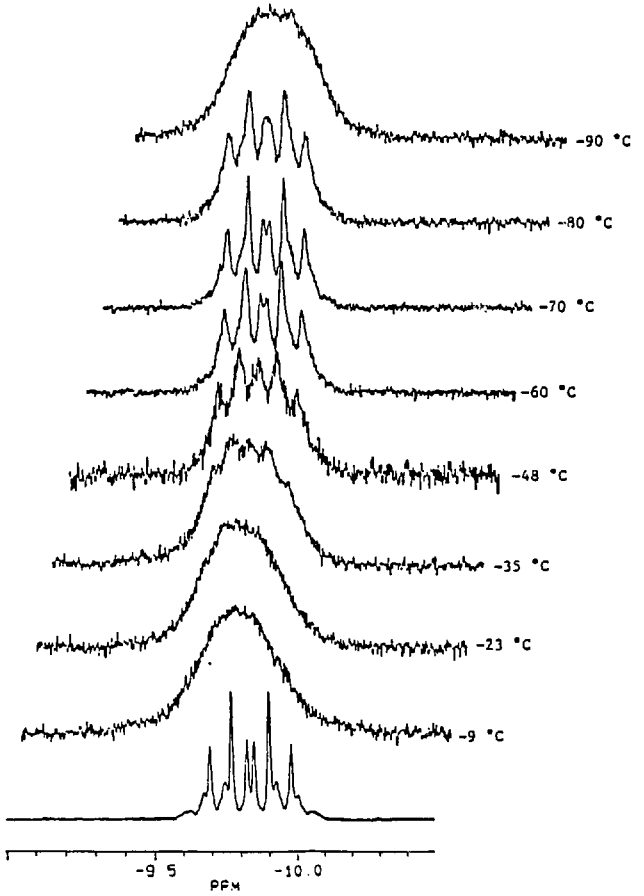

Figure 1. Variable temperature ^1H NMR spectra for the solution resulting from the addition of hydrogen to **1**.

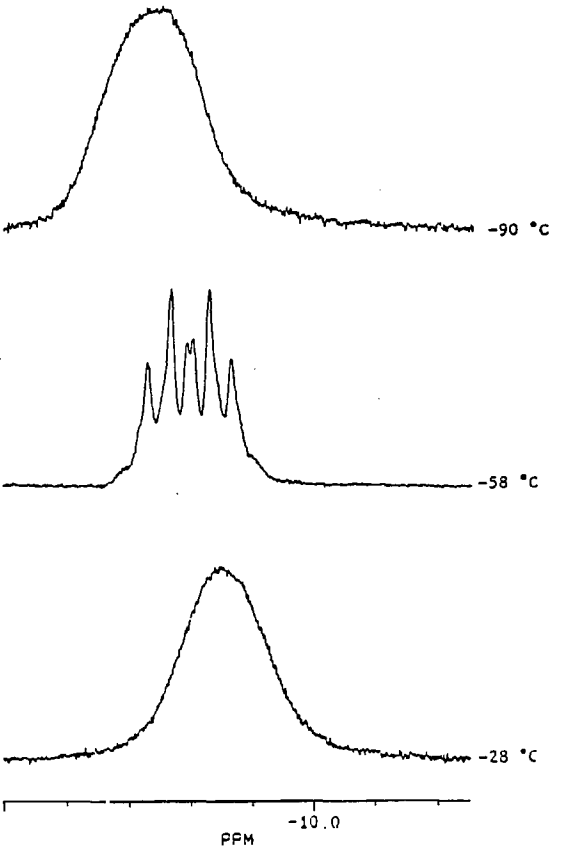

Figure 2. Variable temperature ^{1}H NMR spectra for dihydride **3** and one equiv of *p*-cresol at concentrations similar to those resulting from hydrogenolysis of **1**.

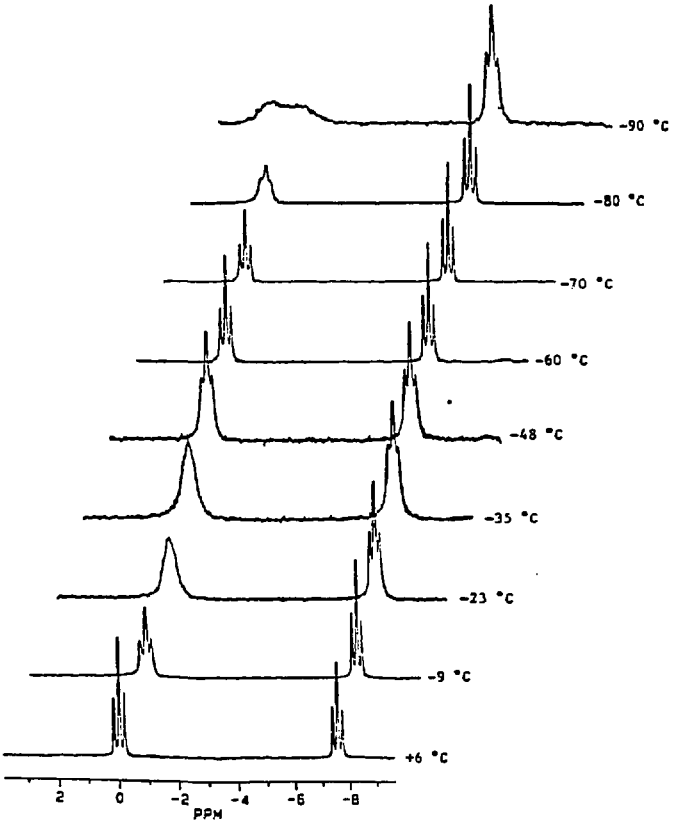

Figure 3 Variable temperature $^{31}P\{^{1}H\}$ NMR spectra for the solution resulting from the addition of hydrogen to **1**.

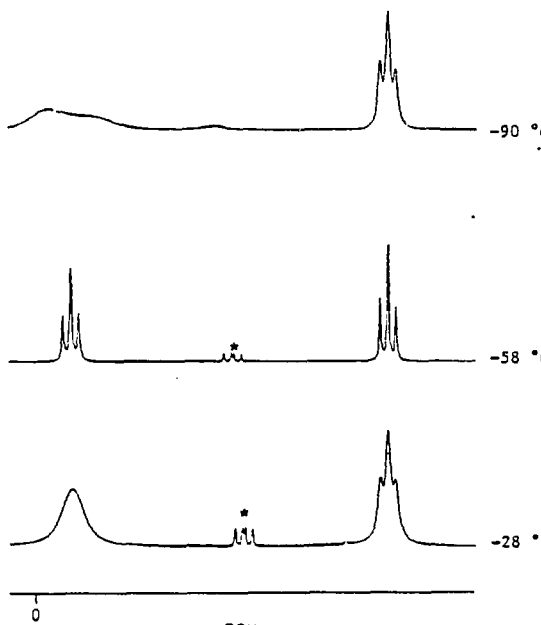

Figure 4. Variable temperature $^{31}P\{^1H\}$ NMR spectra for dihydride **3** and one equiv of *p*-cresol at concentrations similar to those resulting from hydrogenolysis of **1**. The resonance marked with an asterisk corresponds to $(PMe_3)_4Ru(H)(Cl)$ impurity.

generating complex **4** in CD_2Cl_2 by the addition of one equiv of *p*-cresol and four equiv of PMe_3 to **2** in the absence of hydrogen. A ^1H NMR spectrum identical (±0.02 ppm) to that of **5** was observed. Compound **4** was also prepared by the addition of potassium cresolate and cresol to the PF_6 salt **5** in a CD_2Cl_2/THF-d_8 solvent system.

Two possible mechanisms for these hydrogenolysis reactions, one involving a conventional phosphine dissociation and H_2 oxidative addition pathway,[1c] and the other proceeding by proton catalysis, are shown in Scheme 1. Our data demonstrate that the hydrogenolysis of **2** proceeds principally by mechanism b. The autocatalytic kinetic behavior and the dramatic rate increase upon deliberate addition of *p*-cresol demonstrates that the reaction of this molecule with dihydrogen is catalyzed by the phenol. In addition, diversion of the product to cationic species **4** when the reaction is run in the presence of added phosphine provides strong evidence for intermediate **6**.

It is not yet clear how the small amounts of p-cresol needed to catalyze the hydrogenolysis of **2** are formed during the induction period observed for this reaction. However, inhibition of the disappearance of starting material in the presence of added PMe_3 (but no added *p*-cresol), supports generation of a small amount of *p*-cresol by path a, which operates slowly in this case as indicated by the slow rate of phosphine exchange for this system; only catalytic quantities of *p*-cresol are required to make the process proceed at a significant rate.

The weaker acidity of aniline would lead one to expect that autocatalytic pathway b is less likely to operate in the hydrogenolysis of anilide **1**. In fact, addition of aniline to this reaction led to only mild rate increases (2-3 times faster), and first order plots displayed increasing values for k_{obs} during only the third half-life of this reaction. Preliminary phosphine inhibition experiments are consistent with hydrogenation of **1** by path a during the first two half-lives, though we are concerned that trace amounts of a hydrogen-bonding species such as water may catalyze the hydrogenation of **1**.

It is ironic that the reaction of metal-carbon bonds with H_2 has also been shown to be autocatalytic in certain cases,[7] but in such systems the compound responsible for autocatalysis is

the metal hydride rather than the organic product of the hydrogenolysis reaction. The results reported here emphasize that the polarity of metal-heteroatom bonds can make accessible a range of mechanisms for M-X bond cleavage substantially wider than those available to reactions in which M-C and M-H bonds are broken. We believe that future mechanistic investigations will show that reactions of such systems are especially susceptible to catalysis by weak acids such as alcohols and water.

Table 1. ^{1}H NMR spectroscopic data.

	δ (ppm)	multiplicity[a]	J (Hz)	int	assignment[b]
$(PMe_3)_4Ru(H)(NHC_6H_5)$ (1)[a]	6.43	t	6.8	1	Aromatic
	6.59	d	8.0	1	
	7.20	t	7.5	1	
	7.35	m		2	
	1.71	d	7.3	1	NH
	1.81	t	2.6	18	*trans*-PMe_3
	1.03	d	6.8	9	*cis* -PMe_3
	0.96	d	4.9	9	
	-7.69	dq	99, 26	1	Ru-H
$(PMe_3)_4Ru(H)(OC_6H_4$-*p*-Me) (2)[a]	7.18	d	8.6	2	Aromatic
	7.14		8.5	2	
	2.37	s		3	*p*-Me
	1.18	t	2.8	18	*trans*-PMe_3
	1.14	d	5.5	9	*cis*-PMe_3
	0.98	d	7.5	9	
	-7.65	dq	102, 27	1	Ru-H
[$(PMe_3)_5Ru(H)$]	8.69	br s		1	OH
[OC_6H_4-*p*-Me·HOC_6H_4-*p*-Me] (4)[b]	6.80	d	8.0	4	Aromatic
	6.63	d	8.1	4	Aromatic
	2.16	s		6	*p*-Me
	1.52	br s		36	PMe_3
	1.36	d	5.7	9	PMe_3
	-11.42	d quint	74, 25	1	Ru-H
{$(PMe_3)_5Ru(H)$][PF_6] (5)[b]	1.54	br s		36	PMe_3
	1.38	d	5.6	9	PMe_3
	-11.39	d quint	73, 24	1	Ru-H

[a]The multiplicities d and t refer to apparent splitting patterns. Accordingly the values reported for J do not necessarily reflect true coupling constants. [b]The assignment *trans*-PMe_3 refers to the two mutually trans PMe_3 ligands. The other two PMe_3 groups are assigned as *cis*-PMe_3. [c]C_6D_6, 21 °C. [d]CD_2Cl_2, 21 °C.

Table 2. $^{13}C\{^1H\}$ NMR spectroscopic Data.

	δ (ppm)	mult[a]	J (Hz)	assignment[b]
$(PMe_3)_4Ru(H)(NHC_6H_5)$ (1)[c]	21.52	dm	14.2	*cis*-PMe_3
	27.44	dm	24.1	
	23.27	td	12.9, 4.0	*trans*-PMe_3
	107.39	s		Aromatic
	114.64	s		
	117.78	d	4.1	
	128.91	s		
	129.45	s		
	161.83	t	3.2	
$(PMe_3)_4Ru(H)(OC_6H_4$-p-Me) (2)[c]	20.55	d	15.4	*cis*-PMe_3
	27.22	d	23.4	
	22.89	td	12.8, 3.8	*trans*-PMe_3
	20.93	s		*p*-Me
	118.26	s		Aromatic
	120.34	s		
	129.77	s		
	169.13	d	4.5	
$[(PMe_3)_5Ru(H)][PF_6]$ (5)[d]	26.66	m		PMe_3
	26.04	d quint	19.8, 2.0	PMe_3

[a]The multiplicities d and t refer to apparent splitting patterns. Accordingly the values reported for J do not necessarily reflect true coupling constants. [b]The assignment *trans*-PMe_3 refers to the two mutually trans PMe_3 ligands. The other two PMe_3 groups are assigned as *cis*-PMe_3. [c]C_6D_6, 21 °C. [d]CD_2Cl_2, 21 °C.

Table 3. $^{31}P\{^1H\}$ NMR spectroscopic data.

	spin system	δ(ppm)	J(Hz)
$(PMe_3)_4Ru(H)(NHC_6H_5)$ (1)[a]	A_2BC	δ_A=-0.98	J_{AB}=26.4
		δ_B=-14.55	J_{AC}=30.8
		δ_C=5.14	J_{BC}=19.0
$(PMe_3)_4Ru(H)(OC_6H_4$-p-Me) (2)[a]	A_2BC	δ_A=1.54	J_{AB}=32.5
		δ_B=14.92	J_{AC}=27.1
		δ_C=-12.62	J_{BC}=15.9
$[(PMe_3)_5Ru(H)]$ $[OC_6H_4$-*p*-Me·HOC_6H_4-*p*-Me] (4)[b]	A_4B	δ_A=-9.47	J_{AB}=26.1
		δ_B=-22.85	
$[(PMe_3)_5Ru(H)][PF_6]$[b]	A_4BMX_6 ($X=^{19}F$)	δ_A=-9.52	J_{AB}=26.3
		δ_B=-22.92	J_{AM}=0
		δ_M=143.85	J_{BM}=0
			J_{AX}=0
			J_{BX}=0
			J_{MX}=710

[a]C_6D_6, 21 °C. [b]CD_2Cl_2, 21 °C.

Experimental

General. Unless otherwise noted, all manipulations were carried out under an inert atmosphere in a Vacuum Atmospheres 553-2 drybox with attached M6-40-1H Dritrain, or by using standard Schlenk or vacuum line techniques.

^1H NMR spectra were obtained on either the 250, 300, 400 or 500 MHz Fourier Transform spectrometers at the University of California, Berkeley (UCB) NMR facility. The 250 and 300 MHz instruments were constructed by Mr. Rudi Nunlist and interfaced with either a Nicolet 1180 or 1280 computer. The 400 and 500 MHz instruments were commercial Bruker AM series spectrometers. ^1H NMR spectra were recorded relative to residual protiated solvent. ^{13}C NMR spectra were obtained at either 75.4 or 100.6 MHz on the 300 or 500 MHz instruments, respectively, and chemical shifts were recorded relative to the solvent resonance. Chemical shifts are reported in units of parts per million downfield from tetramethylsilane and all coupling constants are reported in Hz. $^{31}P\{^1H\}$ NMR spectra were recorded at 76.4 MHz on the 300 MHz instrument, and chemical shifts were recorded relative to H_3PO_4. ^{19}F NMR spectra were recorded at 376.498 MHz in the 400 MHz instrument and chemical shifts were recorded relative to $CFCl_3$.

IR spectra were obtained on a Nicolet 510 spectrometer equipped with a Nicolet 620 processor using potassium bromide ground pellets. Elemental analyses were obtained from the UCB Microanalytical Laboratory.

To prepare sealed NMR tubes, the sample tube was attached via Cajon adapters directly to Kontes vacuum stopcocks.[8] Known volume bulb vacuum transfers were accomplished with an MKS Baratron attached to a high vacuum line.

Unless otherwise specified, all reagents were purchased from commercial suppliers and used without further purification. PMe_3 (Strem) was dried over NaK or a Na mirror and vacuum transferred prior to use. H_2 was purchased from Air Products and used as received. *p*-Cresol was dried by azeotroping with benzene using a Dean-Stark trap, followed by vacuum distillation. Aniline was dried over sodium and vacuum distilled. $(PMe_3)_4Ru(H)_2$(3) was prepared as described earlier[9] and $(PMe_3)_3Ru(CH_2PMe_2)(H)$ was prepared by literature methods.[6]

Pentane and hexane (UV grade, alkane free) were distilled from $LiAlH_4$ under nitrogen. Benzene and toluene were distilled from sodium benzophenone ketyl under nitrogen. Methylene chloride was distilled from CaH_2 under nitrogen. Ether and tetrahydrofuran were distilled from purple solutions of sodium/benzophenone ketyl. Deuterated solvents for use in NMR experiments were dried as their protiated analogues but were vacuum transferred from the drying agent.

Hydrogenolysis of 1. Into a thin-walled NMR tube was placed a solution containing between 2.5 and 6 mg (0.0050-0.012 mmol) of **1** in 0.6 mL of C_6D_6. The tube was equipped with a Kontes vacuum adaptor, degased by two freeze, pump, thaw cycles, treated with 450 torr of H_2 while submerged in liquid nitrogen, and sealed. This procedure provides a sample containing 2.2 atm of H_2 at 25 °C. The reaction was monitored by ^1H NMR spectroscopy while shaking with an overhead stir motor.

Kinetic Evaluation of Hydrogenolysis of 1. A stock solution was prepared containing 26.6 mg (0.0534 mmol) of **1** and 10 mg of mesitylene as an internal standard in 5.00 mL of C_6D_6 to provide a 0.011 M solution of **1**. Samples for kinetic analysis were prepared in 9" thin walled NMR tubes containing 0.5 mL of the stock solution. The solutions were degassed by two freeze, pump, thaw cycles. Before sealing, appropriate amounts of PMe_3 were added by vacuum transfer and the samples were exposed to 450 torr of H_2 while submerged in liquid nitrogen. The tubes were shaken with an overhead stir motor at room temperature (22 °C -24 °C), and the rates were measured by integrating the disappearance of the PMe_3 resonances relative to the internal standard. Linear first order plots were observed for the first two half-lives ($r^2 > 0.97$), but increasing values for k_{obs} were observed during the third half-life. A typical plot for the samples containing no PMe_3 is shown in Figure 5, and the values for k_{obs} and [PMe_3] are provided in Table 4.

Hydrogenolysis of 2. Into a thin-walled NMR tube was placed a solution containing between 5.4 and 5.6 mg (0.011 mmol) of **1** and 1 mg of mesitylene as an internal standard in 0.6 mL of C_6D_6. The tube was equipped with a Kontes vacuum adaptor, degased by two freeze,

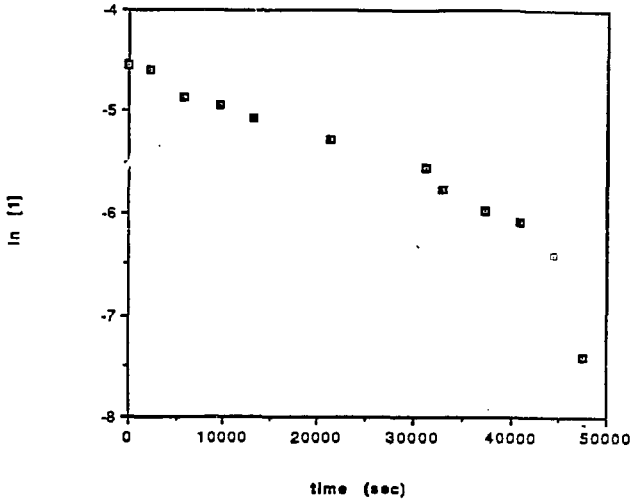

Figure 5. Typical first order plot for the reaction of 1 with hydrogen under conditions that were *pseudo first order in ruthenium complex.*

Table 4. Kinetic data for the hydrogenolysis of 1.

1/[L] ($mmol^{-1}$)	$k_{obs} \times 10^{-5}$ (sec^{-1})
411	1.9±0.3
262	1.1±0.2
222	0.93±0.14
85.7	0.66±0.10

pump, thaw cycles, treated with 450 torr of H_2 while submerged in liquid nitrogen, and sealed. This procedure provides a sample containing 2.2 atm of H_2 at 25 °C. The reaction was monitored by ^1H NMR spectroscopy either in the NMR spectrometer probe at 28°C, or while shaking with an overhead stir motor at room temperature and obtaining NMR spectra at 0.5 to 1.0 h intervals. A plot of ln[2] versus time for the reaction conducted in the spectrometer probe is shown in Scheme 1.

Hydrogenolysis of 2 in the presence of added *p*-cresol. Into a thin-walled NMR tube was placed a solution containing 5.6 mg (0.011 mmol) of 1 and 1 mg (0.01 mmol) of *p*-cresol in 0.6 mL of C_6D_6. The tube was equipped with a Kontes vacuum adaptor, degased by two freeze, pump, thaw cycles, treated with 450 torr of H_2 while submerged in liquid nitrogen, and sealed. This procedure provides a sample containing 2.2 atm of H_2 at 25 °C. The reaction was monitored by ^1H NMR spectroscopy in the NMR spectrometer probe at 22°C. A plot of ln[2] versus time is shown in Scheme 1.

Addition of *p*-cresol, H_2, and PMe_3 to 2 in C_6D_6. Into a thin-walled NMR tube was placed a solution containing 5.6 mg (0.011 mmol) of 2, 1.5 mg (0.014 mmol) of *p*-cresol in 0.6 mL of C_6D_6. The tube was equipped with a Kontes vacuum adaptor, degased by two freeze, pump, thaw cycles and, before sealing, 4 equiv of PMe_3, and 450 torr of H_2 were added to the sample while it was submerged in liquid nitrogen. A ^1H NMR spectrum obtained 5 min after warming to room temperature showed a spectrum containing cation 4, and after this time an oil was observed in the bottom of the sample. This oil was dissolved by opening the sample and adding 0.1 mL of CH_2Cl_2. $^{31}P\{^1H\}$ NMR spectrometry of the resulting sample showed cation 4 in a greater than 20:1 ratio with any other species.

Addition of *p*-cresol and PMe_3 to 2 in CD_2Cl_2. Into a thin-walled NMR tube was placed a solution containing 5.6 mg (0.011 mmol) of 2 and 1.5 mg (0.014 mg) of *p*-cresol in CD_2Cl_2. The tube was equipped with a Kontes vacuum adaptor, degased by two freeze, pump, thaw cycles and, before sealing, 4 equiv of PMe_3 was added by vacuum transfer. ^1H and $^{31}P\{^1H\}$

NMR spectra obtained 5 min after warming to room temperature showed a spectrum containing resonances for only cation 4.

Conversion of 5 to 4 and KPF_6. In one vial was prepared 0.1 mL of a CD_2Cl_2 solution containing 10.6 mg (0.0167) of 5. In another vial was prepared 0.5 mL of a solution containing 2.5 mg (0.0170 mg) of KOC_6H_4-*p*-Me and 2.1 mg (0.0194 mmol) of HOC_6H_4-*p*-Me in a 4:1 mixture of CD_2Cl_2 and THF-d_8. The two solutions were placed into an NMR tube and immediate formation of a white precipitate was observed. A ^1H NMR spectrum of the resulting solution showed a similar pattern to those for 4 and 5. A $^{31}P\{^1H\}$ NMR spectrum showed the appropriate A_4B pattern in the PMe_3 region, while no resonances were observed in the PF_6 region.

$[(PMe_3)_5Ru(H)][PF_6]$ (5) To a solution of 80.6 mg (0.198 mmol) of dihydride 3 in 3 mL of THF-d_8 was added 32.3 mg (1.0 equiv) of NH_4PF_6. Immediate formation of gas was observed. The sample was then placed into a glass reaction vessel fused to a Kontes vacuum adaptor, and 4 equiv of PMe_3 was added by vacuum transfer. Over the course of 8 h, 62.4 mg (50.3%) of pure 5 crystallized from the reaction solution as small white blocks. $^{19}F\{^1H\}$ (CD_2Cl_2, 21 °C, relative to $CFCl_3$) δ73.32 (d, J=712 Hz). IR(KBr) 1894 cm^{-1}(Ru-H).

Notes and References

1. See for example: (a) Mayer, J.M.; Bercaw, J.R.; *J. Am. Chem. Soc.* 1982, *104*, 2157. (b) Gell, K.I.; Schwartz, J.; Williams, G.M. *J. Am. Chem. Scc.* 1982, *104*, 1846. (c) Reamey, R.H.; Whitesides, G.M. *J. Am. Chem. Soc.* 1984, *106*, 81.
2. Parshall, G. *Homogeneous Catalysis*; Wiley-Interscience: New York, 1980
3. Cowan, R.L.; Trogler, W.C. *J. Am. Chem. Soc.* 1989, *111*, 4750.
4. Koenig, K.E. In *Asymmetric Synthesis*; Morrison, J.D., Ed.; Academic: New York, 1985; Vol 5, Chapter 3.
5. Chapter 6.

6. Werner, H.; Werner, R. *J. Organomet. Chem.* **1981**, *209*, C60. A ^{1}H NMR spectrum of this compound was reported. ^{1}H, $^{13}C\{^{1}H\}$, $^{31}P\{^{1}H\}$, $^{19}F\{^{1}H\}$ NMR, and infrared spectral data are provided as supplementary material.

7. Janowicz, A.H.; Bergman, R.G. *J. Am. Chem. Soc.* **1981**, *103*, 2488.

8. Bergman, R.G.; Buchanan, J.M.; McGhee, W.D.; Periana, R.A.; Seidler, P.F.; Trost, M.K.; Wenzel, T.T. In *Experimental Organometallic Chemistry: A Practicum in Synthesis and Characterization*; Wayda, A.L.; Darensbourg, M.Y., Eds.; ACS Symposium Series 357; American Chemical Society: Washington, DC, 1987, p 227.

9. Chapter 1.

Chapter 8

Oxygen- and Carbon-bound Ruthenium Enolates: Migratory Insertion, Reductive Elimination, β-Hydrogen Elimination, and Cyclometallation Reactions

Introduction

Until recently, the organometallic chemistry of late transition metal systems has focused on metal-carbon and -hydrogen bonds. Many routes to formation of metal alkyl, aryl, allyl, and hydride complexes have been investigated, and reactions such as β-hydrogen elimination, reductive elimination, and migratory insertion are well documented. The preparation and reactivity of compounds containing late transition metal-oxygen bonds is less common. It has been proposed that combining a hard ligand with soft late metal center may lead to weak late metal-heteroatom linkages and result in reactive late metal-heteroatom bonds.[1]

Several research groups have been interested in transition metal enolate complexes from the perspective of using the metal center as a potential site of asymmetry in the design of chiral catalysts for aldol reactions. Indeed, transition metal mediated aldol reactions have been observed,[2] and some systems undergo catalytic aldol reactions.[3] Transition metal-enolate complexes also provide a unique system for comparing the structure and reactivity of late metal-oxygen bonds to late metal-carbon bonds. Enolates have been shown to bind to metal centers in an η^1-mode through the oxygen atom[4] or methylene group,[5] or in an η^3-mode as an oxaallyl.[6] Typically, early transition metal enolates exist in the O-bound form, while late metal enolates are C-bound. Only a few cases of late transition metal O-bound enolates are known.[3, 4j, k]

During the course of our studies with the L_4Ru metal system ($L=PMe_3$) we discovered the propensity of enolate substituents to bind to the ruthenium center through the oxygen atom rather than the methylene.[7] Initial studies indicated that this unusual bonding mode gives rise to unprecedented reactivity, and we decided to investigate the synthesis and reactivity of a series of O-bound ruthenium enolates. We provide here a general method for the preparation of a series of O-bound ruthenium enolates and report their rich reactivity which includes processes such as reductive elimination, β-phenyl migration, β-hydrogen elimination, and cyclometallation to form oxametallacycles. Studies of the structure and reactivity of the resulting metallacycles is reported in the next chapter.[8]

Results.

Synthesis of O-bound Enolates. The general synthesis of the ruthenium enolate complexes is shown in equation 1. Addition of the potassium enolates of a variety of ketones and

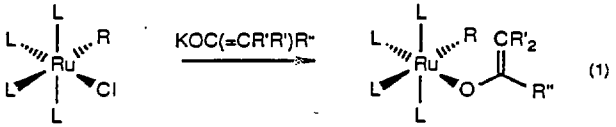

1 R=Ph
2 R=Me
3 R=H

4a R=Ph, R'=H, R"=Me
5a R=Me, R'=Me, R"=H
5b R=Me, R'=H, R"=H
5c R=Me, R'=H, R"=*tert*-Bu
6a R=H, R'=H, R"=Me

aldehydes at room temperature to ruthenium hydrido, alkyl, and aryl halide complexes led in most cases to the generation of O-bound enolates. Exceptions are the addition of the potassium enolate of acetone and 4,4-dimethyl-2-pentanone (methyl neopentyl ketone) to $(PMe_3)_4Ru(Me)(Cl)$ which provided equilibrium mixtures of both the O- and C-bound forms of enolates 8 and 9 (equation 2). The potassium counterion was important for these substitution

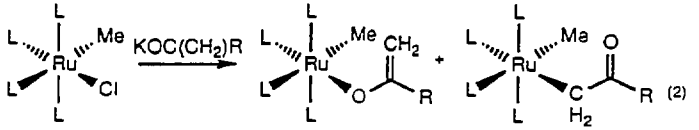

2

8a R=Me
9a R=CH_2CMe_3

8b R=Me
9b R=CH_2CMe_3

reactions. Addition of the lithium enolate of acetone to the ruthenium phenyl chloride (1) led to no reaction, even in THF solvent or with the addition of the appropriate crown ether. The potassium enolates were isolated as solids in the drybox, and they were stored for up to a week in a -40 °C freezer.

The compounds $(PMe_3)_4Ru(Me)(OC(CMe_2)Me)$ (5a) and $(PMe_3)_4Ru(H)(OC(CH_2)Me)$ (6a) were isolated in pure form and were characterized by microanalysis, as well as ^1H, $^{31}P\{^1H\}$, and $^{13}C\{^1H\}$ NMR and infrared spectroscopy. The orthometallated enolate 7 was prepared by addition of the potassium enolate of acetophenone to methyl chloride 2[9] as shown in Scheme 1 or by addition of acetophenone to the benzyne complex $(PMe_3)_4Ru(\eta^2\text{-}C_6H_4)$.[10] This enolate was characterized by X-ray diffraction, as well as microanalysis, ^1H, $^{31}P\{^1H\}$, and $^{13}C\{^1H\}$ NMR and infrared spectroscopy. The other O-bound ruthenium enolates in this study were not stable enough at room temperature to isolate, and so these were characterized by solution NMR spectroscopy.

NMR spectroscopic data for the compounds prepared in thise study are included in Tables 6-8. The ^1H NMR spectrum of all the O-bound enolates contained two inequivalent resonances between δ3.4 and δ4.2 for the olefinic hydrogens. In addition, the $^{13}C\{^1H\}$ NMR spectra contained CH_2 resonances (confirmed by DEPT pulse sequence) between δ73 and δ94. The $^{31}P\{^1H\}$ spectra of the hydrido, alkyl, and aryl ruthenium enolates all displayed A_2BC $^{31}P\{^1H\}$ NMR spectra with P_B resonating downfield and P_C resonating upfield of P_A. The $^{31}P\{^1H\}$ NMR chemical shift of each ligand reflects the trans influence of the ligand located trans to it.[11] For example, the chemical shifts for the phosphines trans to alkoxide,[12] amide,[9,13] halide, and pseudohalides[8,14] in this metal-ligand system lie substantially downfield from those of the mutually trans phosphines, and the chemical shifts of the phosphines trans to hydride,[9,15] alkyl[9,15] and aryl[15,16] substituents lie upfield of the mutually trans phosphines. Therefore $^{31}P\{^1H\}$ NMR spectroscopy is a useful indicator of the O- or C-bound form of these ruthenium enolates.

Scheme 1

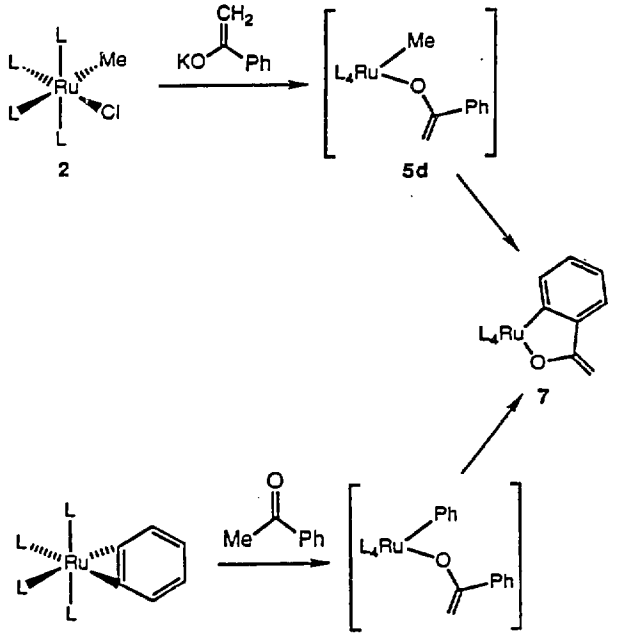

The solid state structure of 7 confirmed the assignments of these O-bound enolates by solution NMR spectroscopy, and it provides the first X-ray structural information on a late metal O-bound enolate. Compound 7 crystallized in space group P1 bar with no abnormally short intermolecular contacts. An ORTEP drawing of the molecule is shown in Figure 1; crystal and data collection parameters are included in Table 1 and intramolecular distances and angles are provided in Tables 2 and 3. The ruthenium atom in this complex is coordinated in an approximately octahedral fashion. The Ru-O distance is 2.120(1) Å, similar to a Ru-O distance in a monomeric cresolate complex (2.161(4) Å)[11] and in a monomeric phenyl hydroxide complex (2.145(4) Å)[12] of this metal-ligand system. The Ru-C bond length (2.100(1) Å) is similar to that observed in the analogous orthometallated benzyl (2.118(3) Å)[17] and benzyne complexes (2.072(2), 2.111(2) Å).[9] The η^1-aryl distance of $(PMe_3)_4Ru(Ph)(OH)$ (2.159(5) Å)[12] is slightly longer than those in the metallacycles. The surface defined by the organic ligand, P1 and P2 is planar to ±0.06 Å. Detailed analysis of the ligand geometry, however, shows that there is a slight twist (3.0 (9)°) of the C-C(O)CH_2 group around the C2-C7 bond. The two axial Ru-P bonds are the same length, but the phosphine trans to the oxygen is significantly shorter than the other three Ru-P distances, reflecting the usual trans influence series in these molecules and in others.[10]

The identity of the oxygen and CH_2 groups was based on the unequivocal location of the two hydrogens on C8 in the difference Fourier map, and is consistent with solution NMR data. The bond distances C7-O and C7-C8 indicate that some delocalization may be occurring. However, the distances in the phenyl group are most likely due to systematic effects of thermal motion, rather than to any peculiar electronic effects.

Synthesis of O- and C-Bound Enolates in Equilibrium. Two enolate complexes were obtained as an equilibrium mixture of their O- and C-bound forms. The addition of the potassium enolate of acetone to $(PMe_3)_4Ru(Me)(Cl)$[8] (2) in aromatic or ethereal solvents led to 8a and 8b (Equation 2). These two compounds were always observed in the same 3:1 ratio in C_6D_6 solvent at room temperature, suggesting that this is the equilibrium mixture. Indeed, the two isomers were shown to rapidly interconvert on the laboratory time scale (*vide infra.*). Therefore,

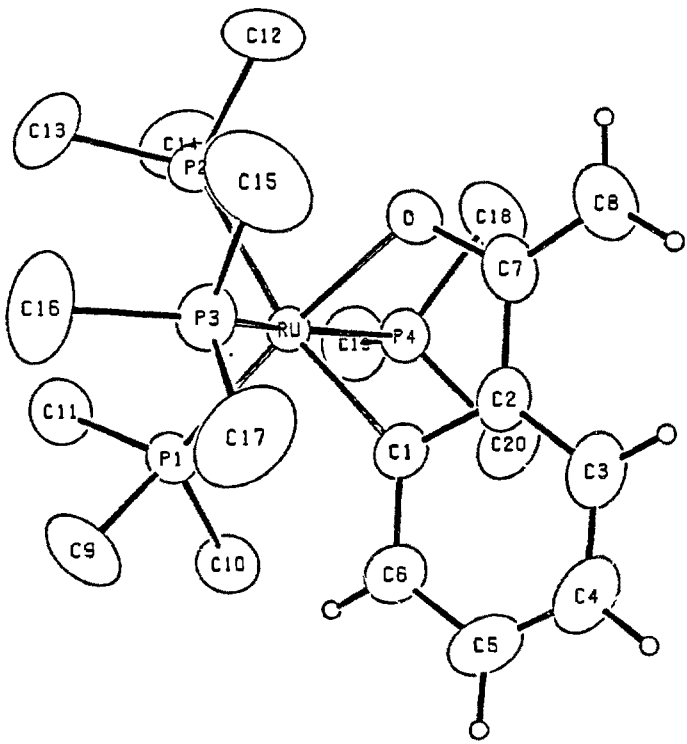

Figure 1 ORTEP drawing of 7. The hydrogen atoms of the PMe_3 ligands have been removed for clarity

Table 1. Crystal and Data Collection Parameters.[a]

	7	**10**
Temperature (°C)	25	-90
Empirical Formula	$RuP_4OC_{20}H_{42}$	$RuP_4OC_{25}H_{49}$
Formula Weight (amu)	523.5	559.7
Crystal Size (mm)	0.25x 0.28 x 0.30	0.25 x 0.30 x 0.50
Space Group	P1	$P2_1/n$
a (Å)	9.3452(9)	8.918(2)
b (Å)	9.7161(9)	37.441(9)
c (Å)	16.278(2)	9.304(9)
α (°)	97.511(10)	90.0
β (°)	117.000(8)	110.71(2)
γ (°)	90.576	90.0
V ($Å^3$)	2301.5(6)	2905.7(26)
Z	2	4
d_{calc} (gcm^{-3})	1.34	1.43
μ_{calc} (cm^{-1})	8.4	7.1
Reflections Measured	+h, ±k, ±l	+h, +k, ±l
Scan Width	$\Delta\theta = 0.55 + 0.35 \tan\theta$	$\Delta\theta = 0.60 + 0.35 \tan\theta$
Scan Speed (θ, °/m)	6.70	6.70
Setting Angles (2θ, °)[b]	26-30	22-26

(a) Parameters common to all structures: Radiation: Mo Kα (λ = 0.71073 Å), except for **1c** λ = 0.70930 Å. Monochromator: highly-oriented graphite (2θ = 12.2°). Detector: crystal scintillation counter, with PHA. 2θ Range: 3-->45°, except for **1c** 2-->45°. Scan Type: θ-2θ. Background: Measured over 0.25(Δθ) added to each end of the scan. Vertical Aperture = 3.0 mm. Horizontal Aperture = 2.0 + 1.0 tanθ mm. Intensity Standards: Measured every hour of x-ray exposure time. Orientation[c] reflections were checked after every 200 measurements. Crystal orientation was redetermined if any of the reflections were offset from their predicted positions by more than 0.1°. Reorientation was required twice for **1b** and **7a**, and once for **8**. (b) Unit cell parameters and their esd's were derived by a least-squares fit to the setting angles of the unresolved Mo Kα components of 24 reflections with the given 2θ range. In this and all subsequent tables the esd's of all parameters are given in parentheses, right-justified to the least significant digit(s) of the reported value.

Table 2. Intramolecular distances for 7

ATOM 1	ATOM 2	DISTANCE
RU	P1	2.275(1)
RU	P2	2.375(1)
RU	P3	2.357(1)
RU	P4	2.357(1)
RU	O	2.120(1)
RU	C1	2.100(1)
C7	C8	1.351(2)
C7	O	1.331(2)
C2	C7	1.478(2)
C1	C2	1.419(2)
C1	C6	1.400(2)
C2	C3	1.392(2)
C3	C4	1.376(3)
C4	C5	1.368(3)
C5	C6	1.391(2)
P1	C9	1.843(2)
P1	C10	1.836(2)
P1	C11	1.839(2)
P2	C12	1.813(2)
P2	C13	1.838(2)
P2	C14	1.835(2)
P3	C15	1.820(2)
P3	C16	1.822(2)
P3	C17	1.811(2)
P4	C18	1.829(2)
P4	C19	1.835(2)
P4	C20	1.823(2)

Table 3. Intramolecular Angles for 7

ATOM 1	ATOM 2	ATOM 3	ANGLE
P1	RU	P2	97.17(1)
P1	RU	P3	97.38(2)
P1	RU	P4	94.71(1)
P2	RU	P3	93.81(2)
P2	RU	P4	93.83(1)
P3	RU	P4	164.77(2)
P1	RU	O	174.59(3)
P2	RU	O	88.09(3)
P3	RU	O	83.47(3)
P4	RU	O	83.64(3)
P1	RU	C1	95.80(4)
P2	RU	C1	167.03(4)
P3	RU	C1	84.30(4)
P4	RU	C1	85.30(4)
O	RU	C1	78.95(5)
RU	C1	C2	112.88(11)
RU	C1	C6	130.91(12)
RU	O	C7	116.16(9)
C2	C1	C6	116.20(14)
C1	C2	C3	120.76(16)
C1	C2	C7	116.48(13)
C3	C2	C7	122.76(15)
C2	C3	C4	120.93(17)
C3	C4	C5	119.68(16)
C4	C5	C6	120.23(17)
C1	C6	C5	122.19(17)
C2	C7	C8	123.94(16)
C2	C7	O	115.39(13)
O	C7	C8	120.67(16)
RU	P1	C9	117.90(7)
RU	P1	C10	118.91(8)
RU	P1	C11	120.26(7)
C9	P1	C10	98.97(9)
C9	P1	C11	98.84(10)
C10	P1	C11	97.54(9)
RU	P2	C12	111.78(7)
RU	P2	C13	121.93(8)
RU	P2	C14	123.21(7)
C12	P2	C13	99.38(12)
C12	P2	C14	99.11(11)
C13	P2	C14	96.83(11)
RU	P3	C15	112.77(8)
RU	P3	C16	124.72(8)
RU	P3	C17	118.47(7)
C15	P3	C16	99.42(13)
C15	P3	C17	98.50(14)
C16	P3	C17	98.44(12)
RU	P4	C18	113.20(6)
RU	P4	C19	122.86(7)
RU	P4	C20	117.65(6)
C18	P4	C19	99.98(9)
C18	P4	C20	100.29(9)
C19	P4	C20	99.18(9)

they were characterized as a 3:1 mixture by solution NMR and infrared spectroscopy, as well as microanalysis. The O-bound isomer 8a displayed spectroscopic features analogous to those of the other O-bound enolates. Resonances for three phosphine methyl groups in a ratio of 2:1:1 were observed in the ^1H NMR spectrum, along with two olefinic hydrogens at δ3.50 and δ3.96 and an enolate methyl group at δ2.06. A metal bound methyl group resonated at δ0.40.

The C-bound isomer 8b exhibited three phosphine methyl groups in a 2:1:1 ratio and an enolate methyl group at δ2.00, along with a second metal bound methyl group at δ-0.26. The $^{13}C\{^1H\}$ NMR spectrum indicated the presence of a Ru-C bond in this compound. A CH_2 resonance in the $^{13}C\{^1H\}$ NMR spectrum was observed at δ22.83, clearly out of the range of methylene resonances for O-bound enolates. In addition, the resonance appeared as a multiplet which displayed coupling to several phosphorus atoms, indicating that this carbon atom is bound to the ruthenium center. The $^{31}P\{^1H\}$ NMR spectrum was also consistent with a mixture of O- and C-bound enolates. In addition to the typical $^{31}P\{^1H\}$ NMR spectrum for the O-bound enolate complexes, the $^{31}P\{^1H\}$ NMR spectrum of this mixture displayed an A_2BC pattern in which both P_B and P_C resonated significantly upfield of the phosphines located trans to O-bound enolates in this system. The chemical shift of these phosphines was closer to the region of PMe_3 ligands trans to simple L_4Ru alkyls.

Addition of the *tert*-butyl substituted analogue, $KOC(CH_2)CH_2CMe_3$, to $(PMe_3)_4Ru(Me)(Cl)$ (2) also led to formation of a mixture of O- and C-bound ruthenium enolates 9a and 9b. Two neopenyyl groups were observed in the ^1H and $^{13}C\{^1H\}$ NMR spectra, as well as two metal-bound methyl groups. The methylene resonances of the O-bound form were observed at δ3.05 and δ3.78 in the ^1H NMR spectrum, and at δ79.45 in the $^{13}C\{^1H\}$ NMR spectrum. The CH_2 portion of the C-bound enolate resonated as a multiplet at δ1.96 in the ^1H NMR spectrum and as a doublet of multiplets (J_{PC}=42.2 Hz) in the $^{13}C\{^1H\}$ NMR spectrum. The two patterns in the $^{31}P\{^1H\}$ NMR spectrum were nearly identical to those of the acetone enolates 8a and 8b.

In order to demonstrate that the ratio of these isomers resulted from rapid equilibration, it was necessary to obtain mixtures containing enhanced amounts of each isomer, and then show

that these both return to the equilibrium ratio. To do this in a simple way, a solution of these isomers was monitored by ^1H and $^{31}P\{^1H\}$ NMR spectroscopy at different temperatures. At 5 °C the observed ratio of 8a to 8b by ^1H NMR spectroscopy was 2.78, and at 60 °C it was 4.46. Both of these mixtures returned rapidly to a 3.50 ratio at 25 °C. At 5 °C equilibrium was established over the course of 10 to 15 min; non-equilibrium ratios were never observed above 40 °C, indicating that interconversion occurs rapidly on the laboratory time scale at these temperatures.

A plot of lnK versus 1/T for the equilibrium written in Scheme 2 is displayed in Figure 2, and indicates that ΔH (1.5±.2 kcal/mol) favors the C-bound form and ΔS (7.6±2.0) favors the O-bound form. The values for both of these parameters are small but significantly different from zero. The equilibrium ratios were reproducible to within 5-10%, and the slope of the lnK versus 1/T plot for the equilibrium indicated in Scheme 2 is clearly negative. Since the dominant form of this complex at room temperature is O-bound, the value of ΔS must be positive, although the absolute value is small. We did not perform this experiment with the *tert*-butyl substituted analogue 9, but we presume that the ratio of isomers observed with this compound at room temperature is also a result of facile equilibration.

A qualitative comparison of the rates of phosphine dissociation and approach to equilibrium was performed by adding 4 equiv of PMe_3-d_9 to a sample of the two isomers and monitoring the solution at 0 °C by $^{31}P\{^1H\}$ NMR spectroscopy. Over the course of 5-10 minutes, complete exchange of the free, labelled phosphine and unlabeled, coordinated phosphine was observed, as determined by observing a 1:1 ratio of free PMe_3-d_9 and free PMe_3-d_0. Thus, the rate of phosphine dissociation is faster than the interconversion of 8a and 8b.

Synthesis of an η^2-Enolate. A complex containing an oxaallyl (η^3-bound enolate) ligand is a possible intermediate in this exchange process. We set out to isolate an η^3-enolate bound to the $L_3Ru(R)$ metal center by using a large enolate substituent which would favor dissociation of phosphine. Indeed, addition of the potassium enolate of 3,3,5,5-tetramethylcyclohexanone to the phenyl chloride 1 led to formation of a 1:1.4 ratio of a compound containing 4 phosphines to which we assign the simple O-bound structure shown in Scheme 3,

Scheme 2

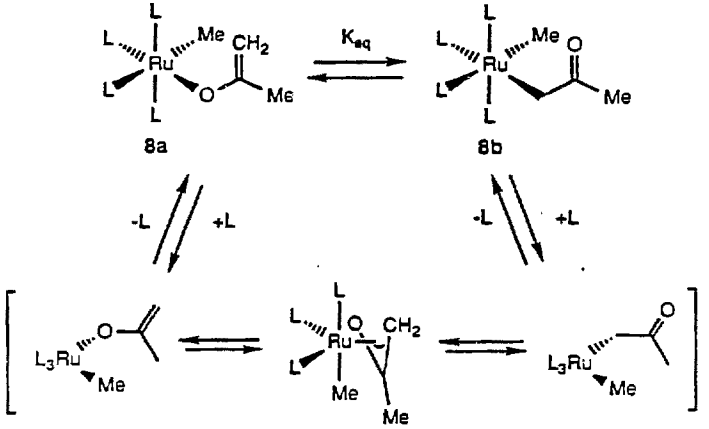

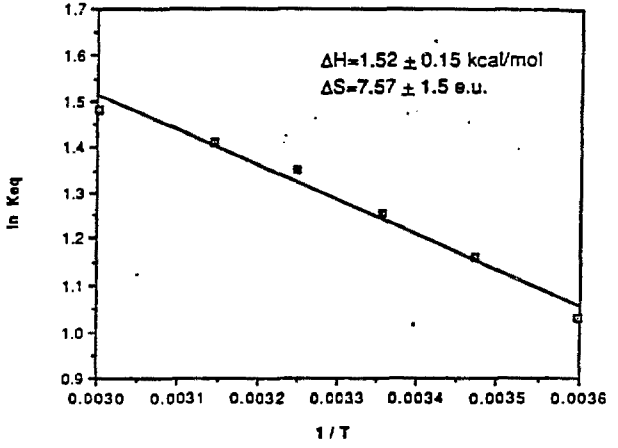

Figure 2. Plot of lnK vs. 1/T to obtain thermodynamic parameters for the equilibrium shown in Scheme 2.

Scheme 3

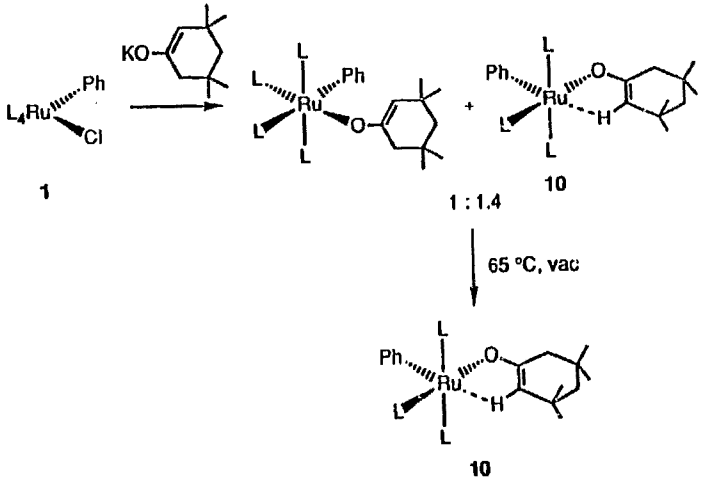

and a compound **10**, containing 3 phosphines. The $^{31}P\{^1H\}$ NMR spectrum of the L_4Ru complex was consistent with those of the other η^1-O-bound enolate complexes. Removal of toluene solvent under vacuum at 65 °C led to complete conversion to **10**. This material possesses two mutually trans phosphines and one resonating in the region characteristic of phosphines located trans to other oxygen-containing substituents. However, several spectroscopic characteristics were inconsistent with an η^3-binding mode. First, only two enolate methyl groups and two methylenes were observed in the ^1H NMR spectrum, indicating that the two sides of the six membered ring are chemically equivalent. Either interconversion between binding to the two sides of the η^3-bound enolate occurs rapidly on the NMR time scale, or the ligand is bound in a more symmetrical fashion. Second, the CH group of the enolate was observed at δ-1.25 in the ^1H NMR spectrum, far from the chemical shift region usual for vinylic hydrogens. However, the $^{13}C\{^1H\}$ NMR chemical shift of the methine carbon was δ76.97, similar to the vinylic resonances of the other enolates reported above.

A single crystal suitable for an X-ray diffraction study was obtained by slow evaporation of a pentane solution of **10**. The structure was solved by standard Patterson and least squares Techniques. An ORTEP drawing of the molecule is shown in Figure 3. Crystal and data collection parameters are included in Table 1; intramolecular distances and angles are provided in Tables 4 and 5. Consistent with the solution NMR data, the enolate is bound symmetrically, and an apparent agostic interaction exists between the metal center and the vinylic C-H bond. The hydrogen atom was not located or refined. Its assumed position is based on idealized sp^2 geometry, but the existence of an agostic interaction is consistent with the ^1H and $^{13}C\{^1H\}$ NMR chemical shifts, indicating that this η^2-binding mode exists in solution as well as in the solid state. The overall geometry is pseudooctahedral with the agostic C-H bond occupying one coordination site. As deduced from the $^{31}P\{^1H\}$ NMR spectrum, two phosphines are bound trans to each other and the other is located trans to the oxygen atom of the enolate. The ring is distorted from planarity, as is expected for a six membered ring system; rapid inversion accounts for the equivalence of C23 and C24 as well as C25 and C26 in the ^1H and $^{13}C\{^1H\}$ NMR spectrum. The

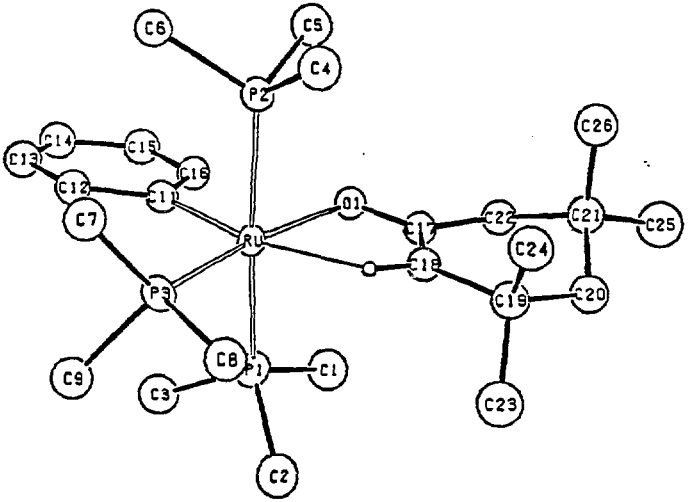

Figure 3. ORTEP drawing of 10. The position of the vinylic hydrogen atom in the drawing is based on idealized sp^2 geometry.

Table 4. Intramolecular distances for 10

ATOM 1	ATOM 2	DISTANCE
RU	P1	2.349(1)
RU	P2	2.332(1)
RU	P3	2.251(1)
RU	O1	2.127(3)
RU	C11	2.030(4)
RU ...	C17	2.776(4)
RU ...	C18	2.766(4)
RU ...	H18	2.14
O1	C17	1.314(4)
C17	C18	1.352(5)
C17	C22	1.526(5)
C18	C19	1.534(5)
C19	C20	1.562(6)
C19	C23	1.553(6)
C19	C24	1.549(6)
C20	C21	1.550(6)
C21	C22	1.556(6)
C21	C25	1.560(6)
C21	C26	1.539(6)
C11	C12	1.415(6)
C11	C16	1.423(6)
C12	C13	1.408(6)
C13	C14	1.364(6)
C14	C15	1.413(6)
C15	C16	1.403(6)
P1	C1	1.855(5)
P1	C2	1.862(5)
P1	C3	1.844(5)
P2	C4	1.849(5)
P2	C5	1.824(5)
P2	C6	1.834(4)
P3	C7	1.856(4)
P3	C8	1.855(4)
P3	C9	1.848(4)

Table 5. Intramolecular Angles for 10

ATOM 1	ATOM 2	ATOM 3	ANGLE
P1	RU	P2	170.66(4)
P1	RU	P3	93.07(4)
P1	RU	O1	86.59(7)
P1	RU	C11	88.47(11)
P2	RU	P3	95.54(4)
P2	RU	O1	85.77(7)
P2	RU	C11	86.71(11)
P3	RU	O1	167.78(7)
P3	RU	C11	98.27(11)
O1	RU	C11	93.93(13)
RU	O1	C17	105.08(22)
O1	C17	C18	123.1(4)
O1	C17	C22	114.6(3)
C18	C17	C22	122.3(4)
C17	C18	C19	125.9(4)
C18	C19	C20	109.6(3)
C18	C19	C23	110.6(3)
C18	C19	C24	110.5(3)
C20	C19	C23	106.4(3)
C20	C19	C24	112.1(3)
C23	C19	C24	107.4(4)
C19	C20	C21	116.2(3)
C20	C21	C22	108.3(3)
C20	C21	C25	108.8(3)
C20	C21	C26	113.5(3)
C22	C21	C25	108.5(3)
C22	C21	C26	109.8(3)
C25	C21	C26	107.8(3)
C17	C22	C21	112.0(3)
RU	C11	C12	128.0(3)
RU	C11	C16	116.0(3)
C12	C11	C16	116.0(4)
C11	C12	C13	122.1(4)
C12	C13	C14	121.1(4)
C13	C14	C15	118.9(4)
C14	C15	C16	120.7(4)
C11	C16	C15	121.3(4)

ATOM 1	ATOM 2	ATOM 3	ANGLE
RU	P1	C1	113.55(15)
RU	P1	C2	119.70(15)
RU	P1	C3	117.46(15)
C1	P1	C2	100.41(21)
C1	P1	C3	100.81(20)
C2	P1	C3	101.95(21)
RU	P2	C4	117.65(15)
RU	P2	C5	111.68(15)
RU	P2	C6	120.53(14)
C4	P2	C5	101.49(21)
C4	P2	C6	102.49(20)
C5	P2	C6	100.05(20)
RU	P3	C7	123.97(15)
RU	P3	C8	109.74(14)
RU	P3	C9	122.23(15)
C7	P3	C8	98.04(20)
C7	P3	C9	97.80(20)
C8	P3	C9	100.39(20)

Ru-O distance (2.127(3) Å) is similar to the Ru-O distance (2.120(1) Å) in the orthometallated enolate **7**. The Ru-C17 and Ru-C18 distances of 2.776(4) and 2.766(4) indicate that the olefinic portion of the enolate is not directly bonded to the metal center. Consistent with an uncoordinated C-C double bond, the C17-C18 distance is not unusually long (1.352(5) Å), and is similar to the uncoordinated C-C double bond distance of 1.351(2) Å in **7**.

Synthesis of Metallacycles. The addition of the potassium enolate of acetone to phenyl chloride (**1**) at room temperature led to formation of the oxametallacyclobutane complex[7a] $(PMe_3)_4Ru(OC(Me)(Ph)CH_2)$ (**11a**), as determined by ^1H, $^{13}C\{^1H\}$ and $^{31}P\{^1H\}$ NMR spectroscopy at -40 °C (equation 3). The room temperature ^1H NMR spectrum of this material

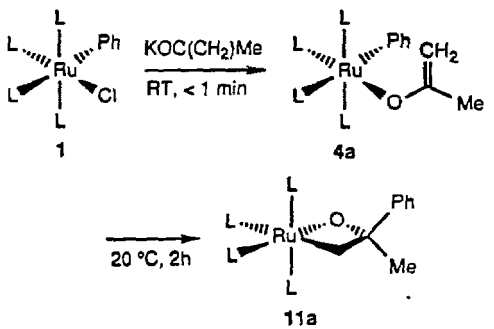

(3)

displayed broad resonances and the room temperature $^{31}P\{^1H\}$ NMR spectrum contained no observable resonances. We presume that rapid, reversible dissociation of phosphine is responsible for the spectroscopic changes between room temperature and -40 °C. Removal of solvent led to decomposition of the ruthenium complex, thus preventing isolation of this material in pure form.

However, an isolable analogue of **11a** was obtained by the addition of 2 equivalents of DMPE (1,2-*bis*-dimethylphosphinoethane) to a benzene solution of **11a**, and confirms the structural assignment of the PMe_3 complex. This simple ligand substitution product $(DMPE)_2Ru(OC(Me)(Ph)CH_2)$ (**11b**), was isolated after reacting for 2 h at room temperature (equation 4). The chelating phosphine prevented the problem of phosphine dissociation

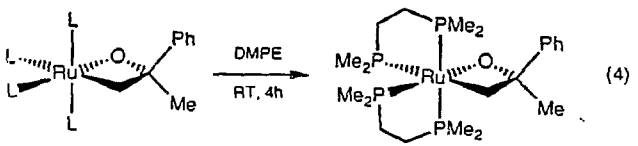

(4)

11a **11b**

experienced when attempting to isolate metallacycle **11a**. Therefore, it was possible to obtain pure samples of **11b**, and this complex was characterized by solution NMR spectroscopy, solid state infrared spectroscopy, and microanalysis. The material was obtained as a white, air sensitive solid which was crystalline, but tended to form thin plates, precluding an X-ray diffraction study. The compound was stored indefinitely at room temperature in the drybox without decomposition. The ^1H and $^{13}C\{^1H\}$ NMR spectra of **2** showed eight DMPM methyl groups, and the $^{31}P\{^1H\}$ NMR spectrum displayed an ABCD pattern. The connectivity of the metallacycle portion of the molecule was clear from ^1H NMR and $^{13}C\{^1H\}$ NMR spectroscopy, with $^{13}C\{^1H\}$ NMR assignments based on spectra obtained with a DEPT pulse sequence. The methyl group was identified by a singlet resonance at δ1.22 in the ^1H NMR spectrum and one at δ41.79 in the $^{13}C\{^1H\}$ NMR spectrum. The appropriate resonances for a static, terminal aryl group were observed in the ^1H and $^{13}C\{^1H\}$ NMR spectrum, and the singlet resonance for the *ipso* carbon indicated that it was no longer bound to the metal center. Instead, the CH_2 group was bound to ruthenium, as indicated

by the multiplet resonance at δ0.62 in the ^1H NMR spectrum and the doublet of multiplets (J=44.7 Hz) at δ1.50 in the $^{13}C\{^1H\}$ NMR spectrum.

The metallacycle portion of **11a** showed features in the ^1H and $^{31}P\{^1H\}$ NMR spectrum similar to those of **11b**. Data for these resonances in **11a** are included in Tables 6 and 7, with the exception of the expected 16 line metal-bound CH_2 resonance, which could not be clearly distinguished from phosphine methyl and impurity resonances in the ^1H NMR spectrum. The phosphine methyl resonances could not be unambiguously distinguished from those of impurities; coupling of these methyl groups to four different phosphorus atoms reduced the peak heights. However, the presence a metal-bound CH_2 group was clear from a $^{13}C\{^1H\}$ NMR spectrum obtained with a DEPT pulse sequence, and the presence of four phosphine ligands was clear from the ABCD pattern in the $^{31}P\{^1H\}$ NMR spectrum. A large trans coupling constant of 363 Hz was obtained from a computer simulation of the spectrum.[18] The inequivalence of the two trans phosphines is consistent with the phenyl and methyl group bound to the β-position, one on each side of the metallacycle.

A likely intermediate in the conversion of **1** to oxametallacycle **11** is the product of simple substitution **4a**, and we were able to directly observe **4a** spectroscopically. Compound 4a was generated by addition of the potassium enolate of acetone to the phenyl chloride complex in THF-d_8 solvent at room temperature for <1 min. ^1H NMR spectroscopic analysis at -40 °C displayed olefinic resonances characteristic of an O-bound enolate, as well as a static, terminal aryl group. The $^{31}P\{^1H\}$ NMR spectrum displayed an A_2BC pattern with chemical shifts similar to those of the other enolate complexes described in the synthesis section. Allowing this solution to warm to 20 °C resulted in the conversion of **4a** to **11** in a yield similar to those resulting from simple room temperature addition of the potassium enolate of acetone to **1** in arene solvents.

A study was performed to determine the role phosphine dissociation plays during this rearrangement. A solution of the phenyl enolate complex 4a was generated by the above procedure and was divided into two NMR tubes. The samples were frozen in liquid nitrogen and to one of them was added 5 equivalents of trimethylphosphine (0.12 M). The rate of formation of

metallacycle 8 was measured at 20 °C for the sample containing no added phosphine, by monitoring the disappearance of starting material resonances in the ^{1}H NMR spectrum. A linear first order plot for this reaction was obtained over greater than three half-lives and provided a rate constant of 4.55 x 10^{-4} sec^{-1}. Thus, the half-life of this reaction was on the order of 25 min. In contrast, the half-life of the sample containing four equivalents of added phosphine was on the order of 9 h, though a precise rate constant was not obtained for this sample. The rate of this phenyl migration step is, therefore, strongly dependent on the concentration of free PMe_3.

The room temperature addition of two equivalents of the potassium enolate of 4,4-dimethyl-2-pentanone to $(PMe_3)_4Ru(OAc)(Cl)$ (12)[13] led to formation of the oxametallacyclobutane $(PMe_3)_4Ru(OC(=CHCMe_3)CH_2)$ (13) in 34% isolated yield, as shown in Scheme 4. This compound was characterized by microanalysis, solution NMR and solid state infrared spectroscopy. The ^{1}H NMR spectrum displayed a multiplet CH_2 resonance at δ1.36 and a vinylic C-H resonance at δ3.75. Similarly the $^{13}C\{^1H\}$ NMR spectrum contained a doublet of triplet of doublets CH_2 resonance at δ-1.57, and a vinylic C-H resonance at δ102.64. The $^{31}P\{^1H\}$ NMR spectrum consisted of an A_2BC pattern with one phosphine resonating upfield and one downfield of the mutually trans phosphines, consistent with one Ru-O and one Ru-C linkage. Results from an X-ray diffraction study on this compound are reported in a companion paper which covers structure and reactivity of the ruthenacycles.[8]

Addition of two equivalents of the potassium enolate of acetone to $(PMe_3)_4Ru(OAc)(Cl)$ (12) led to formation of $(PMe_3)_4Ru(\eta^2\text{-}(CH_2)_2CO)$ (14) and $(PMe_3)_3Ru(\eta^4\text{-}(CH_2)_2CO)$ (15) in roughly equal quantities and in 45-55% total yield by ^{1}H NMR spectroscopy (Scheme 4).[7b] The η^4 complex 15 was isolated in 45-50% yield by sublimation, but we were not able to obtain synthetically useful quantities of 14 due to rapid phosphine dissociation. These two compounds were formed in similar yields by warming a benzene solution of the equilibrium mixture of O- and C-bound enolates 8a and 8b to 65 °C for 6 h. The methane byproduct was formed in 95% yield as determined by Toepler pump techniques.

Scheme 4

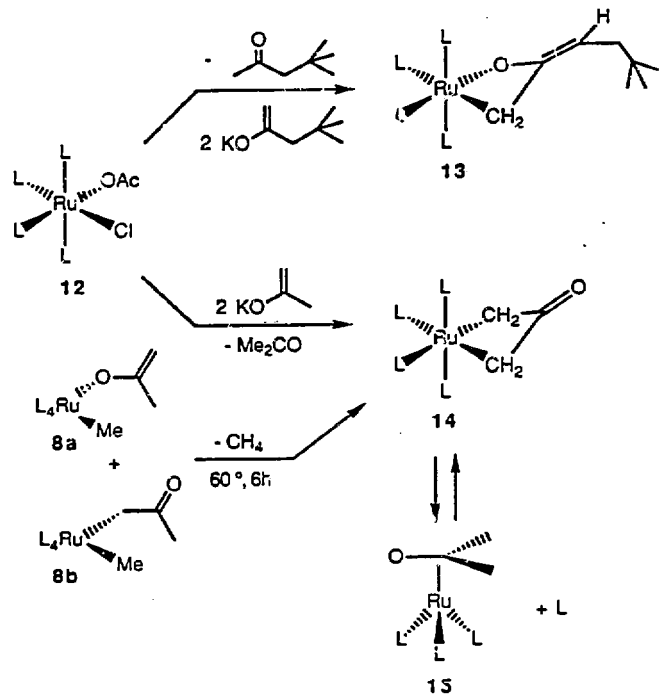
- O
2 KO
L
L
Ru
OAc
Cl
L
L
12
13
H
O
CH2
2 KO
- Me2CO
L4Ru
Me
8a
+
- CH4
60 °, 6h
L4Ru
Me
O
8b
14
O
Ru
+ L
15

Clean samples of metallacycle **14** were generated in solution for NMR spectroscopic characterization by the addition of excess PMe_3 to a solution containing purified tris phosphine complex **15**. At 10 °C in toluene solution, compound **14** displayed an A_2B_2 $^{31}P\{^1H\}$ NMR spectrum. The ^1H NMR spectrum is simple, and contains only one pseudo-triplet CH_2 resonance in addition to the two phosphine methyl resonances. The symmetry required for these two spectra indicates that the ring is planar or is inverting rapidly on the NMR time scale at this temperature. The $^{13}C\{^1H\}$ NMR spectrum contained a doublet of quartets for the metal bound CH_2 and a doublet for the uncoordinated carbonyl group. This structural assignment was confirmed by an X-ray diffraction study on a single crystal obtained by removing the reaction solvent at low temperature and cooling a pentane solution to -40 °C. A detailed description of the crystal structure of this metallacycle is provided in the following paper.

Warming a solution of $(PMe_3)_4Ru(Me)(OC(CH_2)CMe_3)$ (**5c**) to 65 °C for 8 h led to formation of the oxametallacyclobutene $(PMe_3)_4Ru(OC(CMe_3)CH)$ (**16**) in 39% isolated yield, as displayed in Equation 5. Evidence for metallation was obtained from the doublet of triplet of doublets C-H

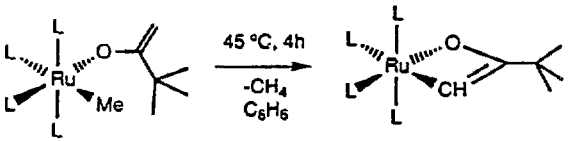

5c **16** (5)

resonance in the $^{13}C\{^1H\}$ NMR spectrum (confirmed by DEPT pulse sequence) at δ90.86, as well as the doublet of doublet C-H resonance at δ5.00. In addition, a methane resonance was observed by ^1H NMR spectroscopy when the thermolysis was performed in a sealed NMR tube. These splitting patterns, resulting from coupling to the phosphine ligands, indicate that the CH group is bound to the metal center. The $^{31}P\{^1H\}$ NMR spectrum displayed an A_2BC pattern with

one phosphine resonating upfield and one downfield of the mutually trans phosphine, indicating that one phosphine is located trans to a Ru-O linkage, and one trans to a Ru-C linkage.

Reductive Elimination Reactions. Thermolysis of the hydrido enolate complex **6a** led to no reaction up to 85 °C. At 110 °C, decomposition of **6a** occurred to form dihydride $(PMe_3)_4Ru(H)_2$ in low yield, and no formation of acetone was observed. However, addition of 2 atm of CO followed by heating to 85 °C for 8 h led to formation of acetone in 79% yield by ^1H NMR spectroscopy and $(PMe_3)_2Ru(CO)_3$ in 62% yield, as shown in equation 6.

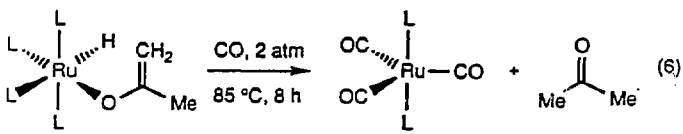

6a

β-Hydrogen Elimination Reactions. Addition of the potassium enolate of acetaldehyde to the phenyl chloride complex **1** (Scheme 5) led to formation of two isomeric complexes **17** and **18**, each containing three phosphines. Warming these two compounds to 45 °C for 4 h led to complete conversion to the major isomer, containing the CO located trans to the ruthenium-bound methyl, $(PMe_3)_3(CO)Ru(Me)(Ph)$ (**17**) in 95% overall yield by ^1H NMR spectroscopy and 23% isolated yield. This compound was characterized by microanalysis, ^1H, $^{13}C\{^1H\}$, and $^{31}P\{^1H\}$ NMR and infrared spectroscopy. Samples of compound **17** were prepared independently by the addition of one equivalent of CO to a C_6D_6 solution of $(PMe_3)_4Ru(Me)(Ph)$ at 65 °C, and the ^1H and $^{31}P\{^1H\}$ NMR spectra were identical to those of the isolated material.

The CO ligand of **17** was identified by a quartet resonance in the $^{13}C\{^1H\}$ NMR spectrum at δ200.56 and an infrared band at 1898 cm^{-1}. A quartet methyl resonance in the ^1H NMR spectrum

Scheme 5

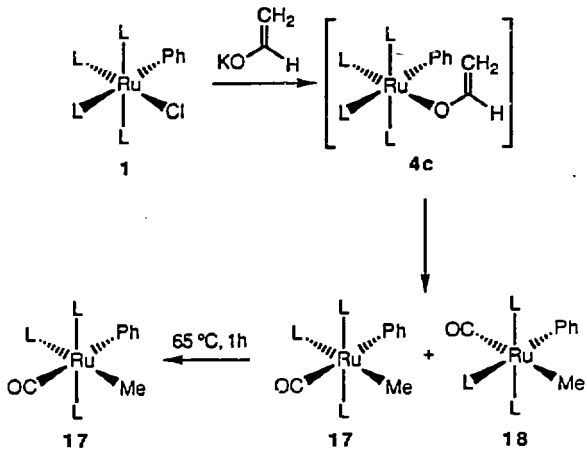
L
Ph
Ru
L
Cl
L
1
CH2
KO
H
L
Ph
CH2
Ru
L
O
H
L
4c
65 °C, 1h
17
17
OC
Me
+
OC
Ph
Me
18

at δ0.33 and a quartet methyl resonance in the $^{13}C\{^1H\}$ NMR spectrum (confirmed by DEPT pulse sequence) at δ-6.55 indicated the presence of a ruthenium bound methyl group. Resonances for a terminal aryl group were also observed, although all five C-H resonances were inequivalent, indicating that rotation of the phenyl group was slow on the ^1H and $^{13}C\{^1H\}$ NMR time scales. The geometry of the molecule was evident from the *ipso* carbon resonance (a doublet of triplets pattern, with a large J_{PC} of 73 Hz). and the A_2B $^{31}P\{^1H\}$ NMR spectrum. The large coupling in the *ipso* carbon resonance indicates that it is located trans to a phosphine, and the $^{31}P\{^1H\}$ NMR spectrum indicates the presence of two equivalent phosphines. Thus, the phosphines must be located trans to each other and the CO ligand must be bound trans to the methyl group, consistent with the pseudoquartet splitting pattern for the resonances corresponding to this substituent.

Warming (65 °C, 1h) a solution of $(PMe_3)_4Ru(Me)(OC(CH_2)H)$ (**5b**), generated from methyl chloride **2** and the potassium enolate of acetaldehyde, led to an 80:14 ratio of methyl hydride $(PMe_3)_4Ru(Me)(H)$ (**17**) and the CO substituted dimethyl complex $(PMe_3)_3(CO)Ru(Me)_2$ (**20**), as shown in Scheme 6. The total yield of these two compounds was 94% by ^1H NMR spectroscopy. The methyl hydride complex **19** has been previously prepared,[9] and was also generated in our laboratory from the addition of C_3H_7MgBr to the methyl chloride complex. The CO substituted dimethyl complex **20** was identified by ^1H and $^{31}P\{^1H\}$ NMR spectroscopy as well as independent synthesis. Two metal bound methyl groups were observed at δ-0.62 and δ-0.38 in the ^1H NMR spectrum. An A_2B pattern in the $^{31}P\{^1H\}$ NMR spectrum with chemical shifts similar to those of the CO substituted phenyl methyl compound **18** indicated the presence of two mutually trans phosphines and one phosphine located trans to a methyl group. This compound was also generated by the addition of one equivalent of CO to the dimethyl complex $(PMe_3)_4Ru(Me)_2$, followed by heating to 45 °C for 2 d.

The stoichiometry of this reaction raised the possibility that ketene CH_2CO might have been formed as a byproduct of β-hydrogen elimination in **5b**. To test this hypothesis we generated a C_6D_6 solution of the methyl enolate complex **5b**, in the presence of 20 equivalents (0.66M) *tert*-

Scheme 6

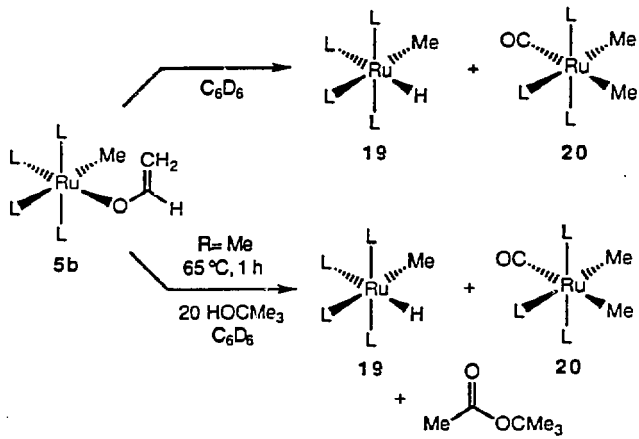

butanol as a ketene trap.[19] This hindered alcohol did not react with the starting ruthenium enolate at room temperature and did not significantly affect the total yield or ratio of the two thermolysis products. However, the formation of *tert*-butylacetate was observed in similar yields (10-15%) for repeated experiments. Increasing the concentration of starting material to 0.1 M and *tert*-butanol to 2.1 M (20 equiv) with the hope of achieving a higher trapping rate, led to low yields of the organometallic product, perhaps due to reaction of the *tert*-butanol with the starting ruthenium enolate. The reaction was also run in the presence of cyclopentadiene as a ketene trap, but this reagent led to decomposition of methyl enolate **5b** and formation of Cp-ruthenium compounds.

Discussion.

Bonding mode. The usual binding mode for late transition metal enolate complexes is the η^1, C-bound form **A** shown in Figure 4.[5] Recently, an extensive report of the synthesis and catalytic reactivity of rhodium O-bound enolates (**B** in Figure 4) was reported from our laboratory.[3] Two other late transition metal O-bound enolates have been reported, although the only spectroscopic data provided for these materials was a ^{1}H NMR spectrum in one case and an infrared spectrum in the other.[4j, k] Examples of isolated η^3-bound enolates are rare,[6] but they have often been invoked as intermediates.[20]

Our results indicate that the free energy difference between the O- and C-bound forms is small for this ruthenium system. The observation of an equilibrium mixture of O- and C-bound enolates and the thermodynamic parameters obtained by variable temperature NMR spectroscopic studies provided values for ΔH and ΔS which were close to zero. The faster rate of phosphine dissociation, as compared to the rate of interconversion, shows that exchange by way of an η^3-oxallyl intermediate is possible, as shown in Scheme 2. If this is the case, the low barrier to interconversion suggests that even the η^3-form is kinetically accessible from both of the η^1-forms, and therefore is within 25 or 30 kcal of the ground state structures.

The η^2-binding mode of the enolate of 3,3,5,5-tetramethylcyclohexanone, which incorporates an agostic metal/vinyl hydrogen interaction, reveals a novel form of transition metal-enolate binding. Once again, a mixture of two forms (η^1 and η^2; 1:1.4) were observed in the

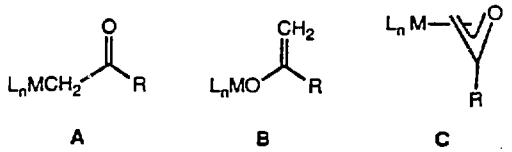

Figure 4. Documented bonding modes for transition metal enolates.

crude reaction mixture. The η^2-enolate results from (presumably reversible) dissociation of phosphine from the η^1-complex, and indicates that the difference in free energy between the two forms is small. We attribute the unusual η^2-binding mode to the steric bulk of the enolate substituent. We believe that steric interaction with the phosphines causes ligand dissociation, but also prevents η^3-coordination, which would bring the methyl groups on the ring prohibitively close to the phosphine methyl groups.

Phenyl Migration. Three possible mechanisms for the formation of oxametallacyfobutane **11a** from phenyl enolate **4a** are shown in Scheme 7. Path a involves migration of the phenyl group directly to the central carbon of the O-bound enolate **4a**. Similarly, path c involves migration within an L_4Ru complex, but to the central carbon of the C-bound enolate **4b**. Since the methyl (acetone) enolate complexes **8a** and **8b** rapidly interconvert on the laboratory timescale the C-bound phenyl (acetone) enolate **4b** may also be present although its concentration may be too small to detect. Path b proposes that **11a** is formed from **22** in an irreversible step in which the phenyl group migrates to the central carbon of the η^3-bound enolate.

The rate expressions for pathways a and c are both first order in ruthenium complex and do not involve the concentration of free phosphine. Pathway a involves migration of the phenyl group directly to the O-bound isomer **4a**, and would display simple first order kinetic behavior. Reaction by pathway c requires either no phosphine dissociation (if **4a** and **4b** interconvert directly) or both phosphine dissociation and recoordination before the rate determining step, either of which results in a rate expression which does not involve ligand concentration. The rate of reaction by pathway c would be dependent on phosphine concentration if the formation of **21b** from **22** is irreversible. However, irreversible conversion of **21a** to **21b** seems unlikely since phosphine dissociation with methyl(acetone)enolate compounds **8a** and **8b** occurs faster than interconversion, and equilibration of these two O- and C-bound isomers is complete after 15 min, much faster than the 2 h necessary for conversion of enolate **4a** to metallacycle **11**. We therefore surmise that pathway b

Scheme 7

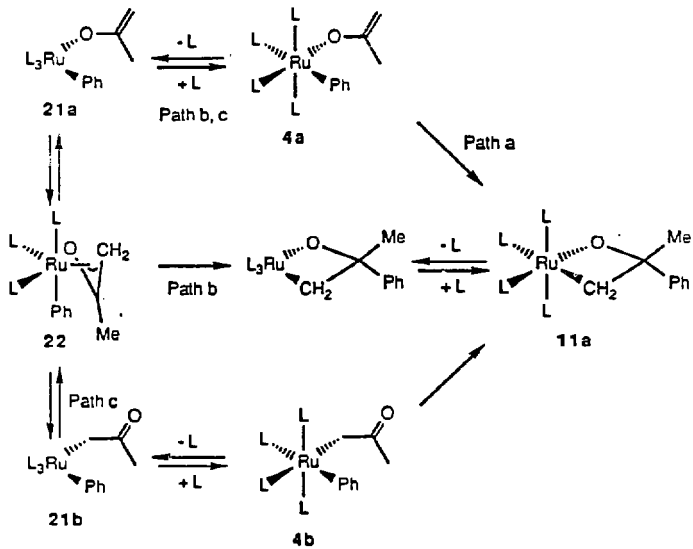
L3Ru
Ph
21a
-L
+L
Path b, c
L
Ru
4a
Path a
CH2
Me
22
Path b
11a
Path c
21b
4b

involves both dissociation and reassociation of phosphine before the rate determining step, and as a result phosphine terms in the rate expression cancel each other out. However, pathway b involves only dissociation of phosphine before the rate determining step, and the rate expression for this pathway includes an inverse dependence of rate on phosphine concentration.

Our observation of a marked inverse dependence of rate on phosphine concentration is inconsistent with pathways a and c, in which the rate determining step involves complexes containing four phosphines. Instead, our results are consistent with a rate determining step which involves a species resulting from phosphine dissociation. It is possible that phenyl migration occurs in coordinatively unsaturated intermediates **21a** or **21b** containing η^1-bound enolates, but we favor migration to the η^3-enolate of intermediate **22** for two reasons. First, it seems unlikely that migration to an η^1-enolate would require predissociation of phosphine. Second, the overall transformation of **4a** to **11a** can be viewed as an insertion of a tethered olefin into the ruthenium-phenyl bond, and many previous studies have demonstrated that olefin insertions into late metal-alkyl bonds typically proceed by coordination of the olefin followed by migration of the alkyl group.[21] Coordination of the olefin of the enolate in intermediate **21a** before insertion forms oxaallyl **22**.

Metallation Reactions. When the group located cis to the enolate is a methyl group rather than a phenyl ring, a variety of cyclometallation reactions occur to produce oxametallacycles and methane. Metallation of aryl groups is a common process,[22] and metallation of alkyl groups by γ-elimination has been observed with this system and several related ones.[23] Studies with this[9] and other late metal systems[21b] are consistent with cyclometallation reactions which proceed by way of phosphine dissociation, followed by intramolecular C-H oxidative addition.

Therefore, the type of metallacycle formed by cyclometallation of these ruthenium enolates reflects the selectivity observed in other C-H oxidative addition processes. Formation of metallacycle **14** from the equilibrium mixture of **8a** and **8b** (Scheme 4) shows that either the allylic C-H bond of the O-bound enolate **8a** or the C-H bond α to the carbonyl in the C-bound form **8b** is favored over addition of the vinylic C-H bond of **8a**. Similarly, the formation of **7** (Scheme 1) from

the methyl enolate intermediate $(PMe_3)_4Ru(Me)(OC(CH_2)Ph)$ (**5d**) demonstrates that addition of the aryl C-H bond to form a 5-membered ring is favored over addition of the vinylic C-H bond to form a 4-membered ring. In contrast to these results, the vinylic C-H bond in complex **5c** reacts preferentially over the sp^3 C-H bond of the *tert*-butyl group (Equation 4). This selectivity forms a 4-membered ring over the 5-membered ring which would result from addition of the sp^3 C-H bond, and it parallels previous results[24] which have demonstrated the greater reactivity of vinylic C-H bonds over alkyl C-H bonds in oxidative addition reactions.

Reductive Elimination Reactions. C-H reductive eliminations are common in alkyl hydride complexes,[25] including an octahedral d^6 rhodium complex containing a C-bound enolate and a hydride ligand.[26] Moreover, we have previously shown that reductive elimination of toluene from the benzyl hydride complex $(PMe_3)_4Ru(H)(CH_2Ph)$ occurs cleanly at 85°C.[14] Therefore, it is interesting to note that C-H reductive elimination from **6a** preceded by conversion of the O-bound enolate to its C-bound form does not occur at temperatures lower than those which lead to other decomposition pathways.

Direct observation of H-X reductive eliminations (X= N, O) are rare,[27] but when observed they have occurred upon addition of an external ligand. CO-induced H-X reductive elimination reactions, similar to that observed with the O-bound enolate **6a**, have been observed to occur from L_4Ru(hydrido)aryloxide and -arylamide complexes.[28] However, in none of these cases does irreversible elimination occur directly from the tetrakisphosphine complex. Reductive elimination reactions are often favored when electron density at the metal center is reduced, and so perhaps this is why elimination of acetone from **6a** occurs only after initial substitution of the poor σ-donating and strong π-accepting CO for a phosphine ligand.

β-Hydrogen Elimination. Our results with the aldehyde enolates provide evidence that β-hydrogen elimination processes occur with these enolate compounds, in contrast to the aldehyde enolates of titanium.[4d] Warming a solution of the methyl enolate **5b** yielded predominantly methyl hydride **19** (Scheme 6). Simple β-hydrogen elimination would form the intermediate **23** with a coordinated ketene, and dissociation of ketene followed by re-coordination

Scheme 8

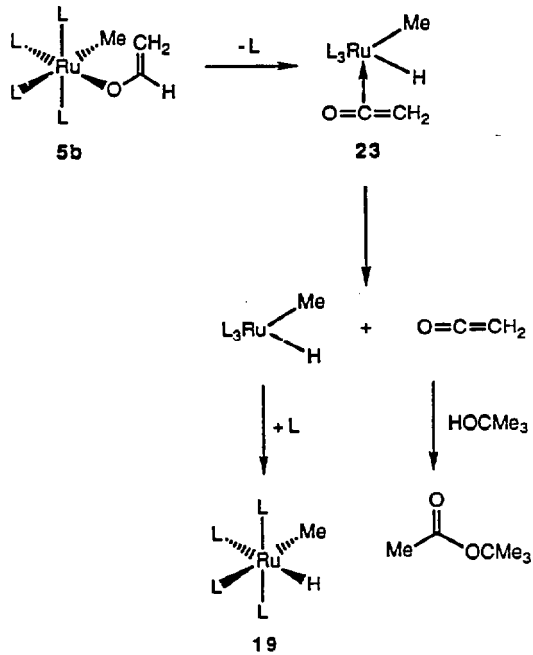
L
L
Ru
Me
CH2
O
H
L
L
5b
-L
L3Ru
Me
H
O=C=CH2
23
L3Ru
Me
H
+
O=C=CH2
+L
HOCMe3
L
L
Ru
Me
H
L
L
19
O
Me
OCMe3

of phosphine would form the final product **19**, as shown in Scheme 8. Although we have not obtained extensive evidence for the formation of free ketene during these reactions, our observation of the trapping product *tert*-butylacetate in 10-15% yield when running the thermolysis of **5b** in the presence of *tert*-butanol provide some evidence that either free or coordinated ketene is formed during the course of the reaction.

The CO-substituted dimethyl complex **20** was formed in lower yields by this thermolysis than was methyl hydride complex **20**. However, the analogous CO-substututed methyl phenyl complex **17** was formed in nearly quantitative yield from the addition of the potassium enolate of acetaldehyde to phenyl chloride **1**. A similar cleavage of the enolate of acetaldehyde was observed with cobalt to form a CO and methylene bridged dimer.[29] A probable mechanism for formation of **17** is shown in Scheme 9, and we attribute the formation of **20** to an analogous pathway. Although the phenyl enolate complex **4c** was not observed, the generality of the enolate substitution reactions provides convincing evidence that this compound is the initial intermediate. As proposed for methyl enolate **5b**, we suggest that β-hydrogen elimination forms phenyl hydride **24**, containing a coordinated ketene. Insertion of the ketene C=C bond into the metal hydride bond forms acyl complex **22**, and deinsertion of the acyl carbonyl forms compounds **17** and **18**.

β-hydrogen elimination reactions from alkyl and alkoxide complexes are common reaction pathways,[30] but elimination of an sp^2-hybridized β-hydrogen is rare. Relevant examples include the deinsertion of CO_2 from formate complexes.[31] Mechanistic studies of this β-elimination from alkyl groups has demonstrated the importance of an open coordination site on the metal.[27] In addition, the mechanistic information available on the formation of hydrides from formate complexes has pointed to a mechanism which involves coordination of the deinserted CO_2 to an open coordination site.[28] Therefore, we propose mechanisms for the enolate β-hydrogen elimination reactions which involve a coordinated ketene that results from initial phosphine dissociation.

Scheme 9

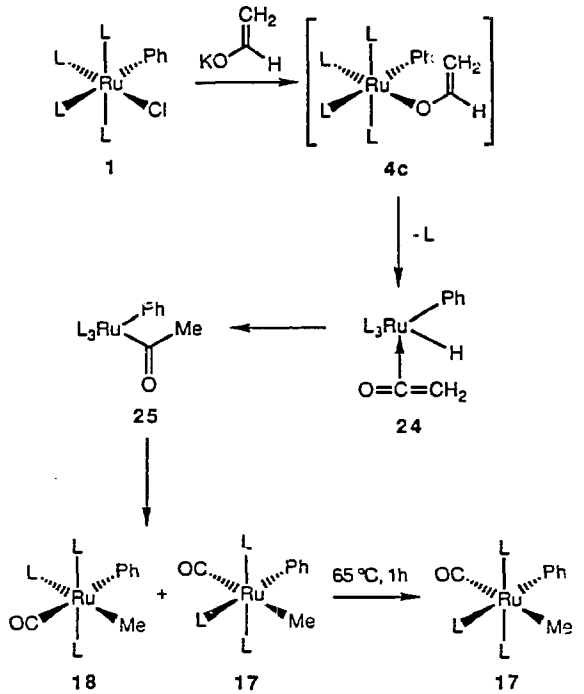
L
Ph
Ru
L
Cl
L
1
CH2
KO
H
L
Ph
CH2
Ru
L
O
H
L
4c
-L
Ph
L3Ru
H
O=C=CH2
24
Ph
L3Ru
Me
O
25
L
Ph
OC
Ru
L
Me
L
18
+
L
Ph
OC
Ru
L
Me
L
17
65 °C, 1h
L
Ph
OC
Ru
L
Me
L
17

Table 6. ^{1}H NMR spectroscopic data.[f]

Compound	δ(ppm)	mult[a]	J(Hz)	int	assignment[b]
cis-(PMe_3)$_4$Ru(Ph)(Cl)[c,d]	1.13	d	7.0	9	*cis*-PMe_3
(*cis*-**1**)	1.14	t	3.0	18	*trans*-PMe_3
	1.25	d	5.6	9	*cis*-PMe_3
	7.04	m			Aromatic[j]
	7.58	m			Aromatic[j]
trans-(PMe_3)$_4$Ru(Ph)(Cl) [c,d]	1.33	br s		36	PMe_3
(*trans*-**1**)	7.04	m			Aromatic[j]
	7.58	m			Aromatic[j]
(PMe_3)$_4$Ru(Me)(OC(CMe_2)H)[d]	0.20	m		3	Ru-Me
(**5a**)	0.87	d	7.2	9	*cis*-PMe_3
	1.14	t	2.8	18	*trans*-PMe_3
	1.17	d	5.6	9	*cis*-PMe_3
	2.12	s		3	OC(CMe_aMe_b)H
	2.15	s		3	OC(CMe_aMe_b)H
	6.73	br s		1	OC(CMe_2)H
(PMe_3)$_4$Ru(Me)(OC(CH_2)H)[d]	0.16	m		3	Ru-Me
(**5b**)	0.84	d	7.3	9	*cis*-PMe_3
	1.12	d	5.7	9	*cis*-PMe_3
	1.15	t	2.7	18	*trans*-PMe_3
	3.90	m		1	OC(CH_aH_b)H
	4.25	dd	13.2, 2.0	1	OC(CH_aH_b)H
	7.25	dd	14.6, 4.8	1	OC(CH_2)H
(PMe_3)$_4$Ru-	-0.15	m		3	Ru-Me
(Me)(OC(CH_2)CMe_3)[g]	0.98	s		9	OC(CH_2)CMe_3
(**5c**)	1.23	d	7.3	9	*cis*-PMe_3
	1.39	t	2.7	18	*trans*-PMe_3
	1.45	d	5.6	9	*cis*-PMe_3
	3.41	d	1.2	1	OC(CH_aH_b)CMe_3
	3.58	br s		1	OC(CH_aH_b)CMe_3
(PMe_3)$_4$Ru(H)(OC(CH_2)Me)[d]	-7.74	dq	104, 17.4	1	Ru-H
(**6a**)	1.01	d	7.3	9	*cis*-PMe_3
	1.13	d	5.5	9	*cis*-PMe_3
	1.37	t	2.9	18	*trans*-PMe_3
	2.07	s		3	OC(CH_2)Me
	3.91	d	2.9	1	OC(CH_aH_b)Me
	4.16	d	2.9	1	OC(CH_aH_b)Me
(PMe_3)$_4$Ru(OC(CH_2)C_6H_4)[g]	1.02	t	6	18	*trans*-PMe_3
(**7**)	1.42	d	6.9	9	*cis*-PMe_3
	1.45	d	6.0	9	*cis*-PMe_3
	3.39	d	1.2	1	OC(CH_aH_b)C_6H_4
	3.95	br s		1	OC(CH_aH_b)C_6H_4
	6.61	tq	7.3, 1.0	1	OC(CH_2)C_6H_4
	6.63	t	7.1	1	OC(CH_2)C_6H_4
	7.11	dt	7.6, 1.6	1	OC(CH_2)C_6H_4
	7.46	m		1	OC(CH_2)C_6H_4

Table 6. (cont'd)

$(PMe_3)_4Ru(Me)(OC(CH_2)Me)$[d] (8a)	0.40	m		3	Ru-Me
	0.86	d	7.4	9	*cis*-PMe_3
	1.18	d	5.3	9	*cis*-PMe_3
	1.27	t	2.8	18	*trans*-PMe_3
	2.06	s		3	$OC(CH_2)\underline{Me}$
	3.50	d	2.2	1	$OC(C\underline{H_a}H_b)Me$
	3.96	d	2.2	1	$OC(CH_a\underline{H_b})Me$
$(PMe_3)_4Ru(Me)(CH_2C(O)Me)$[d] (8b)	-0.26	m		3	Ru-Me
	0.95	d	5.1	9	*cis*-PMe_3
	0.96	d	5.1	9	*cis*-PMe_3
	1.25	t	2.6	18	*trans*-PMe_3
	2.00	s		3	$CH_2C(O)\underline{Me}$
	not obs.				$C\underline{H_2}C(O)Me$
$(PMe_3)_4Ru$-	-0.33	dtd	8.4, 7.0, 4	3	Ru-Me
$(Me)(OC(CH_2)CH_2CMe_3)$	-0.15	dtd	7.9, 4.0, 3	3	Ru-Me
and	0.88	d	7.3		*cis*-PMe_3[k]
$(PMe_3)_4Ru$-	0.97	d	5.0		*cis*-PMe_3[k]
$(Me)(CH_2C(O)CH_2CMe_3)$[d,h]	0.98	d	5.8		*cis*-PMe_3[k]
(9a and 9b)	1.29	m			*tert*-Bu, *trans* and *cis* -PMe_3[k]
	1.96	m		2	$C\underline{H_2}C(O)CH_2CMe_3$
	2.06	s		2	$CH_2C(O)\underline{CH_2}CMe_3$
	2.15	s		2	$OC(CH_2)\underline{CH_2}CMe_3$
	3.05	dd	2.1, 1.1	1	$CH_2C(O)C\underline{H_a}H_bCMe_3$
	3.78	d	2.4	1	$CH_2C(O)CH_a\underline{H_b}CMe_3$
$(PMe_3)_3Ru(Ph)$-	-1.25	s		1	$(O(CC\underline{H}CMe_2CH_2CMe_2CH_2))$
$(O(CCHCMe_2CH_2CMe_2CH_2))$[l]	0.99	d	7.2	9	*cis*-PMe_3
(10)	1.12	t	3.0	18	*trans*-PMe_3
	1.28	s		2	$(O(CCHCMe_2C\underline{H_2}CMe_2CH_2))$
	1.46	s		6	$(O(CCHCMe_2CH_2C\underline{Me_2}CH_2))$
	1.48	s		6	$(O(CCHC\underline{Me_2}CH_2CMe_2CH_2))$
	1.79	s		2	$(O(CCHCMe_2CH_2CMe_2C\underline{H_2}))$
	6.56	m		3	Aromatic
	6.76	d	6.6	1	Aromatic
	7.65	d	7.6	1	Aromatic
$(PMe_3)_4Ru$-	1.60	s		3	$(OC(\underline{Me})(Ph)CH_2)$
$(OC(Me)(Ph)CH_2)$ (11a)[e,l]	7.06	m		2	$(OC(Me)(\underline{Ph})CH_2)$
	7.15	dd	6.9, 7.2	1	$(OC(Me)(\underline{Ph})CH_2)$
	7.30	d	7.2	1	$(OC(Me)(\underline{Ph})CH_2)$

Table 6. (cont'd)

$(DMPE)_2Ru(OC(Me)(Ph)CH_2)$ (11b)[f]	0.29	d	5.8	3	$\underline{Me_2}PCH_2CH_2P\underline{Me_2}$
	1.19	d	6.4	3	
	1.26	d	7.9	3	
	1.47	d	5.2	3	
	1.50	d	7.1	3	
	1.59	dd	6.9, 2.1	3	
	1.70	d	6.8	3	
	1.79	dd	6.7, 2.0	3	
	1.22	s		3	$(OC(\underline{Me})(Ph)CH_2)$
	0.62	m		2	$(OC(Me)(Ph)\underline{CH_2})$
	1.5-2.2	m		8	$Me_2P\underline{CH_2CH_2}PMe_2$
	7.06	t	7.2	1	$(OC(Me)(\underline{Ph})CH_2)$
	7.29	m		2	
	7.42	d	7.2	1	
	8.15	d	7.2	1	
$(PMe_3)_4Ru$-$(CH_2C(=CHCMe_3)O)$[d] (13)	0.83	d	7.1	9	*cis*-PMe_3
	1.05	d	5.4	9	*cis*-PMe_3
	1.33	t	2.8	18	*trans*-PMe_3
	1.36	m		2	$(C\underline{H_2}C(=CHCMe_3)O)$
	1.61	s		9	$(CH_2C(=CHC\underline{Me_3})O)$
	3.75	s		1	$(CH_2C(=C\underline{H}CMe_3)O)$
$(PMe_3)_4Ru((CH_2)_2CO)$[i] (14)	1.05	d	5.4	18	*cis*-PMe_3
	1.13	t	2.4	18	*trans*-PMe_3
	1.54	t	7.9	4	$(C\underline{H_2})_2CO$
$(PMe_3)_4Ru(OCCMe_3CH)$[d] (16)	0.97	d	7.3	9	*cis*-PMe_3
	1.12	d	5.5	9	*cis*-PMe_3
	1.38	t	2.7	18	*trans*-PMe_3
	1.40	s		9	$(OCC\underline{Me_3}CH)$
	5.00	dd	11.2, 4.1	1	$(OCCMe_3C\underline{H})$
$(PMe_3)_3(CO)Ru(Ph)(Me)$[d] (17)	0.33	q	42.4	3	Ru-Me
	0.89	t	2.7	18	*trans*-PMe_3
	1.02	d	6.2	9	*cis*-PMe_3
	7.13	m		2	Aromatic
	7.23	m		1	Aromatic
	7.88	d	6.3	1	Aromatic
	8.21	br, s		1	Aromatic
$(PMe_3)_3(CO)Ru(Me)_2$[d] (20)	-0.62	dt	9.0, 8.4	3	Ru-Me
	-0.38	td	7.7, 3.8	3	Ru-Me
	1.04	d	6.2	9	*cis*-PMe_3
	1.12	t	2.8	18	*trans*-PMe_3

[a]The assignments d and t, when applied to thd PMe_3 resonances are observed patterns, not true multipicity patterns. Accordingly, the values reported as coupling constants for these resonances are the separations between lines and do not necessarily reflect the true coupling constants. [b]The assignment *trans*-PMe_3 refers to mutually trans PMe_3 ligands. The other phosphines are assigned as *cis*-PMe_3. [c]*cis*-and *trans*-$(PMe_3)_4Ru(Ph(Cl)$ was obtained as a 1:1.1 ratio of the *cis* and *trans* isomers. Overlap of the phenyl resonances of these two isomers prevented integration relative to the PMe_3 resonances. [d]C_6D_6, 20 °C. [e]This complex was generated in solution and used *in situ*. We were able to assign the methyl and phenyl groups of the metallacycle. The phosphine and methylene resonances could not be unambiguously distinguished from impurity resonances. [f]THF-d_8, -40 °C. [g]THF-d_8, 20 °C. [h]Some of the resonances for the O- and C-bound isomers could not be distinguished because of the nearly 1:1 ratio of isomers. Assignments are indicated when unambiguous. [i]toluene-d_8, 10 °C. [j]Accurate integrals for the aromatic resonances were prevented by overlap of the signals for *trans*-1 and *cis*-1. [k]Accurate integrals were prevented by overlap of the PMe_3 and *tert*-butyl groups for 9a and 9b. [l]The stereochemistry at the metal center is cis unless stated otherwise.

Table 7. $^{13}C\{^1H\}$ NMR spectroscopic data.

Compound	δ(ppm)	mult[a]	J(Hz)	assignment[b]
$(PMe_3)_4Ru(Me)(OC(CMe_2)H)$[c]	-2.75	dq	59.2, 11.5	Ru-Me
(5a)	18.27	td	22.0, 2.9	*trans*-PMe_3
	21.82	d	15.3	*cis*-PMe_3
	23.90	dd	23.7, 1.9	*cis*-PMe_3
	16.47	s		$(OC(C\underline{Me_a}Me_b)H)$
	21.69	s		$(OC(CMe_a\underline{Me_b})H)$
	93.79	d	3.6	$(OC(\underline{C}Me_2)H)$
	149.94	d	4.3	$(O\underline{C}(CMe_2)H)$
$(PMe_3)_4Ru(Me)(OC(\underline{C}H_2)H)$[c]	1.12	dq	58.7, 11.5	Ru-Me
(5b)	18.39	td	12.1, 2.6	*trans*-PMe_3
	21.62	dd	16.4, 2.0	*cis*-PMe_3
	23.77	d	25.1	*cis*-PMe_3
	78.39	d	3.5	$(OC(\underline{C}H_2)H)$
	162.13	d	4.9	$(O\underline{C}(CH_2)H)$
$(PMe_3)_4Ru(H)(OC(CH_2)Me)$[c]	20.53	dt	17.5, 2.4	*cis*-PMe_3
(6a)	27.27	dm	26.9	*cis*-PMe_3
	22.86	td	12.7, 4.0	*trans*-PMe_3
	25.79	d	4.4	$(OC(CH_2)\underline{Me})$
	77.30	s		$(OC(\underline{C}H_2)Me)$
	168.99	d	4.7	$(O\underline{C}(CH_2)Me)$
$(PMe_3)_4Ru\{OC(CH_2)C_6H_4\}$[f]	19.40	td	12.6, 2.6	*trans*-PMe_3
(7)	22.28	dt	17.0, 1.7	*cis*-PMe_3
	25.23	dm	23.6	*cis*-PMe_3
	72.90	s		$(OC(\underline{C}H_2)C_6H_4)$
	120.68	d	1.3	$[\{O\underline{C}(CH_2)C_6H_4\}$ and
	122.61	d	1.4	Aromatic]
	125.23	m		
	141.27	m		
	152.86	d	3.1	
	176.90	dm	7.7	
	177.71	dq	65.0, 8.2	
$(PMe_3)_4Ru(Me)(OC(CH_2)Me)$[c]	-4.26	dq	60.9, 11.5	Ru-Me
(8a)	19.05	t	8.0	*trans*-PMe_3
	22.74	d	15.8	cis-PMe_3
	13.50	d	26.1	*cis*-PMe_3
	27.63	d	3.7	$(OC(CH_2)\underline{Me})$
	75.68	s		$(OC(\underline{C}H_2)Me)$
	169.23	s		$(O\underline{C}(CH_2)Me)$
$(PMe_3)_4Ru(Me)(CH_2C(O)Me)$[c]	-9.73	dq	56, 12	Ru-Me
(8b)	20.88	t	11.9	*trans*-PMe_3
	23.40	d	18.0	*cis*-PMe_3
	24.17	d	15.4	*cis*-PMe_3
	22.83	m		$(\underline{C}H_2C(O)Me)$
	33.15	s		$(CH_2C(O)\underline{Me})$
	not obs.			$(CH_2\underline{C}(O)Me)$

Table 7. (cont'd)

$(PMe_3)_4Ru$-	19.33	td	12.3, 1.6	*trans*-PMe_3
$(Me)(OC(CH_2)CH_2CMe_3)$	20.91	tt	12.1, 2.4	*trans*-PMe_3
and	23.33	d	20.7	*cis*-PMe_3
$(PMe_3)_4Ru$-	23.56	d	27.5	*cis*-PMe_3
$(Me)(CH_2C(O)CH_2CMe_3)$[c, g]	24.53	d	16	*cis*-PMe_3
(9a and 9b)	24.57	d	16	*cis*-PMe_3
	25.23	dm	42.2	($\underline{C}H_2C(O)CH_2CMe_3$)
	31.16	s		$CH_2C\underline{Me}_3$
	31.29	s		$CH_2C\underline{Me}_3$
	31.53	s		$CH_2C\underline{Me}_3$
	31.58	s		$CH_2C\underline{Me}_3$
	54.27	s		$\underline{C}H_2CMe_3$
	58.27	s		$\underline{C}H_2CMe_3$
	79.45	s		($OC(\underline{C}H_2)CH_2CMe_3$)
	172.07	s		($O\underline{C}(CH_2)CH_2CMe_3$)
	218.10	d	6.0	($CH_2\underline{C}(O)CH_2CMe_3$)
$(PMe_3)_4Ru$-	15.64	t	12.5	*trans*-PMe_3
($O(CCHCMe_2CH_2CMe_2CH_2)$)[e]	22.50	d	23.0	*cis*-PMe_3
(10)	31.27	s		($O(CCHC\underline{Me}_2CH_2C\underline{Me}_2CH_2)$)
	32.30	s		($O(CCH\underline{C}Me_2CH_2\underline{C}Me_2CH_2)$)
	33.13	s		($O(CCH\underline{C}Me_2CH_2\underline{C}Me_2CH_2)$)
	35.13	s		($O(CCHC\underline{Me}_2CH_2C\underline{Me}_2CH_2)$)
	47.67	s		($O(CCHCMe_2\underline{C}H_2CMe_2\underline{C}H_2)$)
	51.72	s		($O(CCHCMe_2\underline{C}H_2CMe_2CH_2)$)
	76.97	s		($O(C\underline{C}HCMe_2CH_2CMe_2CH_2)$)
	119.29	s		Aromatic
	124.65	s		
	125.97	s		
	133.94	s		
	142.22	d	13.0	
	162.51	m		
	164.98	s		($O(\underline{C}CHCMe_2CH_2CMe_2CH_2)$)
$(PMe_3)_4Ru$-	0.99	dm	49	($OC(Me)(Ph)\underline{C}H_2$)
$(OC(Me)(Ph)CH_2)$[d, e]	40.88	s		($OC(\underline{Me})(Ph)CH_2$)
(11a)	93.12	s		($OC(Me)(Ph)CH_2$)
	123.88	s		Aromatic
	125.46	s		
	126.55	s		
	126.86	d	19.2	
	129.07	s		
	164.41	s		

Table 7. (cont'd)

$(DMPE)_2Ru(OC(Me)(Ph)CH_2)$ (11b)[c]	1.50	dm	44.7	$(OC(Me)(Ph)\underline{C}H_2)$
	12.32	dd	20.4, 3.9	$\underline{Me_2}PCH_2CH_2P\underline{Me_2}$
	13.28	pent	5.9	
	14.02	d	17.6	
	15.99	d	8.1	
	17.38	d	15.5	
	19.97	s		
	20.16	dd	20.9, 4.7	
	23.13	d	16.6	
	29.62	t	21.6	$Me_2P\underline{C}H_2\underline{C}H_2PMe_2$
	30.72	dd	28.9, 13.7	
	34.44	dd	26.4, 23.7	
	35.22	dd	31.6, 19.3	
	41.79	s		$(OC(\underline{Me})(Ph)CH_2)$
	92.62	s		$(O\underline{C}(Me)(\underline{Ph})CH_2)$
	123.98	s		$(OC(Me)(\underline{Ph})CH_2)$
	126.30	s		
	126.84	s		
	126.99	s		
	127.10	s		
	164.21	s		
$(PMe_3)_4Ru$-$(OC(=CHCMe_3)CH_2)$[c] (13)	-1.57	dtd	51, 37, 5.1	$(OC(=CHCMe_3)\underline{C}H_2)$
	18.54	td	12.0, 3.1	*trans*-PMe_3
	22.65	d	16.3	*cis*-PMe_3
	24.85	dd	24.9, 2.2	*cis*-PMe_3
	31.56	s		$(OC(=CH\underline{C}Me_3)CH_2)$
	32.88	s		$(OC(=CHC\underline{Me_3})CH_2)$
	102.64	t	2.8	$(OC(=\underline{C}HCMe_3)CH_2)$
	179.88	s		$(O\underline{C}(=CHCMe_3)CH_2)$
$(PMe_3)_4Ru((CH_2)_2CO)$[h] (14)	19.06	td	12.4, 1.5	*trans*-PMe_3
	26.23	m		*cis*-PMe_3
	29.13	dq	38, 6	$((\underline{C}H_2)_2CO)$
	184.00	d	3.0	$((CH_2)_2\underline{C}O)$
$(PMe_3)_4Ru(OC(CMe_3)CH)$[c] (16)	19.27	td	13.1, 2.7	*trans*-PMe_3
	22.93	d	15.7	*cis*-PMe_3
	25.46	dd	25.1, 3.1	*cis*-PMe_3
	29.29	s		$(OC(C\underline{Me_3})CH)$
	38.88	s		$(OC(\underline{C}Me_3)CH)$
	90.86	dtd	64, 16, 6.0	$(OC(CMe_3)\underline{C}H)$
	174.37	t	5.6	$(O\underline{C}(CMe_3)CH)$

Table 7. (cont'd)

$(PMe_3)_3(CO)Ru(Me)(Ph)$[c] (17)	-6.55	q	11.5	Ru-Me
	18.27	t	14.0	*trans*-PMe_3
	20.71	d	19.7	*cis*-PMe_3
	121.71	s		Aromatic
	126.37	d	4.8	
	126.48	s		
	138.59	d	2.1	
	146.83	s		
	166.78	dt	72.7, 17.3	
	200.56	q	10.2	Ru-CO

[a]The assignments d and t, when applied to thd PMe_3 resonances are observed patterns, not true multipicity patterns. Accordingly, the values reported as coupling constants for these resonances are the separations between lines and do not necessarily reflect the true coupling constants. [b]The assignment *trans*-PMe_3 refers to mutually trans PMe_3 ligands. The other phosphines are assigned as *cis*-PMe_3. [c]C_6D_6, 20 °C. [d]This complex was generated in solution and used *in situ*. We were able to assign the resonances of the metallacycle. The phosphine resonances could not be unambiguously distinguished from impurity resonances. [e]THF-d_8, -40 °C. [f]THF-d_8, 20 °C. [g]Some of the resonances for the O- and C-bound isomers could not be distinguished because of the nearly 1:1 ratio of isomers. Assignments are indicated when unambiguous. [h]toluene-d_8, 10 °C.

Table 8. $^{31}P\{^{1}H\}$ NMR spectroscopic data.

Compound	spin system	δ(ppm)	J(Hz)
cis-$(PMe_3)_4Ru(Ph)(Cl)$ (*cis*-**1**)[a]	A_2BC	δA=-8.08 δB=12.02 δC=-15.60	J_{AB}=33 J_{AC}=22 J_{BC}=25
trans-$(PMe_3)_4Ru(Ph)(Cl)$ (*trans*-**1**)[a]	A_4	-7.94	
$(PMe_3)_4Ru(Me)(OC(CMe_2)H)$ (**5a**)[a]	A_2BC	δA=-0.46 δB=14.55 δC=-11.41	J_{AB}=32.4 J_{AC}=26.2 J_{BC}=16.1
$(PMe_3)_4Ru(Me)(OC(CH_2)H)$ (**5b**)[a]	A_2BC	δA=0.26 δB=15.41 δC=-12.01	J_{AB}=33.2 J_{AC}=26.1 J_{BC}=16.6
$(PMe_3)_4Ru(Me)(OC(CH_2)CMe_3)$ (**5c**)[d]	A_2BC	δA=-0.83 δB=9.37 δC=-8.91	J_{AB}=30.6 J_{AC}=26.0 J_{BC}=16.5
$(PMe_3)_4Ru(H)(OC(CH_2)Me)$ (**6a**)[a]	A_2BC	δA=2.12 δB=14.18 δC=-12.63	J_{AB}=33.0 J_{AC}=26.7 J_{BC}=16.4
$(PMe_3)_4Ru(OC(CH_2)(C_6H_4)$ (**7**)[d]	A_2BC	δA=0.69 δB=-13.71 δC=6.86	J_{AB}=25.3 J_{AC}=32.2 J_{BC}=14.3
$(PMe_3)_4Ru(Me)(OC(CH_2)Me)$ (**8a**)[a]	A_2BC	δA=0.49 δB=16.89 δC=-13.20	J_{AB}=34.7 J_{AC}=24.1 J_{BC}=16.8
$(PMe_3)_4Ru(Me)(CH_2C(O)Me)$ (**8b**)[a]	A_2BC	δA=-4.88 δB=-0.73 δC=-16.93	J_{AB}=30.1 J_{AC}=27.5 J_{BC}=14.7
$(PMe_3)_4Ru(Me)(OC(CH_2)CH_2CMe_3)$ (**9a**)[a]	A_2BC	δA=0.70 δB=16.94 δC=-14.26	J_{AB}=36.2 J_{AC}=21.4 J_{BC}=19.0
$(PMe_3)_4Ru(Me)(CH_2C(O)CH_2CMe_3)$ (**9b**)[a]	A_2BC	δA=-4.75 δB=-0.42 δC=-17.06	J_{AB}=29.9 J_{AC}=27.7 J_{BC}=14.5
$(PMe_3)_3Ru(O(CCHCMe_2CH_2CMe_2CH_2)$ (**10**)[b]	A_2B	δA=0.82 δB=13.54	J_{AB}=32.6

Table 8. (cont'd)

$(PMe_3)_4Ru(OC(Me)(Ph)CH_2)$ (11)[b, c]	ABCD	δA=11.36 δB=0.46 δC=-2.02 δD=-12.12	J_{AB}=34.7 J_{AC}=34.8 J_{AD}=5.8 J_{BC}=363.4 J_{BD}=26.3 J_{CD}=26.5
$(PMe_3)_4Ru(O(C=CHCMe_3)CH_2)$ (13)[a]	A_2BC	δA=1.09 δB=11.97 δC=-12.27	J_{AB}=32.5 J_{AC}=23.9 J_{BC}=8.9
$(PMe_3)_4Ru((CH_2)CO)$ (14)[e]	A_2B_2	δA-2.17 δB-9.17	J_{AB}=33.6
$(PMe_3)_4Ru(OCCMe_3CH)$ (16)[a]	A_2BC	δA=-3.43 δB=15.58 δC=-13.28	J_{AB}=35.0 J_{AC}=26.2 J_{BC}=14.47
$(PMe_3)_3(CO)Ru(Me)(Ph)$ (17)[a]	A_2B	δA-4.07 δB=-13.00	J_{AB}=24.6
$(PMe_3)_3(CO)Ru(Me)_2$ (20)[a]	A_2B	δA-0.25 δB=-12.56	J_{AB}=24.0

[a] C_6D_6, 20 °C. [b] THF-d_8, -40 °C. [c] chemical shifts and coupling constants were obtained from a simulated spectrum. [d] THF-d_8, 20 °C. [e] toluene-d_8, 10 °C.

Experimental.

General. Unless otherwise noted, all manipulations were carried out under an inert atmosphere in a Vacuum Atmospheres 553-2 drybox with attached M6-40-1H Dritrain, or by using standard Schlenk or vacuum line techniques.

^{1}H NMR spectra were obtained on either the 250, 300, 400 or 500 MHz Fourier Transform spectrometers at the University of California, Berkeley (UCB) NMR facility. The 250 and 300 MHz instruments were constructed by Mr. Rudi Nunlist and interfaced with either a Nicolet 1180 or 1280 computer. The 400 and 500 MHz instruments were commercial Bruker AM series spectrometers. ^{1}H NMR spectra were recorded relative to residual protiated solvent. ^{13}C{^{1}H} NMR spectra were obtained at either 75.4, 100.6, or 125.7 MHz on the 300, 400, or 500 MHz instruments, respectively, and chemical shifts were recorded relative to the solvent resonance. ^{31}P{^{1}H} NMR spectra were obtained at either 120.8 or 161.9 MHz on the 300 or 400 instruments. ^{1}H and ^{13}C{^{1}H} NMR chemical shifts are reported in units of parts per million downfield from tetramethylsilane and ^{31}P{^{1}H} NMR chemical shifts are reported in units of parts per million downfield from 87% H_3PO_4. All coupling constants are reported in Hz.

IR spectra were obtained on a Perkin-Elmer Model 283 infrared spectrometer or on a Perkin-Elmer Model 1550 or 1750 FT-IR spectrometer using potassium bromide ground pellets. Mass spectroscopic (MS) analyses were obtained at the UCB mass spectrometry facility on AEI MS-12 and Kratos MS-50 mass spectrometers. Elemental analyses were obtained from the UCB Microanalytical Laboratory.

Sealed NMR tubes were prepared by fusing Wilmad 505-PP and 504-PP tubes to ground glass joints which were then attached to a vacuum line with Kontes stopcocks. Alternatively, the tubes were attached via Cajon adapters directly to Kontes vacuum stopcocks.[32] Known volume bulb vacuum transfers were accomplished with an MKS Baratron attached to a high vacuum line.

Unless otherwise specified, all reagents were purchased from commercial suppliers and used without further purification. PMe_3 (Strem) was dried over NaK or a Na mirror and vacuum transferred prior to use. Mesitylene was dried over sodium/benzophenone ketyl and distilled prior

to use. Acetophenone was dried by refluxing over CaH_2, followed by distillation under nitrogen. Hydrogen was purchased from Air Products and was used as received. Acetone was dried with magnesium sulfate before refluxing over magnesium and isolating by vacuum distillation. Carbon monoxide and carbon dioxide were purchased from Matheson and used as received. Trimethylsilane was purchased from Petrarch and used as received. 4,4-dimethyl-2-pentanone and pinacolone were purchased from Aldrich and used as received. *tert*-Butylacetylacetone was prepared by the addition of the potassium enolate of 4,4-dimethyl-2-pentanone to *tert*-butylacetyl chloride. *cis*-$(PMe_3)_4Ru(Me)(Cl)$,[8] *cis*-$(PMe_3)_4Ru(OAc)(Cl)$,[13] and $(PMe_3)_4Ru(\eta^2\text{-}C_6H_4)$[10] were prepared according to methods reported previously.

Many of the satisfactory microanalyses were obtained from sample that were pure by NMR, but recrystallized before submission. Due to the high solubility of these L_4Ru complexes and the small amounts of material used, yields of recrystallized material were not informative. Yields are reported for crystallized samples which provided samples which were pure by NMR spectroscopy.

Potassium enolates of ketones were formed by the addition of a pentane solution of the ketone to a stirred homogeneous solution of $KN(SiMe_3)_2$ in toluene/pentane 1:100. The precipitated enolate was isolated by filtration and stored in the drybox at -40 °C for up to one week. The potassium enolate of 2-methylpropanal was prepared by the addition of KCH_2Ph[33] to $Me_3SiOCH(=CMe_2)$, which was prepared by standard methods.[34] The potassium enolate of acetaldehyde was formed by allowing a solution of KO-*tert*-Bu and *n*-BuLi in dry tetrahydrofuran to warm to room temperature.[35] The lithium-containing products were removed by washing with toluene and the potassium enolate was isolated by filtration and stored in the drybox at -40 °C for up to several weeks.

Pentane and hexane (UV grade, alkene free) were distilled from $LiAlH_4$ under nitrogen. Benzene, toluene, and tetrahydrofuran were distilled from sodium benzophenone ketyl under nitrogen. Dichloromethane was either distilled under N_2 or vacuum transferred from CaH_2. Deuterated solvents for use in NMR experiments were dried as their protiated analogues but were vacuum transferred from the drying agent.

***cis*- and *trans*-$(PMe_3)_4Ru(Ph)(Cl)$ (1).** To a solution of 100 mg (0.208 mmol) of $(PMe_3)_4Ru(\eta^2\text{-}C_6H_4)$ in 2 mL of ether was added 19.9 mg (1.00 equiv) of Me_3NHCl as a solid. The slurry was stirred for 8 h over which time a yellow solid formed. After this time the solid product (pure 1 by ^1H NMR spectroscopy) was filtered, and the resulting clear solution was cooled to -40 °C to provide yellow blocks of analytically pure product. The solids were combined to yield 63.4 mg (59%) of total product which was a mixture of the cis and trans isomers. Anal. Calc'd for $C_{18}H_{42}ClP_4Ru$: C, 41.74; H, 7.95. Found: C, 41.46; H, 7.95.

***cis*-$(PMe_3)_4Ru(Me)(OC(CMe_2)H)$ (5a).** To a solution of 152 mg (0.334 mmol) of $(PMe_3)_4Ru(Me)(Cl)$ in 4 mL of benzene was added 48 mg (1.3 equiv) of $KOC(CMe_2)H$ as a solid. The slurry was stirred for 4 h at room temperature, and then filtered through a medium fritted glass filter using celite filter aid. The solvent was removed from the clear yellow filtrate under reduced pressure, and the resulting solid was extracted three times with a total of 10 mL of pentane. The solution volume was reduced to 3 mL *in vacuo* and cooled to-40 °C to provide 72.4 mg (44%) of analytically pure product. IR(KBr) 1620 (m); Anal. Calc'd for $C_{17}H_{46}OP_4Ru$: C, 41.54; H, 9.43. Found: C, 41.61; H, 9.23.

Generation and Spectroscopic Characterization of $(PMe_3)_4Ru(Me)(OC(CH_2)H)$ (5b). To a solution of 154 mg (0.335 mmol) of $(PMe_3)_4Ru(Me)(Cl)$ in 6 mL of benzene was added 54 mg (1.9 equiv) of $KOC(CMe_2)H$ as a solid. The slurry was stirred for 4 h at room temperature after which time an unlocked $^{31}P\{^1H\}$ NMR of an aliquot showed clean conversion to **5b**. The solution was filtered through a medium fritted glass filter using celite filter aid. The solvent was removed from the clear yellow/orange filtrate under reduced pressure, and the resulting orange solid was extracted three times with a total of 10 mL of pentane. The solution volume was reduced to 5 mL *in vacuo* and cooled to-40 °C to provide 16.4 mg (11%) of powder which was roughly 95% pure by solution NMR. Attempts to obtain analytically pure material were unsuccessful due to partial conversion of **5b** to methyl hydride **19**.

Generation and Spectroscopic Characterization of $(PMe_3)_4Ru(Me)(OC(CH_2)CMe_3)$ (5c). To a solution of 8.2 mg of $(PMe_3)_4Ru(Me)(Cl)$ in 0.6

mL of THF-d_8 was added 7.5 mg (3.1 equiv) of $KOC(CH_2)CMe_3$ as a solid. The resulting solution was placed in an NMR tube and analyzed by ^1H and $^{31}P\{^1H\}$ NMR spectroscopy. It was not possible to isolate pure samples of **5c** due to formation of significant quantities of **16** after several hours at room temperature. Data on **5c** are provided in Tables 6 and 8.

$(PMe_3)_4Ru(H)(OC(CH_2)Me)$ (6a). Into a 1 L glass reaction vessel fused to a Kontes vacuum adaptor was placed a magnetic stir bar and a solution of 350 mg (0.768 mmol) of $(PMe_3)_4Ru(Me)(Cl)$ in 10 mL of C_6D_6. The solution was frozen by immersing the entire vessel in liquid nitrogen, exposed to vacuum, and then treated with 400 torr of hydrogen. The vessel was closed and warmed to room temperature to provide ~2 atm of hydrogen. The solution was stirred for 24 h after which time the reaction vessel was opened under argon. $KOCCH_2Me$ (162 mg, 2.2 equiv) was added, and the slurry was stirred for an additional 6 h. An unlocked $^{31}P\{^1H\}$ NMR spectrum of an aliquot showed clean conversion to **6a**. The solvent was removed under reduced pressure, and the resulting yellow residue was extracted three times with a a total of 20 mL of pentane. The volume was reduced to 5-6 mL and cooled to -40 °C to provide 176 mg (49%) of analytically pure product. IR(Nujol) 1850 (Ru-H), 1579 (C=C); Anal. Calc'd. for $C_{15}H_{42}OP_4Ru$: C, 38.87; H, 9.13. Found: C, 38.55; H, 8.99.

$Ru(PMe_3)_4(\eta^2\text{-}OC(CH_2)C_6H_4)$ (7). (a) preparitive scale. Into a glass reaction vessel fused to a Kontes vacuum adaptor was weighed 31.6 mg (0.0656 mmol) of $(PMe_3)_4Ru(\eta^2\text{-}C_6H_4)$. Benzene (5 mL) was added, and to the resulting solution was added 7.9 mg (1 equiv) of acetophenone. The vessel was heated to 45 °C for 8h, after which time the initial clear solution had turned yellow. The solvent was removed *in vacuo* and the product was crystallized from a pentane/toluene (10:1) solvent mixture to yield 13.6 mg (39.5%) of yellow product. IR (KBr) 3103 (m), 3050 (s), 3043 (s). 3028 (m), 2969 (s), 2903 (s), 1977 (w), 1934 (w), 1624 (w), 1569 (s), 1548 (m), 1431 (s), 1395 (s), 1338 (s), 1316 (s), 1298 (s), 1279 (s), 1262 (s), 1238 (m), 1122 (s), 1021 (m), 990 (s), 938 (s), 854 (s), 841 (s), 784 9s), 736 (s), 712 (s), 700 (s), 662 (s), 647 9(s), 634 (m), 498 (m), MS (FAB) m/e 525 (MH^+).

$(PMe_3)_4Ru(Me)(OC(CH_2)Me)$ (8a and 8b). To a solution of 243 (0.533 mmol) mg of $(PMe_3)_4Ru(Me)(Cl)$ in 4 mL of benzene was added 77 mg (1.5 equiv) of $KOC(CH_2)Me$ as a solid. The slurry was stirred for 4 h at room temperature after which time an unlocked $^{31}P\{^1H\}$ NMR of an aliquot showed clean conversion to 8a and 8b. The aliquot was returned to the reaction mixture, and the solution was filtered through a medium fritted glass filter using celite filter aid. The solvent was removed from the clear yellow filtrate under reduced pressure, and the resulting solid was extracted three times with a total of 10 mL of pentane. The solution volume was reduced to 3 mL and cooled to -40 °C to provide 94.2 mg (37%) of analytically pure enolate product as a mixture of O- and C-bound forms. IR(C_6H_6) 1611 (m), 1583 (s); Anal. Calc'd for $C_{16}H_{44}OP_4Ru$: C, 40.24; H, 9.29. Found: C, 40.50; H, 9.14.

Variable Temperature NMR spectroscopy of 8a and 8b. A solution of 24.6 mg of 8a and 8b in 0.6 mL of THF-d_8 was placed into an NMR tube equipped with a Kontes vacuum adaptor. The sample was degassed by three freeze, pump, thaw cycles and sealed. Ratios of the two isomers were determined by integrating the metal-bound methyl groups. To insure that the equilibrium ratio was measured, spectra were obtained in three minute intervals at one temperature until the integrated spectra from one pulse acquisitions gave ratios within 10% of one another for three successive spectra. Equilibrium ratios were obtained over the temperature range from 5-60 °C. At 5 °C, equilibrium was established over a 15 min time period, and at 60 °C a non-equilibrium ratio was never observed, indicating that equilibrium was established in less than 1 minute. The reversibility of the equilibrium was established by obtaining ratios on the same sample at each temperature twice; a second value was measured after initial values were obtained for each temperature. A plot of ln K versus 1/T is provided in Figure 2.

$(PMe_3)_4Ru(Me)(OC(CH_2)CH_2CMe_3)$ (9a and 9b). To a solution of 150 mg (0.329 mmol) of $(PMe_3)_4Ru(Me)(Cl)$ in 4 mL of benzene was added 59 mg (1.2 equiv) of $KOC(CH_2)CH_2CMe_3$ as a solid. The resulting slurry was stirred for 4 h at room temperature after which time an unlocked $^{31}P\{^1H\}$ NMR of an aliquot showed clean conversion to 9a and 9b. The aliquot was returned to the reaction mixture, and the solution was filtered through a medium fritted

glass filter using celite filter aid. The solvent was removed from the clear yellow filtrate under reduced pressure, and the resulting solid was extracted three times with a total of 10 mL of pentane. The solution volume was reduced to 1.5 mL and cooled to -40 °C to provide 76.2 mg (43%) of analytically pure product as a mixture of O- and C-bound forms. IR(Nujol) 1610 (m), 1581 (s); Anal. Cald'd for $C_{20}H_{52}OP_4Ru$: C, 45.02; H, 9.82. Found: C, 44.71; H, 9.97.

$(PMe_3)_4Ru(Ph)(OC(CHC(Me_2)CH_2C(Me_2)CH_2)$ (10). To a solution of 126 mg (0.243 mmol) of $(PMe_3)_4Ru(Ph)(Cl)$ in 5 mL of C_6H_6 was added 180 mg (2.0 equiv) of $K(OC(CHC(Me_2)CH_2C(Me_2)CH_2)$ as a solid. The solution was stirred for 6 h at room temperature, and an unlocked $^{31}P\{^1H\}$ NMR spectrum of an aliquot showed clean conversion to a product containing four phosphines with an A_2BC spin system (δA=-5.98, δB=5.86, δC=-14.24, J_{AB}=37, J_{AC}=22, J_{BC}=17) and 10 in a ratio of 1:1.4. The aliquot was returned to the reaction mixture; the solvent was removed under reduced pressure, and the yellow residue was redissolved in 20 mL of toluene and placed into a 100 mL Schlenk flask. The toluene was removed over a 15 min period under reduced pressure while heating the flask at 65 °C. A $^{31}P\{^1H\}$ NMR spectrum obtained on a small portion (5 mg) of the yellow residue showed complete conversion to the tris-phosphine complex **10**. The remaining residue was extracted into ether and filtered to provide a clear yellow solution. The solution was reduced to 2-3 mL and cooled to -40 °C to provide 66.2 mg (45%) of analytically pure yellow blocks suitable for X-ray structural analysis. IR(THF) 1601; Anal. Calc'd. for $C_{25}H_{49}OP_4Ru$: C, 53.65; H, 8.83. Found: C, 53.42; 8.86.

Generation and Spectroscopic Observation of $(PMe_3)_4Ru(OC(CH_2)Me)(Ph)$ (4a). To a small vial containing 10.6 mg (0.110 mmol) of $KOC(CH_2)Me$ was added a solution of 32.4 mg (0.0626 mmol) of **1** in 0.6 mL of THF-d_8. The yellow solution of **1** immediately turned orange, and was placed into an NMR tube equipped with a Kontes vacuum adaptor. The sample was quickly frozen in liquid nitrogen and sealed under vacuum. The tube was then placed into the NMR spectrometer probe at -40 °C. ^1H, $^{31}P\{^1H\}$, and $^{13}C\{^1H\}$ NMR spectroscopy showed clean converstion to phenyl enolate **4a**, and the data obtained are included in Tables 6-8.

Generation and spectroscopic Observation of $(PMe_3)_4Ru(OC(Me)(Ph)CH_2)$ (11a). *To a solution of 24.6 mg (0.0475 mmol) cis- and trans-$(PMe_3)_4Ru(Ph)(Cl)$ in 0.6 mL of* THF-d_8 was added an excess (9.4 mg, 0.0979 mmol) of $KOC(CH_2)Me$ as a solid at room temperature. *The suspension was stirred for 2 h over which time the initial yellow solution* turned a darker orange, with a fine precipitate. The reaction was then passed through a small plug of celite, and the resulting clear orange solution was placed into an NMR tube. The tube was equipped with a Kontes vacuum adaptor and sealed under vacuum. ^1H, $^{31}P\{^1H\}$, and $^{13}C\{^1H\}$ NMR spectra were obtained at -40 °C.

$(DMPE)_2Ru(OC(Me)(Ph)CH_2)$ (11b). To a solution of 85.0 mg (0.164 mmol) of a mixture of *cis* and *trans*-$(PMe_3)_4Ru(Ph)(Cl)$ in 8 mL of C_6H_6 was added an excess (40 mg, 0.417 mmol) of $KOC(CH_2)Me$ as a solid at room temperature. The resulting yellow suspension was stirred for 2 h over which time it turned darker orange and a fine precipitate formed. The reaction mixture was then forced through a fritted glas filter with pressure (not vacuum). To the resulting clear orange filtrate was added dropwise at room temperature 2.5 equiv (61.6 mg) of DMPE in 2 mL of Et_2O and the resulting solution cooled to -40 °C to yield 38.6 mg (43.9%) of white solid. This material was recrystallized from ether to provide 15.2 mg (17.3%) of analytically pure white crystals. IR(KBr) 2966(m), 2904(m), 1596(m), 1495(m), 1421(m), 1292(m), 1275(m), 929(s); Anal. Calcd for $C_{19}H_{42}OP_4Ru$: C, 47.10; H, 7.91. Found: C, 46.81; H, 8.00.

$(PMe_3)_4Ru(OC(=CHCMe_3)CH_2)$ (13). To a solution of $(PMe_3)_4Ru(OAc)(Cl)$ (465 mg 0.930 mmol) in 15 mL of THF was added 311 mg (2.2 equiv) of $KOC(CH_2)CH_2CMe_3$ as a solid. After 10 min the solution turned a darker yellow color and an unlocked $^{31}P\{^1H\}$ NMR spectrum of an aliquot showed clean conversion to **13**. The solvent was removed under reduced pressure and the yellow residue was extracted three times with a total of 10 mL of pentane. The resulting slurry was vacumm filtered, and the filtrate was concentrated to 3-4 mL and cooled to -40 °C to provide 162 mg (34%) of product which was pure by solution NMR spectroscopy. This material was recrystallized from pentane at -40 °C before submitting for microanalysis. IR(KBr) 1594; Anal. Calc'd for $C_{19}H_{48}OP_4Ru$: C, 44.09; H, 9.35. Found: C, 43.79; H, 9.40.

$(PMe_3)_3Ru((CH_2)_2CO)$ (15). (a) by thermolysis of $(PMe_3)_4Ru(Me)((OCCH_2Me)$. Into a glass reaction vessel fused to a Kontes vacuum adaptor was placed a solution of 94.2 mg of $(PMe_3)_4Ru(Me)((OCCH_2Me)$ (8a, 8b) in 4 mL of C_6H_6. The solution was degassed using three freeze pump thaw cycles and heated to 65 °C for 24 h. The solvent was then removed under reduced pressure while warming the reaction vessel to 45 °C. The resulting solid was extracted three times with a total of 10 mL of pentane. The yellow solution was then concentrated to ~1 mL and cooled to -40 °C to provide 38.2 mg (42%) of product which was pure by ^1H NMR spectroscopy. This material was recrystallized from pentane before submitting for microanalysis. IR(KBr) 1586; MS(FAB, sulfolane) 387 (MH^+), 330 ($M-(CH_2)_2CO^+$); Anal. Calc'd. for $C_{12}H_{31}OP_4Ru$: C, 37.40; H, 8.10. Found: C, 37.15; H, 8.13.

Alternatively, 15 was be prepared without isolation of the enolate intermediate. A solution of the enolate was generated on a 500 mg scale by addition of excess (1.5-3 equiv) potassium enolate to $(PMe_3)_4Ru(Me)(Cl)$, using the procedure outlined in synthesis of isolated $(PMe_3)_4Ru(Me)(OC(CH_2)Me)$ (8a, 8b). This solution was then filtered and placed into a glass reaction vessel fused to a Kontes vacuum adaptor and heated to 65 °C for 10 h. The product was isolated in 45-55 % yield either by isolation and crystallization from pentane as described earlier of by removal of solvent under vacuum and sublimation at 65 °C.

(b) by addition of $KOCH_2Me$ to $(PMe_3)_4Ru(OAc)(Cl)$. To a solution of 512 mg (0.335 mmol) of $(PMe_3)_4Ru(OAc)(Cl)$ in 6 mL of toluene was added 216 mg (2.2 equiv) of $KOC(CMe_2)Me$ as a solid. The resulting slurry was stirred for 4 h at room temperature. The solution was vacuum filtered through a medium fritted glass filter using celite filter aid. The clear yellow/orange filtrate was transferred to a 100 mL Schlenk flask and the solvent was removed under reduced pressure while heating the flask to 65 °C. The resulting solid was transferred to a sublimation apparatus, and the product was isolated by sublimation at 65 °C over the course of 24 h to provide 186 mg (47%) of product which was *ca.* 90-100% pure by solution NMR spectroscopy.

$(PMe_3)_4Ru((CH_2)_2CO)$ (14). (a) for X-ray diffraction: Synthetically useful quantities of this compound were not prepared due to its propensity to dissociate phosphine, but we were

fortunate enough to obtain a single crystal suitable for an X-ray diffraction study by the procedure described for the formation of $(PMe_3)_3Ru((CH_2)_2CO)$ (**15**), with the following modification of the isolation procedure. The benzene solution obtained from thermolysis of the mixture of **8a** and **8b** was frozen at -40 °C, and the solvent was removed by lyopholization. The solid residue was extracted with 10 mL of pentane and the volume reduced to 2 mL at room temperature. Cooling to -40 °C provided several single crystals one of which was used for an X-ray diffraction study. IR(KBr) 1544 cm^{-1} (C=O).

(b) for solution spectroscopy: Into an NMR tube was placed 0.6 mL of a toluene-d_8 solution containing 35 mg of crystallized tris phosphine complex **15**. The tube was equipped with a Kontes vacuum adaptor and degassed by three freeze, pump, thaw cycles. PMe_3 (4.0 equiv) was added to the sample by vacuum transfer, and ^1H, $^{31}P\{^1H\}$, and $^{13}C\{^1H\}$ NMR spectroscopy at 10 °C showed rapid formation of the tetrakis phosphine complex **14**.

$(PMe_3)_4Ru(OC(CMe_3)CH)$ (16). To a solution of 150 mg (0.329 mmol) of $(PMe_3)_4Ru(Me)(Cl)$ in 10 mL of THF was added 68.2 mg (1.5 equiv) of $KOC(CH_2)CMe_3$ as a solid. The solution was stirred for 4 h at room temperature. The resulting solution of **5c** was then filtered and placed into a glass reaction vessel fused to a Kontes vacuum adaptor. The vessel was heated at 65 °C for 8 h. The solvent was removed under reduced pressure and the solid was crystallized from pentane at -40 °C to provide 64.3 mg of product which was pure by solution NMR spectroscopy. This material was recrystallized from pentane for microanalysis. IR(KBr) 1591(m); *Anal. Calc'd* for $C_{18}H_{46}OP_4Ru$: C, 42.94; H, 9.34. Found: C, 43.25; H, 9.19.

Reductive elimination of acetone from $(PMe_3)_4Ru(H)(OC(CH_2)Me)$ (6a). Into an NMR tube was placed 0.6 mL of a C_6D_6 solution containing 6.4 mg of $(PMe_3)_4Ru(H)(OC(CH_2)Me)$ and 2 mg of mesitylene as an internal standard. The tube was equipped with a Kontes vacuum adaptor. The sample was immersed in liquid nitrogen and exposed to vacuum, followed by 450 torr of CO. The tube was sealed at the top of the liquid nitrogen. This procedure provides a sample containing 2 atm of CO at 25 °C. A ^1H NMR spectrum was obtained of this initial mixture. The solution was then heated at 85 °C for 24 h, after which time

^{1}H NMR spectroscopy showed formation of acetone (79%) and $(PMe_3)_2Ru(CO)_3$ in 62 % yield, as determined by comparison to the initial sample prepared independently in our laboratory during the course of a separate study.[36]

$(PMe_3)_3(CO)Ru(Ph)(Me)$ (17). (a) On a preparative scale from $(PMe_3)_4Ru(Ph)(Cl)$ and $KO(CCH_2)H$. To a solution of 156 mg (0.301 mmol) of $(PMe_3)_4Ru(Ph)(Cl)$ in 6 mL of ether was added 55 mg (2.2 equiv) of $KOC(CH_2)H$ as a solid. The solution was stirred at room temperature for 4 h, after which time the solid was removed by filtration. The resulting clear, pale yellow solution was concentrated to 1-2 mL, layered with 10 mL hexanes, and cooled to -40 °C to provide 30.7 mg (22.7%) of white crystals, judged pure by solution NMR spectroscopy. IR(*THF*) 1898 cm^{-1}.

(b) From $(PMe_3)_4Ru(Ph)(Cl)$ and $KO(CCH_2)H$ to determine NMR yield. 15.2 mg (0.294 mmol) of $(PMe_3)_4Ru(Ph)(Cl)$ and 2 mg of mesitylene as an internal standard were dissolved in 1.2 mL THF-d_8. The solution was divided equally into two NMR tubes. To one sample was added 1.6 mg (1.5 equiv) of $KOC(CH_2)H$. After 2 h at 45 °C, ^{1}H and $^{31}P\{^1H\}$ NMR of the two samples showed a 95% yield of $(PMe_3)_3(CO)Ru(Ph)(Me)$.

(c) from $(PMe_3)_4Ru(Me)(Ph)$ and CO. Into an NMR tube was placed a solution of 8.2 mg (0.017 mmol) of $(PMe_3)_4Ru(Me)(Ph)$ in 0.6 mL of C_6D_6. The tube was equipped with a Kontes vacuum adaptor, and the sample was degassed by two freeze, pump, thaw cycles. One equivalent of CO was added to the sample, as determined by calculating the volume of the NMR tube and adding the appropriate pressure of CO while the NMR tube was immersed in liquid nitrogen (77 K). The tube was then sealed at the top of the liquid nitrogen. Heating the sample to 65 °C for 24 h provided a sample whose ^{1}H and $^{31}P\{^1H\}$ NMR spectra matched those for material isolated by procedure (a) above.

Addition of $KOC(CH_2)H$ to $(PMe_3)_4Ru(Me)(Cl)$ (2). Into an NMR tube was placed 0.7 mL of a THF-d_8 solution containing 8.4 mg (0.018 mmol) of $(PMe_3)_4Ru(Me)(Cl)$ and 2 mg of mesitylene as an internal standard. A ^{1}H NMR spectrum was obtained to use in calculating an NMR yield after addition of the enolate. To this sample was added 4 mg (3 equiv) of $KOC(CH_2)H$

as a solid. The NMR tube was equipped with a Kontes vacuum adaptor and sealed under vacuum. The sample was heated at 65 °C for 1h, after which time ^1H NMR spectroscopy showed formation of $(PMe_3)_4Ru(Me)(H)$[9] in 80% yield and $(PMe_3)_3(CO)Ru(Me)_2$ in 14% yield. The THF-d_8 solvent was then removed under reduced pressure and replaced with C_6D_6 for identification of the two products by comparison of their ^1H and $^{31}P\{^1H\}$ NMR spectra to those reported in C_6D_6 solvent and those obtained by independent synthesis of $(PMe_3)_3(CO)Ru(Me)_2$. Samples of $(PMe_3)_4Ru(Me)(H)$ were also prepared in our laboratory by the addition of $CH_3CH_2CH_2MgBr$ to a THF solution of $(PMe_3)_4Ru(Me)(Cl)$, and the solution NMR spectroscopic data obtained from this preparation were consistent with literature values and those obtained by the above procedure.

Addition of $KOC(CH_2)H$ to $(PMe_3)_4Ru(Me)(Cl)$ (2) in the presence of $HOCMe_3$. Into a small vial was placed 0.7 mL of a THF solution containing 9.1 mg (0.020 mmol) of $(PMe_3)_4Ru(Me)(Cl)$. To this sample was added 4.9 mg (3.0 equiv) of $KOC(CH_2)H$ as a solid. The slurry was stirred for 0.5 h after which time ^1H NMR of this mixture showed formation of $(PMe_3)_4Ru(Me)(OC(CH_2)H)$. The solvent was removed under reduced pressure and the resulting crude ruthenium enolate was dissolved in 0.7 mL of C_6D_6. The solid remaining in this mixture was removed by forcing the solution through a small plug of celite. The clear yellow/orange filtrate was then placed into an NMR tube and to this sample was added 15 µL (20.0 equiv) of $HOCMe_3$ to provide a 0.66 M solution of the alcohol. The NMR tube was then equipped with a Kontes vacuum adaptor, degassed by three freeze, pump, thaw cycles and sealed. The resulting sample was then heated to 65 °C for 1 h, and analysis by ^1H NMR spectroscopy showed that the two organometallic products were formed in roughly the same yield as in the absence of the alcohol. ^1H NMR spectroscopy also showed the presence of $Me_3COC(O)Me$ in 10-11 % yield, as compared to an 80% yield of $(PMe_3)_4Ru(Me)(H)$. The sample was then opened and the solution was forced through a short column of silica, eluting with 1-2 mL of ether to separate the metal containing products from the organic materials. Gas chromatographic analysis showed the presence of $Me_3COC(O)Me$, as determined by coinjection with an authentic sample.

Independent generation of $(PMe_3)_3(CO)Ru(Me)_2$ (20). Into an NMR tube was placed a solution of 7.4 mg (0.017 mmol) of $(PMe_3)_4Ru(Me)_2$ in 0.6 mL of C_6D_6. The tube was equipped with a Kontes vacuum adaptor, and the sample was degassed by two freeze, pump, thaw cycles. One equivalent of CO was added to the sample, as determined by calculating the volume of the NMR tube and adding the appropriate pressure of CO while the tube was immersed in liquid nitrogen (77 K). The tube was then sealed at the top of the liquid nitrogen. Heating to 65 °C for 48 h provided a sample whose ^1H and $^{31}P\{^1H\}$ NMR spectra matched those of material formed by the addition of $KOC(CH_2)H$ to $(PMe_3)_4Ru(Me)(Cl)$.

X-ray Crystal Structure Determination of 7.

(a) Isolation and Mounting: Crystals of the compound were obtained by slow crystallization from toluene/pentane (1:100) at –40 °C. Fragments cleaved from some of these crystals were mounted in thin-wall capillaries in the air. The capillaries were then flushed with dry nitrogen and flame-sealed. Preliminary precession photographs indicated triclinic Laue symmetry and yielded approximate cell dimensions.

The crystal used for data collection was then transferred to our Enraf-Nonius CAD-4 diffractometer and centered in the beam. Automatic peak search and indexing procedures yielded a triclinic reduced primitive cell. Inspection of the Niggli values revealed no conventional cell of higher symmetry. The final cell parameters and specific data collection parameters parameters for this data set are given in Table 1.

(b) Structure Determination: The 3392 raw intensity data were converted to structure factor amplitudes and their esd's by correction for scan speed, background and Lorentz and polarization effects. No correction for crystal decomposition was necessary. Inspection of the azimuthal scan data showed a variation $I_{min}/I_{max} = 1\%$ for the average curve. No correction for absorption was applied. The choice of the centric space group was confirmed by the successful solution and refinement of the structure.

The structure was solved by Patterson methods and refined via standard least-squares and Fourier techniques. In a difference Fourier map calculated following the refinement of all non-

hydrogen atoms with anisotropic thermal parameters, peaks were found corresponding to the positions of most of the hydrogen atoms. Hydrogen atoms were assigned idealized locations and values of B_{iso} approximately 1.25 times the B_{eqv} of the atoms to which they were attached. They were included in structure factor calculations, but not refined. Before the last cycles of refinement, 11 data which showed evidence of interference by multiple diffraction were removed from the data set.

The final residuals for 236 variables refined against the 3174 accepted data for which $F_2>3\sigma$ (F^2) were R = 1.80%, wR = 2.90% and GOF = 2.154. The R value for all 3381 data was 2.22%. In the final cycles of refinement a secondary extinction parameter was included (maximum correction: 9% on F)

The quantity minimized by the least squares program was $\Sigma w(|F_o|-|F_c|)^2$, where w is the weight of a given observation. The p-factor, used to reduce the weight of intense reflections, was set to 0.02 in the last cycles of refinement. The analytical forms of the scattering factor tables for the neutral atoms were used and all scattering factors were corrected for both the real and imaginary components of anomalous dispersion.

Inspection of the residuals ordered in ranges of $\sin\theta/\lambda$, $|F_o|$, and parity and value of the individual indexes showed no unusual features or trends. The largest peak in the final difference Fourier map had an electron density of 0.24 e-/ $Å^3$, and the lowest excursion –0.19 e-/$Å^3$.

The positional and thermal parameters of the non-hydrogen atoms are available as supplementary material.

X-ray Crystal Structure Determination of 10.

(a) Isolation and Mounting: Crystals of the compound were obtained by slow evaporation of a pentane solution and were mounted in a viscous oil. X-ray data were collected as for 7; the final cell parameters and specific data collection parameters are given in Table 1.

(b) Structure Determination: The 3860 raw intensity data were converted to structure factor amplitudes and their esd's by correction for scan speed, background and Lorentz and polarization effects. An empirical absorption correction based on azimuthal scan data

(T_{max}=1.000, T_{min}=0.959) was applied. Inspection of the systematic absences indicated space group $P2_1/n$. Removal of systematically absent and redundant data left 3771 unique data in the final data set.

The structure was solved by Patterson methods and refined via standard least-squares and Fourier techniques. The final residuals for 141 variables refined against the 3230 data for which $F_2>3\sigma(F^2)$ were R = 5.4%, wR = 8.4% and GOF = 3.83. The R value for all 2890 data was 6.3%.

The quantity minimized by the least squares program was $\Sigma w(|F_o|-|F_c|)^2$, where w is the weight of a given observation. The p-factor, used to reduce the weight of intense reflections, was set to 0.03 throughout the refinement. The analytical forms of the scattering factor tables for the neutral atoms were used and all scattering factors were corrected for both the real and imaginary components of anomalous dispersion.

The positional and thermal parameters of the non-hydrogen atoms are provided as supplementary material, as well as a listing of the values of F_o and F_c.

References and Notes

1. Bryndza, H.E.; Tam, W. *Chem. Rev.* 1988, *88*, 1163, and references therein.

2. (a) Mukaiyama, T.; Banno, K.; Narasaka, K. *J. Am. Chem. Soc.* **1974**, *96*, 7503. (b)Evans, D.A.; McGee, L.R. *Tetrahedron Lett.* 1980, 3975. (c) Yamamoto, Y.; Naruyama, K. *Tetrahedron Lett.* 1980, 4607. (d) Stille, J.R.; Grubbs, R.H.. *J. Am. Chem. Soc.* 1983,

105, 1665. (e) Sato, S.; Matsuda, I.; Izumi, Y. *Tetrahedron Lett.* **1986** 5517. (f) Reetz, M.T.; Vougioukas, A.E. *Tetrahedron Lett.* **1987**, *28*, 793.

3. Slough, G.A.; Bergman, R.G.; Heathcock, C.H. *J. Am. Chem. Soc.* **1989**, *111*, 938.

4. Zirconium: (a) Manriquez, J.M.; McAlister, D.R.; Sanner, R.D.; Bercaw, J.E. *J. Am. Chem. Soc.* **1978**, 2716. (b) Gambarotta, S.; Floriani, C.; Chiesi,-Villa, A.; Guastini, C. *J. Am. Chem. Soc.* **1983**, *105*, 1690. (c) Moore, E.J.; Straus, D.A.; Armantrout, J.; Santarsiero, B.D..; Grubbs, R.H.; Bercaw, J.E. *J. Am. Chem. Soc.* **1983**, 105, 2068. Titanium: (d) Curtis, D.M.; Thanedar, S.; Butler, W.M. *Organometallics*, **1984**, *3*, 1855. (e) Straus, D.A.; Grubbs, R.H. *J. Am. Chem. Soc.* **1982**, *104*, 5499. (f) Fachinetti, G.; Biran, C.; Florianai, C.; Villa, A.C.; Buastini, C *Inorg. Chem.* **1978**, *17*, 2995. Thorium: (g) Fagan, P.J.; Manriquez, J.M.; Marks, T.J.; Day, V.W.; Volimer, S.H.; Day, C.S. *J. Am. Chem. Soc.* **1980**, *102*, 5393. (h) Sonnenberger, D.C.; Mintz, E.A.; Marks, T.J. *J. Am. Chem. Soc.* **1984**, *106*, 3484. Molybdenum: (i) Hirao, T.; Fujihara, Y.; Tsuno, S.; Ohshiro, Y.; Agawa, T. *Chem. Lett.* **1984**, 367. Palladium: (j) Ito, Y.; Nakatsuka, M.; Kise, N.; Saegusa, T. *Tetrahedron Lett.* **1980**, *21*, 2873. (k) Dall'Antonia, P.; Graziani, M.; Lenarda, M. *J. Organomet. Chem.* **1980**, *186*, 131.

5. Burkhardt. E.R.; Doney, J.J.; Bergman, R.G.; Heathcock, C.H. *J. Am. Chem. Soc.* **1987**, *109*, 2022. An extensive list of C-bound enolates is provided in this paper.

6. (a) Guggolz, E.; Ziegler, M.; Biersack, H.; Herrmann, W.A. *J. Organomet. Chem.* **1980**, *194*, 317. (b) Bennett, M.A.; Robertson, G.B.; Watt, T.; Whimp, P.O. *J. Chem. Soc., Chem. Commun.* **1971**, 752. (c) Ito, Y.; Aoyama, H.; Hirao, T.; Mochizuki, A.; Saegusa, T. *J. Am. Chem. Soc.* **1979**, *101*, 494. (d) Holmgren, J.S.; Shapley, J.R.; Wilson, S.R.; Pennington, W.T. *J. Am. Chem. Soc.* **1986**, *108*, 508. (e) Robertson, G.B.; Whimp, P.O. *Inorg. Chem.* **1973**, *12*, 1740.

7. (a) Hartwig, J.F.; Bergman, R.G.; Andersen, R.A. *J. Am. Chem. Soc.* **1990**, *112*, 3234. (b) Hartwig, J.F.; Bergman, R.G.; Andersen, R.A. *J. Am. Chem. Soc.* **1990**, *112*, 5670.

8. Chapter 9.

9. Statler, J.A..; Wilkinson, G.; Thornton-Pett, M.; Hursthouse, M.B. *J. chem. Soc., Dalton Trans.* **1984**, 1731.

10. Hartwig, J.F.; Andersen, R.A.; Bergman, R.G. *J. Am. Chem. Soc.* **1989**, *111*, 2717.

11. A trans influence series is given in Appleton, T.G.; Clark, H.C.; Manger, L.E. *Coord. Chem. Rev.* **1973**, *10*, 335. Discussion of correlations between trans influence and ^{31}P chemical shifts is found in: (a) Nixon, G.F.; Pidcock, A. *Ann. Rev. NMR Spectroscopy*, **1969**, *2*, 345. (b) Verkade, J.M.; Quin, eds., *Phosphorus-31 NMR Spectroscopy in Stereochemical Analysis*, VCH Publishers: New York, 1987. (c) Meek, D.W.; Mazanec, T.J. *Acc. Chem. Res.* **1981**, *14*, 266.

12. Chapter 4.

13. Chapter 5.

14. Mainz, V.V.; Andersen, R.A. *Organometallics* **1984**, *3*, 675.

15. Chapter 1.

16. Jones, R.A.; Wilkinson, G. *J. Chem. Soc., Dalton Trans.* **1979**, 472.

17. Tulip. T.H. personal communication.

18. Spectral simulations were performed with the standard Brucker PANIC program.

19. March. J. *Advanced Organic Chemistry*, Wiley: New York, 1985, p. 685.

20. (a) Alper, H.; Keung, E.C.H.; *J. Org. Chem.* **1972**, *37*, 2566. (b) Prince, R.H.; Raspin, K.A. *J. Chem. Soc. A.* **1969**, 612. (c) Goetz, R.W.; Orchin, M. *J. Am. Chem. Soc.* **1963**, *85*, 2782. (d) Shirner, R.L.; *Org. React.* **1942**, *1*, 1.

21. (a) Thorn, D.L.; Hoffmann, R. *J. Am. Chem. Soc.* **1978**, *100*, 2079. (b) Norton, J.R.; Samsel, E.G. *J. Am. Chem. Soc.* **1984**, *106*, 5505. (c) Flood, T.C.; Bitler, S.P. *J. Am. Chem. Soc.* **1984**, *106*, 6076.

22. Ryabov, A.D. *Chem. Rev.* **1990**, *90*, 403.

23 See for example: (a) Andersen, R.A.; Jones. R.A.; Wilkinson, G. *J. Chem. Soc.* **1978**, 446. (b) Foley, P.; DiCosimo, R.; Whitesides, G.M. *J. Am. Chem. Soc.* **1980**, *102*, 6713.

24. Faller, J.W.; Smart, C.J. *Organometallics* 1989, *8*, 602.

25. Collman, J.P. Hegedus, L.S.; Norton, J.R.; Finke, R.G. *Principles and Applications of Organotransition Meal Chemistry* University Science Books: Mill Valley, 1987, p 322.

26. Milstein, D. *Acc. Chem. Res.* 1984, *17*, 221.

27. (a) Newman, L.J.; Bergman, R.G. *J. Am. Chem. Soc.* 1985, *107*, 5314. (b) Glueck, D.S., Newman, L.J.; Bergman, R.G. submitted for publication. (c) Yamamoto, T.; Sano, K.; Yamamoto, A. *Chem. Lett.* 1982,907. (d) Brugo, C.D.; Pasquali, M.; Leoni, P.; Subatino, P.; Braga, D. *Inorg. Chem.* 1909, *28*, 1390. (e) Cowan, R.L.; Trogler, W.C. *J. Am. Chem. Soc.* 1989, *111*, 475.

28. Chapter 6

29. Halbert, T.R.; Leonowicz, M.E.; Maydonovitch *J. Am. Chem. Soc.* 1980, *102*, 5107.

30. Cross, R.J. In *The Chemistry of the Metal-Carbon Bond;* Hartley, R.F.; Patai, S., Eds.; Wiley: New York, 1985; Vol. 2, Chapter 8.

31. See for example, (a) Darensbourg, D.J.; Wiegreffe, P.; Riordan, C.G. *J. Am. Chem. Soc.* 1990, *112*, 5759. (b) Darensbourg, D.J.; Fischer, M.B.; Schmidt, R.E., Jr.; Baldwin, B. *J. Am. Chem. Soc.* 1981, *103*, 1297. (c) Merrifield, J.H.; Gladysz, J.A. *Organometallics*, 1983, *2*, 782.

32. Bergman, R.G.; Buchanan, J.M.; McGhee, W.D.; Periana, R.A.; Seidler, P.F.; Trost, M.K.; Wenzel, T.T. in *Experimental Organometallic Chemistry: A Practicum in Synthesis and Characterization*, Wayda, A.L.; Darensbourg, M.Y. Eds., ACS Symposium Series 357, American Chemical Society, Washington, DC, 1987, p 227.

33. Scholsser, M. *Angew. Chem. Int. Ed. Engl.* 1964, *3*, 362.

34. House, H.O.; Czuba, L.J.; Gall, M.; Olmstead, H.D. *J. Org. Chem.* 1969, *34*, 2324.

35. Bates, R B.; Kroposki, L.M.; Potter, D E. *J. Org. Chem.* 1972, *37*, 560.

36. Burn, M J.; Bergman, R.G.; Andersen, R.A. unpublished results.

Chapter 9

Structure and Reactions of Oxametallacyclobutanes and Oxametallacyclobutenes of Ruthenium

Introduction

Oxametallacyclobutanes have been invoked as intermediates in several reactions that have found widespread utility. For example, processes such as carbonyl methylenation reactions mediated by transition metal complexes, asymmetric epoxidation of allylic alcohols with titanium catalysts, are believed to involve oxametallacyclobutane intermediates.[1] In addition, the intermediacy of oxametallacycles in the epoxidation of olefins by cytochrome P-450 catalysts has been a controversial topic,[1] and the ability to prepare such metallacycles may help to address this issue. Several other reactions of potential utility, such as the rhodium catalyzed synthesis of β-lactams from aziridines[2] and formation of a metallacyclic carbonate of platinum from epoxide and CO_2[3] are also believed to proceed by way of oxa- and azametallacylobutanes.

These results demonstrate that even isolable oxametallacyclobutanes should behave as reactive species. In fact, only a few examples of stable oxametallacyclobutanes are known. Late transition metal examples include the preparation and reactivity of iridaaza- and iridaoxacylobutane complexes reported recently from our laboratories,[4] the generation of an oxametallacylobutane of iridium by reaction of a coordinated olefin with molecular oxygen,[5] the formation of an analogous platinum complex from tetracyanooxirane (2,2,3,3-tetracyanooxacyclopropane),[6] and the recent structural characterization of a rhodium oxametallacyclobutane.[7] Early transition metal oxametallacyclobutanes[8] include titanium and tantalum examples. An oxametallacyclobutane of platinum containing an oxygen atom in the β-position has also been reported.[9]

Even more rare are the analogous complexes containing a C=C bond, the oxametallacyclobutenes. The only isolated examples known so far were prepared by Vaughn and Hillhouse, by the addition of N_2O to zirconocene acetylene and benzyne complexes;[10] the same complex was reported from our laboratories to form from addition of diphenyl acetylene to an oxozirconocene species.[11]

Both oxametallacyclobutane and -butene complexes provide the opportunity to compare the reactivities of the metal-heteroatom and metal-carbon bonds. Metathesis with early metal complexes forms alkene or alkyne and metal-oxo products,[1a] while the iridaoxacyclobutane

complex reported from our laboratory forms ketone and metal-carbene upon photolysis.[4] In addition, insertion reactions occur with the late transition metal heteroatom bonds in both iridium and platinum oxametallacyclobutanes, consistent with the expected reactivity based on the mismatch of a soft metal center and a hard alkoxide or amide substituent.[12]

We have recently reported the unexpected insertion of CO and CO_2 with the metal-carbon bond of a ruthenium oxametallacycle formed by orthometallation of a *p*-cresolate substituent.[13] We have also investigated the reactivities of oxametallacylobutane and oxametallacylobutene complexes with the goal of understanding the factors that control the selectivities these compounds in metathesis, insertion, and epoxide-forming reactions. Several unusual reactivity patterns have been observed, including C-C bond cleavage by an apparent β-methyl elimination process, rapid C-O bond cleavage to extrude alkene upon addition of protic acids and electrophiles, and insertions into the ruthenium-oxygen and ruthenium-carbon bonds. We reported preliminary reactivity with two of the metallacycles,[14] and subsequently set out to rationalize the initially observed reactivity patterns by synthesizing compounds with different connectivity in the ring and with different dative ligands. In this paper we report the results of these reactivity studies. Metallacycles used in this study were prepared from ruthenium enolate complexes, in most cases using methodology described in the accompanying paper.

Results

Most of the results described here focus on the oxaruthenacylobutane complex $(PMe_3)_4Ru(OC(Me)(Ph)CH_2)$ (**1**), containing methyl and phenyl groups in the β-position of the ring. As described in the previous paper, rapid phosphine dissociation at room temperature precluded isolation of this complex in pure form. Therefore, complex **1** was characterized by solution spectroscopy. The most informative spectroscopic data included an ABCD pattern in the $^{31}P\{^1H\}$ NMR spectrum, the metal bound CH_2 resonance in the $^{13}C\{^1H\}$ NMR spectrum, and the resonances for a terminal aryl group not bound to the ruthenium. Reactions with **1** were performed *in situ* following generation of the metallacyle by addition of the potassium enolate of

acetone to $(PMe_3)_4Ru(Ph)(Cl)$ in hydrocarbon solutions, as described in the previous paper. The DMPE analogue of **1**, $(DMPE)_2Ru(OC(Me)(Ph)CH_2)$ (**2**), was stable enough to isolate as described in the previous paper and crystaline samples of it were used for reactivity studies.

Reactions of $(PMe_3)_4Ru(OC(Me)(Ph)CH_2)$ (1). Scheme 1 summarizes the thermal chemistry of compound **1**. Warming a solution containing **1** in roughly 80-90% purity at 45 °C for 8 h led to formation of methane and the cyclic enolate **3** in 51% yield by ^1H NMR spectroscopy (Cp_2Fe internal standard), and in 22% isolated yield. This complex was first isolated as the product of addition of acetone to the ruthenium benzyne complex $(PMe_3)_4Ru(\eta^2\text{-}C_6H_4)$.[15] a transformation that forms one carbon-carbon bond and cleaves another.[16] This reaction occurs by way of compound **1** as described in the previous paper; it is also conveniently formed by addition of acetophenone to the ruthenium benzyne complex $(PMe_3)_4Ru(\eta^2\text{-}C_6H_4)$.[17] We believe an intermediate in the thermolysis of **1** may be the methyl enolate complex $(PMe_3)_4Ru(Me)(OC(CH_2)Ph)$ (**4**), resulting from β-methyl elimination. In order to determine if such an intermediate forms methane and **3**, **4** was generated independently by treating the methyl chloride complex $(PMe_3)_4Ru(Me)(Cl)$[18] with the potassium enolate of acetophenone. This procedure led to the formation of methane and **2** in 97% yield by ^1H NMR spectroscopy, although orthometallation was faster than substitution, precluding direct observation of **4**.

Scheme 2 displays the reactions of **1** with hydrogen and CO. Addition of H_2 (2 atm) to a C_6D_6 solution of **1** cleanly formed the tertiary alcohol $HOCMe_2Ph$ (85% by ^1H NMR spectroscopy) and the dihydride *cis*-$(PMe_3)_4Ru(H)_2$ (**5**)[18,19] (88%). The ^1H NMR spectroscopic identification of the alcohol was confirmed by matching the GC retention time to that of an authentic sample.

Addition of CO (2 atm) to a solution of **1** at room temperature formed compound **6** in 51% isolated yield, the product of CO substitution at the metal center and CO insertion into the metal carbon bond. This complex was characterized by solution NMR spectroscopy, solid state infrared spectroscopy, and microanalysis. Absorptions for coordinated CO was observed at 1907 cm^{-1} and for the inserted CO at 1614 cm^{-1}. The $^{13}C\{^1H\}$ NMR spectrum displayed a resonance at 268.3 for the inserted CO, and one at 201.4 for the coordinated carbonyl. The CH_2 resonance of

Scheme 1

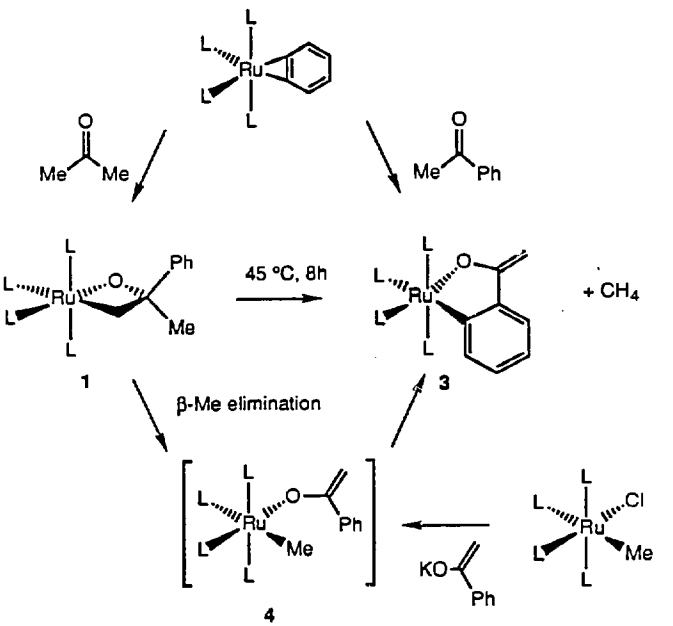

Scheme 2

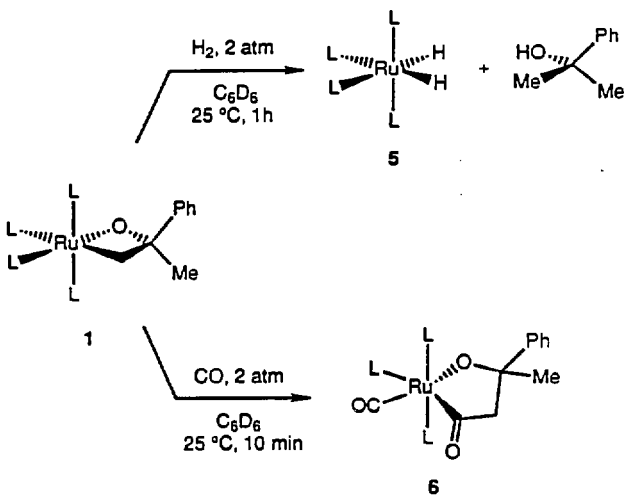

6 was observed as a doublet at δ74.7, indicating that it was located in the position α to a carbonyl group and that it was no longer bound to the metal center. The CH_2 resonance for starting complex 1 was observed at much higher field (δ0.99) and showed coupling to four phosphines. The geometry of 6 was deduced from the $^{31}P\{^1H\}$ NMR spectrum and the splitting pattern of the $^{13}C\{^1H\}$ NMR resonance corresponding to the inserted CO. The $^{31}P\{^1H\}$ NMR spectrum displayed an ABC pattern, with a large trans coupling constant of 321.1 Hz. In addition, the $^{13}C\{^1H\}$ resonance for the inserted CO showed a 100.1 Hz coupling constant, indicating that it is located trans to a phosphine ligand and that the coordinated CO, a strong π-acceptor, is located trans to the potentially π-donating oxygen of the metallacycle.

Addition of protic acids to 1 led to the extrusion of α-methylstyrene, as shown in Scheme 3. The room temperature addition of *p*-cresol to a solution of 1 led to formation of α-methylstyrene in 86% yield by ^1H NMR spectroscopy and *bis*-cresolate complex *cis*-$(PMe_3)_4Ru(OC_6H_4$-*p*-$Me)$ (7) in 74% yield. In order to maintain the proper stoichiometry, water must also be formed by this reaction, although it was not detected. Compound 7 was independently synthesized in 57% isolated yield by the addition of *p*-cresol to the dimethyl complex $(PMe_3)_4Ru(Me)_2$ during the course of a separate study.[20] Even addition of the weak acid acetophenone, followed by warming to 45 °C, led to extrusion of α-methylstyrene (58%) and formation of the cyclic enolate 3 in 61% yield by ^1H NMR spectroscopy. Presumably water was also a byproduct of this reaction.

Addition of carbon electrophiles also led to the extrusion of α-methylstyrene, as shown in Scheme 4. Addition of carbon dioxide to a solution of 1 led to formation of α-methylstyrene in 84% yield and the ruthenium carbonate $(PMe_3)_4Ru(CO_3)$ (8) in 83% yield by ^1H NMR spectroscopy. This complex was prepared in 87% isolated yield by the addition of potassium carbonate to *trans*-$(PMe_3)_4Ru(Cl)_2$.[21] This compound was isolated as a white powder and was identified by ^1H, $^{31}P\{^1H\}$, $^{13}C\{^1H\}$ NMR, infrared and mass spectroscopy. An A_2B_2 pattern was observed in the $^{31}P\{^1H\}$ NMR spectrum, with the phosphines located trans to the carbonate ligand resonating downfield from the mutually trans phosphines. This trend in chemical shift is

Scheme 3

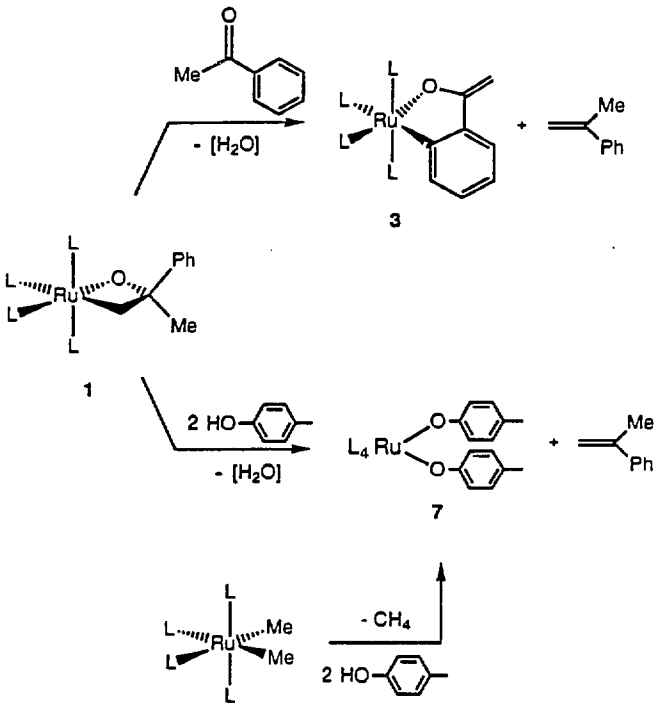
O
Me
- [H2O]
L
L
Ru
L
O
Me
Ph
3
L
L
Ru
L
O
Ph
Me
1
2 HO
- [H2O]
L4 Ru
O
O
Me
Ph
7
L
L
Ru
L
Me
Me
- CH4
2 HO

Scheme 4

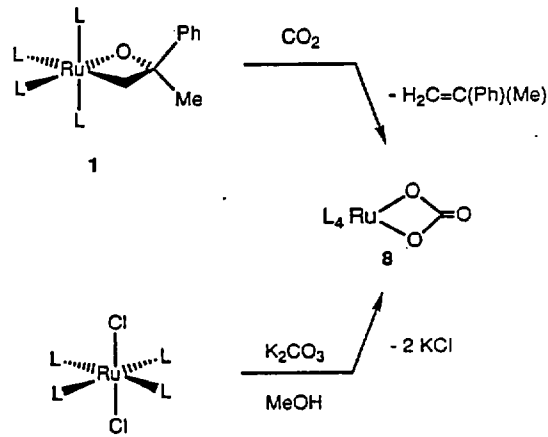
L
L
Ru
O
Ph
Me
L
L
1
CO2
- H2C=C(Ph)(Me)
L4 Ru
O
O
O
8
Cl
L
L
Ru
L
L
Cl
K2CO3
MeOH
- 2 KCl

consistent with other $(PMe_3)_4Ru(X)(Y)$ complexes containing ruthenium-heteroatom bonds,[14, 15, 19, 20] and reflects the weaker trans influence properties of the carbonate substituent, compared to trimethylphosphine.[22] The carbonate ligand was identified by a singlet resonance at δ169.2 in the $^{13}C\{^1H\}$ NMR spectrum, and by an infrared absorption at 1578 cm^{-1}. A parent peak at m/e = 467 in the FAB mass spectrum was consistent with the assignment of **8** as a monomer.

Reaction of **1** with PhNCO, a compound isoelectronic with CO_2, is shown in Scheme 5. Addition of this reagent to **1** led to rapid extrusion of α-methylstyrene and caused precipitation of an initial addition product $(PMe_3)_4Ru(\eta^2\text{-}OC(NPh)O)$ (**9**). This compound stable in the solid state but rearranged to $(PMe_3)_4Ru(\eta^2\text{-}OC(O)NPh)$ (**10**) in solution. Compound **9** was identified by ^1H, $^{31}P\{^1H\}$, and $^{13}C\{^1H\}$ NMR and infrared spectroscopy of a portion of the crude precipitate which contained roughly 90% compound **9**. The NMR spectra of **9** were temperature dependent. At room temperature an A_2B_2 pattern was observed in the $^{31}P\{^1H\}$ NMR spectrum, requiring rapid inversion at the nitrogen atom. However, at -80 °C this inversion was slow, as indicated by the A_2BC pattern in the $^{31}P\{^1H\}$ NMR spectrum, with similar chemical shifts for P_B and P_C. The methyl groups of the phosphine ligands were not resolved in the ^1H NMR spectrum at this temperature, but they were resolved in the $^{13}C\{^1H\}$ NMR spectrum. The organic substituent was identified by the absorption for the C-N double bond at 1706 cm^{-1} in the infrared spectrum, as well as by the resonance at δ171.7 in the $^{13}C\{^1H\}$ NMR spectrum.

Attempts to crystallize **9** from either tetrahydrofuran or methylene chloride led to formation of the more stable isomer, $(PMe_3)_4Ru(\eta^2\text{-}OC(O)NPh)$ (**10**). Simply dissolving compound **9** in methylene chloride and warming to 45 °C for 1 h led to clean formation of **10**. This compound was isolated as a yellow/orange powder by diffusion of ether into the methylene chloride solution of **10**, and it was characterized by microanalysis, as well as ^1H, $^{31}P\{^1H\}$, and $^{13}C\{^1H\}$ NMR and infrared spectroscopy. The room temperature $^{31}P\{^1H\}$ NMR spectrum of **10** displayed an A_2BC pattern, with the phosphines located trans to the carboxamide ligand resonating downfield of the mutually trans phosphines. The carboxamide substituent was

Scheme 5

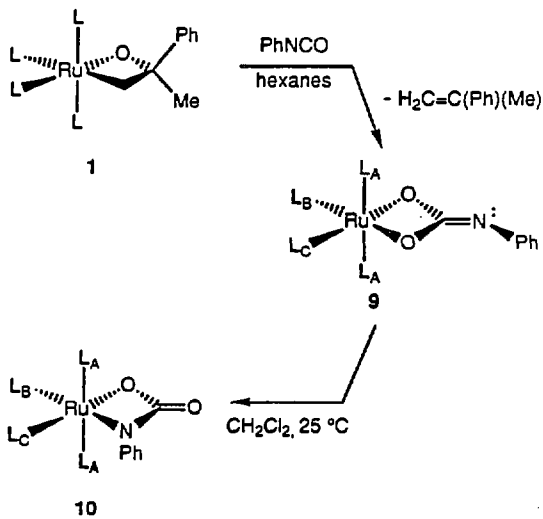
L
L
Ru
L
O
Ph
Me
L
1
PhNCO
hexanes
- H2C=C(Ph)(Me)
LA
LB
Ru
LC
O
O
N
Ph
LA
9
CH2Cl2, 25 °C
LA
LB
Ru
LC
O
O
N
Ph
LA
10

identified by the carbonyl carbon at δ167.7 in the $^{13}C\{^1H\}$ NMR spectrum and by the infrared absorption band at 1595 cm^{-1}.

Addition of benzaldehyde to a C_6D_6 solution of **1** *followed by heating to 45 °C led to* extrusion of α-methylstyrene in 73% yield and provided the hydrido benzoate *cis*-$(PMe_3)_4Ru(H)(OC(O)Ph)$ (**11**) in 53% yield by ^1H NMR spectroscopy (Scheme 6). Compound **11** was prepared independently in 14% isolated yield by the addition of benzoic acid to the ethylene complex $(PMe_3)_4Ru(C_2H_4)$,[23] and was characterized by ^1H, $^{31}P\{^1H\}$, and $^{13}C\{^1H\}$ NMR and infrared spectroscopy, as well as by microanalysis. The hydride substituent was identified by the doublet of quartets resonance (one large trans coupling and three indistinguishable cis couplings) at δ-8.21 in the ^1H NMR spectrum and the absorption band at 1826 cm^{-1} in the infrared spectrum. The presence of the benzoate ligand was confirmed by an absorption at 1599 cm^{-1} in the infrared spectrum, a carbonyl resonance in the $^{13}C\{^1H\}$ NMR at δ172.19, and appropriate resonances for a terminal aryl group in the ^1H and $^{13}C\{^1H\}$ NMR spectrum. An A_2BC pattern in the $^{31}P\{^1H\}$ NMR spectrum established the cis stereochemistry of this complex.

Addition of non-polarizable, unsaturated organic molecules led to no reaction. Addition of *meta*-methyl-α-methylstyrene, styrene, isobutylene, dimethylacetylene, or diphenylacetylene to C_6D_6 solutions of **1** led to no change in its room temperature ^1H and $^{31}P\{^1H\}$ NMR spectra. Warming the solutions to 45 °C led to formation of **3** in roughly the same yield as the thermolysis conducted in the absence of the alkene or alkyne.

Reactions of $(DMPE)_2Ru(OC(Me)(Ph)CH_2)$ (2). A comparison of the reactivities of **1** and **2** should provide information on the role of phosphine dissociation in these reactions, since phosphine dissociation in **2** is less facile than in **1**. The most dramatic difference between these two metallacycles was displayed in their thermal chemistry and reactivity toward CO. While **1** forms methane and cyclometallated product **3** at 45 °C, heating C_6D_6 solutions of **2** to 140 °C for 2 d provided ^1H and $^{31}P\{^1H\}$ NMR spectra which were indistinguishable from those of starting material. No formation of methane, α-methylstyrene, or α-methylstyrene oxide was observed. Similarly, metallacyle **2** was stable toward reaction with carbon monoxide. When a solution of **2**

Scheme 6

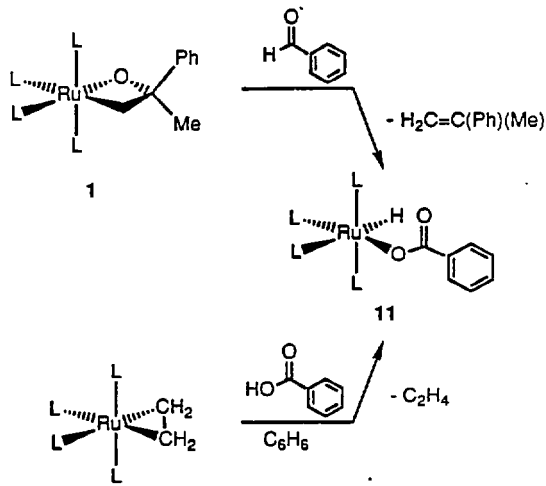
L
L
Ru
O
Ph
Me
L
1
O
H
- H2C=C(Ph)(Me)
L
L
Ru
H
O
O
L
11
L
L
Ru
CH2
CH2
L
O
HO
- C2H4
C6H6

was exposed to 2 atm of CO at 85 °C for 24 h, no evidence for ligand substitution or CO insertion was observed by ^1H or $^{31}P\{^1H\}$ NMR spectroscopy.

Addition of 2 equivalents of *p*-cresol to crystalline samples of **2** in C_6D_6 at room temperature led to rapid, quantitative formation of α-methylstyrene in addition to the DMPE substituted *bis* -cresolate complex $(DMPE)_2Ru(OC_6H_4\text{-}p\text{-}Me)_2$ (**12**) in 74% yield by ^1H NMR spectroscopy (Scheme 7). Compound **12** was prepared independently in 32% yield by the addition of *p*-cresol to $(DMPE)_2Ru(Me)_2$. Yellow crystals of **12** formed from the reaction mixture, and these were characterized by microanalysis, as well as by ^1H, $^{31}P\{^1H\}$, and $^{13}C\{^1H\}$ NMR and infrared spectroscopy. The *cis* -stereochemistry was indicated by a pair of triplets in the $^{31}P\{^1H\}$ NMR spectrum and by the presence of four methyl groups in the ^1H and $^{13}C\{^1H\}$ NMR spectra. The AA'BB' pattern in the aryl region of the ^1H NMR spectrum and the presence of two CH and two quaternary resonances in the aryl region of the $^{13}C\{^1H\}$ NMR spectrum demonstrated the η^1-binding mode of the cresolate substituents. Because the preparation of starting dimethyl compound **12** was reported in 1963 without the aid of NMR spectroscopy, its ^1H, $^{31}P\{^1H\}$, and $^{13}C\{^1H\}$ NMR spectroscopic data are included in Tables 1-3.

The reaction of metallacycle **2** with carbon dioxide in C_6D_6 at room temperature led to extrusion of α-methylstyrene (96%) and precipitation of the DMPE substituted ruthenium carbonate $(DMPE)_2Ru(CO_3)$ (**13**) (Scheme 8). The carbonate complex was dissolved by adding CD_2Cl_2 to the reaction solution containing an internal standard, and ^1H NMR spectroscopy of the homogeneous solution showed that **13** was formed in quantitative yield. This compound was prepared independently in 34% yield and spectroscopically characterized by adding an excess of DMPE to a methanol solution of the PMe_3-substituted carbonate **8**. Compound **13** was isolated as a white powder; its most revealing spectroscopic features were an IR absorption band at 1566 cm^{-1} and a $^{13}C\{^1H\}$ NMR resonance at δ167.5, corresponding to the carbonate substituent. The two DMPM ligands were identified by two triplet resonances in the $^{31}P\{^1H\}$ NMR spectrum in the same chemical shift region as the other DMPM complexes prepared in this study, and by the four methyl resonances observed in the ^1H and $^{13}C\{^1H\}$ NMR spectra.

Scheme 7

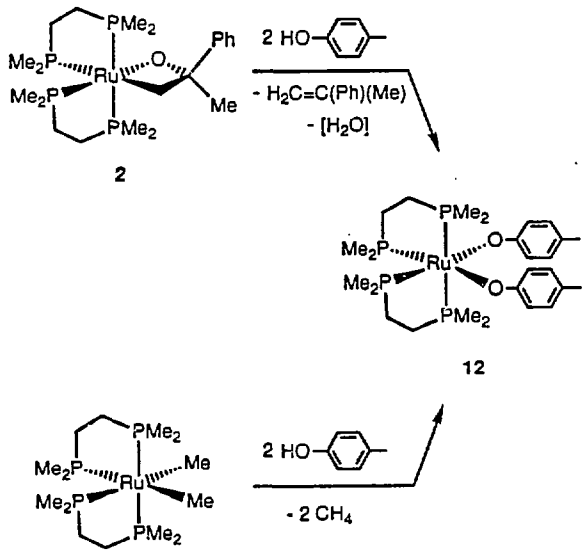
PMe2
Me2P
Ru
O
Ph
Me
Me2P
PMe2
2
2 HO
- H2C=C(Ph)(Me)
- [H2O]
PMe2
Me2P
Ru
O
O
Me2P
PMe2
12
PMe2
Me2P
Ru
Me
Me2P
Me
PMe2
2 HO
- 2 CH4

Scheme 8

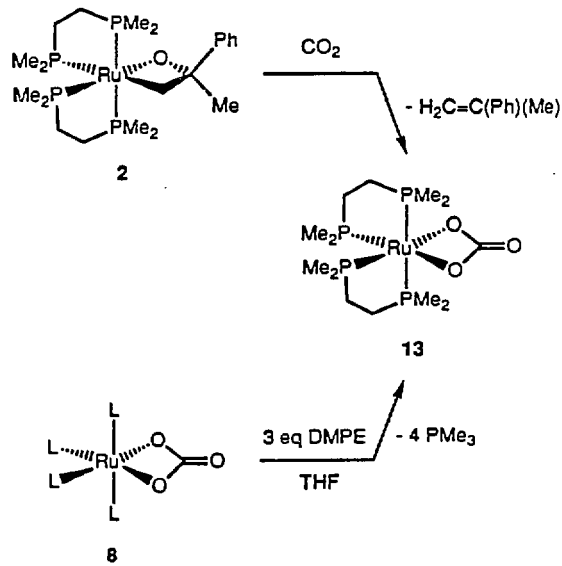
PMe2
Me2P
Ru
O
Ph
Me2P
Me
PMe2
2
CO2
- H2C=C(Ph)(Me)
PMe2
Me2P
Ru
O
O
O
Me2P
PMe2
13
L
L
Ru
O
O
O
L
L
8
3 eq DMPE
THF
- 4 PMe3

Reaction of **2** with one equivalent of benzaldehyde, followed by heating to 110 °C for 2 d led to formation of α-methylstyrene in quantitative yield and hydrido benzoate *trans*-$(DMPE)_2Ru(H)(OC(O)Ph)$ (**14**) in 57% yield (Scheme 9), a transformation analogous to that observed upon addition of benzaldehyde to the PMe_3 substituted metallacycle **1**. However, the reaction with compound **2** required prolonged heating at elevated temperatures. Again the product was prepared independently, this time in 53% isolated yield by addition of 0.25 equivalents of lithium aluminium hydride to the *bis* -benzoate complex **15**. White, crystalline samples of compound **14** were obtained by crystallization from ether, and were characterized by microanalysis, as well as ^1H, $^{31}P\{^1H\}$, and $^{13}C\{^1H\}$ NMR and infrared spectroscopy. The hydride substituent was identified by the quintet ^1H NMR resonance at δ-22.47 and by the absorption at 1907 cm^{-1} in the infrared spectrum. The presence of the benzoate ligand was confirmed by the infrared absorption at 1601 cm^{-1}, by the $^{13}C\{^1H\}$ NMR resonance at δ170.42 and by the presence of the appropriate resonances for a terminal phenyl group in the ^1H and $^{13}C\{^1H\}$ NMR spectra. The trans stereochemistry was indicated by the singlet resonance in the $^{31}P\{^1H\}$ NMR spectrum, the presence of two methyl groups in the ^1H and $^{13}C\{^1H\}$ NMR spectra, and the quintet hydride resonance. The starting *bis*-benzoate complex was prepared in 60-70% isolated yield upon addition of 2 equivalents of benzoic acid to either the naphthyl hydride complex *cis*-$(DMPE)_2Ru(C_{10}H_7)(H)$[24] or the dimethyl complex *cis*-$(DMPE)Ru(Me)_2$.[25] and was spectroscopically characterized. Data for this complex are included in Tables 1-3.

Because C_6D_6 solutions of metallacycle **2** were unchanged upon heating to temperatures below 140 °C, compound **2** could be treated with alkenes and alkynes at higher temperatures than those employed with the PMe_3 metallacycle **1**. However, even heating samples of **2** to 135 °C for 24 h in the presence of *meta*-methyl-α-methylstyrene, styrene, dimethylacetylene, or diphenyl acetylene did not lead to incorporation of these substrates into the metallacycle portion of the molecule. No change in the ^1H and $^{31}P\{^1H\}$ NMR spectra of these reaction mixtures was observed under these conditions.

Scheme 9

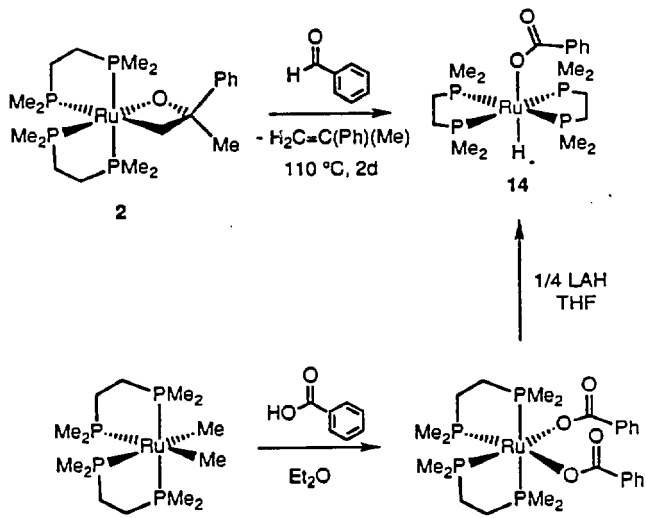
PMe2
Me2P
Ru
O
Ph
Me
Me2P
PMe2
2
H
O
- H2C=C(Ph)(Me)
110 °C, 2d
Ph
O
Me2
Me2
P
Ru
P
P
P
Me2
H
Me2
14
1/4 LAH
THF
PMe2
Me2P
Ru
Me
Me2P
Me
PMe2
HO
O
Et2O
PMe2
Me2P
Ru
O
Ph
O
Me2P
O
Ph
PMe2

Structure and Reactions of $(PMe_3)_4Ru(\eta^2\text{-}OC(CHCMe_3)CH_2)$ (19). We have not been able to crystallographically characterize a ruthenium oxametallacyclobutane containing two sp^3 hybridized carbons in the ring. However, this has been successful with the related sp^2 carbon-containing system, $(PMe_3)_4Ru(OC(CHCMe_3)CH_2)$ (15). This oxametallacyclobutane complex which has a the *tert*-butylmethylene substituent in the β-position, was prepared by the addition of two equivalents of the potassium enolate of 4,4-dimethyl-2-pentanone to the acetate chloride complex $(PMe_3)_4Ru(OAc)(Cl)$, as described in the previous paper. Single crystals suitable for an X-ray diffraction study were obtained by cooling a pentane solution of 15 to -40 °C. The structure was solved by Patterson methods and refined by standard least squares and Fourier techniques. An ORTEP drawing of the molecule is shown in Figure 1. Crystal and data collection parameters are provided in Table 1; intramolecular distances and angles are provided in Tables 2 and 3. The compound crystallized in space group $P2_1/n$, with no unusually short intermolecular distances. The molecule possesses a pseudooctahedal geometry, with the metallacycle occupying two cis sites. The metallacyle portion is flat; the dihedral angle in the ring is 1.9 °. The *tert*-butyl group lies far from the phosphine ligands. All non-bonding distances between the phosphine methyl groups and the *tert*-butyl methyl groups are significantly longer than 4 Å. The C2-O bond length is 1.347(7) Å, similar to the C-O bond length in enols, and the C2-C3 distance is 1.364(9) Å, also similar to the C=C distances in enol tautomers and slighly longer than isolated C=C bonds.[26] The C1-C2 distance is 1.547(9) Å, consistent with a localized carbon-carbon single bond. [26] The phosphine ligands occupy the remaining four sites of the octahedron, and the bond lengths are in the range found in ruthenium compounds of similar structure.[27] The Ru-P(1) distance trans to the oxygen is significantly shorter (2.250(2) Å) than the Ru-P(2) distance trans to the methylene (2.345(2) Å), or the Ru-P(3,4) distance of the mutually trans phosphines (2.341(2) and 2.335(2) Å).

Extrusion of *tert*-butyl allene from 15 upon addition of protic reagents would be analogous to the reactivities of metallacycles 1 and 2. However, addition of 2 equivalents of *p*-cresol to a C_6D_6 solution of 15 led to formation of both the free ketone 4,4-dimethyl-2-pentanone

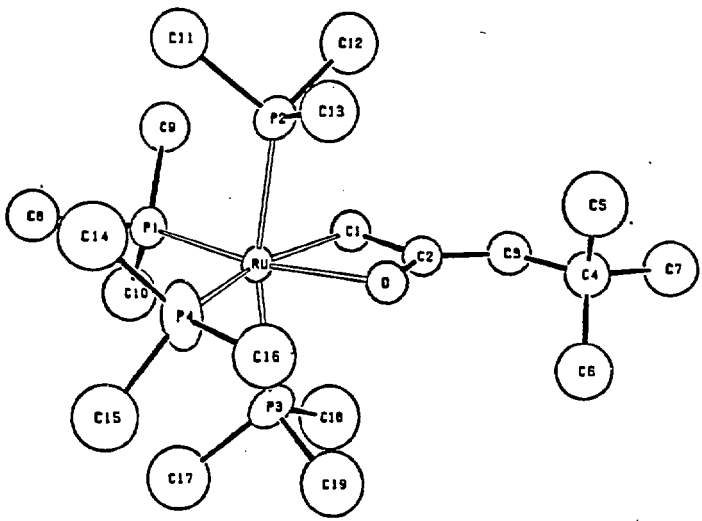

Figure 1. ORTEP drawing of 15

Table 1. Crystal and Data Collection Parameters.[a]

	15	**17**	**18**
Temperature (°C)	-85	-90	-90
Empirical Formula	$RuP_4OC_{19}H_{49}$	$RuP_4OC_{15}H_{42}$	$RuP_3OC_{12}H_{31}$
Formula Weight (amu)	517.6	463.5	385.4
Crystal Size (mm)	0.15x 0.13 x 0.55	0.20 x 0.30 x 0.60	0.12 x 0.26 x 0.27
Space Group	$P2_1/n$	$P2_1/n$	Pnma
a (Å)	9.785(3)	9.337(2)	14.027(2)
b (Å)	19.306(6)	15.615(3)	15.175(3)
c (Å)	14.715(6)	15.536(1)	8.792(1)
α (°)	90.0	90.0	90.0
β (°)	102.73(2)	102.025(15)	90.0
γ (°)	90.0	90.0	90.0
V ($Å^3$)	2711.4(24)	2215.6(13)	1871.4(8)
Z	4	4	4
d_{calc} (gcm^{-3})	1.27	1.43	1.88
μ_{calc} (cm^{-1})	8.1	62.1	14.6
Reflections Measured	+h, +k, ±l	+h, +k, ±l	+h, +k, +l
Scan Width	$\Delta\theta = 0.75 + 0.35 \tan\theta$	$\Delta\theta = 0.85 + 0.35 \tan\theta$	$\Delta\theta = 1.20 + 0.35 \tan\theta$
Scan Speed (θ, °/m)	6.70	6.70	6.70
Setting Angles (2θ, °)[b]	24-28	24-28	22-26

(a) Parameters common to all structures: Radiation: Mo Kα (λ = 0.71073 Å), except for 1c λ = 0.70930 Å. Monochromator: highly-oriented graphite (2θ = 12.2°). Detector: crystal scintillation counter, with PHA. 2θ Range: 3-->45°, except for 1c 2-->45°. Scan Type: θ-2θ. Background: Measured over 0.25(Δθ) added to each end of the scan. Vertical Aperture = 3.0 mm. Horizontal Aperture = 2.0 + 1.0 tanθ mm. Intensity Standards: Measured every hour of x-ray exposure time. Orientation: 3 reflections were checked after every 200 measurements. Crystal orientation was redetermined if any of the reflections were offset from their predicted positions by more than 0.1°. Reorientation was required twice for **1b** and **7a**, and once for **8**. (b) Unit cell parameters and their esd's were derived by a least-squares fit to the setting angles of the unresolved Mo Kα components of 24 reflections with the given 2θ range. In this and all subsequent tables the esd's of all parameters are given in parentheses, right-justified to the least significant digit(s) of the reported value.

Table 2. Intramolecular distances for **15**.

ATOM 1	ATOM 2	DISTANCE
RU	P1	2.250(2)
RU	P2	2.345(2)
RU	P3	2.341(2)
RU	P4	2.335(2)
RU	O	2.146(4)
RU	C1	2.158(7)
C2	O	1.347(7)
C2	C1	1.547(9)
C2	C3	1.364(9)
C3	C4	1.526(9)
C4	C5	1.523(12)
C4	C6	1.524(11)
C4	C7	1.561(10)
P1	C8	1.849(8)
P1	C9	1.854(8)
P1	C10	1.839(9)
P2	C11	1.859(9)
P2	C12	1.838(10)
P2	C13	1.854(9)
P3	C17	1.891(11)
P3	C18	1.861(11)
P3	C19	1.860(11)
P4	C14	1.924(11)
P4	C15	1.834(10)
P4	C16	1.864(10)

Table 3. Intramolecular angles for 15.

ATOM 1	ATOM 2	ATOM 3	ANGLE
P1	RU	P2	94.59(7)
P1	RU	P3	96.14(8)
P1	RU	P4	101.79(7)
P1	RU	O	161.74(12)
P1	RU	C1	94.96(19)
P2	RU	P3	167.78(7)
P2	RU	P4	91.55(9)
P2	RU	O	82.71(13)
P2	RU	C1	87.08(19)
P3	RU	P4	91.98(10)
P3	RU	O	85.27(13)
P3	RU	C1	86.17(20)
P4	RU	O	96.34(13)
P4	RU	C1	163.25(18)
O	RU	C1	66.92(21)
RU	O	C2	94.6(4)
RU	C1	C2	88.5(4)
O	C2	C1	110.0(5)
O	C2	C3	125.5(6)
C1	C2	C3	124.5(6)
C2	C3	C4	125.5(6)
C3	C4	C5	110.7(7)
C3	C4	C6	112.5(6)
C3	C4	C7	107.0(6)
C5	C4	C6	110.5(7)
C5	C4	C7	108.9(7)
C6	C4	C7	107.1(6)
RU	P1	C8	121.9(3)
RU	P1	C9	114.9(3)
RU	P1	C10	118.7(3)
C8	P1	C9	101.9(4)
C8	P1	C10	97.9(4)
C9	P1	C10	97.3(4)
RU	P2	C11	122.6(3)
RU	P2	C12	118.8(3)
RU	P2	C13	113.4(3)
C11	P2	C12	99.8(4)
C11	P2	C13	99.8(4)
C12	P2	C13	98.3(4)
RU	P3	C17	123.5(3)
RU	P3	C18	117.8(4)
RU	P3	C19	111.8(3)
C17	P3	C18	99.0(5)
C17	P3	C19	100.3(5)
C18	P3	C19	101.0(5)
RU	P4	C14	122.6(3)
RU	P4	C15	122.1(3)
RU	P4	C16	111.4(3)
C14	P4	C15	95.4(5)
C14	P4	C16	101.7(4)
C15	P4	C16	99.7(4)

Scheme 10

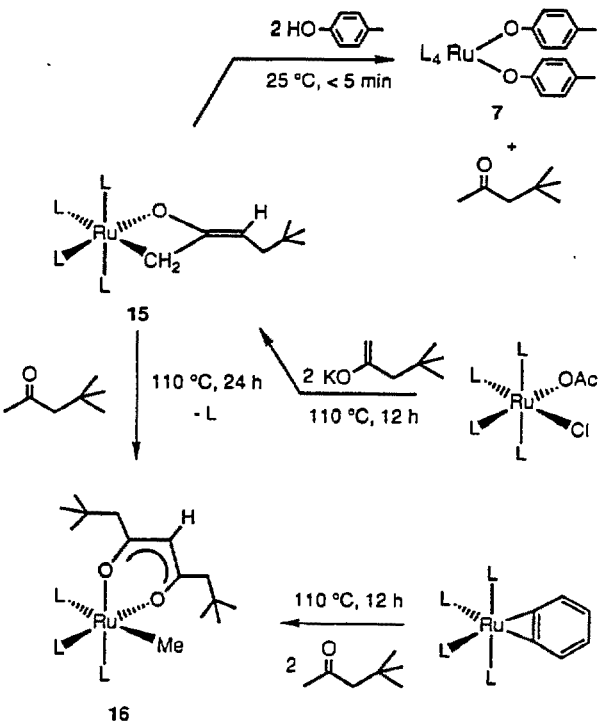
2 HO
25 °C, < 5 min
L4 Ru
O
O
7
+
O
L
L
Ru
O
H
L
CH2
L
15
O
110 °C, 24 h
- L
2 KO
110 °C, 12 h
L
L
Ru
OAc
L
Cl
L
H
O
L
Ru
O
L
Me
L
16
110 °C, 12 h
2
O
L
L
Ru
L

and the *bis*-cresolate complex **7** in quantitative yield (Scheme 10). ^{1}H NMR spectroscopic identification of the organic product was confirmed by comparing the GC retention time with that of an authentic sample.

Although **15** does not extrude alkene by a C-O bond cleavage process analogous to that observed with **1** and **2**, it does undergo a different type of ketone carbon-carbon bond cleavage. Addition of 4,4-dimethyl-2-pentanone followed by heating to 110 °C for 12 h led to formation of the di-*tert*-butyl substituted acetylacetonate complex **16** in 77% yield by ^{1}H NMR spectroscopy. This product is again the result of a carbon-carbon bond formation and a subsequent carbon-carbon bond cleavage process. Compound **16** was more conveniently generated by the addition of 2 equivalents of the potassium enolate of 4,4-dimethyl-2-pentanone to the acetate chloride complex $(PMe_3)_4Ru(OAc)(Cl)$[19] which generated reactants **15** and free ketone *in situ*. Alternatively, compound **16** was synthesized on a preparative scale by the addition of 2 equivalents of 4,4-dimethyl-2-pentanone to $(PMe_3)_4Ru(\eta^2\text{-}C_6H_4)$,[15] followed by heating to 110 °C for 24 h. Yellow crystals of **16** were isolated from this reaction in 35% yield and were characterized by microanalysis as well as by ^{1}H, ^{31}P{^{1}H}, and ^{13}C{^{1}H} NMR and infrared spectroscopy. In addition, the organic ligand was identified by treating a solution of **16** with a slight excess of concentrated HCl to form free *tert*-butyl acetylacetone in quantitative yield by ^{1}H NMR spectroscopy. The free ketone was characterized by comparing its GC retention time and ^{1}H NMR spectrum with those of an authentic sample. The bound organic ligand was identified by the presence of two infrared bands at 1576 cm^{-1} and 1561 cm^{-1}, a methine ^{1}H NMR resonance at δ5.15, and two chemically equivalent neopentyl groups, each exhibiting an AB methylene pattern in the ^{1}H NMR spectrum. An A_2B pattern in the ^{31}P{^{1}H} NMR spectrum was consistent with the presence of equivalent neopentyl groups. The metal-bound methyl group was identified by a doublet of triplets resonance at δ0.34 in the ^{1}H NMR spectrum, integrating to three protons, and a CH_3 resonance (confirmed by a DEPT pulse sequence) with a similar splitting pattern in the ^{13}C{^{1}H} NMR spectrum at δ4.83.

Structure and Reactions of $(PMe_3)_4Ru((CH_2)CO)$ (17). The compound $(PMe_3)_4Ru(CH_2C(O))$ (**17**), a second metallacycle formed by metallation of a ruthenium enolate, has been prepared as described in the previous paper. Unlike its analogue, compound **15**, the acetone dianion complex **17** does not contain a ruthenium-oxygen bond; rather, the complex is bound through the two CH_2 groups. A single crystal suitable for an X-ray diffraction study was obtained by cooling a pentane solution to -40 °C. The structure was solved by Patterson methods and refined by standard least squares and Fourier techniques. An ORTEP drawing of the molecule is shown in Figure 2. Crystal and data collection parameters are provided in Table 1; intramolecular distances and angles are provided in Tables 4 and 5. The compound crystallized in space group $P2_1/n$, with no unusually short intermolecular distances. Although both complexes contain an sp^2-hybridized carbon at the β-position of the ring, the solid state structure of **17** is markedly different from the planar *tert*-butyl substituted analogue **15**. Compound **17** contains two ruthenium-carbon linkages, and a large dihedral angle of 45.6(5)° for the metallacycle, although the Ru-O distance remains long. The C(3)-O distance is 1.261(3) Å, significantly longer than the average C=O bond length in cyclobutanones, while the C(1)-C(3) and C(2)-C(3) distances are 1.468(7) and 1.459(7) Å respectively, significantly shorter than typical carbon-carbon C(O)-C bonds in ketones, including the average of those in cyclobutanones, 1.529 Å.[26] The distances between the carbonyl oxygen atom of the organic substituent and the two nearest phosphine methyl groups are 2.977(6) Å and 3.133(7) Å, much shorter than the closest interactions of the organic substituent of **15** with the trimethylphosphine ligands.

Compound **17** underwent facile phosphine ligand dissociation to form the oxatrimethylenemethane complex **18**, as shown in Scheme 11. Tris-phosphine compound **18** was isolated by removing solvent and excess PMe_3 at 25 °C under reduced pressure, followed by sublimation. The ^1H NMR spectrum displayed two methylene resonances but the $^{13}C\{^1H\}$ NMR spectrum contained only one CH_2 resonance, indicating that the two protons on each carbon are inequivalent. The $^{31}P\{^1H\}$ NMR spectrum displayed an A_2B pattern, consistent with loss of one PMe_3 ligand from **17**.

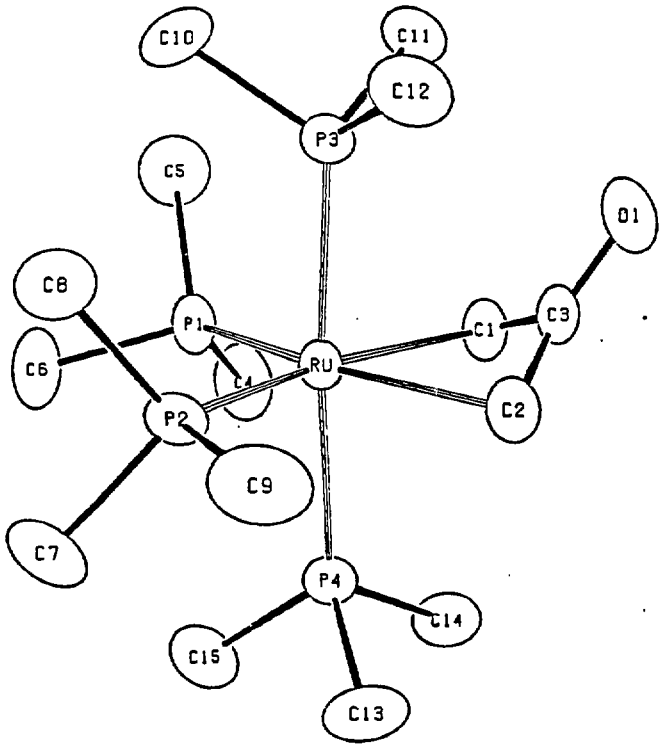

Figure 2. ORTEP drawing of 17

Table 4. Intramolecular distances for **17**.

ATOM 1	ATOM 2	DISTANCE
RU	P1	2.308(1)
RU	P2	2.324(1)
RU	P3	2.358(1)
RU	P4	2.352(1)
RU	C1	2.217(4)
RU	C2	2.222(5)
C1	C3	1.468(7)
C2	C3	1.459(7)
C3	O1	1.261(6)
P1	C4	1.838(5)
P1	C5	1.842(5)
P1	C6	1.827(5)
P2	C7	1.835(5)
P2	C8	1.836(5)
P2	C9	1.837(5)
P3	C10	1.850(5)
P3	C11	1.814(5)
P3	C12	1.814(6)
P4	C13	1.838(5)
P4	C14	1.839(5)
P4	C15	1.836(5)

Table 5. Intramolecular angles for 17.

ATOM 1	ATOM 2	ATOM 3	ANGLE
P1	RU	P2	103.23(4)
P1	RU	P3	92.50(4)
P1	RU	P4	91.72(4)
P1	RU	C1	92.68(13)
P1	RU	C2	158.11(14)
P2	RU	P3	90.78(4)
P2	RU	P4	89.77(4)
P2	RU	C1	163.79(13)
P2	RU	C2	98.15(14)
P3	RU	P4	175.50(5)
P3	RU	C1	88.23(13)
P3	RU	C2	91.86(13)
P4	RU	C1	90.00(13)
P4	RU	C2	83.65(13)
C1	RU	C2	65.72(18)
RU	C1	C3	83.5(3)
RU	C2	C3	83.5(3)
O1	C3	C1	124.1(5)
O1	C3	C2	123.0(5)
C1	C3	C2	110.8(4)
RU	P1	C4	115.36(18)
RU	P1	C5	120.59(19)
RU	P1	C6	121.36(17)
C4	P1	C5	95.6(3)
C4	P1	C6	101.74(24)
C5	P1	C6	97.5(3)
RU	P2	C7	121.99(17)
RU	P2	C8	122.41(16)
RU	P2	C9	113.67(20)
C7	P2	C8	95.93(25)
C7	P2	C9	100.1(3)
C8	P2	C9	98.0(3)
RU	P3	C10	121.47(18)
RU	P3	C11	118.50(18)
RU	P3	C12	115.16(19)
C10	P3	C11	97.82(24)
C10	P3	C12	100.6(3)
C11	P3	C12	99.4(3)
RU	P4	C13	117.94(18)
RU	P4	C14	117.66(17)
RU	P4	C15	122.70(19)
C13	P4	C14	98.26(24)
C13	P4	C15	97.4(3)
C14	P4	C15	98.08(25)

Scheme 11

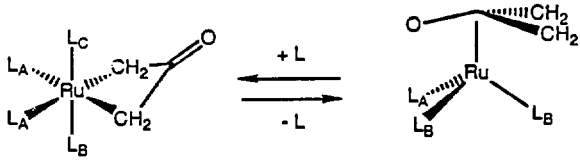

17 18

An X-ray diffraction study was conducted on a single crystal of **18**, obtained by sublimation in a sealed tube over a period of two weeks at 55 °C. The structure was solved by Patterson methods and refined by standard least squares and Fourier techniques. An ORTEP drawing of the molecule is shown in Figure 3. Crystal and data collection parameters are provided in Table 1; intramolecular distances and angles are provided in Tables 6 and 7. The compound crystallized in space group $P2_1/n$, with no unusually short intermolecular distances. The study was hampered by a poor data set, due to poor crystal quality or disorder between the methylene and oxygen positions in the organic ligand. As a result, the data were used principally to confirm the connectivity of **18**, rather than to provide detailed information concerning the bonding mode. Nevertheless, certain overall features of the molecule remained unambiguous. The organic substituent and the three phosphine ligands adopt a staggered conformation, making the overall geometry pseudooctahedral. In addition, the oxatrimethylenemethane substituent is bound in an η^4-fashion. The central carbon is located above the plane of the other three atoms, although the Ru-C(1) distance (1.99(2) Å) remains significantly shorter than the two Ru-C(2) (2.27(1) Å) distances and the Ru-O distance (2.22(1) Å).

$^{31}P\{^1H\}$ NMR spectroscopy of a toluene-d_8 solution prepared from a crystalline sample of compound **17** and one equivalent of phosphine demonstrated that compounds **17** and **18** exist in equilibrium under these conditions. Figure 4 displays a stacked plot of the $^{31}P\{^1H\}$ NMR spectra of such a solution between the temperatures -80 °C and 60 °C. At temperatures below -20 °C, only the complex containing four phosphines (**17**) was observed, while at 60 °C, **18** was the predominant species. Although interconversion of **17** and **18** did not occur rapidly enough to average their distinctive $^{31}P\{^1H\}$ NMR signals, equilibration of the two compounds was complete after less than 5 min even at -20 °C.

Because of the instability of compound **17**, only a few reactivity studies with this complex were attempted. For example, a solution of **17** and free acetone, generated *in situ* by addition of two equivalents of the potassium enolate of acetone to *cis*-$(PMe_3)_4Ru(OAc)(Cl)$,[19] led to clean formation of $(PMe_3)_4Ru(OC(Me)CHC(Me)CH)$ in 45% isolated yield after heating to 85 °C for 8 h

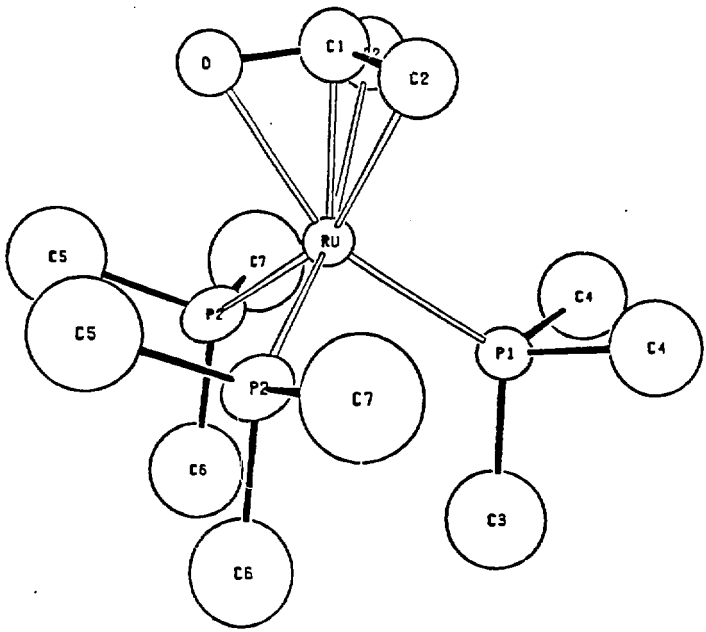

Figure 3. ORTEP drawing of 18

Table 6. Intramolecular distances for 18.

ATOM 1	ATOM 2	DISTANCE
RU	P1	2.237(4)
RU	P2	2.286(3)
RU	O	2.224(10)
RU	C1	1.985(19)
RU	C2	2.265(12)
C1	O	1.325(17)
C1	C2	1.388(13)
P1	C3	1.790(24)
P1	C4	1.820(15)
P2	C5	1.795(17)
P2	C6	1.790(17)
P2	C7	1.828(20)

Table 7. Intramolecular angles for **18**.

ATOM 1	ATOM 2	ATOM 3	ANGLE
P1	RU	P2	96.90(11)
P1	RU	O	157.6(3)
P1	RU	C1	121.4(5)
P1	RU	C2	100.1(3)
P2	RU	P2	98.62(16)
P2	RU	O	97.68(19)
P2	RU	C1	119.0(3)
P2	RU	C2	156.3(3)
O	C1	C2	115.6(9)
C2	C1	C2	123.2(16)
RU	P1	C3	120.8(8)
RU	P1	C4	117.3(5)
C3	P1	C4	101.6(7)
C4	P1	C4	93.6(10)
RU	P2	C5	111.1(6)
RU	P2	C6	124.9(6)
RU	P2	C7	115.8(6)
C5	P2	C6	103.7(7)
C5	P2	C7	101.0(8)
C6	P2	C7	97.1(8)

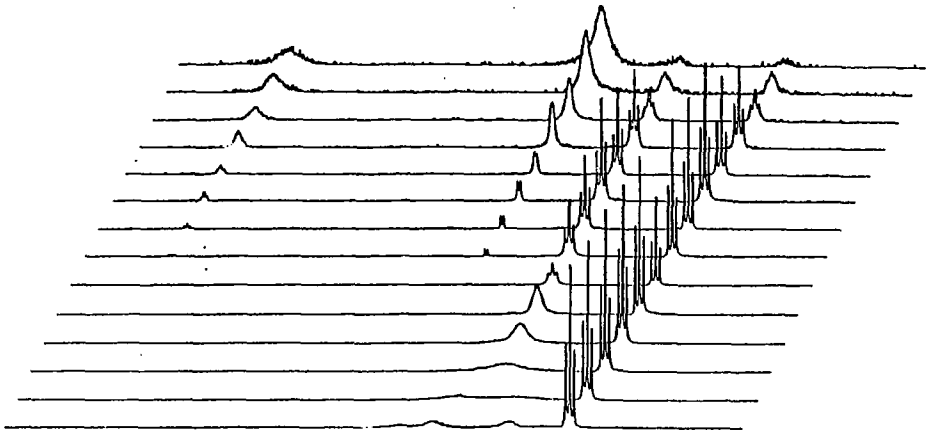

Figure 4. Variable temperature $^{31}P\{^{1}H\}$ NMR spectra of **17** $\rightleftharpoons$ **18** + PMe_3.

Scheme 12

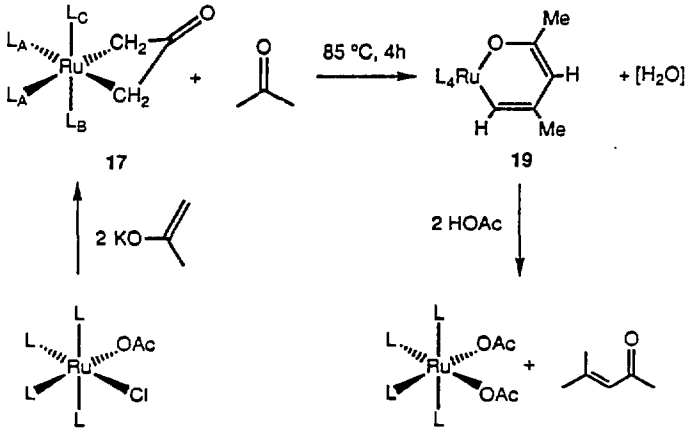

(Scheme 12). The organic portion of **19** can be thought of as a coordinated dianion of the aldol condensation product. This complex was isolated from cold pentane as yellow crystals which were characterized by microanalysis, as well as ^1H, $^{31}P\{^1H\}$, and $^{13}C\{^1H\}$ NMR and infrared spectroscopy. In addition, the identity of the organic ligand was confirmed by treating **19** with two equivalents of acetic acid to form $(PMe_3)_4Ru(OAc)_2$ and free mesityl oxide in 74% yield. This free aldol product was identified by comparison of its ^1H NMR spectrum and GC retention time to those of an authentic sample. The coordinated organic fragment was identified by a doublet of doublet of triplets pattern in the ^1H, and $^{13}C\{^1H\}$ NMR spectra corresponding to one metal bound methine group, and a singlet resonance corresponding to the other. Two resonances for methyl groups not bound to ruthenium were also observed in the ^1H and $^{13}C\{^1H\}$ NMR spectrum. All $^{13}C\{^1H\}$ NMR assignments were confirmed by using a DEPT pulse sequence. The A_2BC pattern in the $^{31}P\{^1H\}$ NMR spectrum, with P_B resonating upfield and P_C resonating downfield of P_A, was consistent with the presence of one ruthenium-carbon and one ruthenium-oxygen bond.

Reactions of $(PMe_3)_4Ru(\eta^2\text{-}OC(tert\text{-}Bu)CH)$ (20). Oxametallacylobutene complex **20** was obtained by extrusion of methane from the methyl enolate complex $(PMe_3)_4Ru(Me)(OC(CH_2)CMe_3)$ at 65 °C over the course of 8 h, as described in the previous paper. Initial reactivity studies with **20** were directed toward determining if addition of protic acids and electrophiles would result in the elimination of *tert*-butylacetylene, in analogy to the behavior of **1** and **2**, or if the organic substituent would remain intact, as it did with complex **15**. The reactions of oxametallacyclobutene **20** with *p*-cresol and CO_2 are shown in Scheme 13. Compound **20** was converted to free pinacolone (3,3-dimethyl-2-butanone) in quantitative yield by ^1H NMR spectroscopy and the *bis*-cresolate complex **7** (91%) when treated with *p*-cresol. Again, the identification of the ketone was confirmed by comparison of GC retention times and ^1H NMR spectra with those of an authentic sample.

Addition of one equivalent of CO_2 to a benzene solution of **20** led rapidly to $(PMe_3)_4Ru(\eta^2\text{-}OC(O)OC(tert\text{-}Bu)CH)$ (**21**), the product of insertion into the metal-oxygen bond. No evidence for formation of *tert*-butylacetylene was observed. Compound **21** was isolated from

Scheme 14

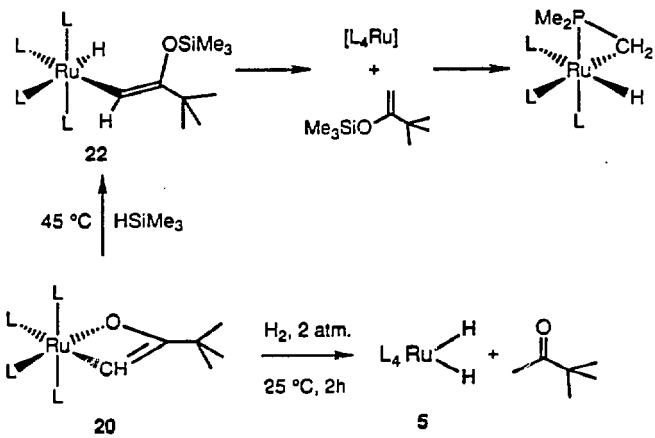
L
L
H
Ru
L
L
H
OSiMe3
22
[L4Ru]
+
Me3SiO
Me2P
CH2
L
Ru
L
H
L
45 °C
HSiMe3
L
L
O
Ru
CH
L
L
20
H2, 2 atm.
25 °C, 2h
L4 Ru
H
H
+
O
5

the reaction mixture as clear crystals in 42% yield, and was characterized by ^1H, $^{31}P\{^1H\}$, and $^{13}C\{^1H\}$ NMR and infrared spectroscopy as well as microanalysis. The inserted CO_2 moiety was identified by its $^{13}C\{^1H\}$ NMR resonance at δ156.6 and an infrared absorption at 1633 cm^{-1}. Conclusive evidence for the presence of a ruthenium-carbon bond in the product was provided by its ^1H NMR spectrum, which contained a doublet of triplets resonance for the methine proton at δ5.34, and by its $^{13}C\{^1H\}$ NMR spectrum, which contained a doublet of triplets of doublets resonance at δ111.0 for the methine carbon. An A_2BC pattern in the $^{31}P\{^1H\}$ NMR spectrum, with P_B resonating upfield and P_C resonating downfield of the mutually trans phosphines, was consistent with the presence of one ruthenium-carbon and one ruthenium-oxygen bond.

Reactions of **20** with hydrogen and trimethylsilane are shown in Scheme 14. When a C_6D_6 solution of **20** was exposed to 2 atm of H_2, formation of free pinacolone in 61% yield by ^1H NMR spectroscopy and dihydride **5**[18, 19] (77%) was observed after 1 h. Similarly, addition of trimethylsilane, followed by heating at 85 °C for 2 h, led to the silyl enol ether of pinacolone in 43% yield as the organic product. In this case, the organometallic product was the previously reported phosphine-cyclometallated complex $(PMe_3)_3Ru(CH_2PMe_2)(H)$[18b, 28] in 40% yield. ^1H NMR spectroscopic identification of both the ketone and silyl enol ether was confirmed by matching GC retention times to those of authentic samples.

A possible mechanism for this reaction is shown in Scheme 14. When a solution of **20** and trimethylsilane was heated to 45 °C, an intermediate was observed by ^1H and $^{31}P\{^1H\}$ NMR spectroscopy but not fully characterized. This intermediate may be the vinyl hydride complex **22**, since formation of cyclometallated compound $(PMe_3)_3Ru(CH_2PMe_2)(H)$ as the organometallic product is consistent with C-H reductive elimination from **17** to form the silyl enol ether and intermediate $(PMe_3)_4Ru$. This Ru(0) intermediate was shown to form **18** cleanly in a separate study.[29]

Scheme 14

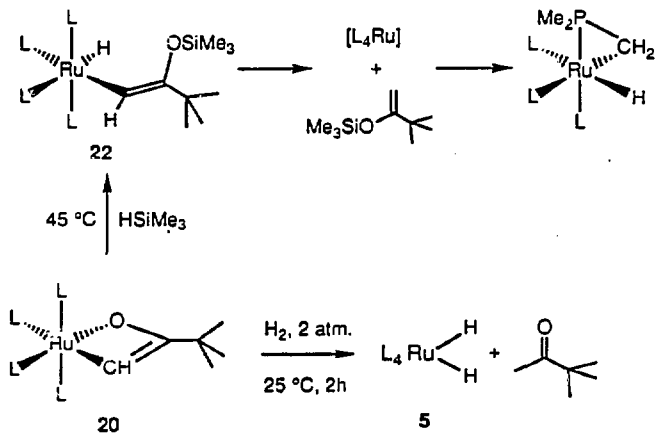
L
L
Ru
H
OSiMe3
L
L
H
22
[L4Ru]
+
Me3SiO
Me2P
CH2
L
Ru
L
H
L
45 °C
HSiMe3
L
L
Ru
O
CH
L
20
H2, 2 atm.
25 °C, 2h
L4 Ru
H
H
+
O
5

Discussion

Effect of dative ligands on reactivity.(a) *Thermal reactions.* The propensity of PMe_3-substituted oxametallacycle **1** to extrude methane and form **3** at 45 °C, compared to the stability of its DMPE-substituted analogue **2** at 140 °C, is consistent with a pathway for this process that is based on the mechanism for the formation of **1** reported in the accompanying paper. A complete mechanism for the C-C cleavage process (including the preparation of metallacycle **1**) is shown in Scheme 15. This mechanism involves β-Me elimination to form $(PMe_3)_4Ru(Me)(OC(CH_2)Ph)$ (**4**), a process that is the reverse of the phenyl migration step to form **1**. Intermediate **4** simply forms methane and **3** by metallation of the aryl ring.[15, 30] The experiments reported in the previous paper in this issue demonstrate that the phenyl migration step proceeds by an initial, reversible dissociation of phosphine to form an η^3-bound enolate substituent. The phenyl group then migrates to the central carbon of this η^3-bound acetone enolate. We therefore propose an analogous β-methyl elimination process to form **4** by way of an η^3-bound acetophenone enolate. Our results with the DMPE analogues are consistent with this hypothesis since the DMPE intermediate that is analogous to **4** is less likely to undergo phosphine dissociation, resulting in the stability of metallacycle **2**. Although we have not obtained any mechanistic data regarding the carbonyl-methyl C-C bond cleavage reaction of 4,4-dimethyl-2-pentanone by **15**, it is possible that *β-methyl elimination from an oxametallacylobutane* complex or another oxametallacycle is involved in this reaction. Previous examples of β-methyl elimination reactions have been reported with electrophilic early transition metal and lanthanide complexes,[16f, g] and a β-cyano elimination was reported to occur from a platinum oxametallacyclobutane.[6b]

Reactions with electrophiles and protic acids. The reactions of oxametallacycles **1** and **2** with the protic acid *p*-cresol and the electrophile CO_2 both occur at room temperature over several minutes. Because dissociation of phosphine would be expected to require higher temperatures for the DMPE complex **2** than for the PMe_3 complex **1**, we conclude that reactions with these reagents occurs directly at the oxygen atom of the metallacycle, and do not involve

Scheme 15

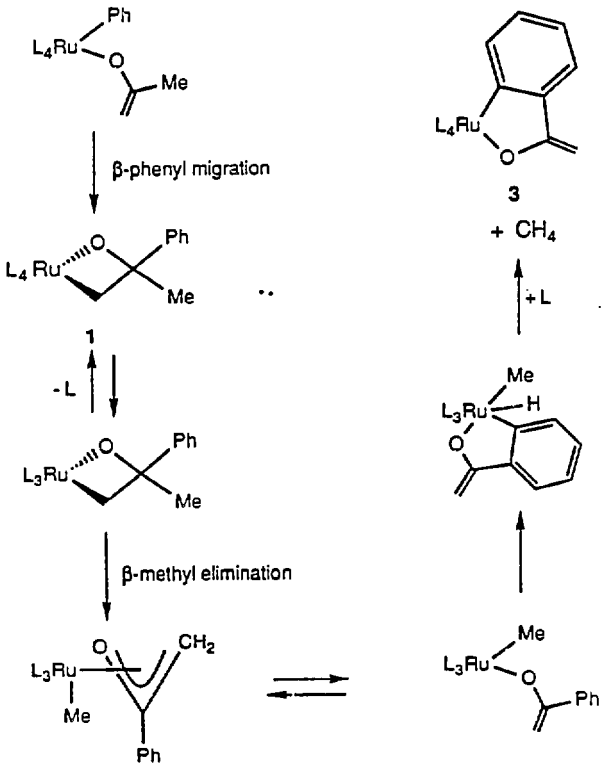
Ph
L4Ru
O
Me
β-phenyl migration
L4 Ru
O
Ph
Me
1
-L
L3Ru
O
Ph
Me
β-methyl elimination
L3Ru
O
CH2
Me
Ph
L4Ru
O
3
+ CH4
+L
Me
L3Ru
H
O
L3Ru
Me
O
Ph

coordination to the metal center by either the organic substrate or the extruded alkene, as shown in Scheme 16. The oxygen atom connected to the electron rich metal center is apparently basic enough to deprotonate *p*-cresol and nucleophilic enough to attack CO_2. Formation of a formal positive charge at the metallacyclic oxygen atom, followed by cleavage of the C-O bond, extrudes alkene. This process is similar to the dehydration of tertiary alcohols catalyzed by protic and Lewis acids.[31] In contrast, the reaction of these two compounds with benzaldehyde under very different conditions may reflect the involvement of phosphine dissociation during this transformation. At 110 °C it is possible that dissociation of one end of the DMPE ligand may allow coordination of the aldehyde. However, no experiments that would address the requirements for ligand dissociation in this reaction were conducted with either complex .

The failure of the oxametallacycles to incorporate alkenes or alkynes suggests that the reactions of these compounds do *not* occur by way of a ruthenium-oxo intermediate. Our results do not rigorously rule out reversible formation of a ruthenium-oxo intermediate with alkene coordinated to the metal center, but it seems likely that the resulting coordinated α-methylstyrene would dissociate at 135 °C and lead to incorporation of another alkene or alkyne into the metallacycle.

Effect of metallacycle on reactivity. In contrast to extrusion of alkene from **1** and **2**, metallacylobutane **17** and metallacyclobutene **20** extrude free ketone upon addition of protic acids. We propose that the aryl group of metallacycles **1** and **2** helps to stabilize the partial positive charge on the β-carbon of the metallacyle that occurs after addition of the acid or electrophile, as shown in Scheme 16. Again, our explanation is analogous to the one used to explain the rate enhancement of ionization caused by phenyl substitution in benzyl alcohols.[30]

Effect of ring substitution on structure. The *tert*-butyl substituent in compound **15** leads to a markedly different solid state structure relative to **17**, as determined by an X-ray diffraction study. First, the enolate dianion in **17** is bound through two Ru-CH_2 linkages, while the organic portion of **15** is bound by one Ru-CH_2 and one Ru-O linkage. The substitution of a bulky group in the methylene position of **17** appears to cause the *tert*-butyl substituted cyclic enolate

Scheme 16

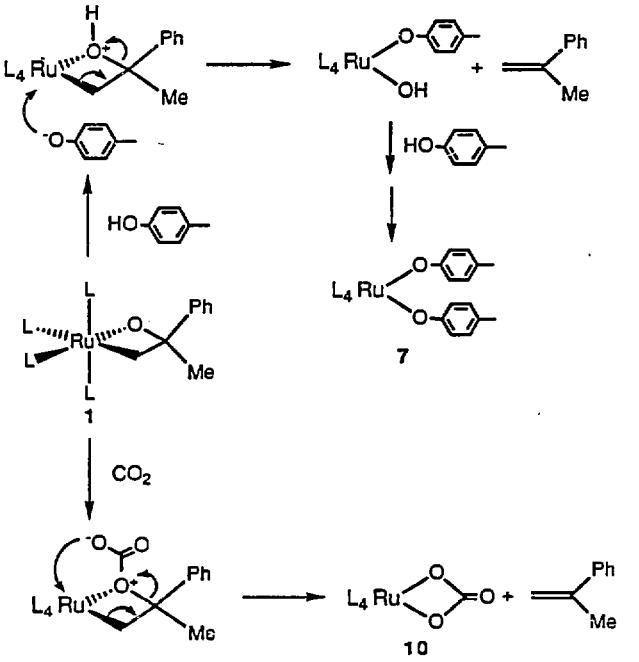
H
Ph
L4 Ru
O+
Me
-O
HO
L
Ru
O
Ph
Me
1
CO2
-O
O
O+
L4 Ru
Ph
Me
L4 Ru
O
OH
+
Ph
Me
HO
L4 Ru
O
O
7
L4 Ru
O
O
O +
Ph
Me
10

15 to bind through one methylene and one oxygen atom rather than to bind through two methylene groups as was observed in **15**.

The two different binding modes apparently give rise to a second dramatic difference between the two structures: the dihedral angle of **15** is 1.9°, while that in **17** is 45.6°. The solid state structure demonstrates that the *tert*-butyl substitution does not significantly affect the steric interactions of the metallacycle with the phophine ligands. In fact, the shortest distance between the *tert*-butyl group in **15** and the nearst phosphine methyl is greater than 1 Å longer than the shortest distance between the carbonyl oxygen atom of **17** and the nearest phosphine methyl group. The $^{31}P\{^{1}H\}$ NMR spectroscopic data indicate that the solution structures are similar to those in the crystalline state. Ring inversion in **17** is slow on the NMR timescale at -70 °C, as indicated by the inequivalent trans phosphine resonances observed at this temperature, but inversion of the metallacycle in **15** is rapid at -90 °C, since the mutually trans phophines are equivalent at this temperature, consistent with a nearly flat ring system for **15** or one with a dramatically lower barrier to inversion in solution.

It seems reasonable to attribute the difference in dihedral angles to electronic differences within the two rings rather than to steric or solid state effects. Theoretical studies have indicated that the large dihedral angles in platinum metallacyclobutan-3-ones are due to a significant contribution of the bonding description **B** shown in Figure 5, and our data are consistent with this proposal.[32e] The C=O bond is significantly longer and the C(O)-C bonds are significantly shorter than those in simple organic ketones,[26] including cyclobutanones. In addition the C=O bond in **17** absorbs at 1544 cm^{-1} (data provided in companion paper), significantly lower in energy than organic ketones. In contrast, the metallacycle portion of **15** contains C-C and C-O bond distances which are similar to those observed for the enol form of organic ketones;[26] these indicate little interaction between the π-system of the ring and the ruthenium metal center.

There are few other structural data relating to the conformation of metallacyclobutane rings. Although several structurally characterized metallacyclobutan-3-ones have been reported, all of these are bound to the metal center through the two enolate carbon atoms; compound **15** is

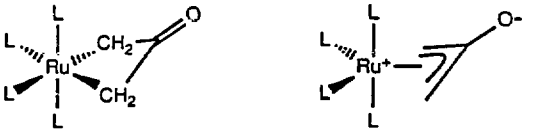

Figure 5. Possible bonding modes for **17**.

the only structurally characterized example of the alternative O- and C-bound isomer.[31] Furthermore, structural data on titanocene complexes shows a trend opposite to that observed with these ruthenium complexes: X-ray structural data for titanacyclobutanes (two Ti-CH_2 linkages) show flat metallacycles,[33] while NMR spectroscopic data on titanaoxacyclobutanes analogous to compound **15** (one Ti-CH_2 linkage and one Ti-O linkage) indicate a puckered ring structure.[8a] In contrast, the structures of a platinum[6a] and a rhodium[7] oxametallacyclobutane display rings that are nearly flat. In addition, the organic analogues display the same trend; cyclobutane is bent, while oxetane is planar in the gas phase.[34]

The overall structural features of the oxatrimethylenemethane complex **18** are similar to those observed with parent trimethylenemethane complexes.[35] Principally, the central carbon atom of the organic ligand is located significantly out of the plane of the other three atoms. This similarity contrasts with observations made on other recently reported heteroatom-substituted systems. In particular, an oxatrimethylenemethane complex of $Fe(CO)_3$ adopts a dimeric structure,[36] and a thiatrimethylenemethane complex of $Fe(CO_3)$[37] shows an unsymetrically bound organic ligand, perhaps due to phenyl substitution at one carbon and *tert*-butyl substitution at the other. A nearly planar oxatrimethylenemethane fragment was observed in a dimeric ruthenium complex.[38] The central carbon was only 0.07 Å above the plane of the other three atoms.

Insertion reactions with CO and CO_2. Extensive mechanistic information indicates that insertion of CO into metal-alkyl bonds involves coordination of free carbon monoxide to the metal center, followed by migration of the alkyl group.[39] Therefore, it is not surprising that the DMPE substituted metallacycle **3** is inert toward insertion of CO into the metal-carbon bond, while PMe_3 substituted metallacycle **1** readily reacts with CO to form insertion product **6**. However, it is interesting to note that CO reacts with the Ru-C bond of **1** in preference to the Ru-O bond, and that metallacycle **2** is inert toward insertion of CO into the metal-oxygen bond. This demonstrates that migration of the methylene end of the metallacycle is faster than migration of the alkoxide end. Moreover, a mechanism involving direct insertion of CO into the

metal-heteroatom bond or dissociation of an alkoxide anion followed by attack of a coordinated or free CO does not occur in this ruthenium system. Such a mechanism has been reported to occur with a square planar iridium system,[40] but intramolecular migration to a coordinated ligand appears to occur with other systems.[41]

In contrast to the alkene extrusion processes that occur upon addition of CO_2 to oxametallacyclobutanes **1** and **2**, as well as the propensity of **1** to undergo insertion of CO into the metal-carbon bond, addition of CO_2 to oxametallacyclobutene **20** led to insertion into the ruthenium-oxygen bond. An extensive report of relative insertion rates of CO and CO_2 with other compounds of the $(PMe_3)_4Ru(X)(Y)$ system is provided in a separate study,[42] including the insertion of CO_2 into the metal-carbon bond of $(PMe_3)_4Ru(OC_6H_3Me)$ (**23**) shown in Equation 1.

The results in that study suggested that selectivities were controlled by the nucleophilicity of the heteroatom of the metallacycle and electrophilicity of the organic substrate. In light of these earlier results, we propose that the greater nucleophilicity of the enolate oxygen atom of **20** (compared to the aryloxide oxygen atom of **23**) and the greater electrophilicity of CO_2 (compared to CO) allows for direct attack of CO_2 by the oxygen atom of **20**. Such a mechanism would account for the observed selectivities of compounds **1**, **20**, and **23** for CO and CO_2.

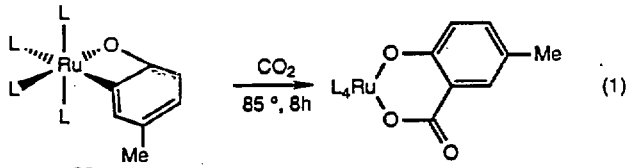

23

(1)

Table 8. ^{1}H NMR spectroscopic data.

Compound	δ(ppm)	mult[a]	J(Hz)	int	assignment[b]
$(PMe_3)_4Ru(OC(CH_2)C_6H_4)$ (3)[d]	1.02	t	3.0	18	*trans*-PMe_3
	1.42	d	6.9	9	*cis*-PMe_3
	1.45	d	6.0	9	*cis*-PMe_3
	3.39	d	1.2	1	$(OC(\underline{CH_aH_b})C_6H_4)$
	3.95	br,s		1	$(OC(CH_a\underline{H_b})C_6H_4)$
	6.61	tq	7.3, 1.0	1	$(OC(CH_2)\underline{C_6H_4})$
	6.63	t	7.7	1	
	7.11	dt	7.6, 1.6	1	
	7.46	m		1	
(CO)(PMe_3)Ru (OC(Me)(Ph)CH_2C(O)) (6)[e]	0.87	d	7.3	9	PMe_3
	1.02	d	6.1	9	
	1.25	d	7.2	9	
	1.47	s		3	$(OC(\underline{Me})(Ph)CH_2C(O))$
	2.98	d	15.5	1	$(OC(Me)(Ph)\underline{CH_aH_b}C(O))$
	3.09	dd	15.5, 4.0	1	$(OC(Me)(Ph)CH_a\underline{H_b}C(O))$
	7.12	t	7.2	1	$(OC(Me)(\underline{Ph})CH_2C(O))$
	7.29	t	7.6	2	
	8.82	d	7.8	2	
cis-$(PMe_3)_4Ru(OC_6H_4$-*p*-$Me)_2$ (7)[e]	0.96	d	7.7	18	*cis*-PMe_3
	1.14	t	3.1	18	*trans*-PMe_3
	2.40	s		6	$(OC_6H_4$-*p*-$\underline{Me})_2$
	7.04	d	8.4	4	$(O\underline{C_6H_4}$-*p*-$Me)_2$
	7.22	d	8.3	4	
$(PMe_3)_4Ru(CO_3)$ (8)[f]	1.40	t	3.3	18	*trans*-PMe_3
	1.40	m		18	cis-PMe_3
$(PMe_3)_4Ru(OC(NPh)O)$ (9)[g]	1.37	m		36	*cis*- and *trans*-PMe_3
	6.55	t	7.7	1	$(OC(N\underline{Ph})O)$
	6.96	t	7.3	2	
	7.22	d	7.5	2	
$(PMe_3)_4Ru(OC(O)NPh)$ (10)[h]	1.28	t	2.8	18	*trans*-PMe_3
	1.44	d	7.9	9	*cis*-PMe_3
	1.47	d	7.4	9	*cis*-PMe_3
	6.53	t	7.1	1	$(OC(O)N\underline{Ph})$
	7.03	t	7.7	2	
	7.27	d	7.9	2	
cis-$(PMe_3)_4Ru(H)(OC(O)Ph)$ (11)[e]	-8.21	dq	101, 25.7	1	Ru-H
	1.00	d	7.4	9	*cis*-PMe_3
	1.28	d	5.4	9	*cis*-PMe_3
	1.32	br s		18	*trans*-PMe_3
	7.21	t	6.8	1	$(OC(O)\underline{Ph})$
	7.30	t	7.5	2	
	8.48	d	7.7	2	

Table 8. (cont'd)

cis-(DMPE)$_2$Ru(Me)$_2$[g]	-0.36	m		6	Ru-Me
	0.95	d	4.6	6	Me$_2$PCH$_2$CH$_2$PMe$_2$
	1.02	d	5.9	6	
	1.04	s		6	
	1.18	t	2.9	6	
	0.87	m		2	Me$_2$PCH$_2$CH$_2$PMe$_2$
	1.23	m		2	
	1.38	m		4	
cis-(DMPE)$_2$Ru-(OC$_6$H$_4$-*p*-Me)$_2$(12)[d]	1.24	s		6	Me$_2$PCH$_2$CH$_2$PMe$_2$
	1.24	t	3.7	6	
	1.37	t	3.5	6	
	1.44	d	9.3	6	
	1.68	m		8	Me$_2$PCH$_2$CH$_2$PMe$_2$
	2.06	s		6	(OC$_6$H$_4$-*p*-Me)
	6.50	d	8.5	4	(OC$_6$H$_4$-*p*-Me)
	6.55	d	8.5	4	
(DMPE)$_2$Ru(CO$_3$) (13)[h]	1.26	d	7.0	6	Me$_2$PCH$_2$CH$_2$PMe$_2$
	1.28	d	4.1	6	
	1.32	t	3.6	6	
	1.44	t	2.3	6	
	1.7-1.9	m		4	Me$_2$PCH$_2$CH$_2$PMe$_2$
	1.9-2.05	m		4	
cis-(DMPE)$_2$Ru(OC(O)Ph)$_2$[h]	1.16	d	8.4	6	Me$_2$PCH$_2$CH$_2$PMe$_2$
	1.35	d	6.8	6	
	1.76	s		6	
	1.84	s		6	
	1.3-1.5	m		8	Me$_2$PCH$_2$CH$_2$PMe$_2$
	7.22	m		3	(OC(O)Ph)
	7.83	d	7.4	2	
trans-(DMPE)$_2$Ru-(H)(OC(O)Ph) (14)[e]	-22.47	quin	21.5	1	Ru-H
	1.14	s		12	Me$_2$PCH$_2$CH$_2$PMe$_2$
	1.36	s		12	
	1.34	m		4	Me$_2$PCH$_2$CH$_2$PMe$_2$
	1.97	m		4	
	7.19	t	7.2	1	(OC(O)Ph)
	7.29	t	7.3	2	
	8.41	d	7.2	2	
(PMe$_3$)$_3$Ru-(CH(C(O)CH$_2$CMe$_3$)$_2$)(Me) (15)[e]	0.34	dt	5.1, 3.4	3	Ru-Me
	1.06	d	5.6	9	PMe$_3$
	1.16	d	6.9	18	PMe$_3$
	1.17	s		18	(CH(C(O)CH$_2$CMe$_3$)$_2$)
	1.97	d	11.4	2	(CH(C(O)CH$_2$CMe$_3$)$_2$)
	2.10	d	11.4	2	(CH(C(O)CH$_2$CMe$_3$)$_2$)
	5.15	s		1	(CH(C(O)CH$_2$CMe$_3$)$_2$)

Table 8. (cont'd)

$(PMe_3)_4Ru$-(OC(Me)CHC(Me)CH) (19)[e]	0.98	d	7.0	9	*cis*-PMe_3
	1.16	d	5.7	9	*cis*-PMe_3
	1.18	t	2.9	18	*trans*-PMe_3
	2.03	s		3	(OC(Me)CHC(Me)CH)
	2.34	s		3	(OC(Me)CHC(Me)CH)
	4.88	d	1.9	1	(OC(Me)CHC(Me)CH)
	6.22	dm	11.1	1	(OC(Me)CHC(Me)CH)
$(PMe_3)_4Ru$ (OC(O)OC(CMe_3)CH) (21)[d]	0.79	d	7.5	9	*cis*-PMe_3
	1.04	d	5.8	9	*cis*-PMe_3
	1.06	t	1.9	18	*trans*-PMe_3
	1.44	s		9	(OC(O)OC(CMe_3)CH)
	5.34	dt	7.1, 2.6	1	(OC(O)OC(CMe_3)CH)

[a]The multiplicities triplet and doublet, when applied to the PMe_3 and DMPE resonances, are apparent splitting patterns. Accordingly, the values reported for J do not necessarily reflect true coupling constants; for example, the tabulated coupling constant in a triplet is the separation between the central line and the outer lines. [b]The assignment *trans*-PMe_3 refers to the mutually trans phosphine ligands; the other two phophines are assigned as *cis*-PMe_3. [c]THF-d_8, -40 °C. [d]THF-d_8, 20 °C. [e]C_6D_6, 20 °C. [f]Methanol-d_4, 20°C. [g]CD_2Cl_2, -62 °C. [h]CD_2Cl_2, 20 °C.

Table 9. $^{13}C\{^1H\}$ NMR spectroscopic data.

Compound	δ(ppm)	mult[a]	J(Hz)	assignment[b]
$(PMe_3)_4Ru(OC(CH_2)C_6H_4)$	19.40	td	12.6, 2.6	*trans*-PMe_3
(3)[d]	22.28	dt	17.0, 1.7	*cis*-PMe_3
	25.23	dm	23.6	*cis*-PMe_3
	72.90	s		$(OC(\underline{CH_2})C_6H_4)$
	120.68	d	1.3	$(OC(CH_2)\underline{C_6H_4})$
	122.61	d	1.4	
	125.23	m		
	141.27	m		
	152.86	d	3.1	
	176.60	dm	7.7	$(O\underline{C}(CH_2)C_6H_4)$
	177.71	dq	65.0, 8.2	$(OC(CH_2)\underline{C_6H_4})$
$(CO)(PMe_3)Ru$-	17.76	dt	23, 4	PMe_3
$(OC(Me)(Ph)CH_2C(O))$ (6)[e]	18.14	dt	15, 3	
	18.20	dt	4, 4	
	38.08	s		$(OC(\underline{Me})(Ph)CH_2C(O))$
	74.65	d	20.0	$(OC(Me)(Ph)\underline{CH_2}C(O))$
	76.82	d	5.8	$(O\underline{C}(Me)(Ph)CH_2C(O))$
	124.24	s		$(OC(Me)(\underline{Ph})CH_2C(O))$
	126.62	s		
	127.52	s		
	157.65	s		
	201.36	m		Ru-CO
	268.31	dm	100.1	$(OC(Me)(Ph)CH_2\underline{C}(O))$
cis-$(PMe_3)_4Ru(OC_6H_4$-*p*-$Me)_2$	18.56	t	12.6	*trans*-PMe_3
(7)[d]	22.57	m		*cis*-PMe_3
	20.75	s		$(OC_6H_4$-*p*-$\underline{Me})_2$
	118.36	s		$(O\underline{C_6H_4}$-*p*-$Me)_2$
	120.66	s		
	129.68	s		
	169.41	s		
$(PMe_3)_4Ru(CO_3)$ (8)[f]	16.98	t	13	*trans*-PMe_3
	22.48	m		*cis*-PMe_3
	169.22	s		Ru-CO_3
$(PMe_3)_4Ru(OC(NPh)O)$ (9)[g]	15.88	t	13.1	*trans*-PMe_3
	21.18	d	23.3	*cis*-PMe_3
	21.43	d	26.2	*cis*-PMe_3
	116.34	s		$(OC(N\underline{Ph})O)$
	122.55	s		
	127.66	s		
	152.69	s		
	171.66	s		$(O\underline{C}(NPh)O)$

Table 9. (cont'd)

$(PMe_3)_4Ru(OC(O)NPh)$ (10)[h]	18.31	t	13.1	*trans*-PMe_3
	22.21	dt	26.1, 2.0	*cis*-PMe_3
	25.57	dq	26.4, 2.1	*cis*-PMe_3
	116.26	s		(OC(O)N<u>Ph</u>)
	122.53	s		
	127.82			
	157.85	d	3.9	
	167.65	s		(O<u>C</u>(O)NPh)
cis-$(PMe_3)_4Ru(H)(OC(O)Ph)$ (11)[e]	22.77	dd	25, 3	*cis*-PMe_3
	26.27	dq	27, 3	*cis*-PMe_3
	23.12	td	14, 3	*trans*-PMe_3
	127.67	s		(OC(O)<u>Ph</u>)
	129.19	s		
	130.21	s		
	139.87	s		
	172.19	s		(O<u>C</u>(O)Ph)
cis-$(DMPE)_2Ru(Me)_2$[e]	-8.03	dq	63.3, 11.6	Ru-Me
	9.02	t	1.8	<u>Me</u>$_2$PCH$_2$CH$_2$P<u>Me</u>$_2$
	15.46	dd	10.6, 7.0	
	19.20	pent	4.5	
	22.71	dd	8.9, 5.6	
	29.20	m		Me$_2$P<u>CH$_2$CH$_2$</u>PMe$_2$
	33.57	m		
cis-$(DMPE)_2Ru(OC_6H_4$-*p*-$Me)_2$ (12)[d]	11.91	t	12.1	<u>Me</u>$_2$PCH$_2$CH$_2$P<u>Me</u>$_2$
	15.56	t	12.0	
	16.25	dd	15.2, 12.3	
	20.26	dd	14.4, 11.6	
	20.89	s		(OC$_6$H$_4$-*p*-<u>Me</u>)
	29.99	m		Me$_2$P<u>CH$_2$CH$_2$</u>PMe$_2$
	32.17	m		
	119.07	s		(O<u>C$_6$H$_4$</u>-*p*-Me)
	121.56	s		(O<u>C$_6$H$_4$</u>-*p*-Me)
	129.01	s		(O<u>C$_6$H$_4$</u>-*p*-Me)
	172.66	t	2.8	(O<u>C$_6$H$_4$</u>-*p*-Me)
$(DMPE)_2Ru(CO_3)$ (13)[h]	8.39	t	12.0	<u>Me</u>$_2$PCH$_2$CH$_2$P<u>Me</u>$_2$
	16.04	t	12.0	
	16.35	t	12.0	
	18.77	t	13.6	
	26.37	m		Me$_2$P<u>CH$_2$CH$_2$</u>PMe$_2$
	33.25	m		
	167.46	s		Ru-CO_3

Table 9. (cont'd)

cis-(DMPE)$_2$Ru(OC(O)Ph)$_2$[h]	13.26	t	13.9	$\underline{Me_2}PCH_2CH_2P\underline{Me_2}$
	15.74	t	12.6	
	17.79	t	13.5	
	18.84	t	15.1	
	27.45	m		$Me_2P\underline{CH_2}\underline{CH_2}PMe_2$
	33.39	m		
	127.62	s		(OC(O)$\underline{Ph}$)
	129.30	s		
	129.55	s		
	139.26	s		
	172.04	s		(O$\underline{C}$(O)Ph)
trans-(DMPE)$_2$Ru-	15.64	pent	5.2	$\underline{Me_2}PCH_2CH_2P\underline{Me_2}$
(H)(OC(O)Ph) (14)[e]	22.49	pent	7.0	
	31.24	pent		$Me_2P\underline{CH_2}\underline{CH_2}PMe_2$
	127.55	s		(OC(O)$\underline{Ph}$)
	128.82	s		
	129.92	s		
	139.97	s		
	170.42	s		(O$\underline{C}$(O)Ph)
$(PMe_3)_3Ru$	4.83	dt	81.2, 11.6	Ru-Me
(CH(C(O)CH_2CMe_3)$_2$)(Me)	19.01	d	13.9	PMe_3
(16)[e]				
	19.93	t	12.5	PMe_3
	30.93	s		(CH(C(O)$CH_2C\underline{Me_3}$)$_2$)
	32.06	s		(CH(C(O)$CH_2\underline{C}Me_3$)$_2$)
	56.53	s		(CH(C(O)$\underline{CH_2}CMe_3$)$_2$)
	103.04	s		($\underline{C}$H(C(O)CH_2CMe_3)$_2$)
	128.90	s		(CH($\underline{C}$(O)CH_2CMe_3)$_2$)
$(PMe_3)_4Ru$	18.66	t	9.4	*trans*-PMe_3
(OC(Me)CHC(Me)CH) (19)[e]	21.52	d	15.1	*cis*-PMe_3
	23.45	d	24.1	*cis*-PMe_3
	26.30	s		(OC($\underline{Me}$)CHC($\underline{Me}$)CH)
	30.50	s		(OC($\underline{Me}$)CHC($\underline{Me}$)CH)
	98.61	s		(OC(Me)$\underline{CH}$C(Me)CH)
	138.18	dtd	64, 16, 10	(OC(Me)CHC(Me)$\underline{CH}$)
	156.41	s		(O$\underline{C}$(Me)CH$\underline{C}$(Me)CH)
		not	observed	(O$\underline{C}$(Me)CH$\underline{C}$(Me)CH)

Table 9. (cont'd)

$(PMe_3)_4Ru$	18.11	td	13.1, 2.0	*trans*-PMe_3
$(OC(O)OC(CMe_3)CH)$ (21)[d]	21.12	d	17.2	*cis*-PMe_3
	22.58	dd	27.0, 2.2	*cis*-PMe_3
	29.53	s		$(OC(O)OC(C\underline{Me_3})CH)$
	38.20	d	6.0	$(OC(O)OC(\underline{C}Me_3)CH)$
	110.98	dtd	60, 18, 8.6	$(OC(O)OC(CMe_3)\underline{CH})$
	151.82	d	2.8	$(OC(O)O\underline{C}(CMe_3)CH)$
	156.58	t	5.3	$(O\underline{C}(O)OC(CMe_3)CH)$

[a]The multiplicities triplet and doublet, when applied to the PMe_3 and DMPE resonances, are apparent splitting patterns. Accordingly the values reported for J do not necessarily reflect true coupling constants. [b]The assignment *trans*-PMe_3 refers to the mutually trans phosphine ligands; the other two phophines are assigned as *cis*-PMe_3. [c]THF-d_8, -40 °C. [d]THF-d_8, 20 °C. [e]C_6D_6, 20 °C. [f]Methanol-d_4, 20°C. [g]CD_2Cl_2, -62 °C. [h]CD_2Cl_2, 20 °C.

Table 10. $^{13}P\{^1H\}$ NMR spectroscopic data.

Compound	spin system[a]	δ(ppm)	J(Hz)
$(PMe_3)_4Ru(OC(CH_2)C_6H_4)$ (3)[d]	A_2BC	δA=0.69 δB=-13.71 δC=6.86	J_{AB}=25.3 J_{AC}=32.2 J_{BC}=14.3
$(CO)(PMe_3)Ru(OC(Me)(Ph)CH_2C(O))$ (5)[e]	ABC	δA=-0.76 δB=8.70 δC=11.26	J_{AB}=26.9 J_{AC}=26.3 J_{BC}=321.1
cis-$(PMe_3)_4Ru(OC_6H_4$-*p*-Me$)_2$[e]	A_2B_2	δA=14.89 δB=-0.98	J_{AB}=31.8
$(PMe_3)_4Ru(CO_3)$ (8)[f]	A_2B_2	δA=23.08 δB=4.75	J_{AB}=30.7
$(PMe_3)_4Ru(OC(NPh)O)$ (9)[g]	A_2BC	δA=1.98 δB=18.96 δC=19.81	J_{AB}=31.1 J_{AC}=32.8 J_{BC}=32.3
$(PMe_3)_4Ru(OC(O)NPh)$ (10)[h]	A_2BC	δA=0.04 δB=5.66 δC=8.99	J_{AB}=30.6 J_{AC}=30.6 J_{BC}=29.8
cis-$(PMe_3)_4Ru(H)(OC(O)Ph)$ (11)[e]	A_2BC	δA=-0.52 δB=6.74 δC=-13.72	J_{AB}=33 J_{AC}=23 J_{BC}=17
cis-$(DMPE)_2Ru(Me)_2$[e]	AA'BB'	δA=45.31 δB=32.69	$J_{AB,AB'}$=19.1
cis-$(DMPE)_2Ru(OC_6H_4$-*p*-Me$)_2$ (12)[d]	AA'BB'	δA=52.28 δB=36.60	$J_{AB,AB'}$=17.3
$(DMPE)_2Ru(CO_3)$ (13)[h]	AA'BB'	δA=57.45 δB=54.86	$J_{AB,AB'}$=20.6
cis-$(DMPE)_2Ru(OC(O)Ph)_2$[h]	AA'BB'	δA=53.99 δB=37.44	$J_{AB,AB'}$=24.4
trans-$(DMPE)_2Ru(H)(OC(O)Ph)$ (11)[e]	A_4	δA=46.90	
$(PMe_3)_3Ru(CH(C(O)CH_2CMe_3)_2)(Me)$ (16)[e]	A_2B	δA=25.43 δB=-8.51	J_{AB}=16.2

Table 10. (cont'd)

$(PMe_3)_4Ru(OC(Me)CHC(Me)CH)$ (19)[e]	A_2BC	δA=-0.35 δB=11.65 δC=-15.13	J_{AB}=35.3 J_{AC}=21.8 J_{BC}=13.7
$(PMe_3)_4Ru(OC(O)CC(CMe_3)CH)$ (21)[d]	A_2BC	δA=0.77 δB=16.49 δC=-13.21	J_{AB}=36.8 J_{AC}=23.4 J_{BC}=17.9

[a] The true spin system for the *cis*-$(DMPE)_2Ru(X)_2$ compounds in this study is AA'BB'. However, all spectra of these compounds were observed simply as a pair of triplets.
[b]THF-d_8, -40 °C. [c]values for δ and J were determined by spectral simulation. [d]THF-d_8, 20 °C. [e]C_6D_6, 20 °C. [f]Methanol-d_4, 20°C. [g]CD_2Cl_2, -62 °C. [h]CD_2Cl_2, 20 °C.

Experimental

General. Unless otherwise noted, all manipulations were carried out under an inert atmosphere in a Vacuum Atmospheres 553-2 drybox with attached M6-40-1H Dritrain, or by using standard Schlenk or vacuum line techniques. Information on methods for solvent purification and for obtaining spectroscopic data is provided in the companion paper.

Unless otherwise specified, all reagents were purchased from commercial suppliers and used without further purification. PMe_3 (Strem) was dried over NaK or a Na mirror and vacuum transferred prior to use. DMPE (1,2-*bis*-dimethylphosphinoethane) (Strem) was used as received. Ferrocene (Aldrich) was sublimed, and mesitylene was dried over sodium/benzophenone ketyl and distilled prior to use. *p*-Cresol was dried by refluxing a solution in benzene using a Dean-Stark trap followed by distillation under argon. Acetophenone and benzaldehyde were dried by refluxing over CaH_2, followed by distillation under nitrogen. Hydrogen, carbon monoxide and carbon dioxide were purchased from Matheson and used as received. Trimethylsilane was purchased from Petrarch and used as received. 4,4-dimethyl-2-pentanone and pinacolone were purchased from Aldrich and used as received. *tert*-Butylacetylacetone was prepared by the addition of the potassium enolate of 4,4-dimethyl-2-pentanone to *tert*-butylacetyl chloride. $Me_3SiOC(CH_2)CMe_3$ was prepared by standard methods.[43] Alkali enolates were prepared as described in the companion paper as was the mixture of *cis*-and *trans*-$(PMe_3)_4Ru(Ph)(Cl)$. $(PMe_3)_4Ru(\eta^2\text{-}C_6H_4)$,[15] *cis*-$(PMe_3)_4Ru(OAc)(Cl)$,[19] and *trans*-$(PMe_3)_4Ru(Cl)_2$[21] were prepared as published previously.

Pentane and hexane (UV grade, alkene free) were distilled from $LiAlH_4$ under nitrogen. Benzene, toluene, and tetrahydrofuran were distilled from sodium benzophenone ketyl under nitrogen. Dichloromethane was either distilled under N_2 or vacuum transferred from CaH_2. Deuterated solvents for use in NMR experiments were dried as their protiated analogues but were vacuum transferred from the drying agent.

$(PMe_3)_4Ru(OC(CH_2)C_6H_4)$ (3). (a) By thermolysis of 1: In 2.4 mL of C_6D_6 was dissolved 25.0 mg (0.0483 mmol) of *cis*- and *trans*-$(PMe_3)_4Ru(Ph)(Cl)$ and 5 mg of ferrocene as an

internal standard. Into an NMR tube was placed 0.6 mL of this solution for determination of the relative concentrations of *cis*- and *trans*-$(PMe_3)_4Ru(Ph)(Cl)$ and the internal standard. To the remaining solution was added 10.4 mg (3.0 equiv.) of $KOC(CH_2)Me$. The resulting suspension was stirred for 2 h, over which time the yellow color turned darker orange. The solid was removed by forcing the suspension through a small plug of celite. The resulting solution containing **1** was equally divided into three separate NMR tubes, one for use in this preparation, a second for part (c) below and a third for use in the preparation of **7** from **1**. The first tube was equipped with a vacuum stopcock, degassed by three freeze, pump, thaw cycles, and sealed under vacuum. The sample was then heated to 45 °C for 8h. ^1H and $^{31}P\{^1H\}$ NMR of the final reaction solution showed formation of **3** in 51% yield, as determined by comparison to the initial sample.

(b) By addition of $KOC(CH_2)Ph$ to $(PMe_3)_4Ru(Me)(Cl)$. In 1.4 mL of C_6D_6 was dissolved 18.8 mg (0.0413 mmol) of $(PMe_3)_4Ru(Me)(Cl)$ and 1.4 mL of ferrocene as an internal standard. Half of this solution was placed into an NMR tube and to the remaining solution was added 5 mg (1.5 equiv.) of $KOC(CH_2)Ph$ as a solid. The resulting suspension was stirred for 5 min at room temperature and then placed into a second NMR tube. The ^1H NMR spectrum of this solution showed the presence of **3** and starting material. No **4** was observed. The solution was allowed to stand at room temperature for 24 h, after which time the ^1H NMR spectrum showed the presence of methane and the formation of **3** in 98% yield, by comparison with the sample of *cis*- and *trans*-$(PMe_3)_4Ru(Ph)(Cl)$ and ferrocene internal standard.

(c) By addition of acetophenone to **1**: To the second sample of **1**, generated as described in part a, was added 2.4 μL (1.2 equiv.) of acetophenone. The tube was equipped with a vacuum stopcock, degassed by three freeze, pump, thaw cycles, and sealed under vacuum. The sample was then heated to 45 °C for 8h. ^1H and $^{31}P\{^1H\}$ NMR of the final reaction solution showed formation of α-methylstyrene (58%) and **3** (61%), [15] as determined by comparison to the initial sample.

Hydrogenolysis of 1. In 1.2 mL of C_6D_6 was dissolved 15.0 mg of *cis*- and *trans*-$(PMe_3)_4Ru(Ph)(Cl)$ and 2 mg of ferrocene as an internal standard. Into one NMR tube was placed

half of the reaction solution and to the remaining solution was added 1.5 mg (1.0 equiv) of $KOC(CH_2)Me$ as a solid. The reaction was stirred for 4 h, after which time the orange solution was filtered through a small plug of celite and the filtrate was placed into a 9" NMR tube equipped with a Kontes vacuum adaptor. The sample was degassed by three freeze, pump, thaw cycles, submerged in liquid nitrogen, and exposed to 450 torr of H_2. The tube was sealed at the top of the liquid nitrogen to give a final length of 8.5 ", and a pressure of approximately 2 atm at 25 °C. After 2 h at 25 °C, the orange solution became pale yellow, and ^1H and $^{31}P\{^1H\}$ NMR spectroscopy showed formation of the dihydride 5 in 88% yield and the alcohol $HOC(Me)_2Ph$ in 84% yield, by comparison to the sample of *cis*- and *trans*-$(PMe_3)_4Ru(Ph)(Cl)$ and ferrocene internal standard. The sample was then opened, the solution passed through a short column of silica to remove the ruthenium complex. After elution with 1 mL of ether, gas chromatographic analysis of the eluent showed the 2-phenyl-2-propanol as the major peak after those of the solvent, as determined by comparison of the retention time to an authentic sample and coinjection of the eluent and a solution of the authentic sample.

$(PMe_3)_3(CO)Ru(OC(Me)(Ph)CH_2C(O))$ (6). To a suspension of 150 mg of *cis*- and *trans*-$(PMe_3)_4Ru(Ph)(Cl)$ in 14 mL of *n*-pentane was added at room temperature 83.5 mg (3.0 equiv) of $KOC(CH_2)Me$ as a solid. The suspension was stirred for 4 h, and after this time the solid was removed by filtration with pressure through a plug of celite. The resulting clear orange filtrate was transferred to a 250 mL glass reaction vessel equipped with a Kontes vacuum adaptor. The vessel was submerged in liquid nitrogen and exposed to vacuum followed by 450 torr of CO. Upon thawing, the yellow solution became clear. The volume was reduced to ~6 mL and cooled to -40°C to provide 76.0 mg (50.1%) of white needles. IR (KBr) 1907 (s), 1614 (s); MS (FAB, sulfolane) 520 (M^+); Anal. Calcd. for $C_{20}H_{37}O_3P_3Ru$: C, 46.23%; H, 7.18%. Found: C, 46.00%; H, 7.38%.

Reaction of 1 with *p*-cresol. A solution of 5 mg (4 equiv) of *p*-cresol in 0.3 mL of C_6D_6 was prepared. To the third sample of 1, prepared as described in the section on the formation of 3 by thermolysis of 1 was treated with the solution of of *p*-cresol dropwise until the

dark orange solution turned yellow (approx 0.2 mL of the solution). ^1H and $^{31}P\{^1H\}$ NMR of the resulting solution showed formation of α-methylstyrene in 86% yield and **7**[20] in 74% yield, by comparison to the sample of *cis*- and *trans*-$(PMe_3)_4Ru(Ph)(Cl)$ and ferrocene internal standard.

$(PMe_3)_4Ru(CO_3)$ (8). (a) From **1**. In 1.8 mL of C_6D_6 was dissolved 14.4 mg (0.0278 mmol) of *cis*- and *trans*-$(PMe_3)_4Ru(Ph)(Cl)$ and 3 mg of ferrocene as an internal standard. Into an NMR tube was placed 0.6 mL of this solution for an integration of starting material versus the internal standard. To the remaining solution was added 3.5 mg (1.3 equiv.) of $KOC(CH_2)Me$. The resulting suspension was stirred for 2 h, over which time the yellow color turned darker orange. The resulting solution containing **1** was divided equally into two NMR tubes. One of the tubes was equipped with a vacuum stopcock, and degassed by three freeze, pump, thaw cycles. To this sample was added 0.0556 mmol of CO_2 by vacuum transfer. Upon thawing, the orange solution turned clear and white crystals formed from the reaction solution. ^1H NMR spectroscopy of this solution showed the presence of α-methylstyrene in 84% yield. The tube was then opened and CD_2Cl_2 (0.2 mL) was added to dissolve the ruthenium complex. ^1H and $^{31}P\{^1H\}$ NMR spectroscopy showed the formation of **8** in 83% yield, by comparison the the sample of *cis*- and *trans*-$(PMe_3)_4Ru(Ph)(Cl)$ and ferrocene internal standard.

(b) Preparative scale. Into a 50 mL round bottom flask equipped with a Kontes vacuum adaptor was placed, in air, 300 mg (0.630 mmol) of *trans*-$(PMe_3)_4Ru(Cl)_2$ and 150 mg (1.09 mmol) of K_2CO_3. To these two solids was added 10 mL of methanol by vacuum transfer. The resulting solution was carefully degassed by three freeze, pump, thaw, cycles and then heated at 50 °C for 1.5 h with stirring. During this time, the initial orange solution turned pale yellow. The solvent was removed under reduced pressure and the resulting solid was extracted with CH_2Cl_2. Removal of the CH_2Cl_2 solvent provided 255 mg (85%) of white solid, which was pure by $^{31}P\{^1H\}$ NMR spectroscopy. This material was further purified by dissolving the material in CH_2Cl_2 and layering the resulting solution with Et_2O to provide 10.6 mg (3.5%) of white powder, used for infrared and mass spectral analysis. IR(KBr): 1578 (s); MS (FAB, 1,2 nitrobenzyl alcohol matrix) 467 (MH^+), 423 ($(M\text{-}CO_2)H^+$), 407 ($(M\text{-}CO_3)H^+$), 391 ($(M\text{-}PMe_3)H^+$).

Synthesis of $(PMe_3)_4Ru(OC(O)NPh)$ (10) *via* $(PMe_3)_4Ru(OC(NPh)O)$ (9). In 10 mL of *n*-pentane was suspended 301 mg of *cis*- and *trans*-$(PMe_3)_4Ru(Ph)(Cl)$ and 120 mg (1.98 equiv.) of $KOC(CH_2)Me$. The reaction was stirred for 4 h at room temperature, after which time the orange suspension was filtered with pressure. To the resulting clear orange solution was added 95.0 mg PhNCO (1.98 equiv) as a solution in 1 mL of *n*-pentane. Upon addition of the isocyanate, a pale yellow solid precipitated from solution. This solid was filtered, washed twice with 1.5 mL of *n*-pentane, and dried under vacuum to provide 194 mg (63%) yield of 9 which was roughly 90% pure by ^1H and $^{31}P\{^1H\}$ NMR spectroscopy. This material was dissolved in 7 mL of CH_2Cl_2 and heated to 45 °C for 1 h to convert 9 to its isomer 10. The solution was concentrated to 1 mL under reduced pressure and layered with 4 mL of pentane. After 12 h at room temperature, 52.6 mg (27.1%) of analytically pure yellow powder was collected. IR(KBr) 2912 (m), 1595 (s), 1577 (m), 1567 (m), 1550 (m), 1492 (m), 1482 (m), 1329 (s), 1314 (m), 1304 (m) 1282 (m0, 1233 (m), 944 (s); Anal. Calcd for $C_{19}H_{41}NO_2P_4Ru$: C, 42.22; H, 7.65; N, 2.59. Found: C, 42.45; H, 7.67; N, 2.49.

$(PMe_3)_4Ru(H)(OC(O)Ph)$ (11). (a) From 1. In 1.2 mL of C_6D_6 was dissolved 10.8 mg (0.0209 mmol) of *cis*- and *trans*-$(PMe_3)_4Ru(Ph)(Cl)$ and 2 mg of ferrocene as an internal standard. Half of this solution was transferred to an NMR tube, and to the remaining solution was added 3 mg (1.5 equiv.) of $KOC(CH_2)Me$ as a solid. The reaction was stirred for 2 h, after which time the solid materials were removed by filtration through a small plug of celite. Benzaldehyde (2.1 µL, 1.0 equiv) was added dropwise at room temperature as a solution in 0.3 mL of C_6D_6. The resulting yellow solution was placed into an NMR tube, equipped with a Kontes vacuum adaptor and sealed under vacuum. The sample was then heated to 45 °C for 24 h, after which time ^1H and $^{31}P\{^1H\}$ NMR spectroscopy showed formation of 11 in 53 % yield and α-methylstyrene in 76% yield.

(b) Preparative scale. In a glass reaction vessel equipped with a Kontes vacuum adaptor was placed a solution of 374 mg $(PMe_3)_4Ru(C_2H_4)$ in 10 mL of C_6H_6. To this stirred solution was added 105 mg (1.0 equiv) of benzoic acid in 2 mL of C_6H_6. The vessel was then closed and

heated to 45 °C for 24 h, after which time the solvent was removed under reduced pressure and the residue was extracted with 10 mL of pentane. Concentration of the solution and cooling to -40°C provided 64.3 mg (14%) of analytically pure white needles. IR(KBr): 1826 (s), 1599 (s); Anal. Calc'd. for $C_{19}H_{42}O_2P_4Ru$: C, 43.26; H, 8.02. Found: C, 43.12; H, 8.10.

$(DMPE)_2Ru(OC_6H_4$-*p*-Me$)_2$ (12). (a) From **2**. In 0.6 mL of C_6D_6 was dissolved 7.1 mg (0.0133 mmol) of **2** and 2 mg of mesitylene as an internal standard. A ^1H NMR spectrum of this solution was obtained. To this solution was then added 2.9 mg (2.0 equiv.) of *p*-cresol as a solid. A second ^1H NMR and $^{31}P\{^1H\}$ NMR spectrum showed formation of α-methylstyrene in quantitative yield and **12** in 74% yield.

(b) Preparative Scale. In 5 mL of toluene was dissolved 325 mg (0.754 mmol) of *cis*-$(DMPE)_2Ru(Me)_2$. To the stirred solution was added, dropwise at room temperature, 179 mg (2.2 equiv.) of *p*-cresol in 1 mL of toluene. During this addition, the initial clear solution turned yellow, and gas evolution was observed. The solution was layered with 3 mL of pentane, and after 12 h, 146 mg (32%) of **12**, judged pure by ^1H and $^{31}P\{^1H\}$ NMR spectroscopy, was isolated. This material was recrystallized for microanalysis by vapor diffusion of pentane into a solution of **12** in toluene. *IR(KBr) 2995(w), 2972 (m), 2906 (s), 2855 (w), 1601 (m), 1500 (s), 1497 (s), 1420 (m),* 1304 (s), 1159 (m), 1099 (m), 929 (s); Anal. Calc'd for $C_{26}H_{46}O_2P_4Ru$: C, 50.72; H, 7.53. Found: C, 50.26; H, 7.52.

$(DMPE)_2Ru(CO_3)_2$ (13). (a) From **2**. In 0.6 mL of C_6D_6 was dissolved 7.1 mg (0.0133 mmol) of **2** and 2 mg of mesitylene as an internal standard. A ^1H NMR spectrum of this solution was obtained. The NMR tube was then equipped with a Kontes vacuum adaptor. To the sample was added 2.0 equiv. of CO_2 by vacuum transfer. Upon thawing, **13** crystallized from the reaction mixture. A second ^1H NMR spectrum showed formation of α-methylstyrene in 96% yield. The tube was then opened and CD_2Cl_2 (~0.2 mL) was added to the solution to dissolve **13**. ^1H and $^{31}P\{^1H\}$ NMR spectroscopy of the resulting solution showed formation of **13** in quantitative yield.

(b) Preparative scale. Into a glass reaction vessel equipped with a Kontes vacuum adaptor was placed 250 mg (0.538 mmol) of **8**, 15 mL of tetrahydrofuran, and 242 mg (3.0 equiv) of DMPE. The reaction vessel was frozen with liquid nitrogen, exposed to vacuum, and heated to 85 °C for 24 h. After this time the $^{31}P\{^1H\}$ NMR spectrum of an aliquot showed complete conversion of **8** to **13**. The solvent was removed under reduced pressure and the resulting solid was washed with hexanes to provide 83.0 mg (33.5%) of white powder, which was roughly 95% pure. Attempts to obtain analytically pure material by crystallization were not successful. IR(KBr) 1566(s).

$(DMPE)_2Ru(H)(OC(O)Ph)$ (14). From **2**. In 1.2 mL of C_6D_6 was dissolved 12.6 mg (0.0237 mmol) of **2** and 2 mg of mesitylene as an internal standard. Half of this solution was placed into an NMR tube, and to the remaining solution was added 1.3 μL (1.1 equiv.) of benzaldehyde. The reaction was then placed into an NMR tube equipped with a Kontes vacuum adaptor and degassed by three freeze, pump, thaw cycles. The sample was then heated at 110 °C for 2 d, and ^1H NMR spectroscopy showed formation of α-methylstyrene in quantitative yield and **14** in 57% yield.

(b) Preparative scale. In 4 mL of hexanes was dissolved 78.4 mg of *cis*-$(DMPE)_2Ru(Me)_2$. To this solution was added 44.4 mg (2 equiv.) of benzoic acid. The reaction was stirred for 24 h at room temperature, over which time the product $L_4Ru(OC(O)PH)_2$ precipitated from the reaction as a white solid. This solid was isolated by filtration and washed twice with 2 mL of pentane to provide 83.5 mg (71.4%) of product which was pure enough (~90%) for preparation of **14**. The *bis*-benzoate (0.130 mmol) was dissolved in 7 mL of tetrahydrofuran. To the stirred solution was added dropwise at room temperature 32.5 μL (0.0325 mmol) of a 1.0 M solution of lithium aluminum hydride in Et_2O. The resulting solution was stirred for 8 h, after which time the solvent was removed under reduced pressure, and the residue was extracted three times with a total of 25 mL of Et_2O. The solution volume was reduced to ~5 mL *in vacuo* and cooled to -40°C to provide 67.9 mg (53.4%) of analytically pure white needles. IR(KBr) 2964 (m), 2921 (m), 2899 (s),

1907 (m), 1601 (s), 1566 (s), 1552 (m), 1419 (m), 1396 (m), 1360 (s), 1291 (m), 1275 (m), 937 (s) 929 (s) cm^{-1}; Anal Calc'd for $C_{19}H_{38}O_2P_4Ru$: C, 43.60; H, 7.32. Found: C, 43.32; H, 7.23.

Reactions of $(PMe_3)_4Ru(OC(CHCMe_3)CH_2)$ (15):

with *p*-cresol. Into an NMR tube was placed a solution of 6.8 mg of **15**, 2 mg of mesitylene as an internal standard, and 0.6 mL of C_6D_6. A ^1H NMR spectrum of this initial solution was obtained. To this sample was then added 3.2 mg of *p*-cresol as a solid. ^1H NMR spectroscopy showed quantitative formation of both **7** and 4,4-dimethyl-2-pentanone, as determined by comparison to the initial spectrum.

with 4,4-dimethyl-2-pentanone to form $(PMe_3)_3Ru(CH(C(O)CH_2CMe_3)_2)$-(Me) (16). From **15**. In 0.6 mL of C_6D_6 was dissolved 12.6 mg (0.0252 mmol) of **15** and 2 mg of mesitylene as an internal standard. To this solution was added 2.9 mg (1.0 equiv.) of 4,4-dimethyl-2-pentanone, and the reaction was transferred to an NMR tube equipped with a Kontes vacuum adaptor. The sample was degassed by three freeze, pump, thaw cycles and sealed. A ^1H NMR spectrum of this initial solution was obtained. The reaction was then heated to 110 °C for 24 h, after which time, ^1H and $^{31}P\{^1H\}$ NMR spectroscopy showed formation of **16** in 77% yield.

(b) Preparative scale. Into a glass reaction vessel equipped with a Kontes vacuum adaptor was placed a solution of 146 mg (0.304 mmol) of $(PMe_3)_4Ru(\eta^2\text{-}C_6H_4)$ and 76.1 mg (2.2 equiv.) of 4,4-dimethyl-2-pentanone in 7 mL of C_6H_6. The solution was heated for 24 h at 110 °C, over which time the initial clear solution turned yellow. The solvent was removed under reduced pressure and the residue extracted into 10 mL of *n*-pentane. The pentane solution was filtered through a small plug of celite, concentrated to ~2 mL and cooled to -40 °C to provide 59.0 mg (35%) of yellow blocks, judged pure by ^1H, $^{31}P\{^1H\}$ and $^{13}C\{^1H\}$ NMR spectroscopy. This material was then recrystallized from pentane for microanalysis. IR(KBr) 2966 (s), 2944(s), 2906 (s), 2861 (m), 1576 (s), 1561 (w), 1514 (s), 1468 (m), 1452 (m), 1446 (m), 1434 (m), 1428 (m),m 1408 (m), 1363 (m), 1293 (m), 1273 (s), 966 (s), 939 (s) cm^{-1}; *Anal. Calc'd for* $C_{21}H_{35}O_2P_4Ru$: C, 49.72; H, 9.61. Found: C, 49.46, H, 9.64

Addition of HCl to 16. Into an NMR tube equipped with a rubber septum was placed a solution of 5.6 mg of **16** and 2 mg of mesitylene as an internal standard in 0.6 mL of C_6D_6. A ^1H NMR spectrum of this solution was obtained. To this solution was then added 3 μL of 37% HCl in water, and immediate formation of a solid occurred. ^1H NMR spectroscopy showed formation of *tert*-butylacetylacetone in quantitative yield, as determined by comparison to the initial spectrum. The sample was then filtered to remove the insoluble ruthenium complex. Gas chromatographic analysis performed on the resulting clear filtrate showed the presence of *tert*-butylacetylacetone, as determined by comparison of the retention time to an authentic sample, as well as coinjection of the reaction solution with the authentic sample.

$(PMe_3)_4Ru(OC(Me)CHC(Me)CH)$ (19). A suspension of $(PMe_3)_4Ru(OAc)(Cl)$ (127 mg, 0.254 mmol) and $KOC(CH_2)Me$ (53.7 mg, 2.2 equiv) in 7 mL of ether was stirred for 2 h at room temperature. After this time, the solution was transferred to a glass reaction vessel equipped with a Kontes vacuum adaptor. The solution was frozen in liquid nitrogen and exposed to vacuum. The vessel was closed and then heated to 85 °C for 8 h. After this time, the solvent was removed and the residue was extracted into 10 mL of pentane. The resulting slurry was filtered through a small plug of celite, concentrated to ~2 mL and cooled to -40 °C to provide 57.7 mg (45%) of yellow crystals of roughly 95% purity by ^1H, $^{31}\{^1H\}$ NMR $^{13}C\{^1H\}$ NMR spectroscopy. This material was recrystallized from pentane to provide an analytically pure sample of **19**. IR(KBr) 2987 (m), 2968 (s), 2967 (s), 2907 (s), 2829 (m), 1581 (s), 1528 (m), 1437 (m), 1419 (m), 1414 (m), 1394 (s), 1295 (s), 13272 (s), 1187 (s), 947 (s); Anal. Calc'd. for $C_{18}H_{44}OP_4Ru$: C, 43.11; H, 8.84. Found: C, 43.22; H, 8.90.

Addition of HOAc to 19. Into an NMR tube equipped with a Kontes vacuum adaptor was placed a solution of 8.6 mg of **19** and 2 mg of mesitylene in 0.6 mL of C_6D_6. A ^1H NMR spectrum of this solution was obtained to determine the relative concentrations of starting material and internal standard. Acetic acid (2.0 μL, 2.0 equiv.) was then added to the sample. The solution was frozen in liquid nitrogen and exposed to vacuum. The tube was sealed and the sample was heated at 85 °C for 2 h, after which time ^1H and $^{31}P\{^1H\}$ NMR spectroscopy showed

formation of $(PMe_3)_4Ru(OAc)_2$ in quantitative yield and mesityl oxide in 74% yield. The sample tube was then opened and the solution was passed through a short column of silica to remove the ruthenium complex, eluting with 1 mL of ether. Gas chromatographic analysis of the eluent showed the presence of $CH_3C(O)CH{=}CMe_2$, as determined by comparison of the retention time to an authentic sample as well as coinjection of the eluent and an authentic sample.

Reactions of $(PMe_3)_4Ru(OC(CMe_3)CH)$ (20):

with *p*-cresol. Into an NMR tube was placed a solution of 7.2 mg of **20** and 2 mg of mesitylene as an internal standard in 0.6 mL of C_6D_6. A ^1H NMR spectrum of this initial solution was obtained. To this sample was then added 3.5 mg of *p*-cresol as a solid. ^1H NMR spectroscopy showed formation of **7** in 91% yield and pinacolone (3,3-dimethyl-2-butanone) in quantitative yield, as determined by comparison to the initial spectrum.

with CO_2 to form $(PMe_3)_4Ru(OC(O)OC(CMe_3)CH)$ (21). Into a medium walled NMR tube was placed a solution of 41.2 mg (0.0819 mmol) of **20** in 0.4 mL of THF-d_8. The tube was equipped with a Kontes vacuum adaptor and degassed by three freeze, pump, thaw cycles. To the solution was added 0.0819 mmol of CO_2 by vacuum transfer. The tube was sealed and the initial yellow solution turned a paler yellow color upon thawing. ^1H, $^{13}C\{^1H\}$, and $^{31}P\{^1H\}$ NMR spectroscopy showed clean conversion to **21**. Upon standing for 12 h, 18.9 mg (42%) of pure **21** as white blocks formed from the reaction solution. This material was recrystallized for microanalysis by diffusing pentane into a THF solution of **21**. IR(KBr): 2972 (m), 2956 (m), 2944 (s), 2910 (m), 1633 (s), 1430 (m), 1325 (m), 1313 (m), 1297 (m), 1279 (m), 1042 (s), 944 (s); Anal. Calc'd. for $C_{19}H_{45}O_3P_4Ru$: C, 41.70; H, 8.47. Found: C, 41.32; H, 8.44.

with H_2. In 1.8 mL of C_6D_6 was dissolved 18.3 mg of **20** and 4 mg of mesitylene as an internal standard. The solution was divided into three equal portions; one portion was placed into an NMR tube to determine the relative concentrations of starting material and the internal standard. The second portion was placed into an NMR tube equipped with a Kontes vacuum adaptor. The latter sample was degassed by two freeze pump thaw cycles, immersed in liquid nitrogen, and exposed to 450 torr of H_2. The tube was sealed at the level of the liquid nitrogen

and heated to 45 °C for 8 h to provide the dihydride **5** in 77% yield and pinacolone in 61% yield, as determined by comparison of the ^{1}H NMR spectrum to that of the initial solution. The sample was then opened and the solution was passed through a short column of silica to remove the ruthenium complex, eluting with 1 mL of ether. Gas chromatographic analysis of the eluent showed the presence of pinacolone, as determined by comparison of the retention time to an authentic sample and coinjection of the eluent and the authentic sample.

with trimethylsilane. The third portion of **20**, prepared as described in the reaction of **20** with H_2, was placed in an NMR tube, and to this tube was added 0.0121 mmol (1.0 equiv.) of trimethylsilane by vacuum transfer. The sample was then heated to 85 °C for 2 h, after which time ^{1}H and ^{31}P{^{1}H} NMR spectroscopy showed formation of $(PMe_3)_3Ru(CH_2PMe_2)(H)$ in 40% yield and $Me_3SiOC(CH_2)CMe_3$ in 43% yield as determined by comparison to the initial solution described in the addition of H_2 to **20**. The sample tube was then opened and the solution was passed through a short column of silica to remove the ruthenium complex, eluting with 1 mL of ether. Gas chromatographic analysis of the eluent showed the presence of $Me_3SiOC(CH_2)CMe_3$, as determined by comparison of the retention time to an authentic sample, as well as coinjection of the eluent and a solution of the authentic sample.

X-ray Crystal Structure Determination of 17.

(a) Isolation and Mounting: Crystals of the compound were obtained by slow crystallization from pentane at –40 °C. Fragments cleaved from some of these crystals were mounted in thin-wall capillaries in an inert-atmosphere glove box and then the capillaries were flame sealed.

The crystal used for data collection was then transferred to our Enraf-Nonius CAD-4 diffractometer and centered in the beam. It was cooled to –90 °C by a nitrogen flow low-temperature apparatus which had been previously calibrated by a thermocouple placed at the sample position. Automatic peak search and indexing procedures yielded a monoclinic reduced primitive cell. Inspection of the Niggli values revealed no conventional cell of higher symmetry.

The final cell parameters and specific data collection parameters for this data set are given in Table 1.

(b) Structure Determination: The 3227 raw intensity data were converted to structure factor amplitudes and their esd's by correction for scan speed, background and Lorentz and polarization effects. Inspection of the intensity standards revealed a reduction of 7% of the original intensity. The data were corrected for this decay. Inspection of the azimuthal scan data showed a variation $I_{min}/I_{max} = 0.94$ for the average curve. An empirical correction based on the observed variation was applied to the data. Inspection of the systematic absences indicated uniquely the space group P21/n. Removal of systematically absent and redundant data left 2890 unique data in the final data set.

The structure was solved by Patterson methods and refined via standard least-squares and Fourier techniques. Hydrogen atoms were assigned idealized locations and values of B_{iso} approximately 1.15 times the B_{eqv} of the atoms to which they were attached. They were included in structure factor calculations, but not refined.

The final residuals for 190 variables refined against the 2430 data for which $F_2>3\sigma$ (F^2) were R = 3.89%, wR = 5.11% and GOF = 2.23. The R value for all 2890 data was 5.60%.

The quantity minimized by the least squares program was $\Sigma w(|F_o|-|F_c|)^2$, where w is the weight of a given observation. The p-factor, used to reduce the weight of intense reflections, was set to 0.03 throughout the refinement. The analytical forms of the scattering factor tables for the neutral atoms were imaginary components of anomalous dispersion.

Inspection of the residuals ordered in ranges of $\sin\theta/\lambda$, $|F_o|$, and parity and value of the individual indexes showed no unusual features or trends. The largest peak in the final difference Fourier map had an electron density of 0.77 e-/ Å^3, and the lowest excursion −0.69 e-/Å^3. Both were located near the Ru atom. There was no indication of secondary extinction in the high-intensity low-angle data.

The positional and thermal parameters of the non-hydrogen atoms were provided as supplementary material with the preliminary report of this compound[44] along with anisotropic

thermal parameters and the positions and thermal parameters of the hydrogen atoms, as well as a listing of the values of F_o and F_c.

X-ray Crystal Structural Determination of 15.

(a) Isolation and Mounting: Crystals of the compound were obtained by cooling slowly a pentane solution of **15**, and were mounted in a viscious oil. X-ray data were collected as for **17**; the final cell parameters and specific data collection parameters are given in Table 1.

(b) Structure Determination: The 3675 raw intensity data were converted to structure factor amplitudes and their esd's by correction for scan speed, background and Lorentz and polarization effects. An empirical absorption correction was applied to the data. Inspection of the systematic absences indicated space group Pnma. Removal of systematically absent and redundant data left 3542 unique data in the final data set.

The structure was solved by Patterson methods and refined via standard least-squares and Fourier techniques. The final residuals for 126 variables refined against the 2497 data for which $F_2>3\sigma$ (F^2) were R=6.3%, wR=7.9% and GOF=2.85. The R value for all 3542 data was 9.4%.

The quantity minimized by the least squares program was $\Sigma w(|F_o|-|F_c|)^2$, where w is the weight of a given observation. The p-factor, used to reduce the weight of intense reflections, was set to 0.03 throughout the refinement. The analytical forms of the scattering factor tables for the neutral atoms were used and all scattering factors were corrected for both the real and imaginary components of anomalous dispersion.

The positional and thermal parameters of the non-hydrogen atoms, anisotropic displacements in angstroms, and tables of least squares planes are provided as supplementary material.

X-ray Crystal Structural Determination of 18.

(a) Isolation and Mounting: Crystals of the compound were obtained by sublimation of **18** in a sealed tube at 55° C for 2 weeks, and were mounted as described for **15**. X-ray data were

collected as for **17**; the final cell parameters and specific data collection parameters are given in Table 1.

(b) Structure Determination: The 1441 raw intensity data were converted to structure factor amplitudes and their esd's by correction for scan speed, background and Lorentz and polarization effects. An empirical absorption correction was applied to the data. Inspection of the systematic absences indicated space group Pnma. Removal of systematically absent and redundant data left 1276 unique data in the final data set.

The structure was solved by Patterson methods and refined via standard least-squares and Fourier techniques. The final residuals for 51 variables refined against the 820 data for which $F_2 > 3\sigma(F^2)$ were R = 7.8%, wR = 9.2% and GOF = 3.07. The R value for all 2890 data was 12.5%.

The quantity minimized by the least squares program was $\Sigma w(|F_o|-|F_c|)^2$, where w is the weight of a given observation. The p-factor, used to reduce the weight of intense reflections, was set to 0.03 throughout the refinement. The analytical forms of the scattering factor tables for the neutral atoms were used and all scattering factors were corrected for both the real and imaginary components of anomalous dispersion.

The positional and thermal parameters of the non-hydrogen atoms, as well as a listing of the values of F_o and F_c were provided as supplementary material with the preliminary report of this compound.[14]

References and Notes

1. For discussions of oxametallacyclobutanes as intermediates in titanium mediated Wittig reactions see: (a) Brown-Wensley, K.A.; Buchwald, S.L.; Cannizzo, L.; Clawson, L.; Ho, S.; Meinhardt, D.; Stille. J.R.; Straus, D.; Grubbs, R.H. *Pure Appl. Chem.* **1983**, *55*, 1733. as intermediates in asymmetric epoxidations see: (b) Sharpless, K.B.; Teranishi, A.Y.; Backvall, J.-E. *J. Am. Chem. Soc.* **1977**, *99*, 3120. (c) Rappe, A.K.; Goddard, W.A. *J. Am. Chem. Soc.* **1982**, *104*, 3287. with P-450 models see: (d) Collman, J.P.; Brauman, J.I.; Meunier, B.; RAybuck, S.A.; Kodadek, T. *Proc. Natl. Acad. Sci. USA* **1984**, *81*, 3245. (e) Walba, D.M.; DePuy, C.H.; Grabowski, J.J.; Bierbaum, V.M. *Organometallics* **1984**, *3*, 498. (f) Collman, J.P.; Kodadek, T.; RAybuck, S.A.; Brauman, J.I.; Papazian, L.M. *J. Am. Chem. Soc.* **1985***107*, 4343. (g) Collman, J.P.; Brauman, J.I.; Meunier, B.; Hayashi, T.; Kodadek, T.; Raybuck, S.A. *J. Am. Chem. Sox.* **1985**, *107*, 2000. (h) Mock, W.L.; Bieniarz, C. *Organometallics***1985**, *4*, 1917. (i) Groves, J.T.; Avaria-Nesser, G.E.; Fish, K.M.; Imachi, M.; Kuczkowski, R.L. *J. Am. Chem. Soc.* **1986**, *108*, 3837. (j) Girardet, M.; Meunier, B. *Tetrahedron Lett.* **1977**, 2955.
2. (a) Alper, H.; Urso, F.; Smith, D.J.H. *J. Am. Chem. Soc.* **1983**, *105*, 6737. (b) Calet, S.; Urso, F.; Alper, H. *J. Am. Chem. Soc.* **1989**, *111*, 931.
3. Aye, K-T.; Ferguson, G.; Lough, A.T.; Puddephatt, R.J. *Angew. Chem. Int. Ed. Engl.* **1989**, *28*, 767
4. Klein D.P.; Hayes, J.C.; Bergman, R.G. *J. Am. Chem. Soc.* **1988**, *110*, 3704.
5. Day, V.W.; Klemperer, W.G.; Lockledge, S.P.; Main, D.J. *J. Am. Chem. Soc.* **1990**, *112*, 2031.
6. (a) Scholdder, T.; Ibers, J.A.; Lenarda, M.; Graziani, M. *J. Am. Chem. Soc.* 1974, *96*, 6893. (b) Lenarda, M.; Ros, R.; Traverso, O.; Pitts, W.D.; Baddley, W.H.; Graziani, M. *Inorg. Chem.* **1977**, *16*, 3178.
7. Zlota, A.A.; Frolow, F.; Milstein, D. *J. Am. Chem. Soc.* 1990, *112*, 6411.

8. (a) Ho, S.C.; Hentges, S.; Grubbs, R.H. *Organometallics*, **1988**, *7*, 780. (b) Bercaw, J.E., personal communication.

9. Hoover, J.F.; Stryker, J.M. *J. Am. Chem. Soc.* **1989**, *111*, 6466.

10. (a) Vaughan, G.A.; Hillhouse, G.L.; Lum, R.T.; Buchwald, S.L.; Rheingold *J. Am. Chem. Soc.* **1988**, *110*, 7215. (b) Vaughan, G.A.; Sofield, C.D.; Hillhouse, G.L. *J. Am. Chem. Soc.* **1989**, *111*, 5491

11. Carney. M.J.; Walsh, P.J.; Bergman, R.G. *J. Am. Chem. Soc.* **1990**, *112*, 6426.

12. Bryndza, H.E.; Tam, W. *Chem. Rev.* **1988**, *88*, 1163.

13. Chapter 5.

14. (a) Hartwig, J.F.; Bergman, R.G.; Andersen, R.A. *J. Am. Chem. Soc.* **1990**, *112*, 3234. (b) Hartwig, J.F.; Bergman, R.G.; Andersen, R.A. *J. Am. Chem. Soc.* **1990**, *112*, 5670.

15. Hartwig, J.F.; Andersen, R.A.; Bergman, R.G. *J. Am. Chem. Soc.* **1989**, *111*, 2717.

16. Other examples of C-C cleavage reactions include: (a) Suggs, J.W.; Cox, S.D. *J. Organomet. Chem.* **1981**, *221*, 199. (b) Suggs, J.W.; Jun, C.-H *J. Am. Chem. Soc.* **1984**, *106*, 3054. (c) Suggs, J.W.; Wovkulich, M.J. *Organometallics*, **1985**, *4*, 1101. (d) Suggs, J.W.; Jun C.-H. *J. Am. Chem. Soc.* **1986**, *108*, 4679. (d) Crabtree, R.H. *Chem. Rev.*, **1985**, *85*, 245. (e) Crabtree, R.H.; Dion, R.P.; Gibbone, D.J.; McGrath, D.V.; Holt, E.M. *J. Am. Chem. Soc.* **1986**, *108*, 7222, and references therein. (f) Watson, P.L.; Roe, D.C. *J. Am. Chem. Soc.* **1982**, *104*, 6471. (g) Buriel, E.; Berger, B.J.; Bercaw, J.E. *J. Am. Chem. Soc.* **1988**, *110*, 976.

17. Hartwig, J.F.; Andersen, R.A.; Bergman, R.G. *J. Am. Chem. Soc.* **1989**, *111*, 2717.

18. (a) Statler, J.A.; Wilkinson, G.; Thornton-Pett, M.; Hursthouse, M.B. *J. Chem. Soc., Dalton Trans.* **1984**, 1731. (b) Hartwig, J.F.; Bergman, R.G.; Andersen, R.A. *submitted for publication.*

19. Mainz, V.V.; Andersen, R.A. *Organometallics* **1984**, *3*, 675.

20. Chapter 4.

21. Sellmann, D.; Bohlen, E.; *Z. Naturforsch. B* **1982**, *37*, 1026.

22. A trans influence series is given in: Appleton, T.G.; Clark, H.C.; Manzer, L.E. *Coord. Chem. Rev.* **1973**, *10*, 335. Discussion of correlations between trans influence and ^{31}P chemical shifts is found in: (a) Nixon, J.F.; Pidcock, A.; *Ann. Rev. NMR Spectroscopy*, **1969**, *2*, 345. (b) Verkade, J.M.; Quin, L.D. eds., *Phosphorus-31 NMR Spectroscopy in Stereochemical Analysis*, VCH Publishers, New York, 1987. (c) Meek, D.W.; Mazanec, T.J. *Acc. Chem. Res.* **1981**, *14*, 266.

23. Wong, W-K.; Chiu, K.W.; Statler, J.A.; Wilkinson, G.; Motevalli, M.; Hursthouse, M.B. *Polyhedron*, **1984**, *3*, 1255.

24. Chatt, J.; Davidson, J.M. *J. Chem. Soc.* **1965**, 843.

25. Chatt, J.; Hayter, R.G. *J. Chem. Soc*, **1963**, 6017.

26. Allen , F.H.; Kennard, O.; Watson, D.G.; Brammer, L.; Orpen, D.G.; Taylor, R. *J. Chem. Soc., Perkin Trans. II* **1987**, S1.

27. Chapter 3, 6, 8.

28. Werner, H.; Werner, R. *J. Organomet. Chem.* **1981**, *97*, 3272

29. Chapter 1.

30. Ryabov, A.D. *Chem. Rev.* **1990**, *90*, 403.

31. March, J. *Advanced Organic Chemistry*; John Wiley and Sons: New York, 1985.

32. (a) Clarke, D.A.; Kemmitt, R.D.W.; Mazid, M.A.; McKenna, P.; Russell, D.R.; Schilling, M.D.; Sherry, L.J.S. *J. Chem. Soc., Dalton Trans.* **1984**, 1993. (b) Kemmitt, R.D.W.; McKenna, P.; Russell, D.R.; Sherry, L.J.S. *J. Chem. Soc., Dalton Trans.* **1985**, 259. (c) Imram, A.; Kemmitt, R.D.W.; Markwick, A.J.W.; McKenna, P.; Russell, D.R.; Sherry, L.J.S. *J. Chem. Soc., Dalton Trans.* **1985**, 549. (d) Jones, M.D.; Kemmitt, R.D.W.; Fawcett, J.; Russell, D.R. *J. Chem. Soc., Chem. Commun.* **1986**, 427. (e) Fawcett, J.; Henderson, W.; Jones, M.D.; Kemmitt, R.D.W.; Russell, D.R.; Lam, B.; Kang, S.D.; Albright, T.A. *Organometallics* **1989**, *8*, 1991.

33. Lee, J.B.; Gajda, G.J.; Schaefer, W.P.; Howard, T.R.; Ikariya, T.; Straus, D.A.; Grubbs, R.H. *J. Am. Chem. Soc.* **1981**, *103*, 7358.

34. (a) Legon, A.C. *Chem. Rev.* **1980**, *80*, 231. (b) Chan, S.I.; Zinn, J.; Gwinn, W.D. *J. Chem. Phys.* **1961**, *34*, 1319.

35. (a) Grosselin, J-M.; Le Bozec, H.; Moinet, C.; Toupet, L.; Köhler, F.H.; Dixneug, P.H. *Organometallics*, **1988**, *7*, 88. (b) Jones, M.D.; Kemmit, R.D.W.; Platt, A.W.G. *J. Chem. Soc., Dalton Trans.* **1986**, 1411. (c) Allen, S.R; Barnes, S.G.; Green, M.; Moran, G.; Trollope, L.; Murrall, N.W.; Welch, A.J.; Sharaiba, D.M. *J. Chem. Soc., Dalton Trans.* **1984**, 1157.

36. Frey, M.; Jenny, T.A.; Stoeckli-Evans, H. *Organometallics* **1990**, *9*, 1806.

37. Ando, W.; Choi, N.; Kabe, Y. *J. Am. Chem. Soc.* **1990**, *112*, 4574.

38. Holmgren, J.S.; Shapley, J.R.; Wilson, S.R.; Pennington, W.T. *J. Am. Chem. Soc.* 1986, *108*, 508.

39. (a) Alexander, J.J. *The Chemistry of the Metal-Carbon Bond*; Hartley, F.R., Ed.; Wiley: New York, 1985; vol 2, chapter 5. (b) Yamamoto, A. *Organotransition Metal Chemistry*; Wiley: New York, 1986. (c) Collman, J.P.; Hegedus, L.S.; Norton, J.R.; Finke, R.G. *Principles and Applications of Organotransition Metal Chemistry*, University Science Books: Mill Valley, 1987, p 356.

40. Rees, W.M.; Atwood, J.D. *Organometallics* **1985**, *4*, 402.

(a) Bryndza, H.E.; *Organometallics*, **1985**, *4*, 406. (b) Bryndza, H.E.; Fultz, W.C.; Tam, W. *Organometallics*, 1985, *4*, 939. (c) Bryndza, H.E.; *Organometallics*, **1985**, *4*, 1687. (d) Cowan, R.L; Trogler, W.C. *J. Am. Chem. Soc.* **1989**, *111*, 4750. (e) Glueck, D.S.; Newman, L.J.; Bergman, R.G. submitted for publication.

42. Chapter 5.

43. Miller, R.D.; McKean, D.R. *Synthesis* **1979**, 730.